DEPARTMENT OF CHEMISTRY
UNIVERSITY OF EDINBURGH

The Vertical Distribution, Associations and Mobility of Pb and other Elements in an Ombrotrophic Peat Bog

A Thesis submitted for the degree of

DOCTOR OF PHILOSOPHY

By Alex Freeman (BSc Hons) (Glasgow)

September 2001

DECLARATION

I hereby declare that this thesis has been composed by myself, and that all of the work described herein is my own

The vertical distribution, associations and mobility of Pb and other elements in an ombrotrophic peat bog

A major aim of this study was to investigate the mobility of Pb in an ombrotrophic peat bog. The vertical distribution of Pb and selected other elements (Mn, Fe, S, P, Al, Ti, Na, K, Mg, Ca, Sr, Ba, Zn and Cu) in the solid phase peat and its porewaters was first established. Other parameters including moisture, organic matter and ash content of the peat as well as porewater pH, conductivity and organic carbon concentration were also determined. On the basis of elemental profiles and those relating to the additional parameters, further investigations of the associations of Pb with organic matter were undertaken. These involved extraction of humic materials by two methods: the International Humic Substances Society method for isolating humic and fulvic acids, and a milder extraction method using 0.045 M Tris-borate (pH 8.5). Stable lead isotope ratios were also obtained for the solid phase peat, its porewater and each of the humic extracts.

The peat cores (1 m depth x 5 cm x 5 cm) were obtained in July 1999 from Flanders Moss, near Stirling, Central Scotland. The approach taken in this study involved sectioning at 2-cm depth intervals. Sections from the same depth interval from several cores were combined: those from five cores were used for the solid phase and porewater investigations whilst those from a further two cores were combined for the purpose of extracting the various humic materials. Elemental concentrations were obtained by FAAS, ICP-OES and ICP-MS as appropriate and isotope ratios were determined by ICP-MS. The activity of ^{210}Pb, a radionuclide often used for dating, was determined by gamma spectrometry. Geochemical modelling of the peat-porewater distribution of Pb was also undertaken.

From the results of this study, elevated Pb concentrations were found mainly in the top 0-30 cm of the solid phase peat. This was consistent with the deposition of anthropogenic Pb, particularly since the onset of the Industrial Revolution. Peak concentrations of 328 and 165 mg/kg were found at 4-6 cm and 20-22 cm respectively.

Porewater Pb concentrations were typically very low with a maximum value of ~0.04 mg/l and values <0.01 mg/l below 30 cm. The two peaks in porewater Pb were coincident with those in the solid phase peat and the porewater/solid phase ratio of Pb concentrations did not vary over significantly over these top sections. From this information alone, it appeared that there was a simple equilibrium distribution of Pb between the solid and aqueous phase and that very little of the total Pb was present in the porewater. The peak at 20-22 cm in both the solid phase and the porewater did, however, coincide with the maximum in porewater organic carbon concentration. Determination of the proportion of Pb in humic extracts showed, however, that very little of the total Pb was associated with humic materials at this depth. In addition, from the distributions and humic-associations of other elements, processes including active plant uptake of nutrients (Mn, Na, K, Ca), reductive dissolution (Fe) and mineral dissolution (Al, Ti) did not affect the vertical distribution of Pb within the peat. Finally, there was good agreement between the $^{206}Pb/^{207}Pb$ isotope ratios obtained for the solid phase peat, the porewater and each of the humic extracts, particularly in the uppermost sections of the core. The isotope signature changes from 1.136 to 1.177 in the solid phase, from 1.143 to 1.179 in the porewater and, for example, 1.143 to 1.180 in the humic acid extract. The similarity of the isotopic profiles provides further evidence to support the post-depositional vertical immobility of Pb in ombrotrophic peat bogs.

Overall, the experimental work provided a dated concentration profile for Pb, which can be used as a historical record of environmental Pb contamination. This (dates, inventories, fluxes) agreed well with records established in previous work using Flanders Moss peat cores and Loch Lomond (southern basin) sediment cores. The work has also extended the understanding of biogeochemical processes occurring in peat bogs although these do not influence the vertical concentration profile of Pb. In particular, the use of stable Pb isotopes established that even humic complexation after deposition was unlikely to affect the vertical distribution of Pb.

Geochemical modelling of the partitioning of Pb between the porewaters and the solid phase peat was also undertaken and the WHAM model predicted strong partitioning onto the solid phase peat in good agreement with the experimental work.

o, each in their own way, have provided
no particular order, Mark, for always
ver on call for advice!), Catherine (for
in plant taxonomy), Leon (for having
!), Clemencia (always able to bring me
e!), Liz (for continual inspiration and
students have also provided help and
challenges for my problem solving,
he years, these have included Nicola,
rdo, Ian, Tim, Daniel, John, Fiona, to

to reality from the monotony of the
g a patient and understanding flatmate
puter!), and Marion, Anna and Karen
o Mark and Cameron for always being
nort notice.

my PhD, has been the escape provided
amates and friends for having to put up
s for experiments and analysis going oft
y, John, Roger and Sarj, but have also
!), Tom, James (both of them!), Wally,
ky, Ben (both of them!), Cazza, Debs,
Lucy, Tolly, Adrianna, Jimbo, Caroline,
es, Dean, Alex (all 3 of them!), Brad,
have forgotten to mention.

pport and assistance particularly in the
uldn't have done it without her!!

ACKNOWLEDGEMENTS

Funding for this PhD was gratefull
from the Macauly Land Use Researc

Thanks to my supervisors; Dr M
encouragement throughout, and Dr
lead isotopic data. Thanks to Dr G
Research Unit, in East Kilbride
interpretation of the dating. Special
his help with the computer modellin
of his computer/printer etc when mi

Thanks to all my family for their
none!), and putting up with a skint
Special thanks to my Mum and
movements a long time ago, but w
both my sisters (and Nigel, my bro
just putting up with me in general.

This PhD involved work over a f
number of colleagues and frien
technical expertise and friendship,
impossible. Past PhD students inc
Lorna Eades, Dr Birgitte Muller,
Special thanks to the latter for his
nights in the lab – it was nice to kno

Always available with advice, and
broke was Dr Rhodri Thomas, with
taken twice the time, and to whom I

CONTENTS PAGE

LIST OF FIGURES

Chapter 2

Chapter 3

Chapter 4

Chapter 5

Chapter 6

LIST OF TABLES

Chapter 2

Chapter 3

Chapter 5

Chapter 1
Introduction

1.1.1 Biogeochemical cycles

The earth can be considered as one giant biogeochemical system (Schlesinger, 1991), within which a number of different components can be identified; including the atmosphere, oceans and surface waters, the geosphere and sediments, and the biosphere (Figure 1.1). These individual components are linked by a number of complex reactions and the entire system is maintained in a state of dynamic equilibrium. The equilibrium is dependent on the size and direction of the fluxes between the various reservoirs or pools (Oeschlager, 1992).

1.1.2 The nature and definition of pollution

Pollution can be defined as "the introduction by man into the environment of substances or energy liable to cause hazards to human health, harm to living resources and ecological systems" (Holdgate, 1979). With recent advances in the understanding of biogeochemical cycles and technological advances in analytical chemistry, it is now possible to measure pollutants at much lower concentrations in the atmosphere, water, and other environmental materials. This has enabled the study of materials from all of the planet's diverse ecosystems, to allow investigation of the spread of ubiquitous pollutants.

1.1.3 The chemistry of metals

Some of the most ubiquitous and pervasive pollutants in the modern environment are heavy metals. "Heavy metals" is a generic name allocated to metals with densities greater than 6 g/cm^3, but is more specifically reserved for the toxic metals including cadmium, chromium, copper, mercury, nickel, lead and zinc (Davies and Jones, 1988: Stumm and Morgan, 1988: Alloway and Ayres, 1993).

Metal elements can be classified as belonging to one of three groups, essential macronutrients, trace metals and essential micronutrients and toxic heavy metals.

Figure 1.1 – Some biogeochemical cycles of metals

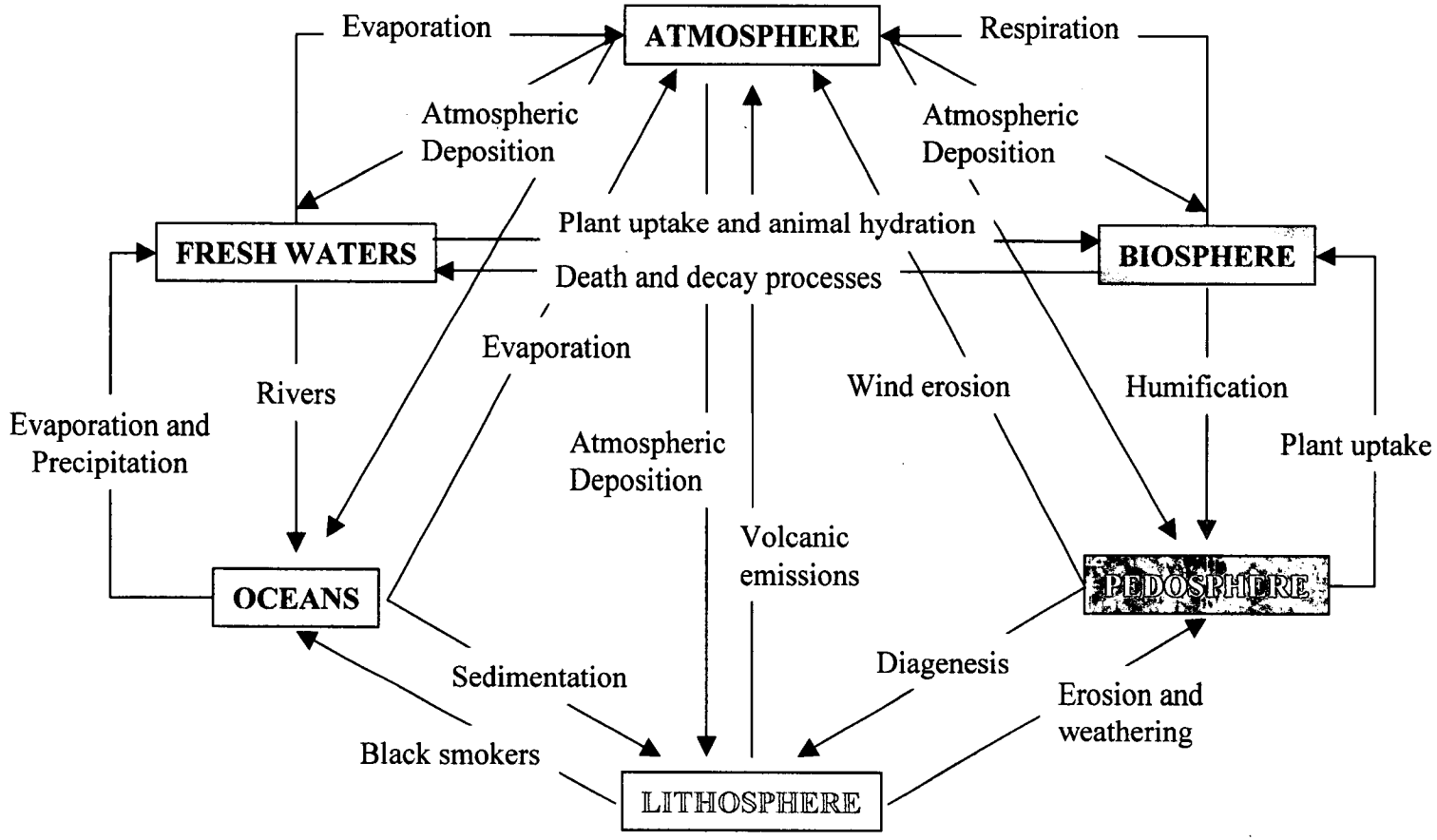

1) Essential elements are those which are essential for life and include carbon, hydrogen, oxygen, nitrogen, sulphur, phosphorus, potassium, calcium and magnesium (Manahan, 1994)
2) Micronutrients (or essential trace elements) are required in small concentrations for metabolic reactions or enzymes. Recognised trace elements include copper, iron, manganese, zinc, and boron (Wild, 1988; Manahan, 1994).
3) Toxic elements can be defined as "harmful to living organisms because of detrimental effects on tissues, organs or biological processes" (Manahan, 1994).

In reality the divisions between the three classes is very difficult to make. Firstly, the very low concentrations of elements, and the very narrow range of concentrations to which living organisms are exposed, necessarily require highly sensitive detection techniques for accurate analysis. Secondly, there is a lack of understanding of the exact role of many trace elements in the human body and living organisms generally, and although an element may be essential for plants, it can be toxic for humans and animals that consume the plant.

1.1.4 Soft and hard metal cations

Another aspect of metal toxicity is the chemical form of the element and the type and intensity of bond formed with organic and inorganic ligands. Pearson (1963), classified metals cations into hard or soft acids and ligands into hard or soft bases (Stumm and Morgan, 1988, Manahan, 1994, Langmuir, 1997). According to Pearson, cations are Lewis acids (proton donors) and ligands are Lewis bases (proton acceptors). "Soft" refers to the cation's electron cloud, allowing easy movement of electrons. The readily polarised nature of soft cations results in the formation of covalent bonds. "Hard" cations, conversely, can be regarded as being rigid, less able to share electrons and more likely to participate in ionic binding (Langmuir, 1993). Likewise, ligands can also be classified as being soft or hard. In general, hard acids are more likely to form bonds with hard bases, and soft acids with soft bases (Stumm and Morgan, 1991). Oxygen and phosphorus ligands are hard bases and have higher affinities for the hard acids, which include sodium, magnesium, calcium, barium, aluminium, titanium, manganese and iron cations.

Sulphur and nitrogen containing ligands are soft bases and more readily form bonds with soft acids (including cadmium and mercury cations), and borderline acids (including copper, lead, and zinc cations: Table 1.1).

Table 1.1A – Classification of hard, soft and intermediate acids (Stumm and Morgan, 1988)

"Hard" Acids	"Intermediate"Acids	"Soft" Acids
Na^+, K^+, Mg^{2+}, Ca^{2+}, Sr^{2+}, Ba^{2+}, Al^{3+}, Ti^{4+}, Fe^{3+}, Mn^{3+}	Cr^{2+}, Mn^{2+}, Fe^{2+}, Co^{2+}, Ni^{2+}, Cu^{2+}, Ti^{2+}, Zn^{2+}, Pb^{2+}	Cu^+, Ag^+, Au^+, Cd^+, Hg^+,

Table 1.1B – Relative affinities of ligands (bases) for hard and soft acids

Ligands binding to Hard acids	Ligands binding to Soft acids
F > O> N=Cl > Br >I > S	S > I > Br > Cl=N > O > F

The ultimate controlling factor on an element's toxicity is the abundance of the element within the biosphere, itself dependent on the abundance of the element within crustal rocks. The concentration of the element in the biosphere is determined by subsequent release through weathering reactions of minerals (and ore bodies), and volcanism.

1.2. NATURAL OCCURRENCES OF METALS AND USES

Metal ores and minerals occur in the three major types of rocks present at the Earth's surface, namely igneous, metamorphic and sedimentary. The most abundant elements at the Earth's crust are the macro-elements (oxygen, silicon, aluminium, iron, calcium, sodium, potassium, magnesium, titanium, hydrogen, phosphorus and sulphur), which comprise 99% of the Earth's crust. Trace elements occur as impurities in the crystal structures of many primary and secondary minerals through substitution. The source minerals for a selection of elements analysed in this study, including macro-elements, trace elements and heavy metals are discussed below, in alphabetical order. Values for the abundance of elements in the continental crust are taken from Wedepohl (1995), who assumed an average composition of the upper continental crust approaching that of granodiorite.

1.2.1 Aluminium (Al) is the most plentiful metal in the Earth's crust (7.96% by weight), and is found in many igneous rocks. Aluminium containing minerals include micas and feldspars, which upon weathering give rise to secondary minerals. Common secondary minerals in temperate regions are vermiculite, montmorrillonite, and kaolinite. It also occurs in many rare minerals including garnet, beryl and turquoise, and gemstones such as emerald, ruby and sapphire. The most important mineral in terms of economic recovery of aluminium metal is bauxite [$AlO_x(OH_{3-2x})$], which is formed from the weathering of aluminosilicate minerals in sub-tropical and tropical regions. Aluminium and its alloys are used in the construction industry; aeroplane, car and bike manufacture, foil and food wrappings, and cans for beer and soft drinks.

1.2.2 Barium (Ba) has an abundance of 584 ppm in the earth's crust, and the most important mineral is the sulphate (barite), which is extensively used in drilling and oil production, because of its high density (barytes in Greek means heavy). As such, it is regarded as a strategically important mineral.

1.2.3 Calcium (Ca) is the third most abundant metal in the Earth's crust, having an abundance of 3.85%. The major form of calcium in the crust is in $CaCO_3$, formed from the deposition of shells of foraminifera and other marine animals. Other important calcium minerals are the sulphate (gypsum) and the fluorite ("blue john"), and the phosphate (apatite). Calcium in the form of limestone has long been used in buildings as building stones or mortars, and on soils as a method of neutralising acidity by liming (Greenwood and Earnshaw, 1997).

1.2.4 Copper (Cu), one of the earliest metals known to man, was extensively used by early civilisations in coinage. It has an average concentration of 25 ppm in the crust and occurs mainly as the sulphide (e.g. chalcocite, Cu_2S), oxide (cuprite, Cu_2O), and carbonate (e.g. malachite $Cu_2CO_3(OH)_2$). The major ore that is mined is chalcopyrite, ($CuFeS_2$). The main use of copper is as an electrical conductor, but its alloys bronze (Cu-Sn) and brass (Cu-Zn) are still in use as coinage.

1.2.5 Iron (Fe) is the second most abundant metal in the crust (4.32%) after aluminium. Man first smelted iron in Asia as early as 3000 B.C., and the wide-scale spread of the technology led to the period of history known as the Iron Age. Because of iron's high inventory it is present in many minerals, including haematite (Fe_2O_3), magnetite (Fe_3O_4), siderite ($FeCO_3$), and pyrite (FeS_2). Iron is the most mined metal, and is used in the production of about 700 Mt of steel each year (Greenwood and Earnshaw, 1997).

1.2.6 Magnesium (Mg) abundances in crustal rocks vary, but an average value is 2.20%, making magnesium the fourth most abundant metal on the planet. The major source of magnesium is dolomite [$MgCa(CO_3)_2$], but it also occurs as a carbonate (magnesite) and a sulphate (epsomite). Magnesium is also present in silicates (olivine), and is an important constituent of asbestos and mica. Magnesium alloys are important in the manufacturing of car engines and aeroplane bodies (Greenwood and Earnshaw, 1997).

1.2.7 Manganese (Mn) is the 12th most abundant element (716 ppm) in the crust, and is found in a variety of primary silicate minerals. Economic minerals are secondary manganese oxides, weathering products of the primary minerals. Manganese nodules of a very high purity have also been discovered on the seabed, close to hydrothermal vents. Economic minerals include the oxide pyrolusite (MnO_2) and the carbonate rhodochrosite ($MnCO_3$). Manganese is a very important constituent in steel production, and in certain non-ferrous alloys.

1.2.8 Phosphorus (P) is an important element in so much as it is an important ligand for metal cations. Phosphorus has an average crustal concentration of 757 ppm. In rocks, phosphorus exists exclusively as phosphate, with the most important minerals comprising the apatite family. The most common members are fluorapatite [$Ca_5(PO_4)_3F$], chloroapatite [$Ca_5(PO_4)_3(OH)$] and hydroxyapatite [$Ca_5(PO_4)_3OH$]. World production of rock phosphate was 151 Mt in 1985. Phosphorus is an essential element because of its role in RNA and DNA, as well as ATP production, and bone

It is often a growth-limiting element, because to be available to plants it has to be in solution and under normal soil conditions, it forms insoluble metal precipitates. The major usage of phosphorus is in fertilisers.

1.2.9 Potassium (K), with a crustal abundance of 2.14%, is the sixth most common crustal metal. Potassium, in contrast to sodium, is strongly bound to complex silicates and when released through weathering is readily taken up by plants because of its role as an essential nutrient. The major use of potassium is in soil fertilisers, but it is also used in detergents, rubber manufacture and as oxidising agents for use in the manufacture of explosives.

1.2.10 Sodium (Na) with an abundance of 2.36% is the fifth most plentiful metal in crustal rocks. Sodium primarily occurs as a chloride, halite or rocksalt, with the formula NaCl. Economically viable deposits form from dried up seas and lakes (Greenwood and Earnshaw, 1997). The size of the sodium ion limits complexation in plants and soils, and its high solubility enables it to build up in seawater. The major use of sodium is in the production of alkalis, road salts, food processing, and the paper, textile, rubber and oil industries.

1.2.11 Strontium (Sr) has an average concentration in Earth's crust of 333 ppm (0.033%). The main strontium minerals are the carbonate (strontianite) and the sulphate (celesite). The main uses of strontium are in the manufacture of computer monitors and TV screens, and for firework production (Greenwood and Earnshaw, 1997).

1.2.12 Sulphur (S) is another essential element, and is very important as a ligand for metal cations in both the reduced (sulphide) and oxidised (sulphate) form. It is also an essential element (Wild, 1988), having an important role in many biological enzymes. Sulphur has been used since antiquity as a medicine and in explosives, and is now used in rubber manufacture (vulcanisation). Major deposits of elemental sulphur are associated with active volcanoes, and it is often found in economic quantities as a caprock for salt domes, where deposits form through anaerobic reduction of sulphate minerals (e.g. gypsum).

1.2.13 Titanium (Ti) has an average crustal concentration of 4010 ppm, and is associated with two minerals, rutile (TiO_2), and illmenite ($FeTiO_3$). These oxide minerals are very stable and highly resistant to weathering. Titanium alloys, used mainly in the aerospace industry, are among the strongest materials known to man.

1.2.14 Zinc (Zn) is another metal used since ancient civilisations, in brass. It has an abundance of 65 ppm in average crustal rock. The main minerals are ZnS (sphalerite), and $ZnCO_3$ (smithsonite). Zinc's major industrial use is as a coating to prevent rusting (galvanising), and in alloys in batteries (Greenwood and Earnshaw, 1997).

1.3 LEAD

1.3.1 Natural occurrence of lead

Lead (Pb) is one of the most abundant heavy metal, with three of the four isotopes (^{206}Pb, ^{207}Pb, ^{208}Pb) being the final product of the radioactive decay of ^{238}U, ^{235}U and ^{232}Th respectively. The isotope ^{204}Pb is termed primordial lead, as it is not produced through radioactive decay, and is a measure of the original concentration of Pb formed early in the universe. The other three isotopes are continually produced from the breakdown of ^{238}U, ^{235}U and ^{232}Th, respectively. The rate of production of the three radiogenic isotopes (^{208}Pb, ^{207}Pb and ^{206}Pb) is dependent on the half-lives of the intermediates in the radioactive decay series (Figure 1.2).

1.3.2 Evolution of lead isotopes

Prior to the crystallisation of the Earth, lead, uranium and thorium existed in uniform proportions throughout the molten planet, and therefore the abundance of lead isotopes was uniform. Upon the beginning of fractionation and crystallisation of the Earth's upper mantle, the three elements were fractionated between the liquid silica melt and the molten mantle. With time, the silica melt crystallised to form minerals and rocks consisting the Earth's crust. The fractionation processes changed the relative ratio of U, Th and Pb, within the various minerals and rocks, which affected the subsequent isotopic ratio of lead within rocks and minerals.

Figure 1.2 – Diagram of the radioactive decay series for ^{206}Pb, ^{207}Pb and ^{208}Pb

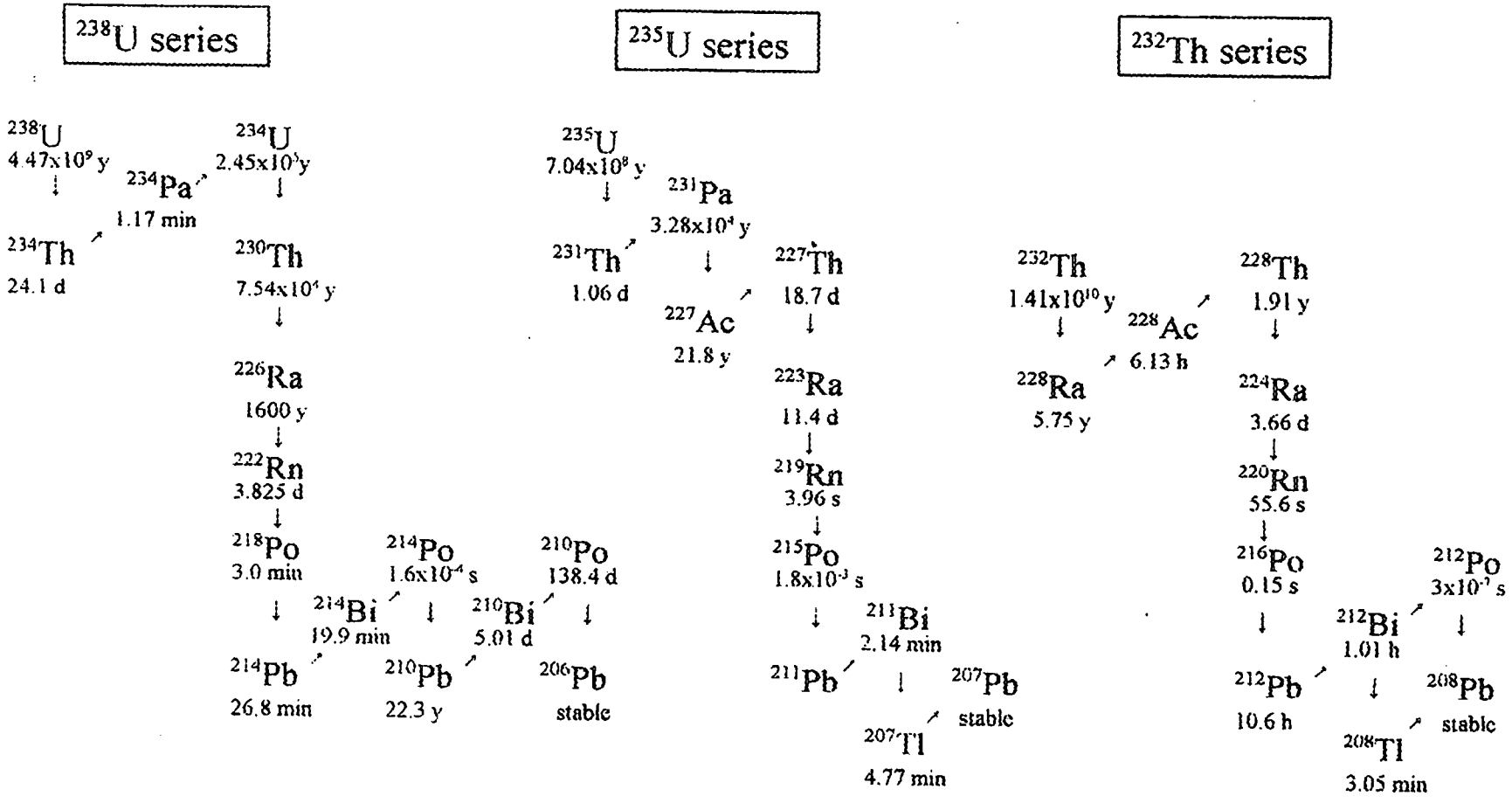

Lead occurs as a trace element in many different rocks, but the major economic mineral containing lead is galena (PbS). Other important minerals include the sulphate anglesite ($PbSO_4$), the carbonate cerrusite ($PbCO_3$) and the phosphate pyromorphite [$Pb_5(PO_4)_3Cl$], which are generally formed from the weathering of galena.

Massive sulphide deposits, composing the bulk of the world's economic deposits of lead contain very little uranium and thorium, due to the processes resulting in the formation of these ore bodies. Galena (PbS) crystallisation generally "fixes" the isotopic composition of lead within the mineral. In ore bodies formed more recently, lead has existed in secular equilibrium with the parent species for a longer period of time, with the result that the concentrations of ^{206}Pb, ^{207}Pb and ^{208}Pb have increased, relative to primordial ^{204}Pb (Figure 1.3). Due to the different rates of decay of the intermediates in the formation of ^{206}Pb, ^{207}Pb and ^{208}Pb the proportion of the three isotopes compared to the original mixture will change with time. More radiogenic lead ore bodies (containing higher relative proportions of ^{206}Pb, ^{207}Pb and ^{208}Pb from the radioactive decay of ^{238}U, ^{235}U and ^{232}Th) are indicative of more recent crystallisation, whereas the less radiogenic ore bodies were formed further back in geological history.

1.3.3 Lead ore genesis and formation

Economic deposits of lead are mostly associated with massive sulphide deposits, which form in different geologic environments. The general mechanism of formation is the same, involving circulating waters, either seawater in the case on the Troodos Mountain ophiolite complex, or continental meteoric waters in the case of the Mississippi Valley deposits, (Hoefs, 1997). The waters circulate through fractures in the Earth's crust generated in extensional regimes, and as the water circulates, it is heated either by local magmas (in the vicinity of volcanoes) or due to the pressure and temperature associated with the depth of circulation. As the waters become heated, anhydrite (MgOH) precipitates, acidifying the waters. The acid solutions then preferentially leach out the larger trace elements from surrounding country rock. The supersaturated solutions are convected towards the surface and the metals are deposited in disseminated forms in the host rock, or in the case of black smokers are deposited on the seabed.

Figure 1.3 – Diagram showing the evolution of lead isotopes in different ore bodies through time

At time t = 0, relative proportions of ^{204}Pb, ^{206}Pb, ^{207}Pb and ^{208}Pb are shown below;

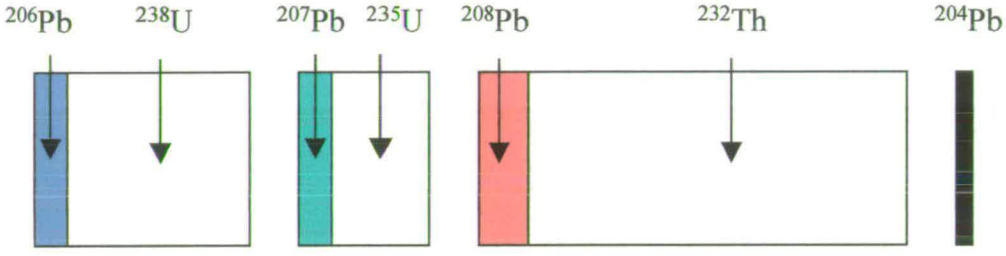

At time t = 1, relative proportions of ^{204}Pb, ^{206}Pb, ^{207}Pb and ^{208}Pb are increasingly different, with the evolution of ^{206}Pb, ^{207}Pb and ^{208}Pb from the decay of parent radionuclides.

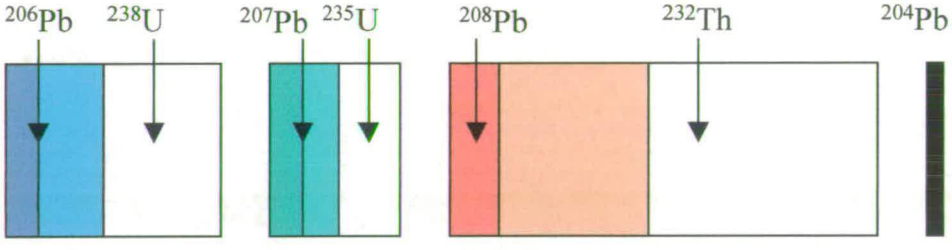

where the darker shaded areas = original concentration at time t=0, and the lighter shaded areas = concentration of isotope evolved from decay of the parent radionuclide. At time t = 2, the relative proportions of ^{204}Pb, ^{206}Pb, ^{207}Pb and ^{208}Pb are considerably different.

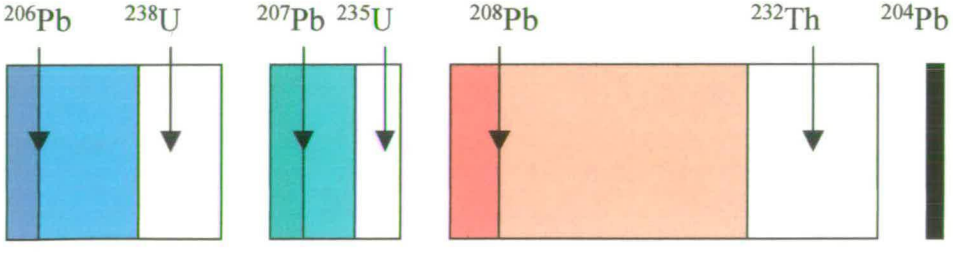

The largest silver, copper, lead and zinc mines are associated with the deposits, and the economies of scale ensure that most of the lead mined today is from one of the very small number of these massive sulphide deposits. By analysing the isotopic "fingerprint" of lead across the globe, the influence of anthropogenic lead (derived from these large ore bodies) can be clearly distinguished from locally derived "natural" lead, (Chow and Earl, 1975). Examples of different isotopic ratios of lead from different ore bodies are given in Table 1.2.

Table 1.2 – Different $^{206}Pb/^{207}Pb$ ratios in galena derived from different orebodies

Name of ore body	Location	206Pb/207Pb ratio
Broken Hill Mt Isa	Australia	1.04
Mississippi Valley	U.S.	1.281-1.396
British Columbia	Canada	1.16
Rio Tinto	Spain	1.164

1.3.4 The toxicity of lead

The Agency for Toxic Substances and Disease Registry in Atlanta (ASTDR) together with the U.S. Environmental Protection Agency (EPA) has ranked toxic substances according to three criteria;

1) Frequency of occurrence at contaminated sites
2) The toxicity of the substance
3) The potential for human exposure

Lead is currently ranked number one on the list. Despite the phasing out of leaded paints, lead in paint remains a threat, with 21 million pre-1940 homes in the U.S. having leaded paint (ATSDR, 1992). Lead is also present in drinking waters, from dissolution of lead solder and pipes used in domestic plumbing.

Lead in soils is derived from the deposition of atmospheric lead (see below) as well as impurities in fertilisers and sewage sludge. Most lead in runoff and rivers is in an insoluble form in colloids (EPA, 1986).

Almost all of the lead inhaled enters the blood, but very little of ingested lead enters the blood through the gastrointestinal tract. The lead in blood generally ends up in soft tissues (brain, kidneys, liver and bone marrow) or mineralising material (bones and teeth). The concentration of lead in bones and teeth is related to the time of exposure, with concentrations increasing with age. Lead in bones exists in two components, a labile component which is in equilibrium with the blood, and an inert form. Even after exposure has finished, and the blood lead level decreases, there is potential for the remobilisation of inert lead from the bones, further exacerbating exposure.

In children, much more of the lead ingested lead is transferred to the blood. A condition exists in some young children known as "pica", where the child places soil and other objects in its mouth (ATSDR, 1988). In children younger than 36 months, the brain blood barrier is insufficiently developed and lead enters the brain, where it can cause neurological effects, and decreased IQ. Children are more likely to have iron and calcium deficiencies and lead in blood will exacerbate anaemia. Other health effects are decreased mental and physical development and decreased levels of Vitamin D. Long-term exposure in both children and adults can lead to more intrinsic health problems including behavioural changes and fatigue, anaemia, and a greater risk of developing cancer (ATSDR, 1992).

1.3.5 Natural sources of lead

Unlike the anthropogenic signature of lead used in industry, which is sourced from the larger lead ore bodies, "natural" lead is also emitted into the atmosphere, from a whole range of different sources. This natural lead component can exhibit similar isotopic ratios ranges to the anthropogenic component. Examples of the varied sources of natural lead are shown below in Table 1.3.

Table 1.3 – World natural sources of atmospheric lead (based on Nriagu, 1989)

Source of natural lead	Median estimated Pb emitted in 1988 (Mt/yr)
Aeolian soil particles	3.9
Seaspray	1.4
Volcanic eruptions	3.3
Forest Fires	1.9
Biogenic sources	1.7
Total	**12.2**

1.3.6 The history of anthropogenic lead pollution

Lead has been exploited by man since antiquity. Lead was first released into the atmosphere through anthropogenic activities about 4500 yr BP, when the technology for smelting lead sulphide ores was developed in Southwest Asia (Patterson, 1971). Studies of lead in the bones of different human civilisations through time has revealed a relationship between the average concentration of lead in the body and the age of the bones, with the highest concentrations found in humans living in the recent past (Grandjean and Holma, 1973; Jaworoski, 1968).

Lead was used by the Egyptians for glazing pottery (Greenwood and Earnshaw, 1997), and by the Romans in water pipes and drinking cups, and lead acetate ("sapa") was used to sweeten wine. The direct route of exposure together with the extensive usage has been postulated as one of the causal factors in the decline of the Roman Empire (Nriagu, 1983a).

1.3.7 Modern uses of lead

The major use of lead currently is in alloys in batteries, from which most of the lead (70%) is recycled. Lead is still used in some countries as an antiknock agent (tetra methyl-lead and tetraethyl-lead) in petrol, although in most western countries legislation has been introduced to curb this usage.

For example, in the U.S. (the first country to reduce lead in petrol), the maximum permitted concentration dropped from 0.52 g/L to 0.28 g/l in 1982, to 0.026 g/l in 1989 (Nriagu, 1990), and leaded petrol was phased out in 1990. Canada started phasing out lead in 1988, and had completed by 1992 (Pacyna *et al.*, 1995). In the UK, the amount of lead permitted in petrol was reduced from 0.40g/l to 0.15g/l in 1986, and this along with increased promotion of unleaded petrol, achieved a reduction in atmospheric lead derived from petrol from 6500 tonnes in 1985 to 800 tonnes in 1997 (DETR, 1998). In Europe, Austria was the first country to ban lead in petrol in the 1990's, closely followed by Sweden and Germany, with the UK and France banning lead in petrol by 2000 (Rosman, 2001). Nriagu (1988) investigated the various sources of atmospheric lead pollution, and the results are presented in Table 1.4 below.

Table 1.4 – World anthropogenic sources of lead (based on Nriagu, 1988)

Source of anthropogenic lead	Median estimate of Pb emitted in 1983 (Mt/yr)
Coal combustion	8.4
Oil combustion	2.4
Non-ferrous metals production	49.6
Steel and iron production	7.6
Waste incineration	2.4
Cement production	7.1
Wood combustion	2.1
Other sources	4.7
Petrol lead	248
Total	**332.3**

Lead has also been extensively used in paints, with several different pigments still in use; $PbCrO_4$ is yellow and used in road markings, $PbMoO_4$ is red-orange and $PbCO_3$ is white. In 1991, 3.3 Mt of lead was produced from lead ore, and a further 5.6 Mt of lead was re-smelted from scrap, (Greenwood and Earnshaw, 1997).

1.4 MONITORING PAST AND PRESENT LEAD POLLUTION

Atmospheric lead is mostly associated with small sub-micrometer particulates, and as a result, can be transported long distances and subsequently deposited in many different environments across the globe. Certain environments on Earth can provide an undisturbed intact record of past pollution. The production of these records is described by Oeschleger (1994) as follows: "constant changes or events occur in systems and are often registered in various earth materials as deposits, layers or growths in time-unit increments on either a local regional or global basis. The recognised global sources of paleo-environmental information include sediments, lake and bog deposits, tree-rings, periglacial features and snow and ice deposits".

1.4.1 Use of enrichment factors to quantify pollution

Zoller *et al.* (1974) introduced the concept of enrichment factors to quantify the amount of pollution. The enrichment factor for an element is calculated from the following equation;

$$EF = (C_{x,p} / C_{Al,p}) / (C_{x,c} / C_{Al,c}), \qquad \text{Equation 1}$$

where $C_{x,p}$ is the concentration of element in sample,

$C_{x,c}$ is the concentration of element in crustal rocks

$C_{Al,p}$ is the concentration of aluminium in sample

$C_{Al,c}$ is the concentration of aluminium in crustal rocks

Aluminium was used for standardisation because of its relative abundance in the Earth's crust (see above), the relatively inconsequential quantities mined, and its conservative nature, meaning that it is not likely to be present in anthropogenic particulates. The equation above compares the concentrations of the element of interest in the sample to what would be present in the sample from a natural source, in this case weathering of the "average" continental crust. The magnitude of difference is termed the enrichment factor. The samples can also be corrected for inputs from sea spray, using sodium as the conservative element instead of aluminium. This approach is useful in determining the relative scale of anthropogenic inputs relative to natural inputs, for example in ice, but not in situations where the anthropogenic inputs swamp the natural inputs.

The use of enrichment factors is not without its critics (Reimann and De Caritat, 2000) who claim that enrichment factors cannot possibly be used to account for "natural" inputs because there are a number of other factors affecting the composition of naturally derived particulates. The biggest problem is that the relative abundances used are obtained for an average continental crust (see Wedepohl, 1995). However, the composition of the local geology may differ considerably from the assumed average, and not accurately account for localised inputs. There are also physical parameters such as the size, shape and density of the particulates that can affect the transport of particulates, as well as chemical factors such as preferential dissolution of certain elements during atmospheric transportation. Other natural inputs may be derived from volcanic eruptions and have compositions completely different from the crustal average.

A further problem comes from the dissolution techniques employed, with most environmental samples being digested using varying concentrations of nitric and hydrochloric acid. This is problematic in that while almost complete dissolution of the anthropogenic aerosols is achieved, complete dissolution of aluminosilicates is only achieved using HF. Thus, the concentration of elements within the anthropogenic aerosols will be exaggerated relative to the concentration of "natural" particulates.

1.4.2 Pb and other metals in snow and ice

Many researchers have attempted to determine temporal trends in lead (Pb) concentrations in snow and ice from a variety of locations. The following section will summarise the most important papers, together with relevant method developments and findings.

Early work on using snow from glaciers suffered from low sensitivity, contamination of samples and poor location. Analysis of continental glaciers was complicated by the presence of large amounts of terrestrial dust. Changes in anthropogenic concentrations of Pb (and other heavy metals) can only be interpreted if the concentrations of Pb and other elements in sea spray and terrestrial dust have been determined. Otherwise, changes in Pb concentration within the ice can wrongly be attributed to changes in pollution when they may in fact result from an increase in lead from natural sources.

In a landmark study by Murozumi *et al.* (1969), snow and ice samples were collected from hand dug pits at sites in Greenland and Antarctica, to avoid both problems of terrestrial dust and contamination from drilling the cores. At Camp Century in Greenland, the samples collected were dated at 1753 to 1965. Pb concentrations in the oldest samples were estimated to have concentrations 25 times greater than background lead (0.001μg/kg), which was determined on ice at the base of the glacier exposed near the coast at Thule and dated at 2800 years old. The concentrations tripled between 1753 and 1815, and further increased by a factor of 3 between 1933 and 1965 to values >0.2 μg/kg. The changes in Pb concentrations (relative to natural levels) in Antarctic ice from New Byrd station were not as significant, with pre- 20^{th} C values being close to detection limits, with an estimated 100-fold increase to levels of 0.02 μg/kg between the beginning of the 20^{th} C and the sampling date in 1965.

Later studies on Arctic and Antarctic ice, (Craigin *et al.*, 1975; Herron *et al.*; 1977), failed to reproduce the trends found by Murozumi and colleagues. In these later studies, general increases were detected, but there was a failure to find the trend of massively increasing lead prior to the 20^{th} C.

Ng and Patterson (1981) argued that, because most of the studies had used drilling to obtain the cores, the ice had become contaminated with traces of oil seeping through to the innermost parts of the cores, effectively raising the concentrations.

Boutron and Patterson (1993) concluded in their study of lead in Antarctic ice that selected contamination of core samples had occurred through partial melting, allowing outside contamination to enter the centre of the core. Some of the fluctuations in lead in the Southern hemisphere reflected natural lead sources, such as exceptional volcanic eruptions (e.g. Krakatoa and Soufriere Hills), as well as anthropogenic inputs, and thus in the southern hemisphere the inputs of anthropogenic lead were less obvious.

Further samples were collected from Greenland, which were analysed for copper, cadmium, and zinc as well as lead, and the results published by Boutron *et al.* (1991).

The samples collected represented a sequence from the 1960's to the 1990's. The concentrations of the heavy metals were normalised against aluminium for terrestrial sources and sodium for sea spray. This normalisation showed that all of the copper was accounted for by natural component inputs, but that the inputs of lead and cadmium, and, to a lesser degree, zinc inputs from these sources were negligible. The other major finding was that the concentrations of all three anthropogenically derived heavy metals had decreased by a factor of 7.5 since 1967, following the introduction of legislation in the 1970's to curb the emissions of these metals to the atmosphere.

Candelone *et al.* (1995) analysed sections of a 70.3 m deep core representing 220 years of snow accumulation at Summit in Greenland. Prior to the Industrial Revolution, concentrations for zinc, cadmium and copper did not show any significant increase in concentration relative to ancient ice. However, this was in marked contrast to the lead concentrations that were already an order of magnitude greater than natural lead concentrations by the late 18^{th} C, highlighting the length of time that humans have been polluting Earth's natural environment

Later studies on Arctic and Antarctic ice concentrated on the use of lead isotopes to identify the source of the lead deposited. The lead was attributed to different sources, as the lead isotopic "fingerprint" of the ice can be used to assess the changing source of the lead. Rosman *et al.* (1993) analysed sub-samples of cores collected by Boutron *et al.*. (1991). The $^{206}Pb/^{207}Pb$ isotopic ratios for 25 snow cores representing snowfall between 1968 and 1988 showed a trend of increasing values up until the early 1980's. This was attributed to increased use of the Mississippi valley lead ore, with more radiogenic values, in petrol additives reflected by the increasing ratio (Table 1.4).

In Antarctic ice, despite relatively low concentrations of in lead in recent snow, the isotopic ratio was significantly less radiogenic than lead in ice form 7500 y BP, proving the anthropogenic influence of lead in Antarctic snow and ice.

The full capabilities of using isotopes was realised in a further paper by Rosman *et al.* (1997), in which the isotopic composition of lead in ancient Greenland ice (from 600 BC to 300 AD) was determined. The relative contributions of lead from each of the mining areas to the total lead in the ice, was assessed using a plot of $^{206}Pb/^{207}Pb$ against $^{208}Pb/^{207}Pb$. These lead isotopic ratios were obtained for lead from the Greek Laurion mines, the British lead mines in Cornwall, Devon, and the Mendips, the German lead mines in the Harz region and finally the massive sulphide deposits of the Southern Iberian Pyrite Belt, including Rio Tinto. Isotopic data were also obtained for Saharan sand, to assess natural inputs. By comparing the sample plots with the plots of known mined areas, the relative contribution of lead to the ice was assigned to each of component areas. Three principal components were identified, a small contribution of natural lead from Saharan dust, a major contribution from the Rio Tinto mine, and a lesser contribution of more radiogenic lead from the other Spanish mines.

More recently, research has switched from Arctic and Antarctic quiescent ice sheets to localised glaciers, e.g. Alpine glaciers (Van der Velde *et al.*, 1998, 1999; Hesterkamp *et al.*, 1999; Rosman *et al.*, 2000) and Canadian glaciers (Cheam *et al.*, 1998; Simonetti *et al.*, 2000). These studies have found similar trends to those observed in the Arctic and Antarctic, with higher concentrations reflecting the proximity to the sources of lead pollution.

In Mont Blanc snow and ice (Hesterkamp *et al.*, 1999), decreasing concentrations of lead and organo-lead complexes, along with changes in the lead isotopic signature at the near surface, reflected the recent phasing out of leaded petrol in Europe.

In a traverse of snowpack from the St Lawrence valley in Canada (Simonetti *et al.*, 2000), the measured lead concentrations were 5 to 10 times higher than those found in Greenland snow for the same period. The highest concentrations of lead, unsurprisingly, were found in the vicinity of the Noranda smelting plant. Enrichment factors for lead (relative to aluminium) were calculated at 370 for the Montreal-Quebec transect, rising to 800 for the North –South transect (closest to Noranda).

The lead isotopic ratios did not plot between the two component sources, namely Canadian lead and U.S. lead, suggesting that there exists a third component, which was proposed to be air masses originating in Eurasia and traversing over the top of the Arctic.

1.4.3 Pb and other metals in lake sediments

One drawback in the use of lake sediments to study anthropogenic inputs is that, unlike the situation in snow and ice, where the only inputs are atmospheric, lakes receive sedimenting material from the surrounding catchments. Both the natural and anthropogenic content of this material can obliterate the anthropogenic signal from direct atmospheric deposition, and in many cases, the localised inputs may reflect reworked sediments, creating a time lag in the anthropogenic signal detected in the sediments. There is also the problem of distinguishing the anthropogenic lead from the total lead. A number of different approaches have been adopted to overcome these difficulties, and this work is summarised below, with the most important and relevant findings.

To avoid the associated problems of sampling snow from continental interiors, Shirahata *et al.* (1980) studied sediments deposited in a remote sub-alpine pond, in Thomson canyon in Yosemite National Park. The sediments were laid down in anoxic conditions (minimising bioturbation of the sediments). The polluted nature of the region, coupled with high sedimentation rates ensured that annual trends of pollution were easily identifiable. ^{210}Pb analysis allowed dating of the annual layers, and identification of nuclear fission products within the layers supported the dating procedure. The changes in isotopic ratio were independent of the lead concentrations, and showed the increasing influence of the Mississippi Valley ores with a $^{206}Pb/^{207}Pb$ ratio of 1.28-1.33, (Table 1.4) in the uppermost two decades of sedimentation of the core. The $^{206}Pb/^{207}Pb$ ratio rose from 1.15 in 1967 to 1.20 in 1974, and 1.23 in 1977.

In a similar manner, Ritson *et al.* (1994) used lead isotopes to trace the historical contamination of Lake Erie. Unlike the sub-alpine pond, Lake Erie had received considerable inputs of anthropogenic lead prior to the introduction of lead in petrol, which was ascribed to coal burning and localised smelting operations. The more recent increases in the isotopic ratios were the result of lead additives to petrol. However, with the reduction of this component following the introduction of the Clean Air Bill (see earlier), the dominant source was shifting from petrol lead to coal burning. Most important perhaps, was the recognition that the lead isotopic composition is more sensitive than lead concentrations to the introduction of anthropogenic lead, because of two factors

1) there is a much smaller analytical error associated with the isotopic composition, and
2) the natural isotopic composition at any one site is more constant than either natural lead concentrations or elemental ratios (e.g. normalising using Pb/Al).

In another study on lead in the Great Lakes, Graney *et al.* (1995) conducted further work to differentiate anthropogenic lead from "natural" lead. In the sediment cores from the Great Lakes, observed lead concentrations were constant prior to 1860, and this lead was deemed "natural" in origin. Pre-1890 isotopic ratios in the lakes were not entirely consistent, with slight differences reflecting the slightly different geology surrounding each of the lakes. Changes in the lead isotopic ratios, firstly due to lead from Pennsylvanian coal, and secondly due to lead from the Missouri lead which was used to manufacture petrol lead additives, were observed. An important observation was that the anthropogenic lead in the sediments was more extractable by acid leaching than the natural lead within mineral lattices.

Further work on lake sediments closer to home in Sweden was conducted by Renberg *et al.* (1994). In this study, long sediment cores were taken from 19 lakes in southern and eastern Sweden. The ^{14}C determined age of some of these cores was > 3000 years. The major finding (analogous to that of Rosman *et al.*, 1997) was that increases in lead concentrations above "background" levels occurred 2600 BP, long before the Industrial Revolution.

The increases in lead concentrations in lake sediments were synchronous across Sweden, illustrating that the lead was not locally derived but more probably the result of long-range transport. One suggested origin was the mining and smelting of lead by the Romans, and this hypothesis agrees with later hypotheses to explain the similar trend of lead contamination of Greenland ice.

Von Gunten *et al.* (1997) collected a 40 m core from sediments in Zurich See, Switzerland. The concentration trends for lead show that a considerable increase occurred in the early 19^{th} C, corresponding to the onset of the Industrial Revolution. The concentrations of lead were elevated and stable from 1920 up to 1975, with the major increase in lead occurring long before the introduction of lead additives to petrol in the 1940's. Von Gunten *et al.* concluded that the predominant source of lead to the Zurich See was not from petrol lead but rather from locally derived industrial lead, and that reductions in "industrial" lead occurred in tandem with increased lead deposition from petrol lead. A chemical plant on the shore of the Zurich See was shown to be the probable source of the early lead contamination, with the decrease in lead concentration after 1975 resulting from decreases in lead in petrol and greater restrictions on vehicular traffic.

Lead isotopic ratios were determined on sediments from Lake Geneva by Monna *et al.* (1999), using a dilute acid to leach out the anthropogenic lead. This methodology was based on the earlier finding of Graney *et al.* (1995), that most of the anthropogenic component of Pb was extractable using dilute acid. Most of the lead added to Swiss petrol is derived from the massive Precambrian lead mines at Broken Hill in Australia and British Columbia in Canada (Doring *et al.*, 1997). In contrast to the situation in the US and Canada, where the petrol lead component has a more radiogenic signature than industrial and natural sources, the lead isotopic signature in Swiss petrol (and European petrol generally) was less radiogenic, with measured values between 1.114 and 1.124 (Table 1.4). The acid leachates for sediments generally produced isotopic ratios slightly lower than the residual material, but the variations in residual ratios suggested that not all of the anthropogenic lead was released by the leaching process.

The leachate fraction was assumed to include lead desorbed from iron, manganese and aluminium oxyhydroxide surfaces, as well as lead carbonates and lead bound to the organic matter. The overall picture was one of relatively radiogenic $^{206}Pb/^{207}Pb$ ratios of 1.17 in sediments from the early 20th C, decreasing in the 1930s and 1940s to ~1.15, with a further decrease to 1.14 occurring in the 1970s. Contrary to the situation in the Zurich See, the isotopic changes correspond to the increased usage of imported ores and coals in the late 1930s/early 1940s and the increased proportion of petrol derived lead in pollution with the expansion in vehicular traffic in the late 1960s/early 1970s.

Following on from earlier work, Branvall *et al.* (1999) analysed varved Swedish lake sediments for lead isotopes. The production of the varves (a light coloured layer deposited in the summer, and a dark layer deposited following snow and ice melt) allowed easy identification of individual annual layers, and facilitated easy dating of the sediments. Natural $^{206}Pb/^{207}Pb$ ratios for the region averaged 1.53, with values much higher than observed in other studied locations (normally ~1.20).

The $^{206}Pb/^{207}Pb$ ratios in the lower sections of the cores varied little between 1.45 and 1.55. This supports earlier findings of a natural origin for lead in the lower sections (pre 500 BC) of the sediments (Renberg *et al.*, 1994). Pronounced declines in $^{206}Pb/^{207}Pb$ values to 1.40, were observed at 0 AD, and this was attributed to Greek and Roman mining and smelting of lead, in agreement with findings from elsewhere (Rosman *et al.*, 1997, Renberg *et al.*, 1994). The decline of these civilisations was marked by an increase in isotopic ratios to more radiogenic "natural" values. Between 900 and 1200 AD, marked increase in lead concentrations were matched by a lowering of the $^{206}Pb/^{207}Pb$ ratio to 1.35, illustrating rapid increases in lead pollution. Reduced lead concentrations with concomitant increases in $^{206}Pb/^{207}Pb$ in the Dark Ages (1200-1400AD) were attributed to reduced mining across Europe. Peaks in lead concentrations were observed in the 1500s coupled to a peak in lead mining and smelting in Europe. The lowest $^{206}Pb/^{207}Pb$ values of <1.3 were observed in sediments ~1970. Due to the much higher $^{206}Pb/^{207}Pb$ values of the natural lead in this region, (determined by the geology), the final isotopic ratios reached in the sediments are still much more radiogenic than those reported in other studies (see above).

The important factor is that the decrease in $^{206}Pb/^{207}Pb$ ratio in this locale was observed occurring in the same time scale (middle to late 20th C) as the decrease in other studies.

A further study warranting inclusion in this section and the most relevant for this project was the study of lead isotopes in Loch Lomond by Farmer *et al.*, (1996). Loch Lomond, the largest freshwater loch in Britain, is situated 30 km to the northwest of Glasgow. Three distinct trends in excess lead in the sediments were identified, based on lead isotopic ratios and concentrations in the sediments. Lead concentrations and isotopic ratios were relatively stable prior to the early 19th C. Between 1817 and 1929, the flux in excess lead increased considerably while the isotopic ratio remained stable. In sediments deposited since 1929 (the introduction of lead additives in petrol), the flux of lead remained high, and the isotopic ratio decreased due to the use of Australian and Canadian Pb in the manufacture of lead isotopes (Table 1.4).

1.4.4 Lead in mosses and tree rings

As noted by Oeschlager, records of atmospheric concentrations of lead and other heavy metals are stored within materials with known temporal accumulations, e.g. snow and sediment accumulations. Lead is also stored however, in growing material receiving lead inputs from atmospheric deposition, and is not readily translocated from roots (Wild, 1988). This section will summarise the main research in this field, together with relevant trends identified.

Bacon *et al.* (1996) determined lead isotopic ratios in archived grassland samples from IACR Rothamsted, following earlier determination of lead concentrations (Jones and Johnstone, 1991). The samples analysed represented a sequence commencing in 1856 and running through to the late 1980s. The $^{206}Pb/^{207}Pb$ ratios remained stable at 1.17 up until 1890, and then decreased steadily until a minimum of 1.098 was reached between 1980 and 1985. Importantly, the isotopic ratio decrease started three decades prior to the introduction of lead to petrol, and as with the sediments from Lake Geneva, the introduction of imported (e.g. Australian) ores and coals was proposed to account for these changes. An increase in $^{206}Pb/^{207}Pb$ ratios was observed after 1986, which followed legislation reducing the concentration of Pb in petrol from 0.4 g/L to 0.15 g/L.

Mosses can also be used for identification of temporal trends in lead pollution because they acquire their nutrients solely from atmospheric deposition and rainfall (Rühling and Tyler, 1970). Berg *et al.* (1995) related the concentrations of elements within Norwegian mosses to concentrations of elements in atmospheric deposition. Rosman *et al.* (1998) analysed Norwegian moss samples collected in 1977, 1990 and 1995. A distinct split between sites was identified using the $^{206}Pb/^{207}Pb$, with aerosols deposited at coastal sites coming mainly from the U.K and Western Europe, while inland atmospheric depositions were affected by aerosols originating in Eastern Europe and Russia. The concentrations of Pb in the coastal samples all exhibited decreases in lead concentration with time, the more recent mosses having lower concentrations. The $^{206}Pb/^{207}Pb$ ratios decreased to values <1.13 between 1977 and 1990, but increased by 1995. These changes were attributed to the usage of alkyl lead additives, manufactured from non-radiogenic Australian ores, in petrol in the U.K. and France. This was followed by bans on Pb in petrol and a reduction in car-exhaust emissions, with $^{206}Pb/^{207}Pb$ decreasing this source, with values returning towards more radiogenic "natural" values. A similar pattern was observed for the inland samples, although the isotopic ratios were >1.14, reflecting the lower influence of aerosols from Western Europe.

Carignan and Gariepy (1995) used epiphytic lichens instead of mosses to study lead deposited in the St Lawrence valley and around Quebec. In a similar manner to mosses, epiphytic lichens depend entirely on atmospheric deposition for nutrients, which are received in the form of rain, snow fog, dew, mist, and dry deposition. Trace metals accumulate through complexation with plant exudates and confinement within the growing surface. Lichens nearest the smelting operation at Noranda had much lower $^{206}Pb/^{207}Pb$ ratios (~1.054) than ranges recorded in the Great Lakes from U.S. and Canadian sources (cf results of Graney *et al.*, 1995). The lichens collected further away from Noranda exhibited more radiogenic isotopic ratios, in line with the radiogenic Pb in petrol from the Mississippi Pb deposits (Table 1.4). Tree bark and lake sediments were also analysed.

The uptake of atmospheric lead by trees is via two pathways (Robitaille, 1981), the first being direct deposition onto foliage (through wet and dry deposition) and the second being uptake of atmospherically deposited heavy metals from the soil and subsequent translocation into xylem.

Carignan and Gariepy (1995) reported lead isotopic ratios in spruce needles similar to those obtained for lichens. The isotopic ratios for the sediments, tree bark and leaves were all progressively more radiogenic. The reasons given for the differences were that the tree bark and wood undoubtedly contained an unquantified input of soil lead, while the sediments contained lead from locally eroded geological formations. The tree leaves had a much shorter lifespan than either the needles or lichens, and it was proposed that the more radiogenic isotopic ratios in the leaves resulted from a short-term change in the overall lead isotopic signature derived from atmospheric deposition.

Weiss *et al.* (1999) used mosses to study the atmospheric deposition of lead in Switzerland. Mosses collected annually and stored in a herbarium were used to carry out a retrospective analysis of temporal lead isotopic variations, in a similar approach to that adopted by Bacon *et al.* (1996). The moss samples represented a time span from 1867 to 1997, although samples between 1897 and 1950 were unavailable. The $^{206}Pb/^{207}Pb$ ratio declined from values of 1.18 in the 19th C to 1.16 in 1950, 1.14 in 1970, a minimum of 1.12 in the 80's before a recovering to 1.14 in 1999. This pattern clearly indicates the change from a radiogenic signal in the last century, to a less radiogenic signal presumably due to the influence of Australian lead, and then an increase in the $^{206}Pb/^{207}Pb$ ratio following the banning of lead in petrol in W Europe.

Watmough *et al.* (1999) successfully used $^{206}Pb/^{207}Pb$ ratios in tree rings to reconstruct changes in isotopic lead signature. The sycamores used in this study were from two different environments in northwest England. The woodland site at Prescot was located close to a metal refinery, while the site at Croxteth was part of woodland remote from conurbations. The tree rings sampled represented a 30-year sequence from 1965 to 1995. Surface soils at both sites were contaminated with Pb; although as expected, concentrations at the Prescot site were far higher.

The $^{206}Pb/^{207}Pb$ ratios in the soils were both relatively radiogenic (1.197 at Prescot and 1.174 at Croxteth). However, a weak acid leachate extracted up to 60% of the soil lead, and yielded much lower isotopic ratios (1.156 and 1.142), illustrating the petrol lead component of the total lead pool. In the tree cores from Croxteth, the Pb concentrations were shown to have decreased by a factor of 5 (from 8 mg/kg to 1.6 mg/kg) between 1970 and 1993. Despite the decrease in concentration, an associated decrease in isotopic ratio was not observed, with values staying close to 1.16 up to 1987. In the most recent tree rings, (post 1987) the ratio increased from 1.16 to 1.17. The decrease in Pb concentrations was attributed to a decline in industry and associated "industrial" emissions of lead, while the increase in $^{206}Pb/^{207}Pb$ was attributed to a decrease in petrol-lead, resulting in a greater influence of the radiogenic "industrial" signal.

In a study of Sicilian lichens, Monna *et al.* (1999) used isotopic ratios to distinguish between anthropogenic lead ($^{206}Pb/^{207}Pb$ ranging from 1.141 to 1.165) and geogenic lead derived from localised volcanic activity associated with Mt Etna and Vulcano island ($^{206}Pb/^{207}Pb$ ranging from 1.230 to 1.280).

Source apportionment was also used by Kunert *et al.* (1999), who determined $^{206}Pb/^{207}Pb$ ratios for moss samples collected from Innsbruck between 1987 and 1996. The $^{206}Pb/^{207}Pb$ ratio increased from 1.131 to 1.154 over the period of the study, and in line with the findings of Weiss *et al.* (1999), and Watmough *et al.* (1999), the increase in isotopic ratio was attributed to a decline in petrol lead deposited on the mosses.

Ceburniss and Steinnes (2000) compared the concentrations of heavy metals in mosses and Norway spruce needles collected in Lithuania. This study showed that mosses are preferable for use as biomonitors, because of the higher concentrations of metals received and consistency of retention, whereas the needles were only able to retain certain metals, importantly including lead.

1.4.5 Atmospheric Lead

Instead of using depositional environments to investigate atmospheric lead pollution, Pb in rainfall and atmospheric particulates can be sampled directly. In an attempt to quantify changes in the transport of atmospheric Pb, Grousset *et al.* (1994) analysed atmospheric aerosols collected throughout Western Europe between 1979 and 1992. Their results showed a general reduction in the concentration of Pb with time, although the overall observed trend was largely dependent on the geographical location. In order to discount the geographical effect, the isotopic ratios of Pb were measured, providing a characteristic independent of Pb concentration. Reported literature values for other areas were included in the discussion. A similar trend was observed to those in mosses, snow cores and lake sediments, with decreasing $^{206}Pb/^{207}Pb$ ratios up to the 1980's, followed by increasing values more recently. The isotopic signature in southern Europe was assumed to represent linear mixing between two end components, one being anthropogenic lead ($^{206}Pb/^{207}Pb \sim 1.09$) the second being crustal-derived lead in Saharan loess ($^{206}Pb/^{207}Pb \sim 1.20$). However, it was noted that the Saharan dust particles could scavenge anthropogenic lead during precipitation events instigated by the mixing of warm Saharan siroccos and colder air masses from continental Europe. These particulates would then give a lead isotopic ratio that was more characteristically anthropogenic.

Similar work by Monna *et al.* (1997) involved isotopic analysis of atmospheric particulates, incinerator ash, and petrol in France and the south of England. Isotopic ratios were obtained for petrol in France ($^{206}Pb/^{207}Pb \sim 1.084$) and for southern England ($^{206}Pb/^{207}Pb \sim 1.067$). The similarity between the two values reflected the monopoly of Octel Co in providing lead additives in both Britain and France, although the company operated independently in both countries, resulting in slightly different sourcing of lead. French petrol additives consisted of a mix of Australian ore (Broken Hill and Mount Isa) with Moroccan ore, while in Britain the Australian ore was mixed with Canadian ore.

French incinerator ash yielded a more radiogenic average of 1.149. Isotopic ratios ranging from 1.084 to 1.158 were determined for airborne particulates collected in France and southern England in 1995. The incinerator ash value was used as an average "industrial" signature, because of the mixing of lead from a variety of industrial sources (Hamester, 1994). The results indicate that lead isotopic ratios can be used to assess the relative contributions to atmospheric lead from different locations.

Äberg *et al.* (1999) used the ^{206}Pb /^{204}Pb ratio to evaluate atmospheric composition of aerosols in Oslo. It has been shown in previous studies on lead in Arctic ice cores, Swedish lake sediments and Norwegian mosses that lead is subject to long-range transport, and lead from central Europe can be transported to the remoter regions of Northern Europe, with lower intrinsic lead pollution. Recent phasing out of petrol-lead in Europe decreased atmospheric lead burdens, but atmospheric lead pollution is still significant albeit from different sources. Äberg *et al.* identified lead from unleaded petrol and wood stoves as contributing to recent atmospheric lead in Oslo.

Veron *et al.*, (1999) used Pb isotopic ratios for source apportionment of atmospheric Pb pollution in Northwest France. In conjunction with air mass trajectory models, the isotopic ratio was used to distinguish between lead sourced from Britain and that sourced from France. The lead sourced from France was further differentiated into petrol lead and industrial lead. Aerosols sampled at a rural site showed an increase in $^{206}Pb/^{207}Pb$ ratios from 1.108 in 1983 to 1.148 in 1994.

Chiaradia and Cupelin (2000) investigated the source of atmospheric lead at a city and a country site in Switzerland using lead isotopes. Three potential sources were identified, these being petrol lead, incinerator lead and lead from coal burning. Unsurprisingly the city site generally exhibited less radiogenic ratios due to the increased effect of petrol lead, whereas the incinerator provided a greater portion of lead at the country site. Temporal variations were also observed, with coal burning becoming a more important component in the city during winter.

In the most ambitious study yet carried out, Rosman *et al.* analysed aerosols collected from sites across the Northern Hemisphere between 1994 and 1999. The average $^{206}Pb/^{207}Pb$ values for Western Europe ranged from 1.097 in Madrid to 1.165 in Germany. The differences were mainly attributed to the variation in lead used for lead additives, with petrol in Spain and the UK being produced by Associated Octel UK, whereas lead additives in France and Germany were produced by subsidiaries of Associated Octel in France and Germany respectively.

Farmer *et al.* (2000) compared the lead isotopic signature of lead in rainwater, atmospheric particulates, pine needles and leaded petrol in Scotland between 1982 and 1998. The isotopic ratios in all of the samples reflected a consistent increase in the $^{206}Pb/^{207}Pb$ ratios in the last decade, from 1.120 in 1989-91 to 1.144 in 1997-98. This increase was attributed mostly to the decrease in the use of leaded petrol in the intervening time period.

1.4.6 Lead in peat bogs

In order to be of use in historical monitoring, a peat bog has to meet a number of criteria. There are two types of bog, minerotrophic and ombrotrophic. Plants growing on minerotrophic peat bogs receive their mineral nutrition not only from atmospheric deposition (rainfall and dry deposition) but also from percolating groundwaters (Shotyk, 1996). Ombrotrophic peat on the other hand receives nutrition solely from atmospheric deposition (Glooshenko, 1982).

Minerotrophic bogs are unsuitable for use in historical studies because any elements present in atmospheric deposition will be susceptible to mobilisation by groundwaters, and subsequent percolation through the core, disrupting the historical trends. Secondly, in analytical terms it is often extremely difficult to distinguish between elements imported to the peat profile in percolating groundwaters and those deposited on the growing surface of the bog.

The two types of bog can be distinguished from each other according to a number of factors. The most obvious of these is visual inspection of the vegetation growing on the bog surface. Differences in vegetation arise from the different nutritional status of minerotrophic and ombrotrophic peat bogs, itself due to the mechanisms by which each receives nutrients. Ombrotrophic bogs, dependant entirely on rainfall and dry deposition, have limited nutrition, whereas minerotrophic peat receives significant concentrations of elements such as Mg, Ca and K from groundwaters. Thus, the plant species growing on ombrotrophic bogs will consist of particular species that have low nutritional requirements, whereas minerotrophic peat can support a much greater range of vegetation (Shotyk, 1996).

However, visual inspection of a peat bog is insufficient for classification as being ombrotrophic or minerotrophic, as there is no means of telling how deep the ombrotrophic zone of the peat extends. This can only be assessed using geochemical classification of the core once collected.

One such telltale geochemical indicator of the intrusion of percolating groundwaters is the Ca/Mg ratio in the peat. In seawater, the Ca/Mg ratio is roughly 1:5 (Shotyk, 1996). Rainwater derived from seawater will have a similar ratio, and in the surface layers of bogs, a similar ratio will be observed. In groundwaters however, the Ca/Mg ratio will be much higher due to preferential release of Ca from plagioclase feldspars, the most abundant rock type in the Earth's upper crust. Mg tends to be associated with the more resistant minerals pyroxene and biotite, and is therefore less prone to release through weathering. The Ca/Mg ratio in groundwaters is therefore enriched in Ca. Sharp increases in the Ca/Mg ratio at depth in the peat can be indicative of the influx of Ca-enriched groundwaters (Shotyk, 1996).

Following correct identification, ombrotrophic peat bogs can provide good historical records of past atmospheric deposition, and have several advantages over the use of ice cores, lake sediments, mosses and tree rings.

The major drawback with the use of ice cores is the very low concentrations of metals present and the ease with which the cores can become contaminated, either during sampling, or during preparation for analysis. A number of different approaches have been utilised to circumvent these problems and these have been discussed earlier in section 1.4.2. The other more obvious problem is that of location of suitable glaciers for use. While the rationale behind sampling ice and snow at the poles is a valid one in terms of quantifying the extent of pollution across the globe, one of the inherent problems is the difficulty in reaching the sampling sites in the first place, let alone removing large samples of ice to the laboratory for analysis.

Lake sediments are much more widespread across the planet, and are more accessible than glaciers but there are several factors that need to be taken into consideration. There are processes operating in lake sediments, physical processes (e.g. slumping of sediments), chemical processes (e.g. redox cycling) and biological processes (e.g. bioturbation), which can disturb the sediment profile to such an extent that obtaining an interpretable profile is untenable. A secondary consideration is the need to distinguish between natural inputs (e.g. suspended sediments in inflowing streams) from atmospherically deposited anthropogenic inputs, although as discussed earlier there are ways of overcoming these difficulties.

While mosses provide valuable information on atmospheric deposition of metals ongoing at the time of sampling, they represent only a "snapshot" of deposition over a relatively short time span, and their use in reconstruction of past atmospheric depositional trends is limited. Their main use is in conjunction with peat bog profiles for example, providing a check on observed short-term trends.

Tree rings represent possibly the easiest environmental material to sample in terms of abundance and comparability from one location to another, but there are also many problems. As with lake sediments, metal concentrations within the tree rings cannot be attributed solely to atmospheric deposition, and must be resolved into two or more components: metals received directly from deposition, and metals taken up from the soil and translocated into the xylem.

Other difficulties include the differences between tree species in the uptake of metals, and the partitioning of metals into different parts of the tree following uptake.

In contrast to the above options, peat bogs are widely spread across the temperate regions of the Earth and can be used in spatial studies. Ombrotrophic peat has evolved to hold on to metals received through atmospheric deposition (Madsen, 1981). The organic nature of peat provides numerous exchange sites to which cations can be bound. Both of these properties allow relatively large concentrations of metals to accumulate in peat, ensuring that levels of the metals are sufficiently high to allow analysis on relatively simple instruments without the need for utilising "clean techniques".

The slow accumulation rates of peat can be both an advantage and disadvantage. The drawback is that it is difficult to obtain high-resolution temporal increments within the peat, not allowing identification of short-term depositional events. The beneficial side of this property is the ability of even a relatively short core to provide a historical record covering periods of centuries and in extreme cases millennia.

It has been shown in work by numerous researchers that ombrotrophic peat bogs provide valuable records of past pollution. Generally speaking, providing simple checks are completed (e.g. that the peat is ombrotrophic), peat can be sampled, analysed and the data interpreted with relative ease, in comparison to other environmental materials with the capability of recording past metal pollution. Examples of these earlier studies are discussed below.

One of the first studies on historical lead pollution using a peat bog was conducted by Lee and Tallis, (1973). Peat in Derbyshire was sampled to a depth of 2 m, and was dated using pollen records. The sampling site was adjacent to where a previous sample, which had been dated using ^{14}C, had been collected. The major finding of the study was a peak in the lead concentration at 90 cm depth, which was tentatively attributed to local lead mining by the Romans, dated at around 500 AD.

The applicability of using peat cores to reconstruct past atmospheric deposition of metals was fully investigated by Damman *et al.*, (1978). The use of peat bogs as effective records was questioned, due to reported mobilisation of microelements (including Cu), and physical changes within the peat column. These physical changes included;

1) compaction of the peat with burial,
2) changes in the plant species growing on the bog surface (affecting the composition of the organic matter produced on decay),
3) varying growth rates due to changing climatic conditions (affecting accumulation rates), and
4) fluctuations in the water table, causing concomitant changes in the anoxic/oxic zones, in turn affecting the rate of decomposition of the decaying organic matter in the peat.

The elements analysed were classed into four groups according to their vertical concentration variations. The first group included sodium and potassium, with maximum concentrations in the near surface layers, decreasing below 10 cm. The second group of elements included Ca, P, Mn and Pb. These elements also exhibited maximum concentrations in the near-surface sections, but the decrease in concentration occurred lower in the peat at 35 cm depth. The third group of elements all had maximum concentrations between 20 and 35 cm below the peat surface, and included Fe, Al, and Zn. Nitrogen concentrations varied little down the core, while the Mg concentrations at depth were double those observed at the surface.

The concentrations of elements in precipitation were used to estimate the retention of elements within the peat, and some of the trends identified are relevant for this study and are summarised briefly below.

Potassium was effectively retained, due to plant uptake, although Damman noted that *Sphagnum* mosses have no vascular structure, and therefore have a restricted capability to take up nutrients. In contrast, Na was lost from the core. Fe and Mn were shown to participate in redox cycling below the oxic zone of the peat.

However, the most important conclusion of this study was that, based on the observed similarity between the behaviour of Pb and Fe, the Pb was mobile within the peat. More evidence to support this conclusion was the apparent observed difference between the concentrations of Pb in the hummocks and Pb in hollows, with the concentration in hollows being a factor of 3-5 times greater than those determined in the hummocks. The following mechanism was proposed to explain the mobilisation of Pb in the form of Pb sulphide. Fluctuating ground waters cause vertical variations in the oxic/anoxic boundary. The lead sulphide is oxidised to soluble lead sulphate, and is translocated down the profile in percolating rainfall, until reaching the anoxic boundary and the lowered water table. The sulphate would then be reduced back to the insoluble sulphide and re-precipitated in the peat.

More recently, Cole *et al.* (1990) analysed a core from a calcareous fen for a range of metals including Al, Pb, and Zn. The core was dated using ^{210}Pb, ^{14}C, and pollen analysis. The agreement of the three dating methods suggested that although the study site was not a truly ombrotrophic bog, there was little or no mobilisation of Pb in the core. The observed variations in metal concentration showed that the highest rate of deposition of metals had occurred in the most recent 130 years.

Urban *et al.* (1990) investigated the mobility of Pb in peat profiles following conflicting evidence from a number of sources questioning the assumption of immobility. Differences between Pb in hummocks and hollows were observed, but in this study, the concentrations of Pb were higher in hummocks relative to hollows, the opposite trend to that observed by Damman. By measuring Pb inputs to the bog and using mass balance calculations, Urban *et al.* demonstrated that there was an overall loss of Pb from the peat bog. This, coupled with observed Pb enrichments in the peat below the water table led Urban *et al.* to argue that in peat hollows, the Pb was subject to remobilisation and loss from the peat through lateral migration of organic-rich ground waters.

In contrast to the findings of Damman and Urban, Vile *et al.* (1990) showed that ^{210}Pb dating of peat cores from the Czech republic agreed with pollen dating of the cores, supporting the immobile nature of ^{210}Pb.

A further study by Vile *et al.* (1999) involved collection of peat cores from Marcell Forest, Minnesota. These were placed in lysimeters and various amounts of lead (both in soluble form and in coal fly ash) were added. Rainfall was added to each of the lysimeters, and the resulting water levels sustained at different levels in each. The lead in drainage waters was collected and the concentrations determined. The aqueous Pb was retained through binding to organic matter, and the coal fly ash was retained within the peat structure. Under the conditions of fluctuating water levels, no mobility of lead was observed. This led Vile to conclude that peat bogs do effectively retain Pb.

More recently, two separate studies have utilised ^{210}Pb dating on several peat bogs in Switzerland (Appleby *et al.*, 1997) and in Scotland (MacKenzie *et al.*, 1998). In Scotland, two cores (one from an ombrotrophic bog and one from a minerotrophic bog) using both the CIC (Constant Initial Concentration) method and the CRS method (Constant Rate of Supply) described in Appleby and Oldfield (1992). MacKenzie *et al.* used both the CRS and CIC dating methods, and found good agreement between the dates yielded by both in the ombrotrophic bog. The results of both these studies suggest that if care is taken in selecting an ombrotrophic bog, ^{210}Pb dating is a valid method for obtaining dates from the depth increments. In the Swiss ombrotrophic bogs, the ^{210}Pb dates obtained using the CRS method were in good agreement with pollen analyses.

One of the other associated problems with identifying elemental pollution within peat bogs is distinguishing anthropogenic lead from "natural" lead inputs. In many peat cores, increased Pb concentrations are not indicative of anthropogenic lead pollution (see Urban and Damman above). The complex relationship between total lead concentrations and the deposition of naturally derived mineral material first has to be considered, as this mineral material itself can contain traces of lead within the mineral lattices. To account for any natural lead within the peat, one method adopted involves normalisation using a "conservative" element, not present in anthropogenically-derived aerosols and particulates, and originating solely from crustal rocks. By knowing the relationship between the conservative element and lead, a correction factor can be used to account for natural inputs of lead to the peat. Subtracting this from the total lead leaves the anthropogenic input.

This differs from the use of enrichment factors (section 1.4.1), which are useful in situations where the anthropogenic input is on the same scale as natural sources (e.g. ancient Arctic ice. Enrichment factors applied to situations where the natural lead component is obliterated by the scale of the anthropogenic lead component, rendering the resultant enrichment factors meaningless in terms of comparison. Normalisation, and the subtraction of the natural component is a much better technique. Many different elements have been used for normalisation, and these include aluminium, titanium (Gorres and Frentzel, 1997), scandium (Weiss *et al.*, 1997), zircon and yitrium (Shotyk, 1996, 2001). Acid Insoluble Ash (AIA) has also been used to quantify inputs of terrestrial origin (Vile *et al.*, 1995).

The difficulty with this method is that the natural abundances used are those determined for an average upper continental crust, which is not one specific rock type but an average of all the different rock types in the Earth's upper crust. As with enrichment factors (section 1.4.1) the localised geology may be completely different from this assumed "average" upper crust, with the result that normalisation may fail to correctly account for local inputs of Pb.

Recently a large number of studies have been conducted using peat bogs as archives of metals. These include Pb (Vile *et al.*, 2000; Weiss *et al.*, 1999), Cu (Kempter and Frenzel, 2000), As (West *et al.*, 1997), Hg (Benoit *et al.*, 1998), Cd (Steinnes, 1997) and other trace metals. Studies have been conducted on peat in countries as widespread as the Czech republic (Vile *et al.*, 2000) and Bolivia (Espi *et al.*, 1997), and in conjunction with other records such as mosses and lake sediments (Branvall *et al.*, 1997; Farmer *et al.*, 1997; Norton *et al.*, 1997). A review of the more important papers is provided below.

One of the most studied areas in terms of peat bogs is Switzerland, where deep peat cores have been obtained and analysed from a number of sites across the country (Shotyk, 1996, 1998, 2001). The isotopic ratios for lead determined on these peat cores have provided a 12,000-year record of lead pollution.

The peat bogs were classified as ombrotrophic down to 4.2 m, through visual inspection and identification of the vegetation, and the use of geochemical indicators. In the sections of the core dated (using ^{14}C from 12,000 before present (BP) to 3000BP), the lead concentrations were consistently low, with radiogenic isotopic signatures (^{206}Pb /^{207}Pb >1.194), indicating the lead originated from natural sources. Identified sources included aeolian soil particulates and Saharan dust. In the sections of the peat younger than 3000BP, there was a decrease in the ^{206}Pb /^{207}Pb ratio together with an increase in Pb concentrations. This was attributed to lead smelting by the Phoenicians, Greeks and Romans in the Southern Iberian Pyrite Belt in Spain (Shotyk *et al.*, 1998). A further decrease in isotopic ratios was observed at 240BP, together with a massive increase in Pb concentration. This correlated with increased industrialisation in the 19th C.

Peat bogs in the proximity of mines (Martinez-Cortinez, 1997; Kempter and Frenzel, 1999) and heavily industrialised areas (Gilbertson *et al.*, 1997) have also been extensively studied. Martinez-Cortinez *et al.* (1997) collected a 2.5 m deep core from an ombrotrophic peat bog in the Iberian Peninsula (close to the extensively mined Southern Iberian Pyrite Belt). As well as measuring the total concentration of lead (and Cd and Zn), a KCl extraction was used to assess the more labile Pb component of the peat. Interestingly, the proportion of total lead extracted by the KCl was constant at around 20%, throughout the peat profile. Enrichment factors for Pb, Zn and Cd were calculated relative to titanium. Early anthropogenic pollution was first identified at 2800 BP. The overall fluctuating pattern of lead was similar to others reported (Renberg *et al.*; Shotyk *et al.*; see above) but with a few differences which were attributed to regional pollution not detected in Switzerland or Sweden.

Another mining region extensively studied is the Harz region in Germany (Kempter *et al.*, 1997; Kempter and Frenzel, 2000). In the 1997 paper, a comparison of a number of peat profiles obtained from across Europe was made. Elemental concentrations were measured using XRF. Notably, while many of the cores in Europe exhibited lead enrichment during Roman times, the greatest lead concentrations were observed in The Middle Ages for the peat cores in the Harz region, reflecting intensive mining in the area.

Enrichment factors were calculated relative to Ti, and these showed the highest values during the Middle Ages. This study highlights the differences that can arise due to localised anthropogenic disturbances such as mining, which can be detected in peat on top of the typical European anthropogenic Pb signal.

In a more detailed paper on peat from Sonnenburg Moor in the Harz Mountains, Kempter and Frenzel (2000) found elevated lead concentrations were detected in the peat by 300 AD. Lead concentrations steadily increased to peak between the 12 and 13th C AD, before decreasing dramatically due to widespread pestilence and plague, in Western Europe. Increases in lead concentrations were not detected until the beginning of the 17th C, when large-scale mining again led to significant deposition of lead. Improved efficiency of lead smelting and a gradual decrease in lead mining in the region led to a steady decrease in lead emissions to the present. Thus, it has been shown that the lead concentrations,in mining areas can be directly related to human activity in the area.

Alternatively, peat bogs well away from mining and industrial sources have been used to assess the long-range transport of Pb, and popular countries for these studies are Sweden (Branvall *et al.*, 1997) and Norway (Steinnes, 1997; Dunlap *et al.*, 1999). Branvall *et al.* (1997) used lead isotopes to analyse $^{206}Pb/^{207}Pb$ ratios in three peat bogs, which were then compared to $^{206}Pb/^{207}Pb$ trends in lake sediments in the same region (Renberg *et al.*, 1994). Dating was achieved using pollen analysis in conjunction with ^{14}C. The $^{206}Pb/^{207}Pb$ ratios in these peat cores steadily decrease from very radiogenic values of >1.2 in peat sections dated at 3000 to 5000 BC, to 1.17 in the 20th C, with sharp decreases to < 1.14 in the near surface sections. The overall decreasing trend was interpreted as increasing deposition of Pb from outwith the region, initially from long-range transport of soil particulates and burning of vegetation from Europe. Lead mining and smelting in Spain, Germany and the UK led to further decreases in the ratio, with the importation of Australian ores also being reflected, especially in the later half of the 20th C in petrol additives. Similar trends were identified by Dunlap *et al.* (1999).

Earlier work on the Flanders Moss peat supported the lead isotopic trends identified in Loch Lomond sediments, with a decrease in ^{206}Pb /^{207}Pb in the upper sections of the peat, corresponding to the increased influence of lead in petrol in the recent past. These results will be discussed in more detail in conjunction with the results obtained from this study later in the thesis.

1.4.7 – Summary of the use of environmental records to reconstruct past records of Pb pollution

In summary, Pb is a widespread toxic pollutant that is now a ubiquitous pollutant at the farthest reaches of the globe. Analysis of Pb concentrations in environmental media from remote regions provided clear evidence for the anthropogenic influence on these lead concentrations. A number of environmental records have been identified and their use in reconstructing past and current Pb deposition has been discussed. The major advantages and disadvantages for each of the methods have been summarised. The use of lead isotopes greatly enhanced the quantification of lead and identification of possible sources. It is clear that despite the assumptions and limitations inherent in using ice cores, sediments, mosses, and peat bogs, records from local, regional and global studies can be used to demonstrate the impact of anthropogenic lead pollution on the globe.

With particular reference to the use of peat bogs, one of the most important factors controlling the mobility of Pb (and other elements) is binding to organic matter. To a large extent the immobility of the organic-Pb complexes has been assumed, and before experimentally investigating the binding of Pb to organic matter and humic substances, it is necessary to review the current extent of understanding of the characteristics and binding of humic materials. This will be explored in the following section.

1.5 HUMIC SUBSTANCES

1.5.1 Introduction

Humic substances are defined as the macromolecular brown-coloured components of organic matter, which bear no morphological resemblances to the plant or animal tissues from which they were derived (Hayes and Swift, 1978). They are found in a range of different environments including peat bogs but also more generally in soils, sediments and natural waters. One property, which makes them so important in natural systems, is their ability to bind metals. This has important implications not only in plant nutrition and growth (and in turn animal welfare), but also for the mobility and availability of potentially toxic heavy metals, which have contaminated many natural environments as a result of man's activities. Thus, an important area of research is the investigation of the role of humic materials in the complexation of heavy metals in soils, sediments and waters.

1.5.2 Historical context

Humic substances have long been of interest to scientists, since their role in maintaining soil fertility was recognised in the 18th Century. Early workers such as Achard, in 1736 (Stevenson, 1982) attempted to devise a scheme for extracting humic substances from soil. Initially a polymeric, highly coloured material was extracted using an alkaline extractant. Precipitation of one fraction termed humic acid (HA) was achieved by addition of acid. This left a second fraction in solution, which was termed fulvic acid (FA). The chemical fractionation of humic molecules into HA and FA on the basis of solubility in acid solution is still extensively used to date. More elaborate fractionation schemes have also been adopted, and an increasing number of humic fractions have been isolated (Figure 1.4). Even in the 1930s, however, several key workers including Hobson and Page (1932) questioned the applicability of such fractionation schemes. Many of the identified characteristics of the isolated fractions were discovered to result from the fractionation method used (Waksman, 1936). Researchers started to view humics more as a continuum of molecules of heterogeneous nature, than a collection of discrete molecules.

Figure 1.4 - Fractionation of Humic Substances

(adapted from Kononova, 1966)

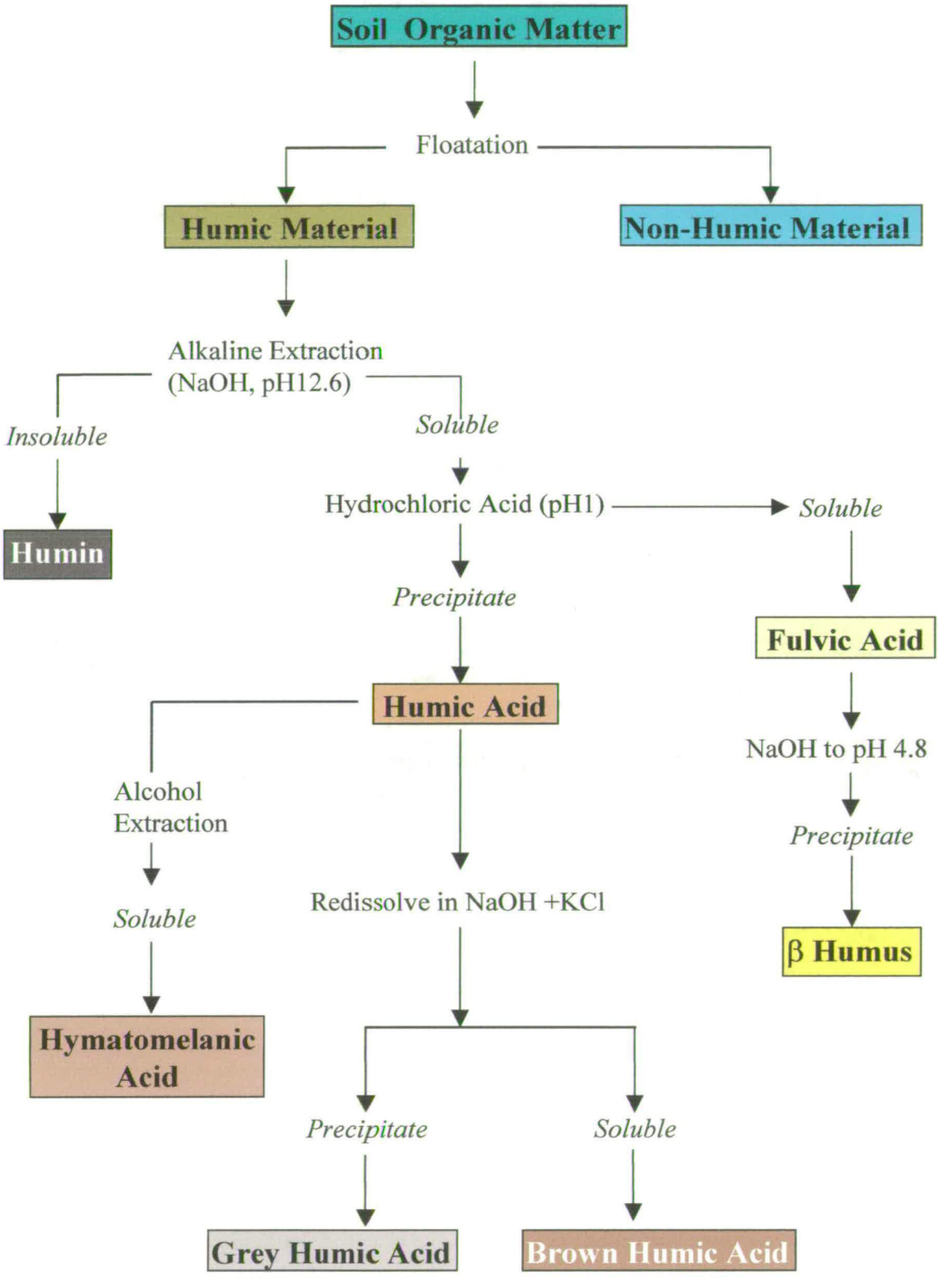

1.5.3 Formation of humic substances

One of the uncertainties associated with humic substances is the question of how they are formed in soils and sediments. There are two main ideas, which are:

a) that humics form directly from degradation products in the soil, and have similar properties, or

b) that the polycyclic molecules are formed by microbial action in the soil.

The first theory was popular early in the 20th Century, when it was realised that the degradation products of humic acids and their properties were similar to those of lignin (Stevenson, 1982). At this time however Maillard (1917), succeeded in synthesising a nitrogenous brown polymer compound from condensation reactions between amino acids and sugars. Other suggested pathways in the same vein include microbiological production of quinones, which could combine to form humics, while others suggest that these quinones could equally react with the amino acids and sugars to produce humics. A schematic diagram of the various pathways is illustrated in (Figure 1.5).

It now appears that both pathways may operate in the formation of humic substances, although to varying extents depending on the environment. Two opposing examples are considered. Humic substances in acidic or waterlogged conditions (e.g. peat) are much more likely to form through the lignin pathway, due to limited microbial activity in the acidic, anaerobic conditions. In contrast, humic substances formed in warm, aerated, tropical soils with higher levels of microbial activity are more likely to form through microbiological action, (Stevenson, 1985). An outcome of these different modes of formation is one of the reasons for the different functionality observed in humic substances from different environments (Malcolm and MacCarthy, 1991) and extracted from soils in various locations around the world (Schnitzer and Khan, 1972). The functionality of humic substances has particular relevance for the metal binding ability of the humic substances, as will be discussed in Section 1.6.3.

Figure 1.5 - Proposed pathways for the formation of humic substances from precurser organic matter (adapted from Stevenson, 1994)

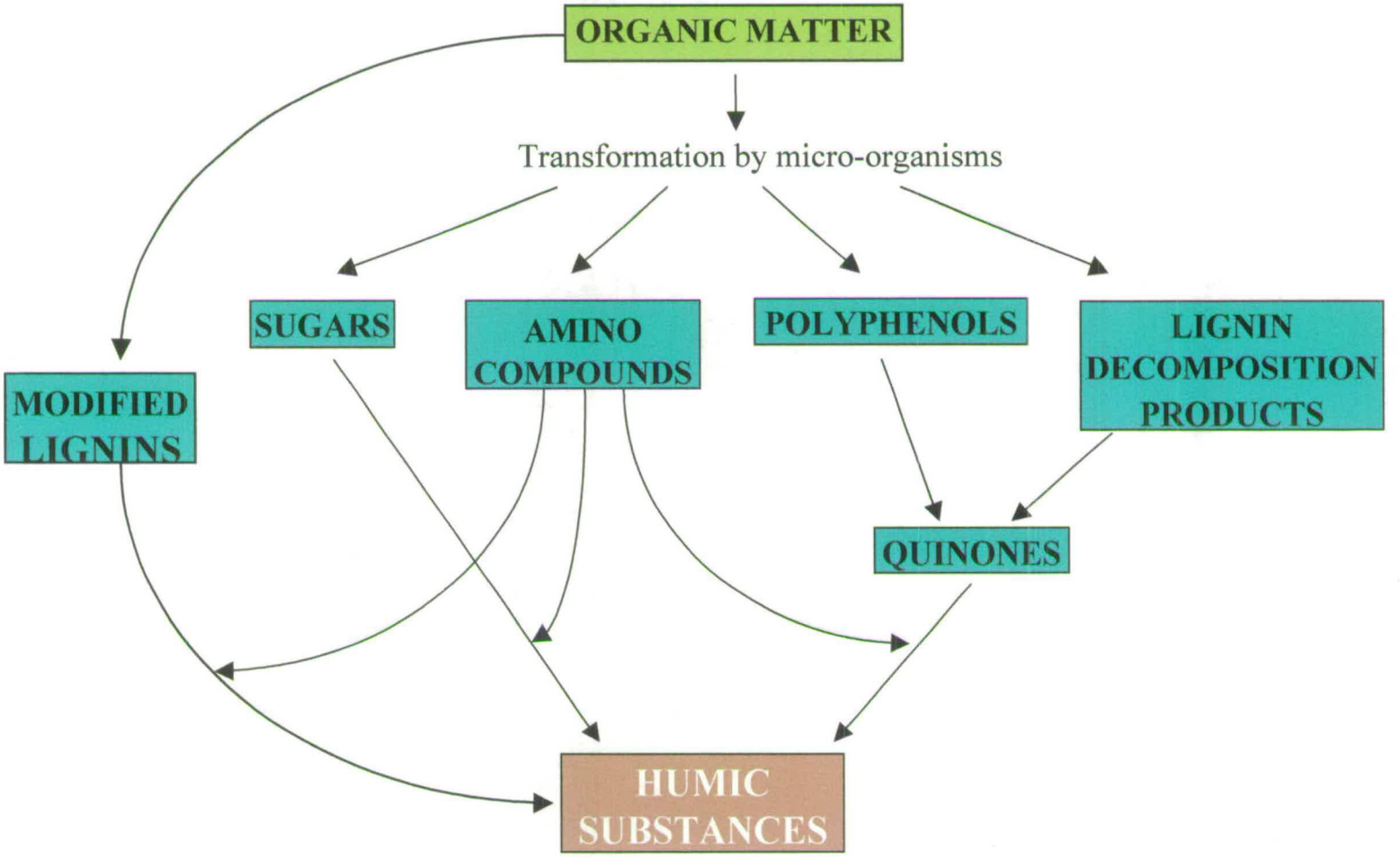

1.6 EXTRACTION OF HUMIC SUBSTANCES

1.6.1 Introduction

In order to characterise humic substances, it has been necessary to isolate them from the soil, sediment or water. Stevenson (1982) has described the four conditions that should be satisfied for an extraction of humic substances. These are:

1) the humic extract should be unaltered *i.e.* as close to its natural condition as possible, to ensure that any further characterisations of the extract are directly related to natural conditions and not merely an artefact of the method.

2) the extract should be relatively pure and free of contaminants. For humics, it is normally advantageous to have no inorganic components present, including clays, silicate minerals and metal ions. Organic contaminants such as carbohydrates, which may be bound to the humic molecules may also be undesirable.

3) the extract should be fully representative of the sample from which it was taken. For the full range of humic substances found in soil (as opposed to a specific aquatic fulvic acid fraction), this means that both end members of humic substances, i.e. the smallest fulvic acids to the largest humic acids have to be encompassed. Due to their heterogeneous nature, sizes range from 3-500 Daltons for the smaller fulvics up to an estimated 1,000,000 Daltons for the larger humic molecules (Aiken and Wershaw, 1985).

4) the method of extraction should be easily reproducible and transferable between all the different types of samples, from coal to stream fulvic acids.

Currently, no single extractant has been found which satisfies all of the above criteria. Traditional extractions have been done using 0.1/ 0.5M sodium hydroxide (NaOH) solution. This alkaline extractant is at a pH of 13 or above and the validity of using such a harsh extractant has been called into question (Stevenson, 1982). At a pH as high as this, oxidation of the humic molecules is known to occur at a rapid rate, leading to changes in functionality, and possibly even structure (Swift and Posner, 1972). For this reason it is normally necessary to undertake any experiments in a nitrogen atmosphere.

This, however, does not entirely solve the problem of alteration as other parts of the extraction procedure also involve exposure of the humic material to harsh conditions, e.g. pH 1 during the acid precipitation of HA, dilute HF during the removal of co-extracted siliceous materials. The one factor in favour of using a strong alkaline reagent in the initial extraction step is that it can extract upwards of 80% of the total humic content from soils, and is able to dissolve the more recalcitrant fraction of humic substances.

Once the sample has been extracted, it is necessary in most cases to purify it by removing any metal ions and carbohydrates, fatty acids etc., which are bound to the humics. This is important in the case of the former to protonate all the functional groups and hence aid their detection, and in the case of the latter, remove these known components (not part of the core humic molecule), which may affect any average weights or properties of the extractant (Hayes, 1985). One method of doing this involves using a strong acid such as HF to try and remove any transitory organics bound to the humics, lower the pH sufficiently to remove metal ions into solution, and dissolve any inorganic components such as clays or silicates.

Purification often results in a loss of up to 40% of the total weight of extracted humic substances, and while the relative aromatic and aliphatic contents increase showing that the backbone is present, it is thought that many of the functional groups are altered. Indeed ^{13}C NMR studies have shown that this is the case (Preston and Schnitzer, 1986), with a resultant change in the spectra recorded. Dissolution in an organic compound and methylation of the humics has also been used, again to remove any metals from the groups, and aid their detection. The argument against this technique is that in order to be soluble in an organic extractant, the hydrophilic groups are repelled to the centre of the molecule (Wershaw, 1983), where the resultant hydrogen bonds mean they are not methylated. Any subsequent characterisation is unfairly biased towards the hydrophobic molecules, which are on the outside of the molecule and readily methylated.

Other purification methods have developed, including passing the extracted humic substances through successive anion and cation exchange resins (Malcolm and Thurman, 1986), although there is the problem of adsorption of some of the humic molecules to the resin.

Alternatives to this have been used, in order to obtain a sample more like the actual humics found in nature. A variety of these, are shown below (Hayes, 1985):

1) **MILD EXTRACTANTS** ***e.g.*** **$Na_2P_2O_7$, 0.045M Tris Borate,** which work using the same mechanism as above, only with using less severe pHs (7-9) there is less risk of alteration. A disadvantage is that the extraction is less efficient at ≤ 30% (Piccolo and Mirabela, 1987; Piccolo *et al.*, 1989; Stevenson, 1994).

2) **COMPLEXING AGENTS** ***e.g.*** **E.D.T.A,** work by preferentially chelating di- and `tri-valent cations, changing the humic substances from an insoluble to a soluble form. A drawback is that this extractant attacks aluminium and iron oxyhydroxides as well.

3) **ORGANIC ACIDS** ***e.g.*** **Formic acid, Acetylacetone** work by disrupting hydrogen bonds and complexing some of the cations. These extractants can provide a purer extract of organic material, relatively free of associated inorganic complexes, but are generally unable to extract the larger size molecules.

4) **DILUTE MINERAL ACIDS** ***e.g.*** **HF** work by dissolving silicates and clays to which the humic molecules are bound, but the extremely low pH causes structural alteration, aggregation and loss of some of the functionality.

Of these alternative extraction methodologies, the most favoured is the use of mild aqueous solvents. In particular, mild solvents such as 0.045 M Tris-borate (pH 8.5) (e.g. Vinogradoff, 2000) and Tris-borate/EDTA (e.g. Eloff and Pauli, 1975) have been used.

These solvents have been shown to extract up to 45 % of soil humic material. Moreover, Vinogradoff (2000) showed that, although the extraction efficiency was lower than that obtained using 0.1 M NaOH, 0.045 M Tris-borate was capable of extracting very large (~200,000 Da) as well as smaller humic molecules. A criticism of mild aqueous solvent extraction has often been that only smaller molecules were extracted. Thus, this method, which avoids exposure to extremes of pH, may have the potential to extract a less-altered component that is representative of the total humic substances in soils.

1.7 CHARACTERISATION OF HUMIC SUBSTANCES

Once the humic substances have been extracted, a range of techniques can be used to characterise the humic substances. These include:

- Elemental analysis and ash content
- Molecular size determination
- Acidity and assignment of this acidity to specific functional groups
- Functionality

1.7.1 Elemental composition and ash content

The elements that are used to characterise humic materials are mainly C, H, and N (O is often calculated by mass difference). Other elements analysed for include S and P, and ash content. These values can be used for the following, as outlined by Steelink (1985);-

1) To identify the type of humic substance

This can be done by checking the C:O ratio against a plot of percentage C against percentage O (Stevenson and Butler, 1969) and hence can differentiate between kerogen-forming aquatic fulvic acids, and soil humic acids.

2) To monitor the structural changes of humic substances in soils and sediments

Increasing humification with depth is seen to cause increasing aromaticity and an associated decrease in the oxygen content due to microbial action.

3) To devise structural formulas for humic substances

Normally elemental analysis can provide an accurate structural formula, from which the structure can be determined. This is not the case with humics because of their polymeric nature (Huffman and Stuber, 1985). Indeed any attempts to use the results from elemental analysis to define an average formula for humics has been ridiculed by Steelink (1985). He points out that a formula of $C_{10}H_{12}O_5N$ obtained for fulvic acid, is the same average formula as wood.

4) To eliminate the role of inorganic material

The most widely used ranges of elemental values in humic and fulvic acids are those of Schnitzer and Khan (1972), shown below in **Table 1.5-**

Element	Fulvic acid	Humic acid	Humin
% C	40-50	50-60	55-60
% O	44-50	30-35	30-35
% H	4-6	4-6	5-6
% N	<1-3	2-6	4-5
% S	<2	<2	<1

These authors have also used elemental analysis to compare the difference between soils from around the world.

1.7.2 Molecular weight and size determinations

This has been attempted using a variety of different methods (Swift, 1989);-

- Gel filtration chromatography
- Ultrafiltration
- Light scattering abilities
- Scanning Electron Microscopy (SEM)

The above methods have been used to determine molecular sizes, by comparison with known standards, of a known size. The problem with the gel permeation is coagulation of the humic compounds, resulting in a situation where even though most of the molecules are smaller than the cut-off, coagulation will increase the size of the molecules to way above the cut-off, ensuring that they are retained. For example, Reuter and Perdue (1981) used G50 Sephadex gel with an exclusion limit of 30,000 Daltons to fractionate humics. Subsequent number average weight analysis produced a figure way below this cut-off, of only 1231 Daltons. It should be noted however that number-average molecular weights are lower than weight-average molecular weights. Electrostatic repulsion can also cause problems with gel permeation.

Ultrafiltration is also imprecise due to the exact precision of the cut-off. Most are manufactured so that 90% of the material greater than the cut-off will be retained, but 10% will pass through. Concentration effects at the surface of the filter are also a problem and can lead to clogging with high concentration samples (Buffle, 1988). The two methods described above are the main ones utilised in the determination of molecular weight and size determinations, but studies involving light scanning properties (Jones et al, 1995), and SEM (Tan, 1985) have also been undertaken.

It must be noted that any results can be expressed in a number of different ways (Swift, 1989).

1) The number average molecular weight, *Mn*, uses the following formula;-

$$Mn = \frac{\Sigma n_i M_i}{\Sigma n_i} \qquad \text{Equation 2}$$

where n_i is the ith number of molecules of weight M_i.

2) The weight average molecular weight, *Mw*, uses the following formula;-

$$Mw = \frac{\Sigma n_i M_i^{\,2}}{\Sigma n_i M_i} \qquad \text{Equation 3}$$

Generally, *Mn* produces smaller averages than *Mw*, and tends to favour the smaller fractions, which although they can represent a large proportion of the total number of molecules, represent a far smaller fraction in terms of weight. For this reason, *Mw* is generally favoured over *Mn* (Buffle, 1988).

1.7.3 Total acidity and the relative contribution from different functional groups

Total acidity can be measured by titration of the humic against barium hydroxide (Perdue, 1985), with the remaining barium hydroxide back-titrated against acid. The problem with this method is that it is very difficult to ascertain whether all the acid groups are dissociated, but with a pH of 13, it is hoped that this is achieved. Carboxylate acidity is measured using calcium acetate.

This differs from the barium hydroxide titration in that it is poorly buffered and the pH of the titration is dependant on the concentration of humic acid used. The only way of estimating the phenolic contribution to the total acidity is to subtract the carboxyl acidity from the total acidity. This is far from ideal, and a better method of determining functionality is by using spectroscopic methods.

1.7.4 Functionality

There are two main methods for assessing the functionality of humic substances. While UV spectroscopy is useful in terms of assessing changes in functionality, using the ratio of absorbance's at 465 and 665nm (E_4/E_6 ratio), it does not provide any useful information on the nature of the functionality (Perdue, 1985). IR spectroscopy can be used with more accuracy to determine functionality, and has the advantage that solid samples can be used. Groups identified include carboxyl, phenolic, alcoholic, amine and amide (MacCarthy and Rice, 1985). Bonds identified include ester linkages and C=C double bonds.^{13}C NMR has also been increasingly used on humics, both in aqueous and solid forms, and the earlier identifications have been verified (Wershaw, 1985).

Table 1.6 ^{13}C-NMR chemical shift regions for various types of carbons

Region I	Region II	Region III	Region IV	Region V
0- 50 ppm	50 - 100 ppm	110 - 160 ppm	160 - 190 ppm	190 - 220
Paraffinic groups	Alcohols, Amines, Carbohydrates, Ethers, Acetals	Aromatic - C Olefinic - C	Carboxyls, Esters, Amides	Aldehydes and Ketones

There are however, differences between the functionality observed between using IR and NMR, and these differences have been investigated by Lobartini and Tan (1988).

1.8 METAL BINDING BY HUMIC SUBSTANCES

In many environmental situations, the speciation of metals is controlled by their binding to organic matter and in particular, to the humic and fulvic components of organic matter. In order to assess the likely speciation of metals, it is necessary to know the stability constant of the metal-organic bond.

1.8.1 The affinity of functional groups for metal ions and the relative abundance of these groups in humic materials

The affinity of the various functional groups for metal ions as assessed by Chabarek and Martell (1959) is shown below:

$-O^-$ (enolate)>$-NH_2$ (amine)> -N=N- (Azo)> =N- (Ring N)> COO^- (Carboxylate) > -O- (Ether) > C=O (Carbonyl).

Although the nitrogen groups have the highest affinity for metal ions, they are scarce on humic molecules, and as a result, most of the groups participating in metal binding are carboxyl and phenolic groups. The metal ions also have a range of affinities for the sites on the humic molecules, and these have been assessed (Schnitzer and Hanson, 1970):

For 1:1 complexes (using the ion exchange equilibrium method), the following stability constants were determined:-

Log K	Cu > Ni > Co > Pb = Ca > Zn = Mn > Mg
At pH = 3.5	(3.3 > 3.2 > 2.8 > 2.7 = 2.7 > 2.2 = 2.2 > 1.9)
Log K	Ni > Co > Cu = Pb > Mn > Zn > Ca > Mg
At pH = 5	(4.2 > 4.1 > 4.0 > 4.0 > 3.7 > 3.6 > 3.3 > 2.1)
Irving – Williams series	Cu > Ni > Co > Zn > Fe > Mn

1.8.2 Stability constants

For the reaction of a metal cation (M^{i+}) with an anionic ligand (A^{j-}), the formation constant, or stability constant (K) is calculated using the following equation;

$$K = \frac{[M_j A_i]}{[M]^j [A]^i} \qquad \text{Equation 4}$$

The ligand's complexing ability is normally expressed as a molarity, but in the case of humics, it is necessary to express it in terms of the concentration of complexing sites. The amount of metal bound is normally assessed by titration of the humics with a known concentration of metal, and then measuring the concentration of the metals remaining in solution. The amount of metal bound is the difference between the initial and final free metal concentrations. There are ways of measuring the free metal concentration (Stevenson, 1982); -

- Ion Selective Electrode - these are easy to use and specific to certain ions, but have low sensitivity.
- Anodic Stripping Voltametry - the preferred method as it is highly sensitive, and can be done on small volumes

The reactive site concentration can be determined by;-

- Molecular weight measurements
- Potentiometric titrations
- Estimation of the total complexing sites from metal retention data

Methods of calculating stability constants (reviewed in Stevenson, 1982) include;-

1) THE ION EXCHANGE EQUILIBRIUM METHOD

This is based on the competition between the humic groups and a cation exchange resin for the metal cations. Two assumptions are made for this method;-

- The metal ion is the central ion
- The aqueous metal ion concentration is almost negligible in comparison to the concentration of the humic ligands.

It is clear that in certain cases, both of these assumptions cannot be made, and this seriously reduces the validity of constants determined in this fashion.

Briefly, the distribution co-efficient for the metal (λ) is calculated from the measurements of the free metal concentration, the metal in the complex and the metal bound to the resin. A second distribution co-efficient (λ_0) is calculated in the absence of the ligand. A graph of log $[(\lambda_0 / \lambda) -1]$ against log A_0 (initial concentration of the unbound ligand), yields log K as the intercept.

2) BASE TITRATION METHOD (also known as the Bjerrum approach)

In this method, the binding of the metal *M* to the humic ligand *A* yields one or two hydrogen ions, the concentration of which can be determined by titration with a base

$$HA + M^{2+} \Leftrightarrow MA^{+} + H^{+}$$

$$HA + MA^{+} \Leftrightarrow MA_2 + H^{+}$$

$$B_2 = b_1 b_2 = \frac{[MA_2][H^+]^2}{[HA]^2[M^{2+}]} \qquad \text{Equation 5}$$

where B_2 = overall Bjerrum constant, b_1 = first formation constant and b_2 = second formation constant. This method requires the calculation of the concentration of the dissociated ligand, and the average number of ligands bound per metal ion (n, also known as Bjerrum's formation function). The major problem with this method is that the titration graphs of base added against pH are shifted horizontally, because of release of non-titratable H^+ in the presence of the metal. This has been solved by adding sequential amounts of metal to the humic at a constant pH (by returning the solution to it's initial pH by addition of base).

3) SCATCHARD PLOT METHOD

The humic ligand is presumed to be the central group

$$\nu = \frac{M_b}{A_t} \qquad \text{Equation 6}$$

where M_b is the concentration of the metal ion, A_t is the concentration of the ligand and ν is the average number of metal ions associated with each macromolecule. A plot of $\nu/[M^{2+}]$ against ν produces K_0 as an intercept. Scatchard plots give evidence of two sites, but Saar and Weber (1979) found continuous variation in the site strength.

1.9 COMPUTER MODELS - WHAM

In recent years, it has become desirable to model humic-metal interactions for understanding the cycling of potentially toxic metals in the environment, and aid speciation calculations of metals in water. Computer modelling is one way of trying to predict the mobility of these complexes, and such information is badly needed, especially for two main areas of research. The first of these deals with the upcoming prospect of dumping sewage sludge enriched in heavy metals from industrial sources onto agricultural land, and the associated health implications. The second of these, and more relevant for this project, is the use of peat profiles in monitoring changes in pollution and heavy metal deposition to the land from a variety of different sources. The assumption that has been made in the past is that the metal-humic complexes present in peat are immobile (Shotyk *et al*, 1997; MacKenzie *et al*, 1997) and once in the profile remain there. This assumption has been called in to doubt by results and predictions from the computer models (Tipping and Woof, 1990) and more information is now required to test the various models. One such model developed is called WHAM.

1.9.1 The WHAM Model

The Windermere Humic Acid Model (WHAM) model was developed by Tipping (1994), for modelling the release of humic-metal complexes into water bodies. Initially, a simple model was developed to calculate the amount of Al bound to the dissolved humic and fulvic molecules in order to calculate the complete speciation of the metal in stream waters (Tipping et al, 1988). The amount of metal bound was calculated using an equation with three constants (α, β, and γ);

$$[Al_m\text{-}org] = \alpha\,[HS]\{Al^{3+}\}^{\beta}\{H^{+}\}^{\gamma} \qquad \text{Equation 7}$$

where $[Al_{m\text{-}org}]$ = organically complexed Al, $[HS]$ = concentration of humic substances, $\{Al^{3+}\}$ = monomeric aluminium activity, and $\{H^{+}\}$ = proton activity. The activities of the ionic species were calculated using the extended Debye-Hückel equation (see below).

Electrostatic interactions were taken into consideration using an empirical expression derived from the Poisson-Boltzmann equation (Tanford, 1961);

$exp(-2wzZ)$, Equation 8

where z = the charge on the complexing ion, Z = the charge on the HS (mequiv/g) and w = the electrostatic interaction factor. The factor w was related to the ionic strength of the solution and charge as follows;

$w = P\,(log_{10}I)exp(Q/Z/)$, Equation 9

where P *and* Q = (-ve) constants, I = the ionic strength, and $/Z/$ = the modulus of Z.

In a further development of the model, the functionality of the humic molecules was recognised, and split into carboxylic groups (COOH) and phenolic groups (WAH). Each group was assigned a dissociation constant (pK) and a metal binding constant, which varied according to the metal bound. Extra parameters were introduced, increasing the number of parameters to eight, shown below;

- Total acidity (*Ac*, which was measured)
- Carboxyl content (*n*)
- Four intrinsic equilibrium constants; one each for proton dissociation for the two groups (K_I and K_{II}) and one for Al binding (K_{Al}), and one for proton binding (K_H)
- Two parameters for ionic strength effects (P and Q)

Of these eight parameters (P, Q, K_{Al}, K_H, K_I, K_{II}, n, Ac) only the total acidity, was experimentally determined. The remaining seven were set using least-fit-squared analysis.

A further development in the model was an increased definition of the functionality, (Tipping et al, 1988a), achieved by sub-dividing the existing carboxyl content into two fractions (COOH I and COOH II). Bidentate binding was assumed to occur for all of the metals ions, and therefore three different possible sites were created for metal binding (see Table 1.6).

Table 1.6 - Possible binding conformations

Site Name	Functional Groups
Type A	COOH I+ COOH 2
Type B1	COOH I + WAH
Type B2	COOH II + WAH

The major problem associated with this model was the neglect of competition from other cations and therefore an over estimation of the binding capacity. It was found that Ca competition had little effect on the aluminium binding. Thus, it was concluded that the aluminium and calcium ions were not in direct competition for the same sites. A further adaptation of the model was needed to account for this.

In the next development, the Complexation of Humic Acids by Organic Soils (CHAOS), an extra mechanism was introduced to describe the binding of Ca ions. A diffuse double layer was used to account for metal ions not specifically bound but held in close association with the humic molecule, but which could still balance the negative charge of the dissociated acid groups of the humic. Thus the metal cations used in the model, could exist in one of the three states;-

1) **cations specifically bound** (chelated) to functional groups on the humic molecule (Compartment H)

2) **aqueous cations** (in free solution) (Compartment S)

3) **cations in the double diffuse layer**, (Compartment D) weakly associated with the humic molecule to neutralise the delocalised charge

The number of metal ions in the third compartment was related to the volume of the diffuse layer. The volume of the diffuse layer was in turn dependent on the following;-

- pH - this affects the dissociation of the acid functional groups, which controls the charge on the molecule (Z).

- Ionic strength - the higher the ionic strength, the greater the competition for the diffuse layer, the closer the cations approach the molecule, and subsequently the smaller the Donnan volume.

The relationship between the concentration of cations in the D and S compartments was described in terms of a simple Donnan-exchange process, using a modified Schofield equation, shown below;

$$\frac{[H^+]_D}{[H^+]_S} = \left\{\frac{[M^{Z+}]_D}{[M^{Z+}]_S}\right\}^{1/Z} \qquad \text{Equation 10}$$

where $[]_D$ = signifies protons and metal cations in the diffuse layer, and $[]_S$ = signifies protons and metal cations in solution

The Donnan volume was calculated using the Debye-Hückel equation;

$$V_D = \frac{10N}{M}.\frac{4\pi}{3}.[(r+1/\kappa)^3 - r^3] \qquad \text{Equation 11}$$

where V_D = the diffuse layer volume, N = Avogadro's number, M = humic molecular weight, r = the radius of the humic molecule and κ = the Debye-Hückel parameter.

The next development of the model was to determine the solubility of the humic molecule (Tipping and Woof, 1990). This had been shown in earlier papers to be related to the charge on the humic substance (Z), with the greater charged molecules being more soluble. However, the charge on the molecule is itself determined by the number of bound cations.

The metal binding of the humic molecules was calculated as before and these humic molecules were divided between a mobile compartment (HSM) and an immobile compartment (HSI). The charges of the humic molecules (Z_{HSI} and Z_{HSM}) are determined mainly by the binding of Al^{3+} and H^+. For a selection of soils investigated, there were large variations in the concentrations of humic substances associated with the HSM fractions, relating to the different charge and binding characteristics of the humic molecules present.

Model V was the successor to CHAOS, with further developments in functionality (Tipping and Hurley, 1992). The old description was discarded, as, in line with other workers in the field, (*e.g.* Perdue and Lytle, 1983), carboxyl and phenolic pK's were no longer regarded as discrete, but rather two continua normally distributed around two medians. To translate this to modelling, four parameters were needed (as opposed to the two constants in CHAOS). Two values (pK_A and pK_B) were adopted for the median (around which the pK values were distributed) and two further values (ΔpK_A and ΔpK_B) defined the extent to which the distribution occurred.

The other major development of the model was that not all of the metals specifically bound (*i.e.* in the H compartment) were bound bidentately. Due to steric effects, not all of the cations had the right orientation in relation to the functional groups to form bidentate bonds. An arbitrary value of 0.4 was chosen as the fraction of the total number of metal ions able to achieve the right conformation to form bidentate bonds. The number of different sites was increased to eight, four for each type of group:

$$pK_1 = pK_A - (\Delta pK_A / 2) \qquad pK_5 = pK_B - (\Delta pK_B / 2)$$

$$pK_2 = pK_A - (\Delta pK_A / 6) \qquad pK_6 = pK_B - (\Delta pK_B / 6)$$

$$pK_3 = pK_A + (\Delta pK_A / 6) \qquad pK_7 = pK_B + (\Delta pK_B / 6)$$

$$pK_4 = pK_A + (\Delta pK_A / 2) \qquad pK_8 = pK_B + (\Delta pK_B / 2)$$

Thus, the total number of sites on the humic molecule was increased to 21; 12 for bidentate binding, eight for monodentate binding and one for diffuse binding. After application of the model to studying competition between alkaline and trace metals. (Tipping, 1993), the model was converted into a computer code for computer modelling (the WHAM model; Tipping, 1994). The computer programme incorporates a series of metal binding constants and thermodynamic data from the literature, together with a full set of default parameters, which can be changed upon measurement of new parameters. The model can be used to calculate the speciation of a variety of metals, both in waters and soils, and takes into account processes such as sorption onto clays and precipitation of oxyhydroxides.

1.10 AIMS

The introductory material presented in Chapter 1 has described the use of a number of environmental media to reconstruct records of the past deposition of atmospheric Pb. Included in these media were ombrotrophic peat bogs which differ from the others in that they are highly organic in character. For many elements in addition to Pb, little is known about the chemical form of the elements following deposition into the peat bog. Moreover, little is known about the changes that may occur with increasing time from deposition. The construction of historical records, however, requires the assumption of post-depositional immobility within the peat. This has previously been assumed but not unambiguously established for Pb in such environments.

Thus, there were three main aims of the project:

(i) to establish the relationship between porewater and solid phase concentrations of Pb within the peat and to compare the vertical distribution of Pb with that of other elements with varying chemical characteristics (highly conservative to non-conservative behaviour) (Chapter 3).

(ii) to investigate the associations of Pb within the peat and also the stable isotope ratios of Pb in different components of the peat bog (solid phase, solid phase humic materials and porewaters) to establish the importance of any changes occurring with depth that might influence the solid phase profile (Chapters 4 and 5).

(iii) to attempt to model the partitioning of Pb between the porewater and solid phase peat using the geochemical model, WHAM, and to assess the potential use of modelling to predict changes in the partitioning of Pb under different environmental conditions (Chapter 6).

Chapter 2

Sampling Procedures and Experimental Methodology

The following chapter includes a description of the peat bog sampling location and the procedures adopted for the collection of peat cores. The protocols for storage of samples, preparation prior to analysis, together with the various methods of analysis and characterisation adopted in this study are then described.

2.1 PEAT CORE COLLECTION

2.1.1 Location of Flanders Moss peat bog

The site chosen for the collection of peat cores was Flanders Moss peat bog in Central Scotland (Figure 2.1A), 34 km north of Glasgow and 18 km west-northwest of Stirling. Flanders Moss, located on the north bank of the River Forth, is the largest lowland raised peat bog in Britain. The peat bog is bounded on the southern edge by the Fintry Hills and on the northern edge by the Menteith Hills. Figure 2.1A also shows the location of two freshwater lochs from which dated sediment cores, used for the construction of historical records of anthropogenic Pb deposition, have previously been obtained (Farmer *et al,* 1996). These are the Lake of Menteith, which is located 5 km east north east of Flanders Moss, whilst Loch Lomond lies 23 km to the west of the peat bog.

Flanders Moss lies between two major local roads, the A873 Stirling to Aberfoyle road to the north, and the A811 to Stirling to Drymen road to the south. These roads run parallel to each other in an east-west orientation. Running parallel in a north-south orientation, linking the above roads, are minor B roads: the B822 to the east and the B8034 to the west (Figure 2.1B). The peat bog is relatively remote from major and minor local roads as the minimum distance from any of these to the centre of the bog is 2.5 km. Moreover, the largest intercity road in the vicinity is the M9, a four-lane motorway, lies some 15 km to the east (Figure 2.1A).

Figure 2.1A – Map of central Scotland, with Flanders Moss in the centre of the picture (red arrow). Note also the location of the Lake of Menteith and the edge of Loch Lomond (blue arrows).

Figure 2.2B – Close up of the location of Flanders Moss, including the surrounding roads and towns

Flanders Moss is also quite remote from centres of population (18 km from Stirling) and is surrounded by small farms and villages. South Flanders and Easter Poldar farms are situated within a 2 km radius of the centre of the bog, the nearest village of Thornhill lies 4 km northeast, while the villages of Kippen and Buchlyvie lie 5 km southeast and 8 km southwest respectively (Figure 2.1A).

2.1.2 Description of sampling site on Flanders Moss

The site chosen for collection of the peat cores was the highest point of the bog, situated ~2 km north west of Easter Poldar farm (indicated by the red arrow in Figure 2.1B). The exact location of the site was Grid Ref. 6309 9819 (OS Landranger Map 57). The entrance to the bog (from the track leading from East Poldar) was marked by a stance of mixed deciduous trees whilst the bog itself supported mostly heather, as well as scattered birch trees (*Betula Pubescens*) (Proctor, 1992) and a range of mosses and lichens (Figure 2.2A). A number of different examples were identified with the aid of a guide to mosses and lichens (Jahns, 2000). These included the moss species *Sphagnum papillosum*, *Sphagnum capillifolium*, *Sphagnum fallax*, and *Polytrichum commune* were identified, together with the lichen *Cladonia potentosa*, and the cranberry plant *Erica vulgaris*.

Figure 2.2A – Photograph of Flanders Moss sampling site, with examples of heather in the foreground and *Betula Pubescens* in the background.

2.1.3 Collection of peat cores from Flanders Moss peat bog

A coring technique was adopted in order to obtain peat from depths down to 1 m from the surface of the bog. Other methods of sample collection, e.g. excavation of a pit, had previously been unsuccessful in obtaining material from depths of greater than 50 cm. Multiple cores, however, were required so that sufficient material could be obtained for all planned experimental and analytical procedures. Thus, eleven cores ~1 m in length were obtained from Flanders Moss on 8th July, 1999, using a Waardenar corer (Waardenar, 1982). This corer consisted of a three-sided box made from galvanised steel (Figure 2.2B), with dimensions 0.05 m by 0.05 m by 1 m. The box had an open base consisting of three blades, which cut three sides of the core as the box was inserted vertically into the peat bog. On the remaining open side of the box, there were two runners, into which a separate cutting blade plate was then inserted to cut the fourth side of the core.

Figure 2.2B – Photograph of Wardenaar corer with extracted peat core

The enclosed core was carefully extracted from the peat bog and immediately laid horizontally on an acid-washed polythene sheet. Only cores that remained wholly intact after removal were retained. The corer was cleaned between consecutive core extractions by inserting both parts of the corer into a waterlogged hollow of peat.

Each peat core was cut with a stainless steel knife into 2-cm depth sections in the field. These sections were placed first into labelled polythene Ziploc bags, and then inside a second, larger Ziploc bag, which was immediately placed in an ice-filled cool box. Powder-free latex gloves were worn throughout the core sectioning procedure.

2.1.4 Peat core designation

On return to the laboratory, equivalent sections (with respect to depth) from five of the cores were bulked, re-bagged, and returned to the cool box, which was placed in a cold store (4 °C). These samples were designated Core 1. Core 2 consisted of two cores bulked together and then stored as described for Core 1. The remaining four cores were simply stored.

2.1.5 Sample storage

The bulked sections for Cores 1 and 2 and the individual sections for the remaining four cores were placed in a freezer (–20 °C) for storage.

2.2 SAMPLE PROCESSING AND ANALYSIS

2.2.1 Cleaning of glassware and plastic equipment

Unless otherwise specified, all equipment (glassware, e.g. Pyrex conical flasks and beakers, and plastic equipment, e.g. polypropylene bottles and centrifuge tubes) was subjected to an acid cleaning procedure. This involved thoroughly rinsing the equipment with tap water to remove any dust or dirt and then with acetone to remove any permanent ink labels. Following this, the equipment was soaked in a solution of Decon 90 overnight to remove any organic material and persistent stains.

On removal from the Decon 90 solution, the equipment was thoroughly rinsed again in tap water to remove all traces of the detergent, and transferred to a 5 M Analar HNO_3 acid bath. The acid bath was covered with cling film, placed on a hotplate and heated at 90°C for at least four hours. Following cooling, the equipment was thoroughly rinsed in de-ionised water to remove all traces of the acid, and then placed in a bath containing de-ionised water. The water bath was also covered with cling film, placed on a hotplate and heated to 90°C for a further four hours.

Upon cooling, the equipment was transferred to a drying cabinet and left overnight. Finally, all equipment was sealed with the appropriate lids or with cling film, put in polythene zip bags, and stored in a cupboard until use.

2.2.2 Sample processing procedures and analyses carried out on Cores 1 and 2 from Flanders Moss peat bog

A flowchart summarising the sample processing and analytical procedures carried out on each of Core 1 and Core 2 is presented in Figure 2.3A and B, respectively. Sections 2.3-7 describe each part of the procedures in more detail.

Figure 2.3A - Flowchart outlining sample processing and analytical procedures for Core 1

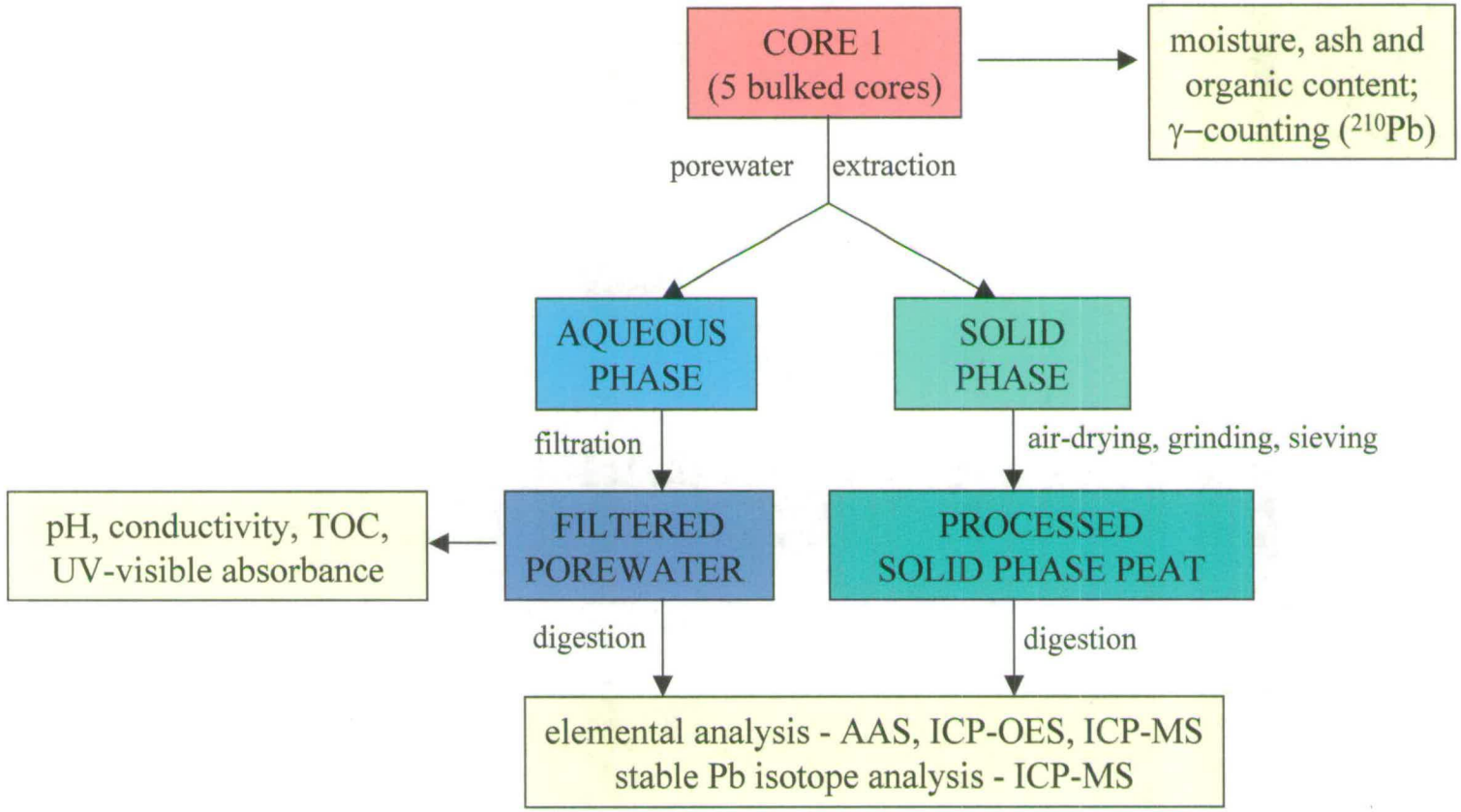

Figure 2.3B - Flowchart outlining sample processing and analytical procedures for Core 2

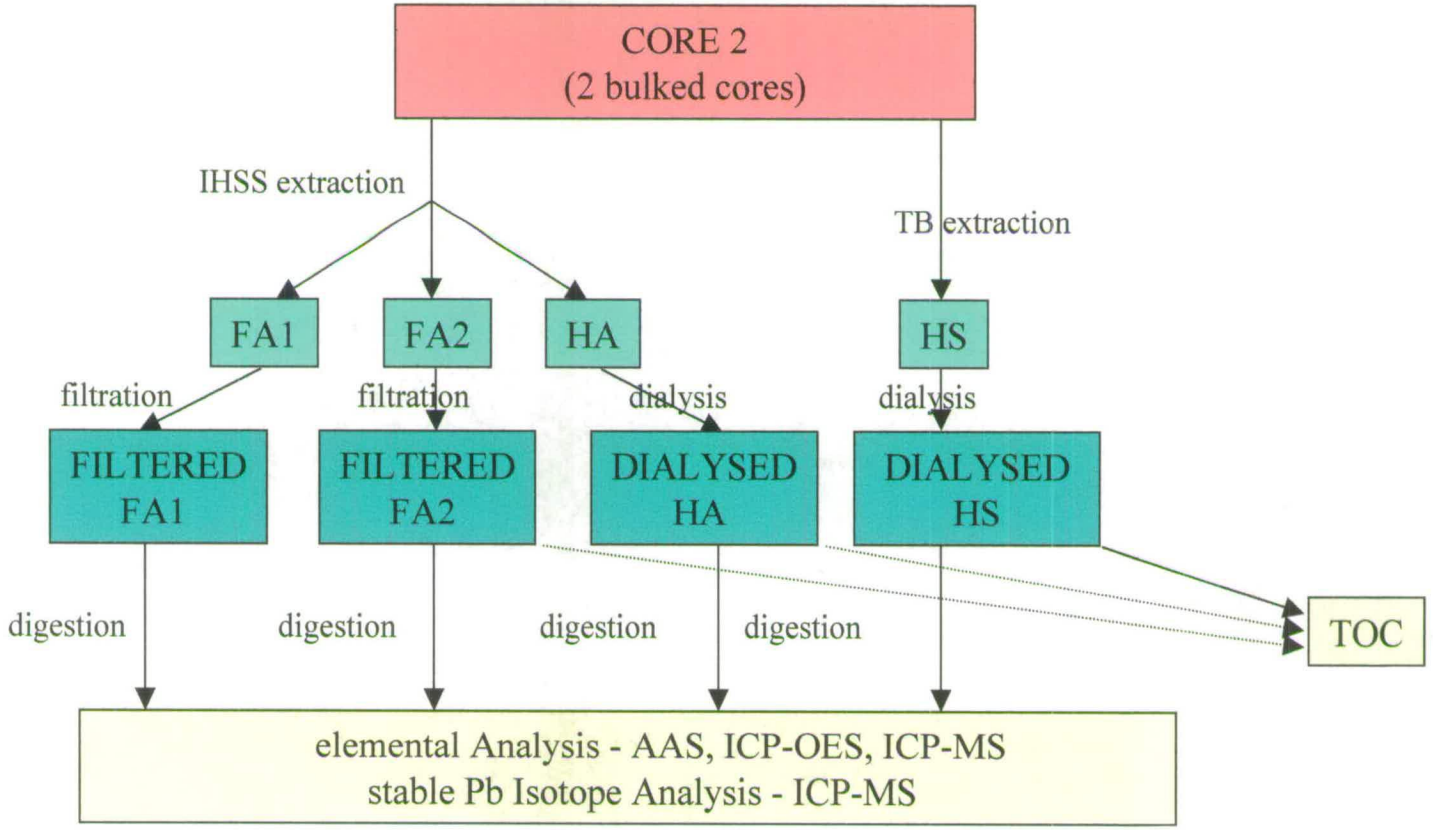

2.3 POREWATERS

2.3.1 Extraction of porewaters

A small hole was cut in the centre of the base of each Sterilin bottle using a sterile, stainless steel scalpel blade. Any polypropylene shavings in the bottle were removed by rinsing out the inside of the bottles with de-ionised water. The bottles were then dried in a drying cabinet, transferred to a desiccator and allowed to cool before weighing.

The bulked 2 cm depth sections from the five cores (designated Core 1) were defrosted overnight. Sub-samples were obtained using a stainless steel apple corer, which was inserted into the centre of each of the core sections. Any root material protruding from the base of the corer was removed. The peat was then transferred into the weighed 30 ml polypropylene Sterilin bottles.

In total, between 10 and 15 grams of the defrosted wet peat was accurately weighed into the bottles, with approximately eight bottles being used for each of the fifty 2 cm sections of the core. Each Sterilin bottle (minus lid) was placed inside a 50 ml polypropylene centrifuge tube (Figure 2.4).

The centrifuge tubes were sealed with polypropylene screw caps and spun in a centrifuge at 4000 rpm for 10 minutes. The bottles were removed and the extracted pore waters were transferred to a second set of centrifuge tubes. The bottles containing the residual peat were returned to the original centrifuge tubes and spun for a further 10 minutes at 6000 rpm (Figure 2.5). After the second centrifugation, the residual peat remaining in the bottles was loosely covered with cling film and air-dried (see Section 2.4.1).

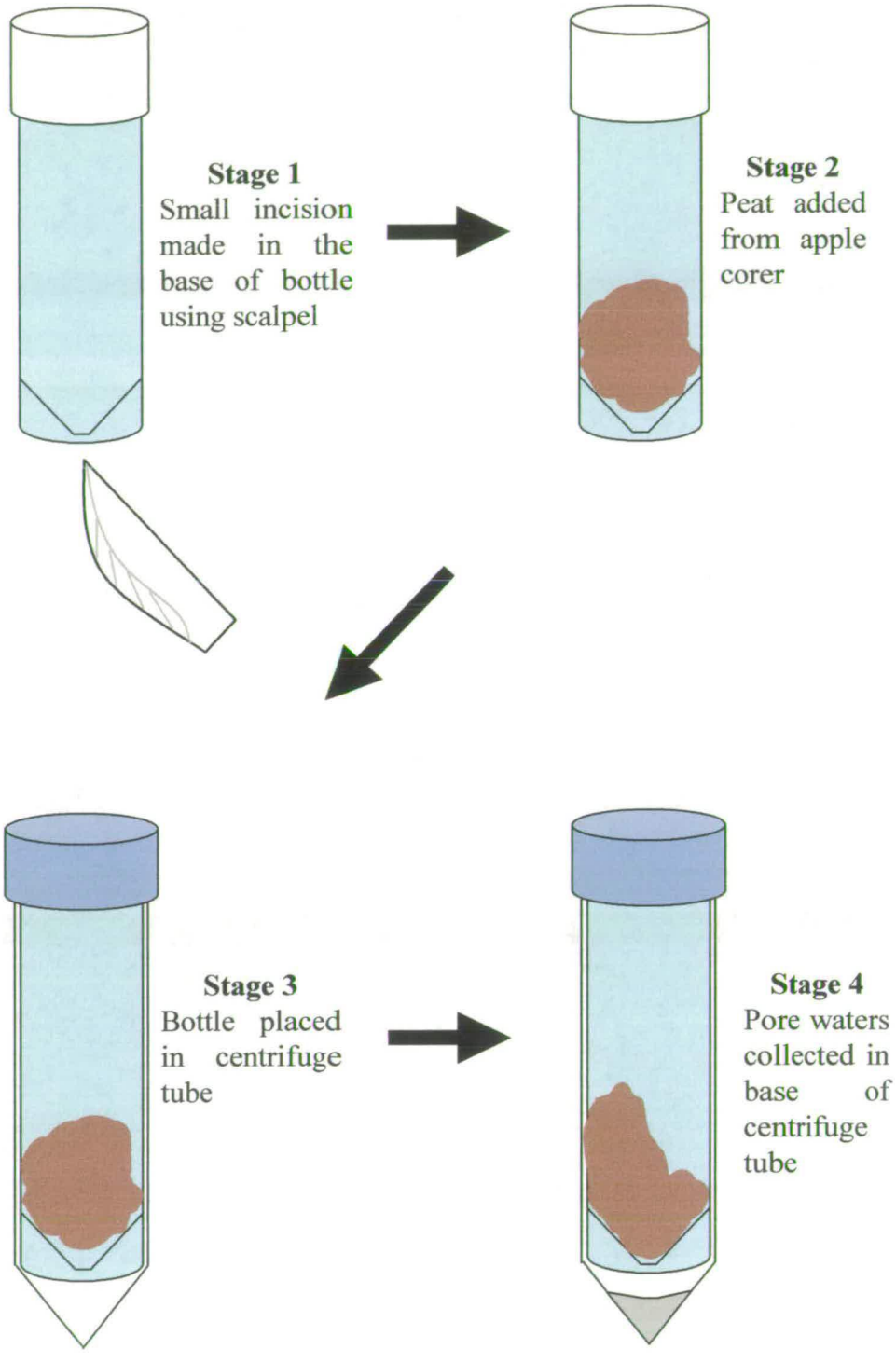

Figure 2.4 – Diagram showing the equipment used to extract the porewaters from Core 1

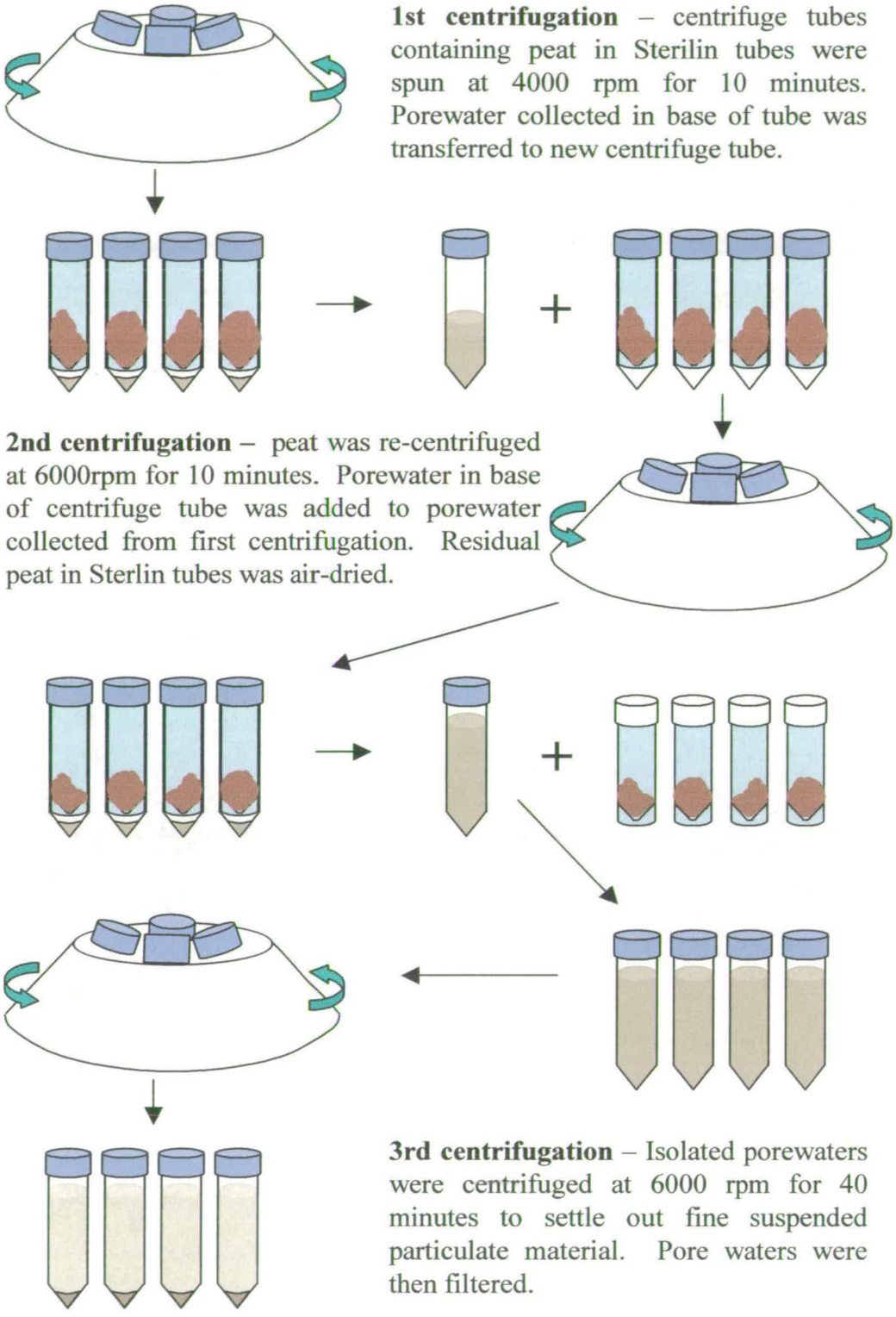

Figure 2.5 - Diagram showing porewater extraction methodology

2.3.2 Filtration of porewaters

The porewaters from the second centrifugation were combined with those isolated from the first centrifugation. The combined porewaters (~ 30-35 ml) were spun at 6000 rpm for 40 minutes to remove the remaining particulate material (Figure 2.5). The combined porewaters were then carefully transferred to a Nalgene polycarbonate filtration system and filtered under vacuum through a 0.2 μm Whatman cellulose nitrate filter paper. The filtered porewaters were transferred to set of Sterilin bottles and stored at 4 °C.

2.3.3 Subdivision of porewater samples and sample preparation procedures

For each of the pore waters, a 13 ml sub-sample was transferred into a 15 ml Corning centrifuge tube for TOC analysis. A further sub-sample of 5 ml was retained for measurements of pH, conductivity, and UV absorbance. The remainder of each pore water sample (~ 15 ml) was acidified to pH < 2 with the addition of 100 μl 16 M Aristar HNO_3 to produce a 2% (v/v) HNO_3 solution for elemental analysis by AAS, ICP-OES or ICP-MS. The acidification procedure was carried out in accordance with the U.S. EPA Method 6010B for "Determination of trace elements in solution using Inductively Coupled Plasma-Atomic Emission Spectrometry".

Following the acidification step, however, precipitation (presumably of humic acids) was noted to have occurred in several of the pore water samples. An additional digestion procedure was required before the samples could be analysed.

2.3.4 Porewater digestion procedure

The digestion utilised the remaining solution (i.e. 15ml) of each of the acidified pore water samples. The acidified pore water volumes were determined gravimetrically prior to digestion by weighing a set of empty Sterilin bottles, and then reweighing the bottles filled with the samples. The samples were transferred to Teflon beakers which were placed on a hotplate. The volumes of the samples were reduced to less than 5 ml. The sample and washings (2% (v/v) Aristar HNO_3) were transferred into Teflon microwave digestion tubes. The volume of the samples was made up to 10 ml using the 2% (v/v) Aristar HNO_3 acid. Five ml of 16 M Aristar HNO_3 was also added to each of the tubes to give a total volume of 15 ml.

The digestion method (Table 2.1) was based on the U.S. EPA Method 3015 ("Microwave-assisted digestion of aqueous samples and extracts"). A smaller total solution volume than the recommended 45 ml was used because of the presence of the organic precipitates (section 2.3.3). This increased the reactivity of the sample in the microwave tube. The smaller total volume also avoided the unnecessary dilution of the pore waters which could have increased elemental concentrations in the sample blanks from added digestion reagents.

Table 2.1 - Microwave digestion parameters for porewater samples

Parameters	Values for porewater samples
Total volume	15 ml
Volume of Aristar HNO_3	5 ml
Ramp time	25 mins
Maximum ramp pressure	180 psi
Hold time	5 mins
Maximum temperature	210°C

Following digestion and cooling, the samples were returned to the Teflon beakers (the same beakers as had been used previously, thereby minimising any contamination of the original samples) and reheated until the volume was reduced to near dryness. The samples were then transferred (with 2% (v/v) Aristar HNO_3 washings) to pre-weighed 15 ml polypropylene centrifuge tubes, which were made up to the 15 ml mark with 2% (v/v) Aristar HNO_3. The exact final volume was determined by weighing the tubes once full, the weight of solution then being converted to yield a volume (Appendix 9.1). A 10 ml aliquot of these samples was analysed using ICP-MS (Section 2.6.3).

2.3.5 pH measurements

The pH measurements were made using a BDH pHase electrode (Merck, UK), which was first standardised using three buffer solutions (pH 4, 7 and 9.2) made up from Fisher buffer tablets. The electrode was placed in the porewaters (in Sterilin tubes), which were swirled around the electrode. The pH readings were allowed to stabilise for at least 20 seconds and then recorded.

2.3.6 Conductivity measurements

Conductivity measurements were made using a Jenway Model 4200 Conductivity Meter (Jenway Ltd., UK). This was standardised with 1 M, 0.1 M and 0.01 M solutions of KCl respectively, against the corresponding conductivities, specified in the manufacturer's manual. The probe was placed in each of the porewater samples and allowed to equilibrate for 2 minutes before the conductivity (μS) was recorded.

2.3.7 UV-visible absorbance measurements

A sub-sample of the pore water was placed in a disposable cuvette and the absorbance relative to that of de-ionised water in a reference cell measured in a Unicam UV2-100 UV spectrometer (Thermospectronic, UK).

A scan of the spectrum from wavelengths of 250 to 750 nm was taken for each sample, and the specific absorbances at 254, 465 and 665 nm recorded. The absorbance at 254 nm was used as a measure of the concentration of organic matter in solution, (Chen *et al*,1977).

2.3.8 Dissolved organic carbon (DOC) measurements

The organic carbon concentration of the porewaters was determined via non-dispersive IR spectrometric measurements of CO_2 from sodium persulfate oxidation of the organic carbon remaining after initial acidification with phosphoric acid, using a Model 700 Total Organic Carbon Analyser (O.I. Analytical, USA). By strict definition, the isolation of the porewater extracts entails that the organic carbon represented both dissolved and colliodal organic carbon, although for the purposes of this study, and for simplicity, the total colloidal and dissolved organic carbon present in the porewaters will be referred to as Dissolved Organic Carbon (DOC).

2.4 SOLID PHASE PEAT

2.4.1 Air-drying, grinding and sieving

The residual peat material from the pore water extractions (Figure 2.5) was allowed to air dry over several weeks. The dried material was then ground into a fine powder using a porcelain mortar and pestle. The ground material was repeatedly passed through a stainless steel < 2 mm particle size sieve, with all the retained material being reground until it passed through the sieve. Root material and shards of quartzite that didn't pass through the sieve were discarded. The final ground samples (< 2 mm) were stored in labelled polythene zip-bags.

2.4.2 Preparation of samples for γ-counting (^{210}Pb)

The activity of ^{210}Pb in sub-samples of peat from Core 1 (5 bulked cores) was determined by γ-spectrometry. The sub-samples comprised the remainder of peat from each 2-cm depth section that had not been used for the pore water extraction (Figure 2.3a). The air-drying, grinding and sieving of this material was identical to that described above in Section 2.4.1. Again, any root material not passing through a 2 mm sieve was removed. The weight of each of the processed samples was accurately determined. For samples in the weight range 2-5 g the entire sample was used for analysis, but for larger weights either 5 or 10 g was used depending on the amount of material available. The 5 g and 10 g samples were pressed into discs using a hydraulic press and were sealed in polystyrene containers by Araldite. Samples with weights of less than 5 g were too small to be pressed into discs and, in these cases, the sample was compressed into the polystyrene container and held in position by tissue paper and the container was then sealed with Araldite. After sealing, the containers were left for a period of at least 21 days before analysis in order to allow ^{222}Rn to grow in secular equilibrium with ^{226}Ra.

Analysis was performed using an EG & G Ortec LoAx planar intrinsic Ge gamma photon detector housed inside a graded shield comprising 10 cm of Pb lined with Cd and Cu. Each sample was placed inside an annular plastic holder, which accurately located it on the window of the detector.

In order to obtain acceptable counting statistics, the analysis times varied between three days and seven days depending upon the sampling size and the specific activities of the radionuclides of interest. Detection efficiencies were determined using a series of standards produced by addition of known activities (traceable to Harwell primary standards) of ^{210}Pb and ^{226}Ra (and ^{137}Cs) to peat samples from a horizon that contained no detectable, unsupported ^{210}Pb (or ^{137}Cs). Standards of weights 2, 3, 4, 5 and 10 g were used to determine detection efficiencies for the range of sample and appropriate corrections were recorded before and after analysis of the suite of samples and appropriate corrections were made to all sample count rates.

Gamma spectra were recorded using an EG & G Ortec 919 ADCAM unit interfaced to a PC running the EG & G GammaVision software package. Evaluation of peak areas was performed by manual calculation. An example of this calculation is contained in Appendix 9.2.

2.4.3 Moisture, organic matter and ash content determination

The moisture content was obtained using sub-samples of Core 1 (not used for pore water extraction). Triplicate samples, each of ~ 1 g, of the 2 cm depth sections were accurately weighed into porcelain crucibles. The crucibles were covered with porcelain lids and placed in a Carbolite muffle furnace (Model GSM 11/8), in batches of 15, at 110 °C for 12 hours. The furnace was then switched off and the crucibles allowed to partially cool, whereupon they were transferred to a desiccator (filled with silica gel) and allowed to cool to room temperature. The crucibles were then reweighed. The crucibles were repeatedly returned to the furnace and reheated at 110 °C for a further 12 hours, until there was no change in the final weight of the crucible between runs. The difference between the final weight and the original weight was taken to be the moisture content (Sparks, 1988).

In order to obtain the organic matter and ash content, the crucibles were returned to the muffle furnace and heated at 450 °C for 12 hours. The cooling procedure as described above was again used, before the samples were reweighed. As above, the heating procedure was repeated, until a constant weight for the crucibles was achieved. The difference between the weight after heating at 110 °C and the weight after heating at 450 °C was taken to be the weight of organic matter, and the difference between the weight after heating at 450 °C and the weight of the crucible was taken to be the weight of ash.

2.4.4 Digestion of peat for pseudo-total elemental analysis

The method used was based on the US EPA Method 3051 for the microwave digestion of soils, sludges and sediments. This was preferred to Method 3052, as it did not involve the use of hydrogen peroxide, which, during earlier work, had resulted in elevated elemental concentrations in sample blanks.

Triplicate 0.5 g samples of the ground, air-dried residual peat material (Section 2.4.1) were accurately weighed out into 100 ml Pyrex beakers. To reduce the organic content the beakers were placed in the muffle furnace for 8 hours at 450 °C, prior to digestion. On removal, after partial cooling, the samples were immediately placed in a desiccator and allowed to cool to room temperature. De-ionised water (10 ml) was used to transfer all of the ash from the beakers into the Teflon microwave digestion tubes. To each of the tubes, 10 ml 16 M Aristar HNO_3 was added, and the tubes placed in the CEM Mars 5 microwave digestion unit. The digestion program used is shown below in Table 2.2.

Table 2.2 - Microwave digestion parameters for peat samples

Parameters	Values for peat samples
Total volume	20 ml
Volume of Aristar HNO_3	10 ml
Ramp time	20 mins
Maximum ramp pressure	160 psi
Hold time	15 mins
Maximum temperature	210°C

Following digestion, the samples were filtered through Whatman No 542 hardened ashless filter papers into pre-weighed 50 ml centrifuge tubes. The tubes were weighed and the solution volume made up to the 50 ml mark using de-ionised water. In order to determine the exact final solution volumes, the weights of the full centrifuge tubes were recorded. Subtracting the initial weights of the empty centrifuge tubes yielded the weights of the digest solutions (Appendix 9.1). The addition of de-ionised water reduced the Aristar HNO_3 concentration in the solutions from 50% (v/v) to 10% (v/v), to provide a lower background concentration of acid (and hence lower blanks) for analysis. The solutions were stored in the fridge (4°C) until elemental analysis could be conducted.

2.5 HUMIC AND FULVIC ACID EXTRACTION USING INTERNATIONAL HUMIC SUBSTANCES SOCIETY METHODOLOGY

2.5.1 Sample preparation

The bulked 2 cm depth sections from the two cores (designated Core 2) were defrosted overnight. Humic and fulvic acids were extracted from a 10 g portion of the wet peat from each section which was accurately weighed into a 250 ml screw-top Pyrex conical flask. The extraction method used was a modified version of the International Humic Substances Society (IHSS) extraction procedure (Swift, 1988) and is summarised in the flowchart in Figure 2.6. Sections 2.5.2-2.5.4 describe each step in the extraction procedure in more detail.

2.5.2 Isolation of fulvic acid fraction 1 (FA1) from Core 2 samples

To each conical flask, 50 ml of 0.1 M Analar HCl acid was added. The conical flasks (x 6) were placed on a wrist-action shaker for 1 hour. The contents of each flask were allowed to settle before decanting into two 50 ml centrifuge tubes, which were centrifuged at 6000 rpm for 15 minutes. The solutions were then carefully decanted into a fresh set of centrifuge tubes (Figure 2.7).

The acid-soaked residues of peat material were re-centrifuged, and the supernatant again removed. The solutions were combined with the solution previously isolated. The combined acid solutions were re-centrifuged to remove floating debris. The extracted solutions were transferred into polypropylene Nalgene filtration units and filtered through a 0.2 μm Teflon filter. These were then labelled as FA1 extract solutions.

2.5.3 Isolation of fulvic acid fraction 2 (FA2) from Core 2 samples

The residual peat materials from the isolation of FA1 were washed back into the conical flasks with 50 ml aliquots of 0.1 M NaOH (Figure 2.8).

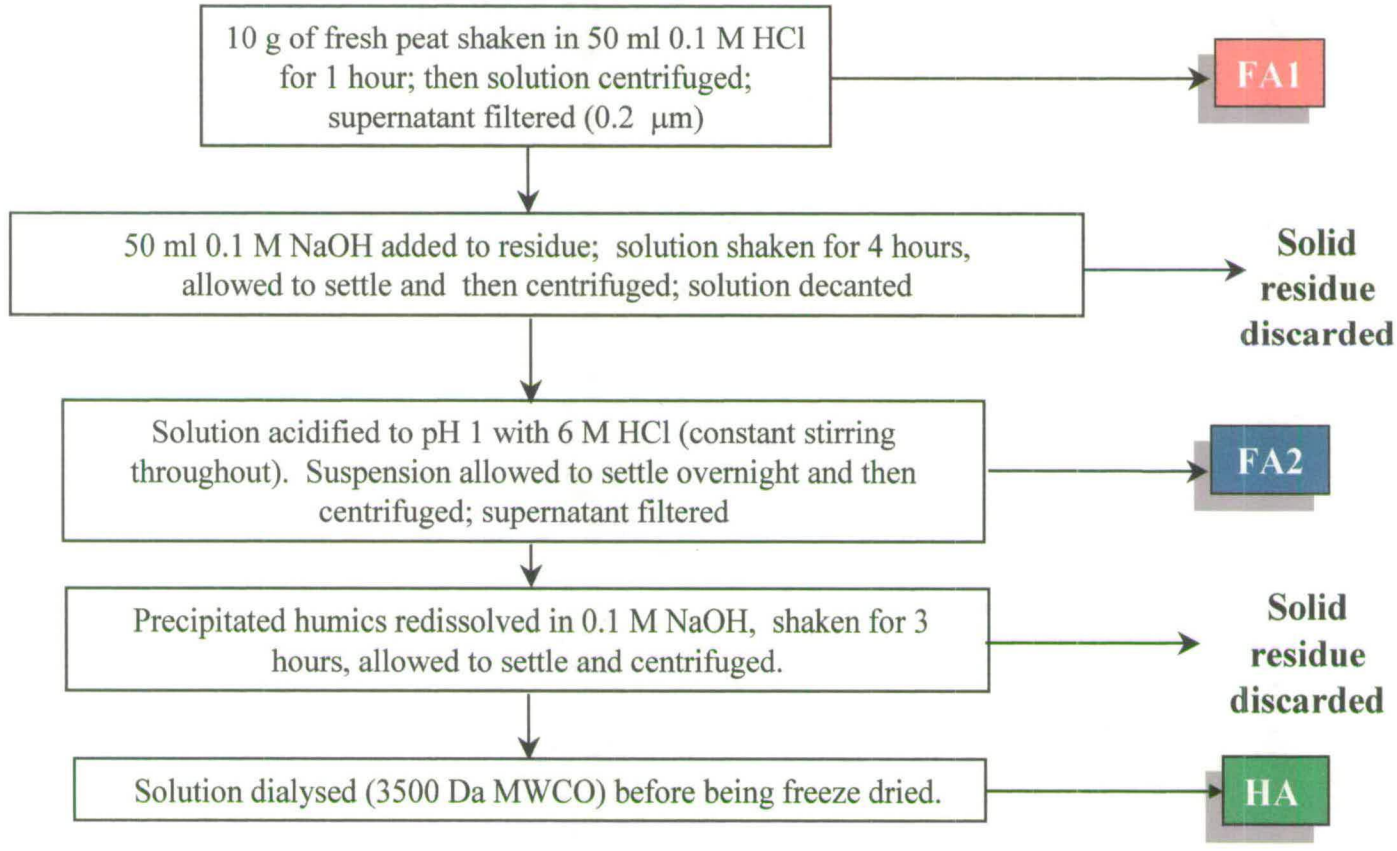

Figure 2.6 - Modified IHSS Method for extraction and purification of FA1, FA2 and HA from Core 2

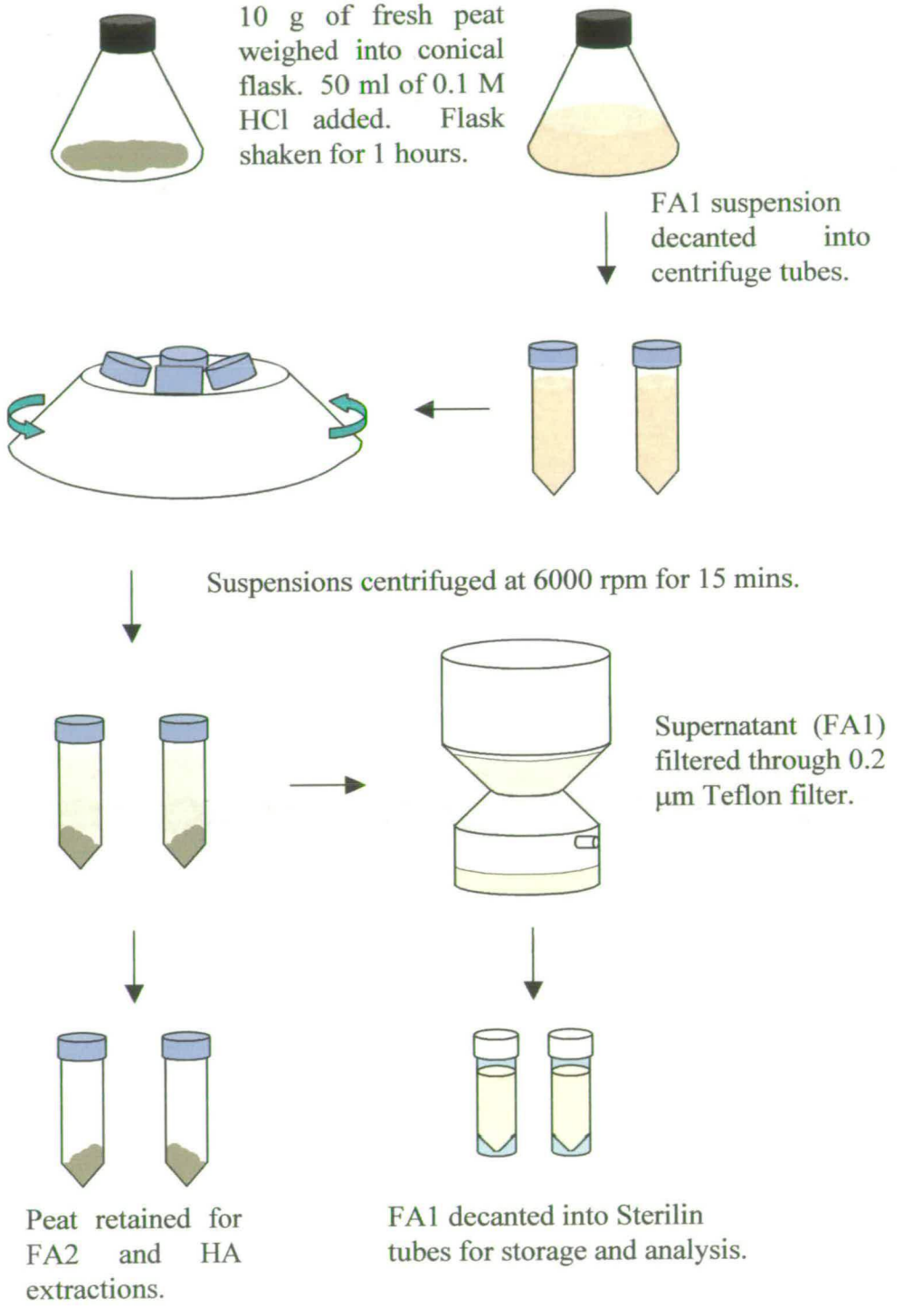

Figure 2.7– Diagram illustrating FA1 extraction from Core 2

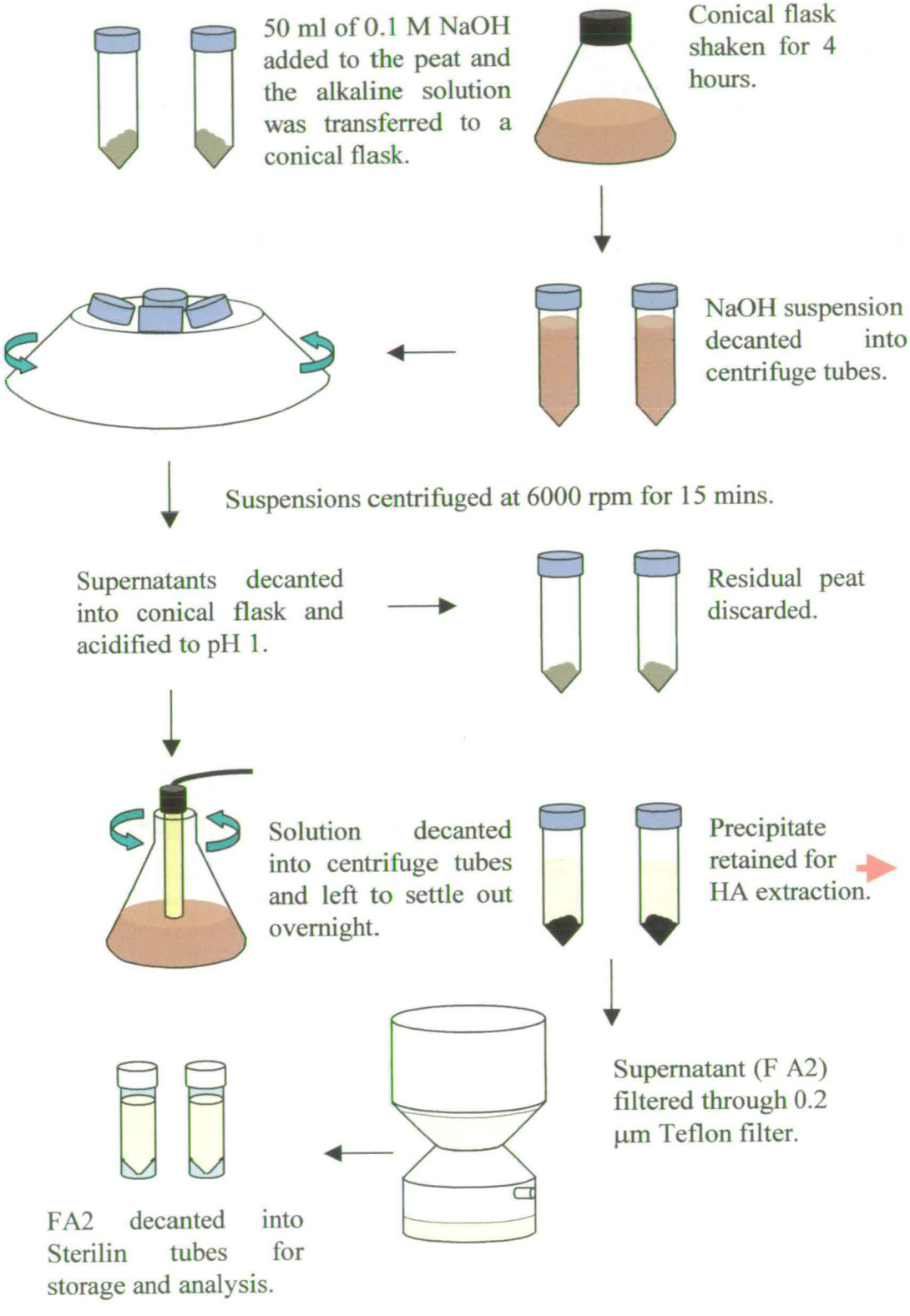

Figure 2.8 – Diagram illustrating FA2 extraction from Core 2

Nitrogen gas was bubbled through the 0.1 M NaOH to purge the solution of oxygen. The conical flasks containing the NaOH-humic suspension (under a nitrogen atmosphere) were placed on a wrist-action shaker for 4 hours. On removal from the shaker the solutions were decanted into two centrifuge tubes and centrifuged at 6000 rpm for 15 minutes.

The supernatants from the centrifuge tubes were decanted into Pyrex conical flasks. A pre-calibrated pH probe was placed in the supernatant in the flasks, which were swirled vigorously. The pH of the solution was lowered to 1 with the drop-wise addition of 6 M HCl, under constant stirring. The acidified solutions were transferred to centrifuge tubes and left overnight to allow the humic acid precipitate to settle out of solution.

The supernatants of the acidified humic suspensions, designated as fulvic acid fraction 2 (FA2), were decanted into Sterilin bottles and filtered through 0.2 μm filters in the same manner as described for FA1. The settled out humic acid precipitate was retained for the next stage (Section 2.5.4).

A subsample of each of the FA2 extracts was analysed for DOC following the procedure outlined in Section 2.3.8.

2.5.4 Isolation of the humic acid fraction (HA) from Core 2 samples

The acidified Humic Acid precipitates (Section 2.5.3) were washed into conical flasks with 50 ml of 0.1 M NaOH (Figure 2.9), and the flasks were purged with nitrogen gas as described in Section 2.5.3. The conical flasks were placed on a wrist-action shaker for a further 3 hours. The alkaline solutions were removed from the shaker, transferred to centrifuge tubes and centrifuged for 30 minutes at 6000 rpm. Using Pasteur pipettes the solutions were transferred to Spectropor Biotech regenerated cellulose dialysis tubing, with a molecular weight cut-off (MWCO) of 3500 Daltons.

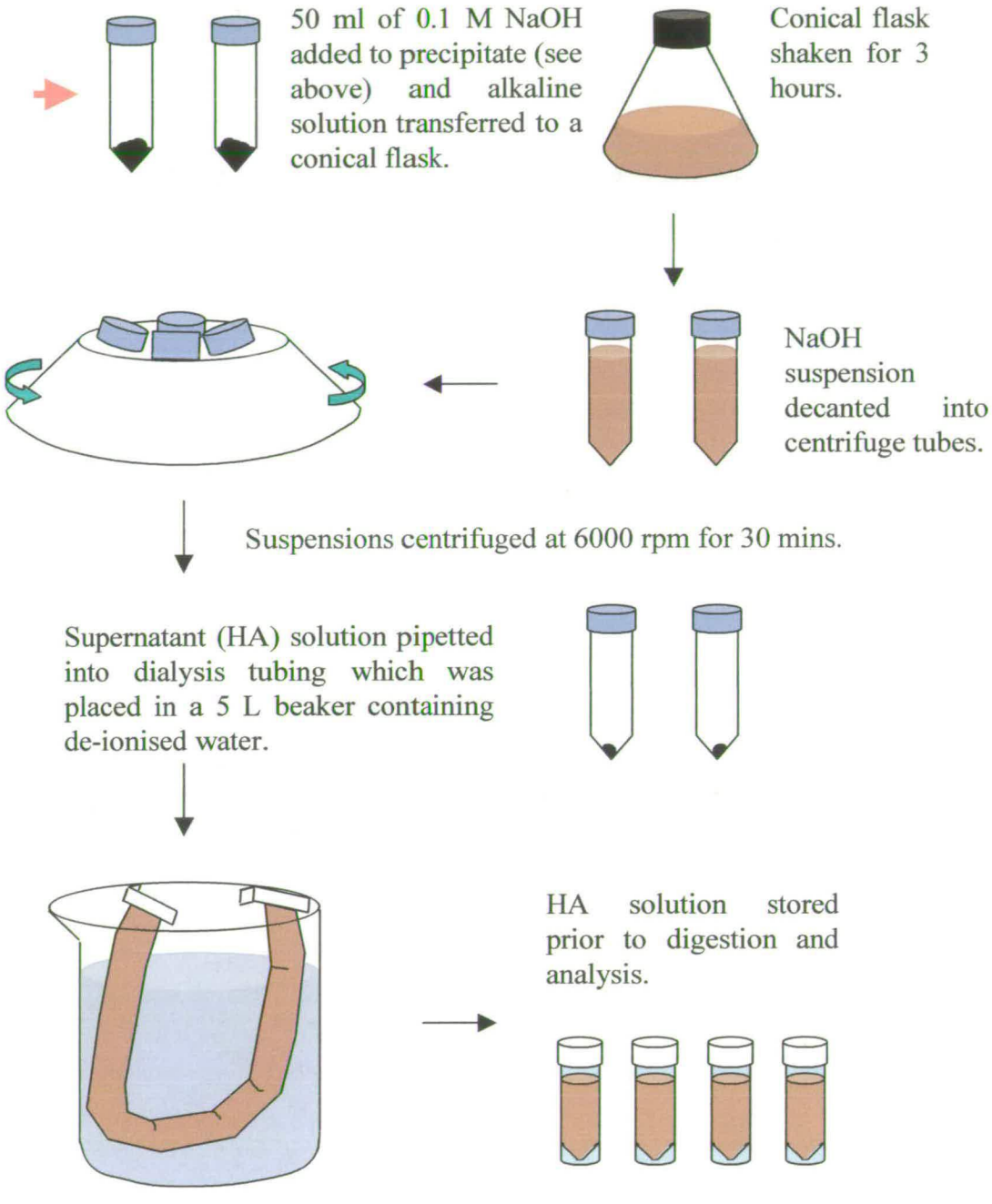

Figure 2.9 – Diagram illustrating HA extraction from Core 2

2.5.5 Dialysis of the humic acid fraction (HA) extracted from Core 2 samples

Prior to use, the dialysis tubing was cut into sections of about 20-30 cm in length and soaked in de-ionised water to remove any trace of preservatives. Upon removal from the water, the sections of tubing were sealed at one end with a dialysis clip. The HA solutions (Section 2.5.4) were carefully pipetted into the open ends of the sections of tubing, which were folded down, trapping a small bubble of air above the humic solution. The folded end of the tubing was then sealed with a dialysis clip, and the sealed tubes were carefully folded into a U-shape. During folding, the air bubbles in the tubing were forced to either end of the sealed tubes. The folded tubes were placed into large, clean Pyrex beakers, which were then filled with de-ionised water to a level just below the position of the air-bubbles in the tubes (Figure 2.9). This minimised the risk of solution leakage through the clips, by raising them above the water level. The water in the beakers was initially changed every 3 hours, and then every 6 hours, for the first 3 days. The pH of the dialysis waters were monitored using a BDH Gelplas electrode connected to a Griffin pH Meter Model 50.

When the pH of the de-ionised water bath remained below pH 5.5 for more than twelve hours after the last change of the water bath, it was assumed that the concentration of NaOH inside the dialysis tube had sufficiently diminished. The dialysis tube was removed from the bath, the clip removed from one end, and the humic solution carefully transferred into a set of pre-weighed Sterilin bottles. The bottles were reweighed, and the difference in weight was used to calculate the volume of the HA. A 10 ml aliquot of each of the dialysed humic solutions was digested (Section 2.6.3), with the remaining solutions being frozen in preparation for freeze-drying (Section 2.6.4).

2.6 HUMIC SUBSTANCE EXTRACTIONS USING A MILDER AQUEOUS SOLVENT (0.045 M TRIS-BORATE; pH 8.5)

2.6.1 Isolation of humic substances (HS) from Core 2 samples

As with the IHSS extraction method, 10 g portions of wet peat from the two bulked cores designated Core 2 were accurately weighed into 250 ml screw-top conical flasks. A 10 L solution of 0.045 M Tris-Borate (TB) was prepared by dissolving 54.5 g of tris(hydroxymethyl)aminomethane and 27.9 g of boric acid in 10 L of de-ionised water. A 50 ml aliquot of the Tris-Borate solution was added to each of the conical flasks containing the peat. The flasks were then purged with nitrogen and placed on a wrist-action shaker for 4 hours.

On removal from the shaker, the contents of the flasks were carefully decanted equally into two 50 ml polypropylene centrifuge tubes. These were placed in a centrifuge and spun at 6000 rpm for 15 minutes. The solutions from both tubes were carefully pipetted into a fresh set of centrifuge tubes, using a Pasteur pipette. Both initial tubes containing the peat residue were returned to the centrifuge and the procedure was repeated. Following the removal of the supernatant as before, the residue from the second tube was added to that in the first centrifuge tube. The residue was re-centrifuged for a final time and the final aliquot of separated solution added to the previous extracts. The extracted solutions were then centrifuged for 15 minutes at 6000 rpm to remove any suspended colloids transferred with the liquid.

2.6.2 Dialysis of humic substances (HS) extracted from Core 2 samples

The centrifuged solutions were transferred immediately to dialysis tubing following the final centrifugation step. The dialysis tubing used was the same as the tubing used in the dialysis of the humic acid extracts, namely Spectropor Biotech regenerated cellulose membranes with a MWCO of 3500 Daltons.

As with the dialysis of HA, the HS solution was emptied from the dialysis tubing after the pH had remained below pH 5.5 for a period of more than 12 hours after the last change of de-ionised water in the beaker. The HS solutions were again transferred to a set of pre-weighed Sterilin tubes. Once full, these tubes were weighed and the final dialysis volume was calculated from the weight difference (Appendix 9.1).

2.6.3 Digestion of HS (and HA) extracts

The HS (and HA) solutions contained too much organic matter for them to undergo elemental analysis directly. Reduction of the organic content of the extract solutions was required prior to analysis but the addition of H_2O_2 was not favoured for the reasons described in Section 2.4.4. The easiest method for reducing the organic content was a digestion of a portion of each solution.

Table 2.3 - Microwave digestion parameters HS (and HA) extracts

Parameters	Values for HS (and HA) extracts
Total volume	10 ml
Volume of Aristar HNO_3	5 ml
Ramp time	15 mins
Maximum ramp pressure	180 psi
Hold time	10 mins
Maximum temperature	210°C

Aliquots (5 ml) of the humic solutions were pipetted into the Teflon microwave tubes and 5 ml of concentrated HNO_3 was added from a measuring cylinder. The digestion program used is displayed in Table 2.3. After the Teflon tubes were removed from the microwave and allowed to cool, the digest solutions were transferred to Sterilin bottles for storage until analysis. The tubes were not weighed at this stage, as the volume of the digest solution was still 10 ml (i.e. there was no loss of sample during the digestion, and there was a complete transferral of the samples from the digestion vessels to the Sterilin tubes).

2.6.4 Freeze-drying of HS (and HA) solutions

The remainder of the HS (and HA) solutions, which had not been digested, were frozen (–20 ^{o}C). The bottles containing the frozen HS (and HA) solutions were removed from the freezer and left at room temperature for 15- 20 minutes prior to use, to allow the outsides of the frozen samples to melt, whilst the central core of each sample remained frozen. This aided in the degassing of the sample. With the entire sample in one cylindrical block of ice, the only way for air to escape from the degassing sample was through the frozen sample, which often caused the entire cylindrical block of ice to be forcibly ejected from the Sterilin container. This not only resulted in possible contamination of the sample, but also mixing of the samples. In order to negate this event from occurring, it was found that if the sample was partially melted, the degassing air was afforded an easy escape from the sample, and did not cause sample ejection.

The plastic lids were taken off the Sterilin bottles and the bottles placed twelve at a time in a polycarbonate chamber. Three of these chambers were attached to the E-C Modulyo freeze-drier, which was connected to an Edwards EV 5 vacuum pump. The freezer unit was turned on half an hour prior to use and the temperature was allowed to fall below –40 ^{O}C. The vacuum was initialised and the valves on each of the chambers were opened slightly to allow degassing of the partially frozen humic samples. After a period of 10 minutes, the valves were fully opened.

The freeze-drier was left on for 2-3 days, after which time the vacuum was disengaged. The samples were removed and shaken, a rattling sound being produced by residual ice. If any ice was present, the samples were returned to the freeze-drier. If no ice was present, the samples were re-sealed with the original lids, and weighed. This weight minus the original weight of the Sterilin tube gave the total weight of the freeze-dried sample. This was used to calculate the concentration of humic material extracted (see Chapter 3).

2.7 ELEMENTAL ANALYSIS

2.7.1 Flame Atomic Absorption Spectrometry (FAAS)

The concentration of Pb in solid phase peat and porewater digest solutions, FA1 and FA2 extracts and digested HA and HS extracts was obtained by flame atomic absorption spectrometry (FAAS). These analyses were performed on a Pye Unicam SP9-800 and an ATI Unicam Model Solaar 929 atomic absorption spectrometer. The FAAS analyses were necessary to screen the concentration range of the samples, so that appropriate dilutions could be carried out prior to further analysis, e.g. by ICP-MS. FAAS was also the preferred method for determining the concentration of Pb (particularly at low concentrations) because there were also potential interferences affecting determination by ICP-OES. The instrumental conditions for these analyses are shown in Table 2.4.

Table 2.4 – Instrumental parameters used for analysis by FAAS

Element	Lamp current (mA)	Wavelength (nm)	Burner type	Angle of Burner Rotation	D_2 Background Correction
Pb	10	217.0	50 mm	0	YES

Standards for calibration of the instrument were prepared from 1000 mg/L m lead nitrate solution (Fisher Scientific, UK). All standards were prepared in an identical reagent matrix to that of the samples being analysed. At least three concentration standards and a zero concentration blank were used in each calibration, and only calibrations with a least-squares linear correlation co-efficient of more than 0.995 were accepted.

2.7.2 Multi-element analysis by Inductively Coupled Plasma-Optical Emission Spectrometry (ICP-OES)

Following single-element analysis for Pb by FAAS, the samples were analysed by inductively coupled plasma-optical emission spectrometry (ICP-OES). The TJA IRIS instrument (ThermoElemental, USA) was used in this study. The solutions were analysed for the following elements:

- Aluminium
- Barium
- Calcium
- Copper
- Iron
- Potassium
- Magnesium
- Manganese
- Sodium
- Phosphorus
- Lead
- Sulphur
- Strontium
- Titanium
- Zinc

Due to the number of different elements simultaneously determined using the ICP-OES, it was unrealistic to calibrate 3 or 4 individual concentration standards for each individual element. Four multi-element solutions were used for calibrations, and the associations were decided according to the expected similarity of concentration of the elements in the various samples analysed. The element groupings used are shown in Table 2.5.

Table 2.5 - Multi-element groupings for ICP-OES standards

	Elements
Multi-element solution 1	Aluminium (Al), Copper (Cu), Lead (Pb), Strontium (Sr), Titanium (Ti)
Multi-element solution 2	Phosphorus (P), Sulphur (S)
Multi-element solution 3	Barium (Ba), Calcium (Ca), Potassium (K), Magnesium (Mg), Sodium (Na)
Multi-element solution 4	Iron (Fe), Manganese (Mn), Zinc (Zn)

A 100 mg/L stock solution of each of the four multi-element solutions was prepared by pipetting 1 ml of each of the individual 1000 mg/l Fisher stock solutions into a Sterilin tube and making the total volume up to 10 ml with further incremental 1ml additions of the reagent matrix (e.g. 10% (v/v) Aristar HNO_3). Each of the stock solutions was weighed to provide a very precise standard concentration.

The concentration standards for each sample run were made up from the 100 mg/L stock solutions (Figure 2.10), which were refrigerated between runs. When the stock solutions ran out, a fresh set was made up. The comparability was checked using the internal calibration on the instrument. The concentration of standards used for the calibrations varied according to the expected concentration range of the analyte elements analysed. A full list of the concentrations used is provided in Table 2.6.

Figure 2.10 - Flowchart showing standard preparation for ICP-OES analysis

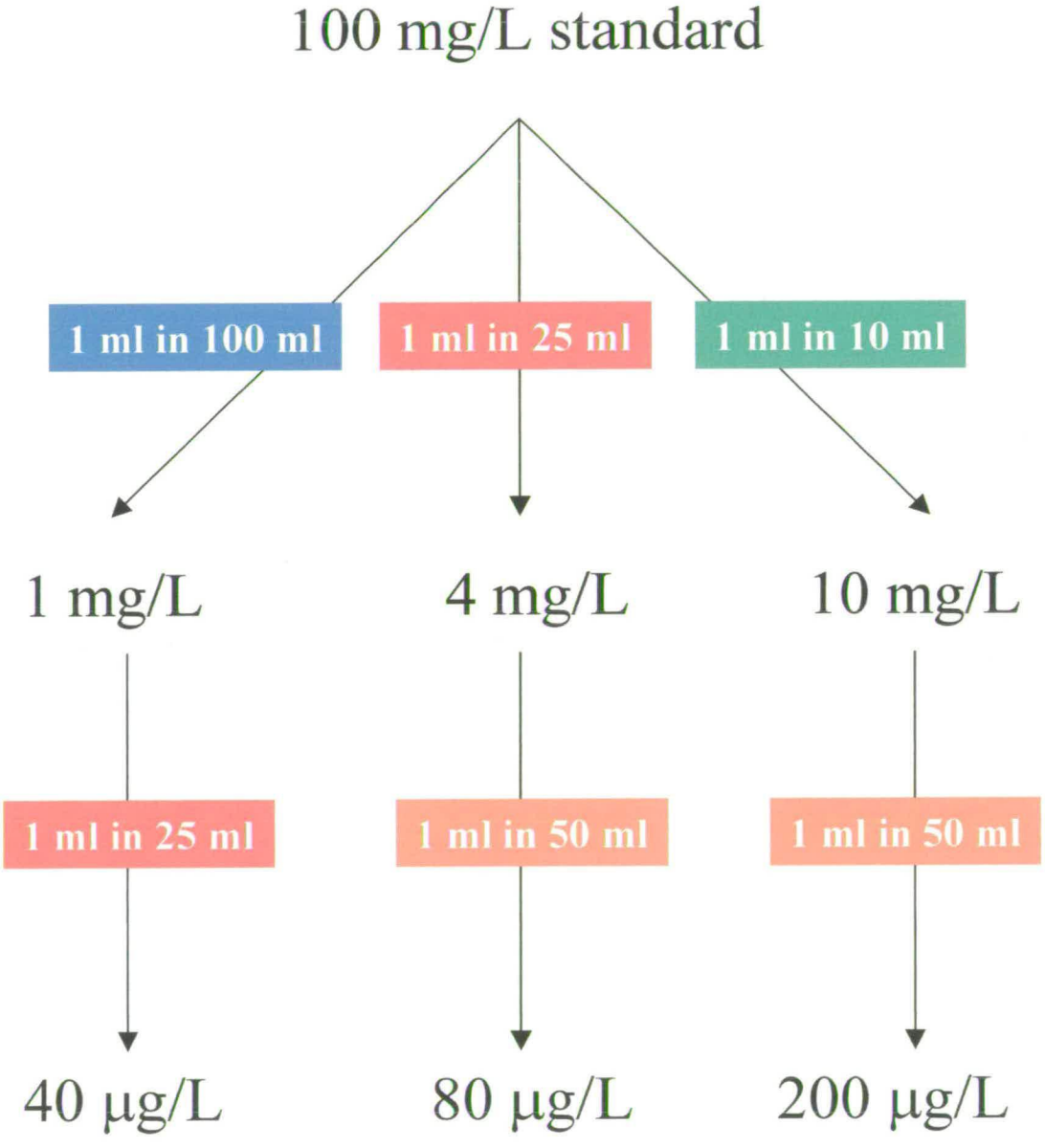

Table 2.6 – ICP-OES calibration standard concentrations

Analysis	Solution Matrix (v/v)	Standard Concentration (mg/L)			
		Solution 1 standards	Solution 2 standards	Solution 3 standards	Solution 4 standards
Digested porewaters	2% HNO_3	0.04, 0.2, 1, 10	0.4, 2, 10	0.04, 0.2, 1, 10	0.04, 0.2, 1, 10
Digested solid phase peat	10% HNO_3	0.04, 0.2, 1, 10	0.2, 2, 10	1, 4, 10	0.1, 1 10
FA1	0.1 M HCl	0.04, 0.08, 0.2, 1, 4	0.2, 1, 10	0.08, 0.2, 1, 4, 10	0.08, 0.2, 1, 4
FA2	0.1M HNO_3	0.04, 0.08, 0.2, 1, 4	0.2, 1, 4, 10	0.08, 0.2, 1, 10	0.04, 0.08, 0.2, 1, 10
Digested HA	50% HNO_3	0.04, 0.08, 0.2, 1, 4	0.2, 1, 4, 10	0.08, 0.2, 1, 10	0.04, 0.08, 0.2, 1, 10
Digested HS	50% HNO_3	0.04, 0.08, 0.2, 1, 10	0.2, 1, 4, 10	0.08, 0.2, 1, 10	0.04, 0.08, 0.2, 1, 10

The ICP-OES was calibrated using the concentration standards, and the software used a least linear squares fit line through the points. If the linear regression was less than 0.95, the standards were remade and the calibration was repeated. The matrices of the standards were identical to the final sample matrices (i.e. if the sample solutions were made up to 10% (v/v) Aristar HNO_3 for analysis, the standards were also made up in 10% (v/v) Aristar HNO_3). The raw reagent solutions were used as zero concentration standards. A series of reagent blanks and method blanks were analysed. To check instrumental drift, a series of appropriate concentration standards was re-analysed after every ten samples. If the readings varied by more than 10%, the run was aborted. To avoid memory effects from the standard solutions, the standards were followed by a further blank to flush out the instrument. The ICP-OES instrumental parameters employed during the analyses are outlined in Table 2.7.

Table 2.7 – ICP-OES operation parameters

Instrument	**Parameters**
Pump rate	100 rpm
Nebuliser type	Crossflow
Nebuliser pressure	32 PSI
RF power	1150 W
Argon flow	0.5 l/min
Uptake rate	1.85 ml/min
Method	**Parameters**
Auto sampler	On
No. of repeats	3
Delay time	5s
Uptake time Low WL	5s
High WL	30s
Acquisition time	30s
Wash out	15s

After the instrument was calibrated, the emission intensity for each element of interest was measured at the appropriate wavelengths for each sample and for reagent blanks. These wavelengths are summarised Table 2.8.

Table 2.8 Wavelengths used for the detection of elements by ICP-OES

Element	Wavelength (nm)	Element	Wavelength (nm)
Aluminium	396.1	Sodium	588.9
Barium	455.4	Phosphorus	178.2
Calcium	393.3	Lead	220.3
Copper	324.7	Sulphur	180.7
Iron	259.9	Strontium	407.7
Potassium	769.8	Titanium	334.9
Magnesium	279.5	Zinc	213.8
Manganese	257.6		

An estimate of the detection limit for each element was made using three times the standard deviation of the appropriate emission signal from the reagent blank, which was run 10 times through the instrument. It should be noted that these detection limits are usually different from the manufacturers quoted instrumental detection limits. The "real" detection limits are largely dependent on the concentration of elements in the reagent blanks and, in most cases, this was in excess of the manufacturer's detection limits. Thus for the calculation of the concentration of elements in samples, the raw sample concentration readings were determined by the sample signal being greater than three times the standard deviation of the reagent blank. Any values lower than the detection limits were classed as below the detection limit (B.D.L.). For those above the detection limits, the average of the counts for the method blanks was then subtracted from the sample counts, yielding a net signal subsequently transformed to give the concentration of elements, expressed in mg per kg of dry weight peat (see sample calculation in Appendix 9.3).

2.7.3 Inductively Coupled Plasma-Mass Spectrometry (ICP-MS)

All samples being analysed for lead isotopes were pre-diluted to Pb concentrations of less than 100 µg/L. They were analysed for stable lead isotopes, ^{206}Pb, ^{207}Pb and ^{208}Pb. The analysis was conducted using a VG Plasmaquad 3, connected to a Gilson Minipuls 3 peristaltic pump. The pump introduced the sample into the Meinhard nebuliser in the instrument. The instrument was operated using the parameters shown in Table 2.9, which had been optimised for Pb isotope analysis (Eades, 1999).

Table 2.9 – ICP-MS Operation Parameters

Instrument	**Parameters**
Dwell time	2.0 ms
Points/peak	3
D.A.C. step	5
Mode	Pulse counting
Mass range	203.6 to 209.4 amu
Reflected power	1-3 W
Argon flow	0.76-0.84 l/min
Uptake ratio	0.55 ml/min
Method	**Parameters**
Auto sampler	Gilson
No. of repeats	5
Settle time	30 s
Uptake time	150 s
Acquisition time	60 s
Wash out	30 s

The instrument was calibrated at the beginning of each run using lead concentration standards, prepared in a similar manner to the ICP-OES standards. A standard reference solution, SRM 981 (NIST), was used to calibrate the instrument for stable isotopes of lead.

The certified isotope abundance and ratios for the reference material SRM 981 are shown in Table 2.10.

Table 2.10 – SRM 981 Certified Reference Material: Pb isotopic abundance and atomic ratios

Isotopic Abundance (%)		Atomic Ratios	
^{206}Pb	24.1442 +/- 0.0057	$^{206}Pb/^{207}Pb$	1.093
^{207}Pb	22.0833 +/- 0.0027	$^{208}Pb/^{207}Pb$	2.370
^{208}Pb	52.3470 +/- 0.0086	$^{208}Pb/^{206}Pb$	2.168

A blank solution of 2% v/v HNO_3 Aristar was analysed at the beginning of the run and the counts were subtracted from the corresponding counts obtained for each of the SRM 981 standards. Mass bias factors were calculated from the corrected standard counts using the PQVision software. The mass bias factors account for deviations from the certified values, caused by mass fractionation within the instrument arising from different sensitivities to different isotopes. Examples of typical values of mass bias ratios for $^{206}Pb/^{207}Pb$, $^{208}Pb/^{207}Pb$, and $^{208}Pb/^{206}Pb$ are 1.000, 1.050 and 1.050, respectively.

The raw data for the samples were expressed as counts. Five readings were obtained for each sample, with the standard deviation of the five values representing a measure of the internal precision. Sample blanks and acid blanks from the digestion procedure were run with every set of samples. For the concentration data, the average of the blanks was subtracted from the samples. The ^{208}Pb readings were used as a measure of concentration. The PQVision was capable of automatically calculating the concentration of the samples, but this software allowed correction using only one blank. The concentrations were therefore calculated manually from the concentration calibration. The isotopic ratios were also calculated manually, using the blank corrected counts from the concentration calculation. The calculated mass bias corrections were used in the calculation of isotopic ratios, from the individual counts for each of the isotopes (Appendix 9.4).

2.8 CERTIFIED REFERENCE MATERIALS

In order to validate the digestion procedures and to provide a check on all the analyses, certified reference materials were digested and elemental concentrations determined using FAAS and ICP-OES.

2.8.1 Digestion procedure for certified reference materials

Replicate 0.5 g air-dried reference material was weighed into 100 ml beakers. These were ashed at 450°C for 4 hours to reduce the organic matter content. Upon cooling, the beakers were removed from the ashing furnace and placed in a desiccator. The contents of the beaker were carefully washed into the Teflon Microwave tubes using 5 ml of deionised water, followed by 5 ml of concentrated Aristar HNO_3, (producing a 50% (v/v) solution). The digestion conditions are outlined in Table 2.11.

Table 2.11 - Microwave digestion parameters for certified reference materials

Parameters	Values for reference materials
Total volume (ml)	10
Volume of Aristar HNO_3 (ml)	5
Ramp time	15 mins
Maximum ramp pressure	180 psi
Hold time	10 mins
Maximum temperature	210°C

Following digestion, the samples were filtered through Whatman No.542 hardened ashless filter papers to remove any particulate material. Following filtration, the samples were diluted with de-ionised water according to the necessary dilution required for analysis. The instrument conditions were the same as previously described (Sections 2.7.1-2.7.3). The reference materials used and the number of replicates are listed in Table 2.12.

Table 2.12 – Certified reference material parameters

Sample Code	No. of replicates	Sample description
7004	3	CMI Loam reference material
O.L.	3	NBS Orchard Leaves reference material

2.8.2 7004 Reference Material Loam

The reference loam was obtained from the Czech Metrological Institute, together with a list of certified concentrations for selected elements in the loam. The elemental concentrations were available for four different digestion methods, and these values these together with the results obtained from this analysis are displayed in Table 2.13. All of the following concentrations are expressed as mg/kg dry weight.

Table 2.13 – CMI 7004 reference material certified elemental concentrations (mg/kg)

Element	This study	Total (HF)	Aqua Regia	Hot 2M HNO_3	Cold 2M HNO_3
Cu	155 ± 4	183 ± 5	167 ± 1	159 ± 5	137 ± 4
Mn	642 ± 1	869 ± 34	741 ± 36	572 ± 35	527 ± 24
Pb	88 ± 1*	93.4 ± 3.4	83.1 ± 2.3	82.6 ± 1.9	71.7 ± 2.5
Zn	204 ± 1	227 ± 7	198 ± 6	169 ± 8	119 ± 5

*obtained by FAAS; all other values from this study were obtained by ICP-OES

The above results show that the digestion method employed in this study extracts similar proportions of the total metal content to aqua regia and hot 2M HNO_3 extractions. The certified total value was determined for a total digestion procedure involving the use of HF for a complete digestion of the sample, including mineral material. The digestion procedure utilised in this study was a "pseudo-total" extraction, and did not involve the complete digestion of all the mineral material.

Thus the results obtained for this study are not as high as the total certified values, but instead are closer to the aqua regia extractable, which is the most vigorous of the pseudo-total extractants. These results indicate that the digestion procedure employed is indeed valid for this study. The difference in the relative amount of the total certified values extracted for each element probably reflects the different associations of these elements with the mineral matrix.

2.8.3 Orchard Leaves Reference Material

The Orchard Leaves reference material (SRM 1571) was obtained from the National Bureau of Standards in the U.S., where it was certified for a large number of different elements. A range of non-certified concentrations have been determined, and presented in the literature, and this range is shown here for comparison. The obtained concentrations are compared with the certified values and the range of published values in Table 2.14.

Table 2.14 – Orchard Leaves Reference Material certified elemental concentrations (mg/kg)

Element	Certified total values	Range of published values	This analysis
Al	(410)	99 - 428	187 ± 31
B	33 ± 3	23.7 - 38	28.7 ± 11.2
Ca	20900 ± 300	16300 - 24100	15 000 ± 3300
Cu	12 ± 1	9.8 - 20	11 ± 0.2
Fe	300 ± 20	151 - 367	217 ± 8
Mn	91 ± 4	52 - 144	60 ± 3
Pb	45 ± 3	37 - 53	43 ± 2
Sr	37	23 - 45	28 ± 2
Zn	25 ± 3	18 - 81	26 ± 3

The certified values for Orchard Leaves are for total concentrations. In this respect the results displayed above for Al, Fe and Mn seem surprisingly low, as the measured concentrations in the digests would be expected to be much more akin to the certified total values, given the comparative lack of mineral material in the Orchard Leaves reference material. However, the digestion of the Orchard Leaves reference material yielded digest solutions containing a small residue of solid material. No such residue was encountered in any of the peat digest samples, suggesting that digestion of the peat for determination of "pseudototal" provided a more complete assessment of total concentrations.

Chapter 3

Vertical distribution of elements in the solid phase and porewaters in Flanders Moss peat Core 1

3.1 INTRODUCTION

This chapter contains the results of elemental analysis of (i) the solid phase peat material and (ii) porewaters extracted from each 2-cm depth section of combined (see section 2.1.4) 1-m cores from Flanders Moss. Other parameters that help to characterise the peat and porewaters and may be important for the interpretation of the elemental data, e.g. moisture content, organic content, ash content and density of the solid phase material and conductivity, pH, UV-vis absorbance, DOC concentration in the porewaters, are also included.

The data for peat and porewater characterisation are presented in sections 3.2 and 3.4 respectively, and are followed by sections 3.3 and 3.5, which contain the results of elemental analysis of solid phase peat and porewaters.

3.2 CHARACTERISATION OF SOLID PHASE PEAT SAMPLES FROM FLANDERS MOSS PEAT CORE 1

Table 3.1 displays the values for the dry weight, water volume, density, moisture content (% wet weight), wet/dry ratio, organic content (% dry weight) and ash content (% dry weight). Figures 3.1A-F are constructed from the data presented in Table 3.1.

Table 3.1A – Characterisation of solid phase peat samples from the upper half of Flanders Moss peat Core 1

Section Depth (cm)	Dry Weight (g)	Water Volume (ml)	Density (g/cm^3)	Wet/Dry Ratio	Moisture Content (%)	Organic Matter (%)	Ash (%)
0-2	18.35	17.97	0.073	7.54	86.75	12.89	0.37
2-4	18.87	16.73	0.075	8.07	87.60	11.35	1.05
4-6	21.72	23.91	0.087	9.85	89.84	9.01	1.15
6-8	33.09	18.99	0.132	6.79	85.28	13.36	0.93
8-10	32.54	22.37	0.130	6.51	84.64	14.66	0.70
10-12	35.80	22.69	0.143	6.70	85.07	14.43	0.50
12-14	34.94	18.91	0.140	6.77	85.23	14.02	0.75
14-16	28.33	23.01	0.113	8.61	88.38	11.41	0.21
16-18	32.04	21.95	0.128	7.71	87.02	12.68	0.30
18-20	33.24	21.27	0.133	7.98	87.47	12.31	0.22
20-22	25.02	20.50	0.100	9.82	89.82	10.05	0.18
22-24	28.41	21.50	0.114	8.74	88.56	11.29	0.15
24-26	24.92	13.73	0.100	10.25	90.24	9.69	0.17
26-28	23.21	17.61	0.093	10.00	90.00	9.85	0.15
28-30	21.11	23.95	0.084	11.69	91.44	8.52	0.10
30-32	20.96	21.44	0.084	11.75	91.49	8.41	0.18
32-34	15.39	15.97	0.062	14.50	93.10	6.81	0.09
34-36	13.45	23.77	0.054	15.94	93.73	6.16	0.11
36-38	14.98	23.69	0.060	15.65	93.61	6.35	0.04
38-40	18.24	23.72	0.073	13.48	92.58	7.39	0.06
40-42	18.08	24.31	0.072	13.90	92.81	7.17	0.02
42-44	15.73	23.75	0.063	15.04	93.35	6.58	0.07
44-46	13.01	23.08	0.052	19.02	94.74	5.19	0.06
46-48	11.69	22.10	0.047	20.21	95.05	4.87	0.07
48-50	20.96	25.76	0.084	11.49	91.30	8.62	0.09

Table 3.1B - Characterisation of solid phase peat samples from the lower half of Flanders Moss peat Core 1

Section Depth (cm)	Dry Weight (g)	Water Volume (ml)	Density (g/cm^3)	Wet/Dry Ratio	Moisture Content (%)	Organic matter (%)	Ash (%)
50-52	18.59	23.20	0.074	12.87	92.23	7.71	0.05
52-54	16.40	22.29	0.066	14.67	93.18	6.74	0.08
54-56	14.86	21.77	0.059	15.35	93.49	6.45	0.06
56-58	14.69	23.10	0.059	16.14	93.80	6.08	0.11
58-60	16.09	23.55	0.064	16.29	93.86	6.05	0.08
60-62	18.04	22.31	0.072	13.08	92.35	7.59	0.06
62-64	17.29	23.55	0.069	14.45	93.08	6.86	0.06
64-66	16.47	21.37	0.066	13.26	92.46	7.52	0.02
66-68	16.95	23.76	0.068	16.45	93.92	6.06	0.02
68-70	18.43	23.75	0.074	12.31	91.88	8.05	0.07
70-72	19.19	20.91	0.077	12.77	92.17	7.73	0.10
72-74	18.28	15.02	0.073	13.11	92.37	7.53	0.10
74-76	19.33	23.14	0.077	12.15	91.77	8.15	0.08
76-78	19.40	23.92	0.078	12.82	92.20	7.69	0.11
78-80	19.50	22.81	0.078	12.77	92.17	7.78	0.06
80-82	15.57	23.71	0.062	14.75	93.22	6.72	0.06
82-84	15.58	22.54	0.062	15.30	93.46	6.48	0.05
84-86	15.12	22.34	0.060	15.39	93.50	6.47	0.03
86-88	13.91	27.91	0.056	17.36	94.24	5.71	0.05
88-90	13.37	23.35	0.053	18.49	94.59	5.35	0.06
90-92	10.05	22.28	0.040	22.21	95.50	4.47	0.03
92-94	8.88	24.13	0.036	23.42	95.73	4.24	0.03
94-96	11.44	23.16	0.046	21.52	95.35	4.59	0.05
96-98	10.50	23.31	0.042	22.83	95.62	4.34	0.04
98-100	12.21	23.86	0.049	22.51	95.56	4.39	0.05

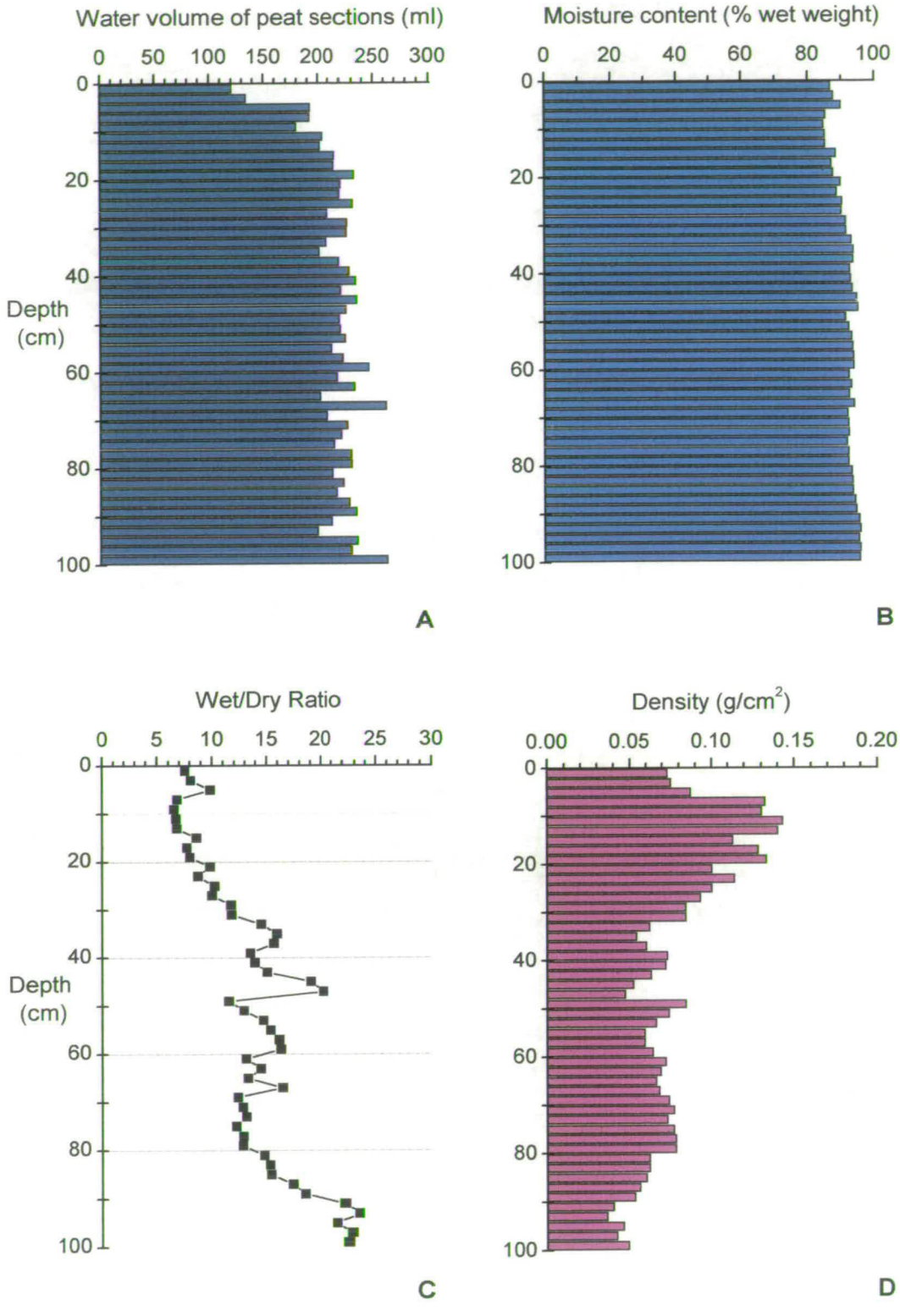

Figures 3.1A-D: Vertical variations in the water volume, moisture content, wet/dry ratio and density from Flanders Moss peat

3.2.1 Water volume and moisture content

Figure 3.1A shows the variation in water volume (wet weight – dry weight) with vertical depth for Core 1 (five bulked cores – total volume per section = 5 x 5 cm x 5 cm x 2 cm = 250 cm^3). The volume of water in each section increased almost linearly from the surface to 20 cm. Below this depth, the value was almost constant at ~216±13 ml.

Figure 3.1B shows the variation in moisture content (% wet weight) with vertical depth in the peat core. Moisture content were typically high with values ranging from ~84 to ~96 %. Beneath the sharp peak at 4-6 cm, values of ~84-85 % were obtained for the next four sections. Values then gradually increased to ~93% at 32 cm. With the exception of the small peak at 44-48 cm, the moisture content was almost constant down to a depth of 80 cm. Below this depth, values again increased to a maximum in the bottom five sections of ~96%.

3.2.2 Wet/Dry Ratio

Figure 3.1C displays the wet/dry ratios for the peat profile. Values ranged from ~6.5 in the near surface sections to ~23.6 at the bottom of the core. Notably the position of a small near-surface peak (4-6 cm) coincides with the peak in moisture content but there was no marked minimum in the next four sections. Additionally, the peak at 44-48 cm is more accentuated than in the moisture content profile. The final feature in the wet/dry ratio profile was the marked increase from 80 cm to the maximum values observed for the bottom five sections.

3.2.3 Density

Figure 3.1D shows the vertical variations in the density of the peat. Lower values of ~ 0.08 g/cm^3 at the surface were underlain by a broad maximum at 6-20 cm of ~0.13-0.14 g/cm^3. Below this values were generally in the range 0.05-0.07 mg/cm^3 with perhaps a small increase to a maximum of ~0.08 mg/cm^3 at 70-80 cm. The density decreased in the bottom sections to ~0.04-0.05 mg/cm^3.

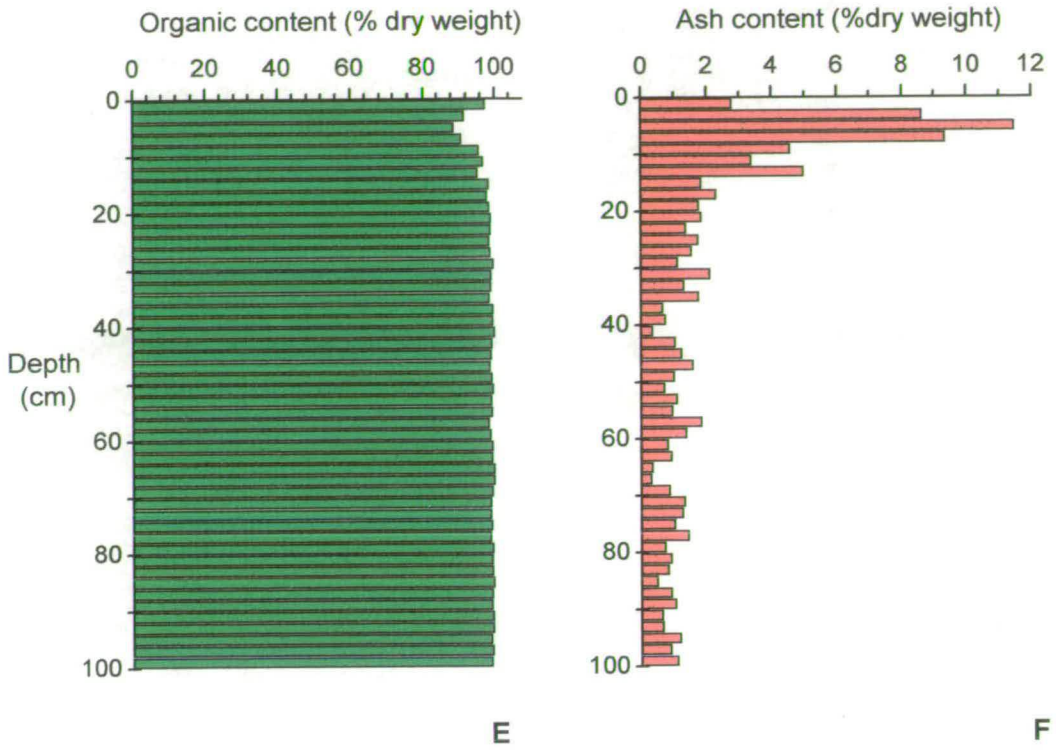

Figures 3.1E-F – Vertical variations in the organic matter and ash content of dried Flanders Moss peat

3.2.4 Organic Content

The vertical profile of organic content (% dry weight) is shown in Figure 3.1E. With the exception of the top 0-18 cm, the organic content was typically in the range 98-100%. In this part of the core, there did not appear to be any correlation between organic content and moisture content or wet/dry ratio. The major feature in the 0-18 cm section was the minimum at 4-6 cm, the position of a small maximum in both the moisture content and wet/dry ratio profiles.

3.2.5 Ash Content

Figure 3.1F shows the ash content profile, which is simply the inverse of the organic content profile (100%-organic content). Clearly, the peak in ash content coincided with the features occurring at 4-6 cm in each of the other profiles. The minimum in moisture content lies just below this peak. The ash content at the peak was ~11%, at the upper end of values quoted for ombrotrophic peat bogs (Shotyk, 1996). Most of the values, however, were < 2%.

3.3 VERTICAL DISTRIBUTION OF ELEMENTS IN THE SOLID PHASE OF FLANDERS MOSS PEAT CORE 1

For the purpose of establishing the mobility of Pb in peat, the suite of elements included in this study has been separated into five groups. The basis for this selection is also outlined below (Table 3.2):

Table 3.2 Groupings of elements used to elucidate biogeochemical processes occurring in Flanders Moss peat bog

Group	Elements	Basis for selection
I	Mn and Fe	Susceptible to redox cycling
II	S and P	May participate in other important biogeochemical cycles
III	Al and Ti	Mineral components used as indicators of soil inputs
IV	Na, K, Mg, Ca, Ba and Sr	Alkali metals and alkaline earth metals which may be susceptible to plant uptake
V	Zn, Cu and Pb	Heavy metals from anthropogenic sources

All elemental concentrations for Flanders Moss Core 1 solid phase are displayed in Appendix 9.5.

3.3.1 Group I – Mn and Fe

Figures 3.2A-B show the vertical distribution of Mn and Fe, respectively. The Mn profile had a near-surface maximum of 75 mg/kg at 0-2 cm. Thereafter, the Mn concentration decreased rapidly to a near-constant value of ~1 mg/kg below 20 cm.

The main feature of the Fe profile was also a near-surface maximum of ~3000 mg/kg at 0-4 cm which was slightly broader than that observed for Mn. The concentration of Fe decreased less rapidly than that of Mn to 630 mg/kg by 12-14 cm and to ~ 300 mg/kg by 46-48 cm. Below this depth, concentrations were almost constant at ~230 mg/kg.

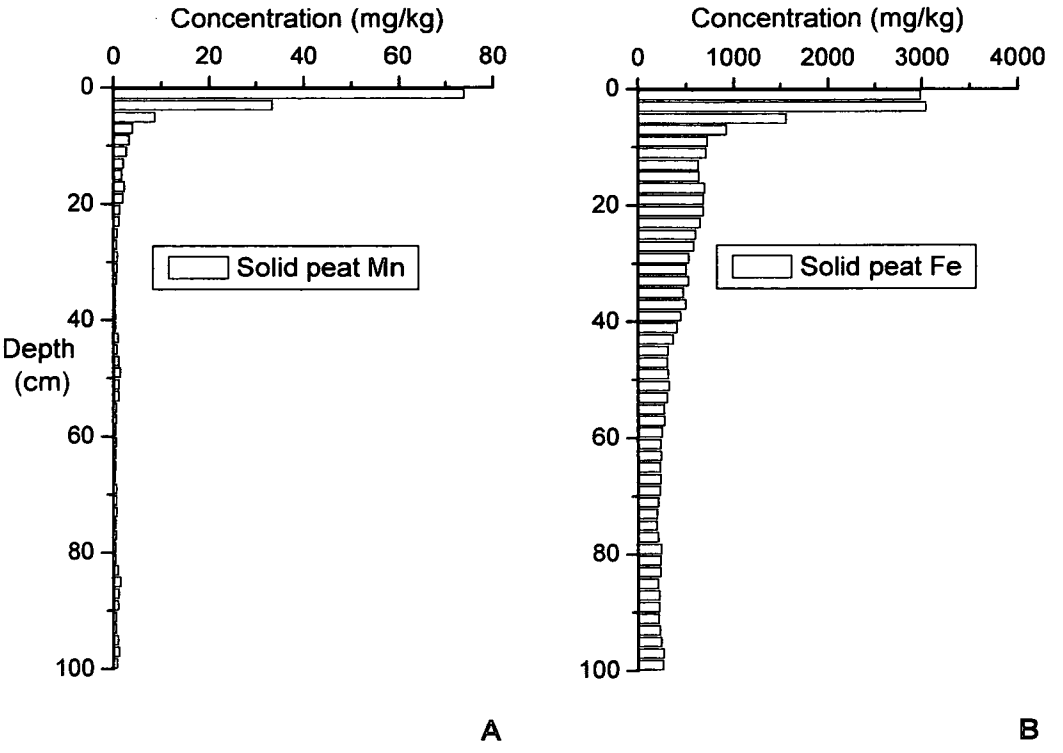

Figure 3.2A-B: Vertical concentration profiles of Fe and Mn in solid phase Flanders Moss peat

3.3.2 Group II – S and P

The S profile (Figure 3.3A) differed from that of Mn and Fe in that there was no near-surface maximum and no sharp decrease in concentration with increasing depth. Values of ~1000 mg/kg were typical of the concentration of S in the solid phase peat samples. It would appear, however, that there were small variations in the form of broad maxima (and minima) occurring over the entire length of the core, e.g. maxima at 0-10 cm, ~ 20 cm, ~ 40 cm, ~ 50 cm, ~ 80 cm. Some of the peaks below 30 cm did coincide with peaks in moisture content (Figure 3.1B).

Figure 3.3B shows the vertical distribution of P for peat Core 1. The concentration of P at the surface maximum was 698 mg/kg and the surface peak extended over the top three sections. Between 6-18 cm, concentrations were almost constant at ~ 250 mg/kg and between 24-68 cm, values were typically ~ 110 mg/kg. There was a broad peak (up to 224 mg/kg) at 70-80 cm, below which values decreased to 73 mg/kg at the bottom of the core.

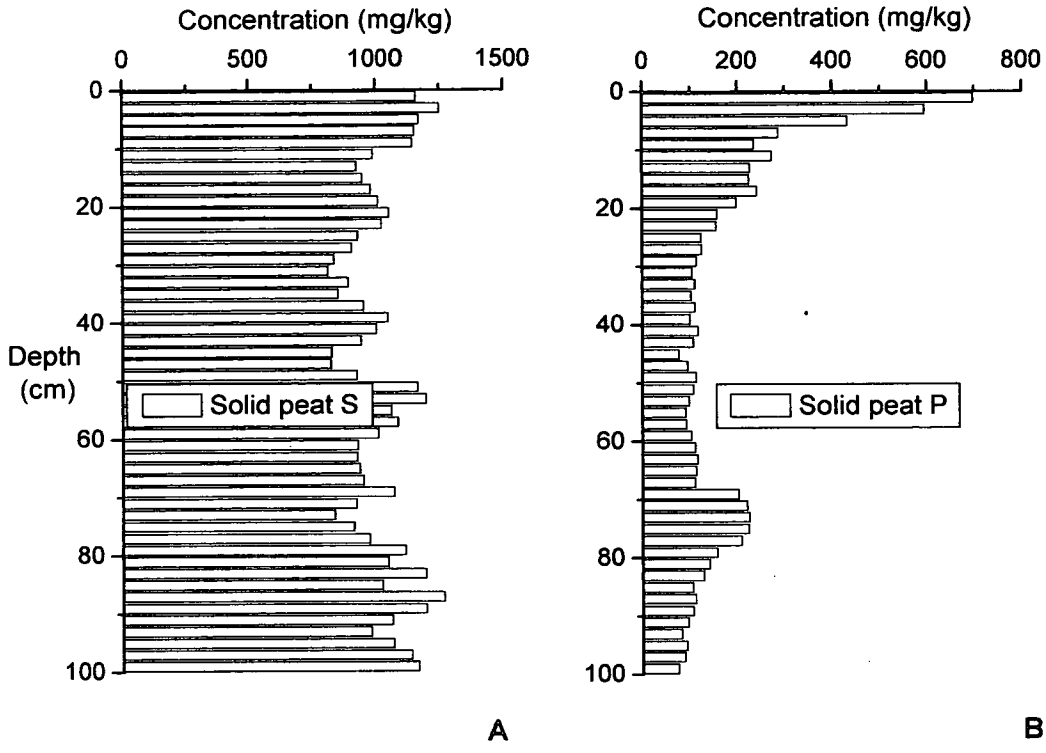

Figures 3.3A-B: Vertical concentration profiles of S and P in solid phase Flanders Moss peat

3.3.3 Group III – Al and Ti

Figure 3.4A-B shows the vertical profiles for Al and Ti. The Al profile had a broad maximum in the 2-14 cm depth sections and the concentrations at the maximum were ~ 2250 mg/kg. There was also a broad shoulder below the main maximum at ~ 20 cm. Below this, there was a general decrease to ~400 mg/kg by 60-62 cm. A smaller broad maximum was also observed in the 70-80 cm depth sections of the peat.

The Ti profile was very similar to the Al profile with the exception that there was an additional broad peak at 30-40 cm. Concentrations of Ti ranged from ~ 120 mg/kg at the near-surface maximum to ~20 mg/kg at the bottom of the core. Although the maximum concentrations of Al and Ti coincided with the maximum in the ash content profile, the Al and Ti peaks were significantly broader than the ash peak. In addition, there was little similarity between the Al (and Ti) and the ash content profiles in the deeper sections of the peat core.

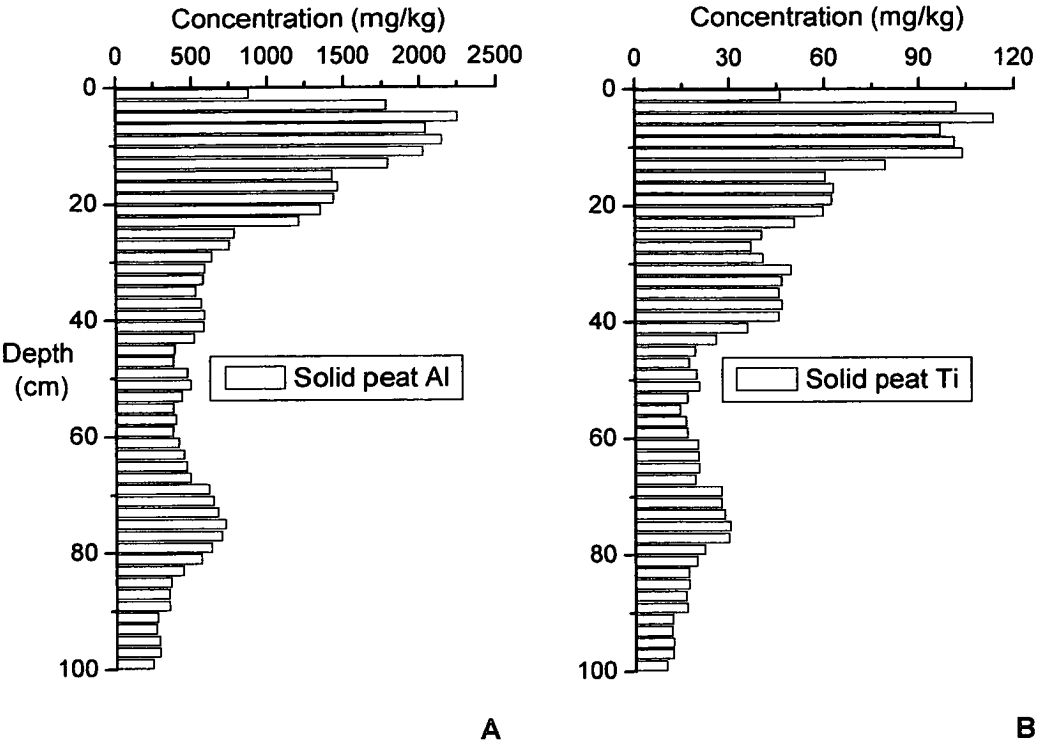

Figures 3.4A-B:Vertical concentration profiles of Al and Ti in solid phase Flanders Moss peat

3.3.4 Group IV – Na, K, Mg, Ca, Sr and Ba

The vertical concentration profiles for Na, K, Mg, Ca, Sr and Ba are shown in Figures 3.5A-F. Maximum concentrations of 440, 1200 and 1840 mg/kg for Na, K and Ca, respectively, were found in the 0-2 cm sections. Although there was a slight maximum of 1000 mg/kg at 0-4 cm in the Mg profile, the maximum concentrations of up to 1700 mg/kg were found in the bottom sections of the core. Each of the profiles for the four major cations had further distinctive features.

In the Na profile (Figure 3.5A), after a sharp decrease in concentration below the 0-2 cm section to 160 mg/kg, there was a slight increase in concentration to a broad maximum of ~210 mg/kg centred at about 30 cm. Below 40 cm, concentrations decreased very gradually from ~ 160 mg/kg to 110 mg/kg at the bottom the core.

In contrast, K concentrations decreased almost exponentially below the 0-2 cm section to ~ 90 mg/kg by 20 cm (Figure 3.5B). Values were typically less than 50 mg/kg in the deeper sections of the core.

Superimposed upon the general increase in Mg concentration with increasing depth were a number of broad maxima, e.g. 50-70 cm and 80-100 cm, that coincided with similar features in the moisture content profile (Figure 3.5C).

Although the general trend in the Ca profile was a decrease in concentration with increasing depth, the broad maxima observed in the Mg profile were also evident at the same depths in the Ca profile (Figure 3.5D). The Ca profile had an additional broad maximum at ~ 20 cm. It should also be noted that there was an absence of peaks at ~ 30 cm (observed in Na profile) or ~ 40 cm (observed in S profile).

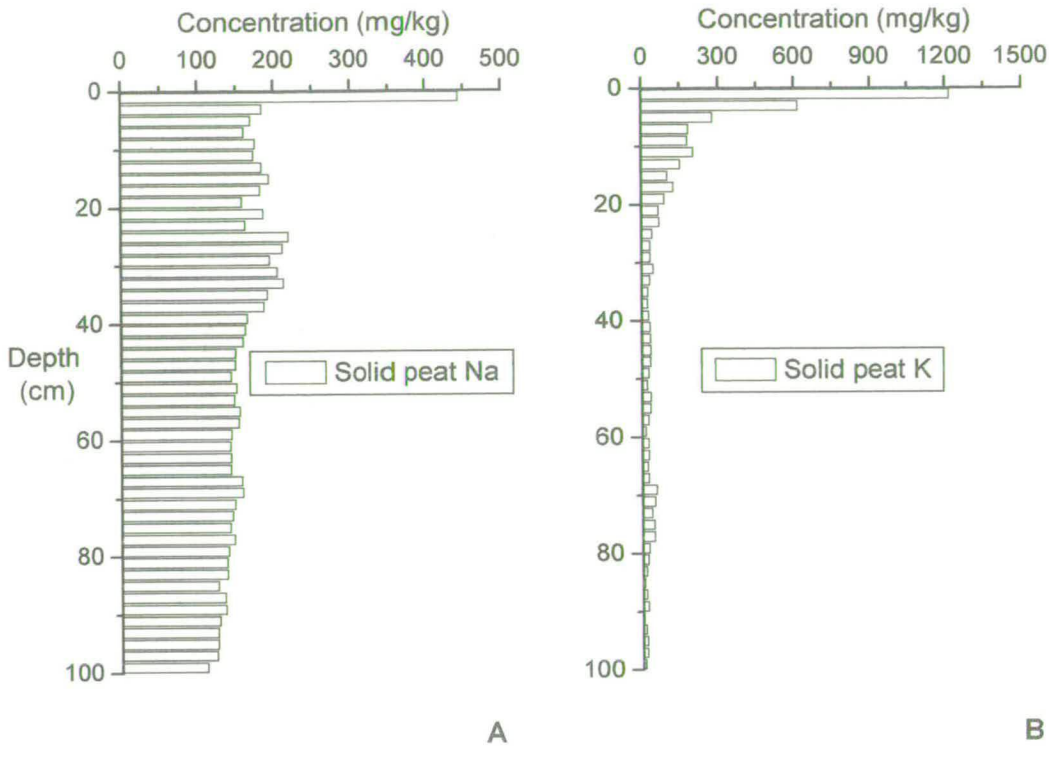

Figures 3.5A-B:Vertical concentration profiles of Na and K in solid phase Flanders Moss peat

The Sr concentration profile (Figure 3.5E) differed from those of Na, K, Ca and to a lesser extent Mg in that there was no pronounced near-surface peak but only a gradual decrease from ~25 mg/kg in the top 0-20 cm section to ~19 mg/kg in the 80-100 cm section. The position of the smaller maxima, e.g. ~20 cm and ~ 40 cm, coincided with those observed in the Ca and S profile.

Figure 3.5F shows the gradual decrease in the concentration of Ba from surface values of 33 mg/kg to 8 mg/kg at 24-26 mg/kg and then to ~ 1 mg/kg at the bottom of the core. The shape of the Ba profile has more similarity to the P profile than to any of the other Group IV elements.

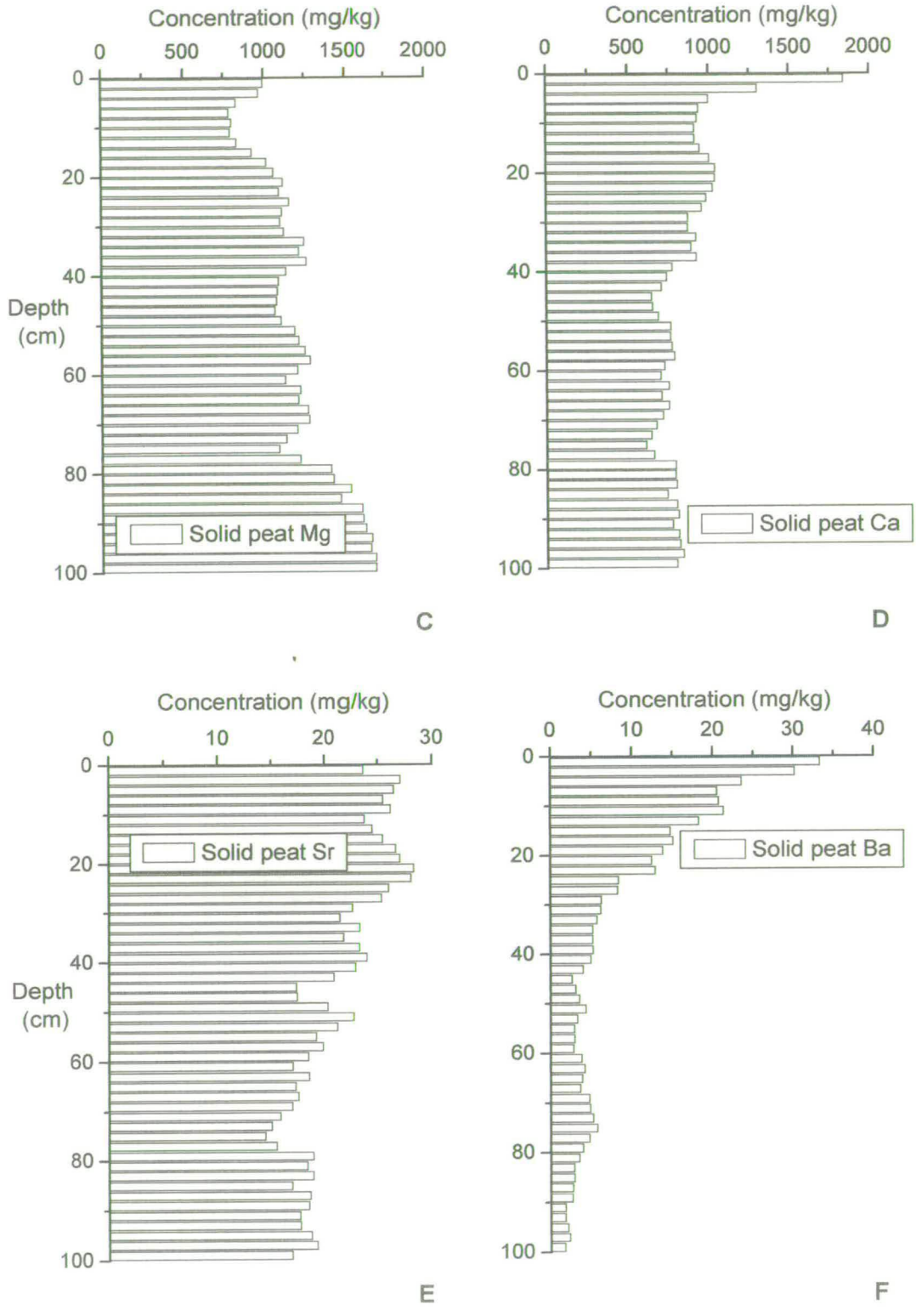

Figures 3.5C-F:Vertical concentration profiles of Mg, Ca, Sr, and Ba in solid phase Flanders Moss peat

3.3.5 Group V – Zn, Cu and Pb

The vertical concentration profiles for the heavy metals, Zn, Cu and Pb are displayed in Figure 3.6A-C. From these profiles, it was immediately apparent that the Pb and Cu concentrations were greatest in the 0-30 cm and 0-20 cm regions, respectively, of the peat core. In contrast, Zn was distributed more evenly over the entire core.

The Zn concentration profile (Figure 3.6A) was very noisy but there was the suggestion of a maximum of ~300 mg/kg at ~ 30 cm, the same position as the broad peak observed in the Na concentration profile. Below this depth, there was only a gradual decrease in Zn concentrations to ~ 200 mg/kg at the bottom of the core.

The Cu profile (Figure 3.6B) had a peak concentration of ~16 mg/kg at 2-4 cm, slightly above the position of the upper Pb peak. There were perhaps two other peaks in the Cu profile of ~7 mg/kg and ~ 4mg/kg at 10-12 cm and 16-20 cm, respectively. Thereafter, Cu concentrations were typically less than 1 mg/kg.

There were two clear peaks in the Pb profile (Figure 3.6C), the first at 4-6 cm and the second at 20-22 cm and the peak concentrations of Pb were ~330 and ~165 mg/kg, respectively. The upper Pb peak coincided with the peak in the ash content profile but there was no secondary peak in the ash content at the position of the lower Pb peak. There is, however, a peak in S concentration at the position of the lower Pb peak. Below 30 cm, Pb concentrations were less than 10 mg/kg.

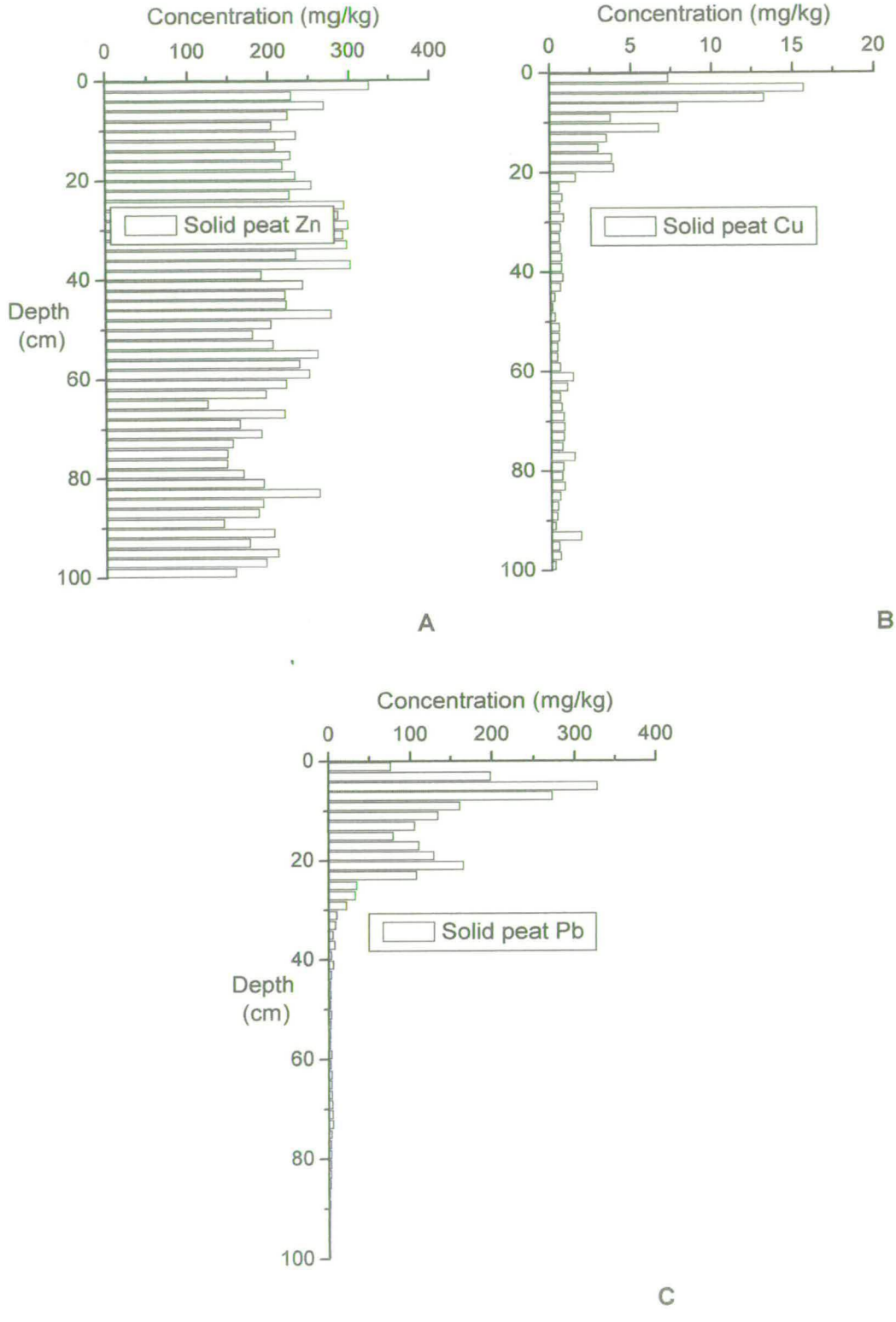

Figures 3.6A-C:Vertical concentration profiles of Zn, Cu, and Pb in solid phase Flanders Moss peat

3.4 CHARACTERISATION OF THE POREWATERS EXTRACTED FROM FLANDERS MOSS PEAT CORE 1

All porewater characterisation data are contained in Appendix 9.6.

3.4.1 pH

Figure 3.7A shows the vertical variations in porewater pH for peat Core 1. The value at the surface of 4.18 decreased to a minimum of 3.64 at 18-20 cm depth. A gradual increase to 4.12 at the bottom of the core was then observed.

3.4.2 Conductivity

The maximum conductivity values of ~190-200 μS were observed for the porewaters extracted from the 10-20 cm sections of the peat core (Figure 3.7B). Although the maximum conductivity value coincides with the minimum pH of the porewaters, the main part of the broad conductivity peak is located slightly above the pH minimum. Below 20 cm, in contrast with the gradual change in pH, there is a sharp decrease in conductivity to values of ~140 μS. Below 40 cm, the conductivity of the porewaters is almost constant at ~100-110 μS.

3.4.3 DOC

The maximum DOC concentration of 173 mg/l occurred in the porewater extracted from the 0-2 cm section of the peat core (Figure 3.7C). In the 2-4 cm section, however, the DOC concentration dropped to 63 mg/l. Below this, a more gradual increase to a maximum of 173 mg/l at 20-22 cm was observed. It is notable that the maximum DOC concentration also occurred at the same depth as the pH minimum and conductivity maximum. Additionally, the conductivity peak occurred slightly above the DOC peak. The DOC concentrations then decreased gradually from the peak value down to ~72 mg/l at 60-62 cm. In the porewaters from the 62-78 cm sections, there was a slight increase to values of 80-90 mg/l but thereafter concentrations were almost constant at ~65 mg/l.

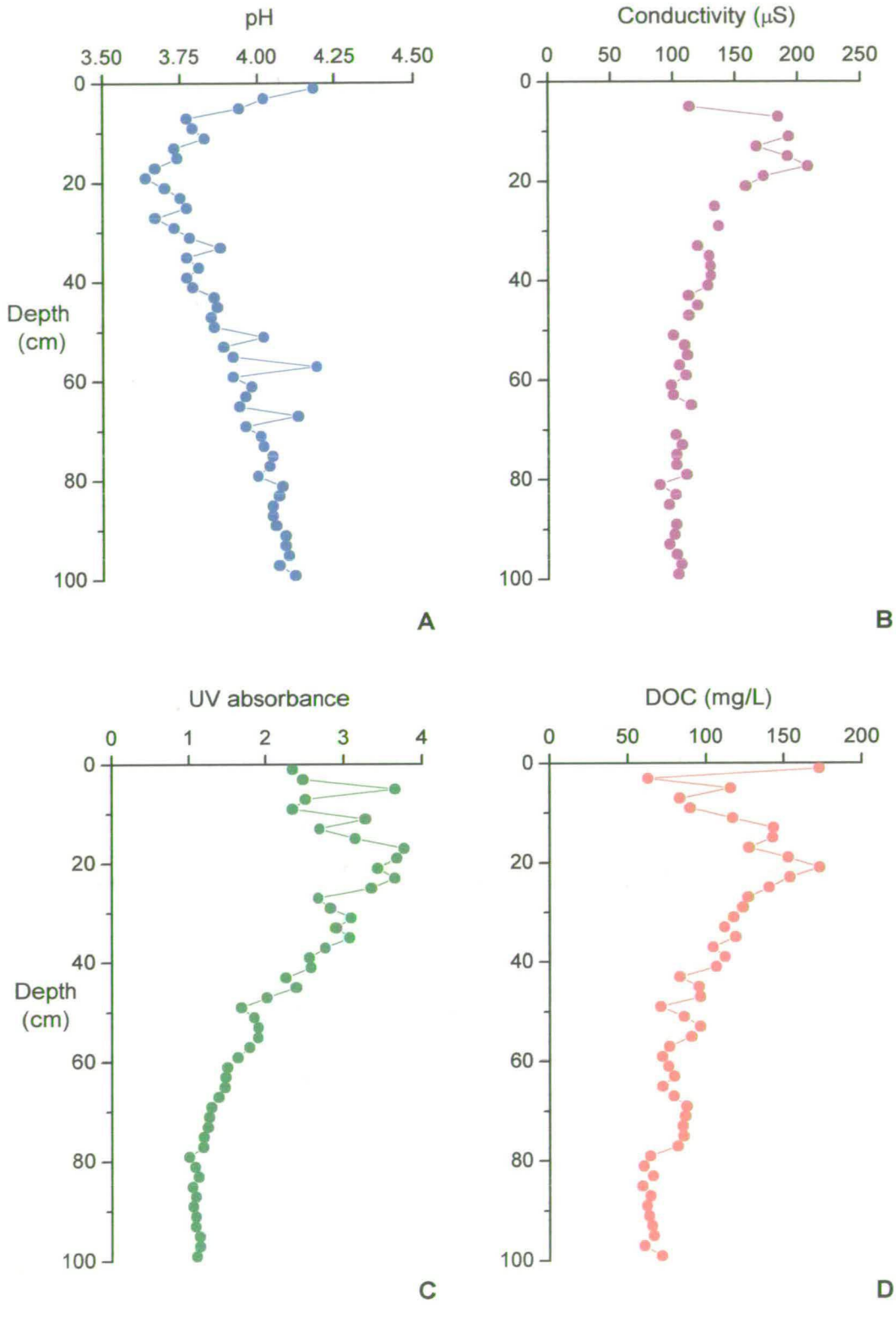

Figures 3.7A-D: Vertical variations in pH, conductivity, DOC and UV absorbance in the porewaters collected from a Flanders Moss peat core

3.4.4 UV Absorbance

The UV absorbance, used as a measure of the concentration of humic substances was also recorded for each of the porewater samples (Figure 3.7D). There is a good degree of similarity between the DOC and UV absorbance profiles although there are also some important differences. Excluding the top 0-10 cm sections in which there are obvious differences between the two profiles, e.g. the absence of a UV absorbance peak in the 0-2 cm section, the general shape of the profiles is very similar with the maximum values occurring at similar depths (16-24 cm – UV; 20-22 cm – DOC). The peak in the UV absorbance profile is clearly broader than that in the DOC profile. In addition, there would appear to be two shoulders lying below the broad UV absorbance peak at ~30-40 cm and ~50-60 cm, respectively. The overall decrease from the broad peak down the near-constant values in the porewaters from the bottom 80-100 cm sections of the core was also more extensive than that in the DOC profile.

3.5 VERTICAL DISTRIBUTION OF ELEMENTS IN THE POREWATERS EXTRACTED FROM FLANDERS MOSS PEAT CORE 1

All porewater elemental concentrations are displayed in Appendix 9.6. As in section 3.3, the elements will be separated into five groups:

Group I – Mn and Fe

Group II – S and P

Group III – Al and Ti

Group IV – Na, K, Mg, Ca, Sr and Ba

Group IV – Zn, Cu and Pb

3.5.1 Group I – Mn and Fe

The shape of the porewater profile for Mn was almost identical to that obtained for the solid phase peat profile (Figure 3.8A). The maximum Mn concentration of ~0.13 mg/l occurred in the porewater from the 0-2 cm section. Concentrations then decreased rapidly with increasing depth to less than the concentrations in the blanks by 14 cm. There was perhaps a very small broad Mn peak at ~ 8-16 cm in the porewater.

The overall shape of the Fe porewater profile was quite similar to that of the solid phase peat profile (Figure 3.8B). The maximum Fe concentration of 0.93 mg/l occurred in the porewater from the 0-2 cm section. The ratio of the peak porewater concentration of Fe to that at, for example, 18-20 cm (ratio value = 2.8) was, however, smaller than the same ratio of Fe concentrations in the solid phase peat (ratio value = 4.4). Porewater Fe concentrations decreased markedly below 50 cm to values of less than 0.1 mg/l.

3.5.2 Group II – S and P

In contrast to the Mn and Fe profiles, there was significantly less similarity between the porewater and solid phase profiles for S (Figure 3.9A). In general, porewater concentrations were typically ~7 mg/l in the upper 30 cm, ~3 mg/l down to 80 cm and ~1 mg/l in the 80-100 cm sections of the core.

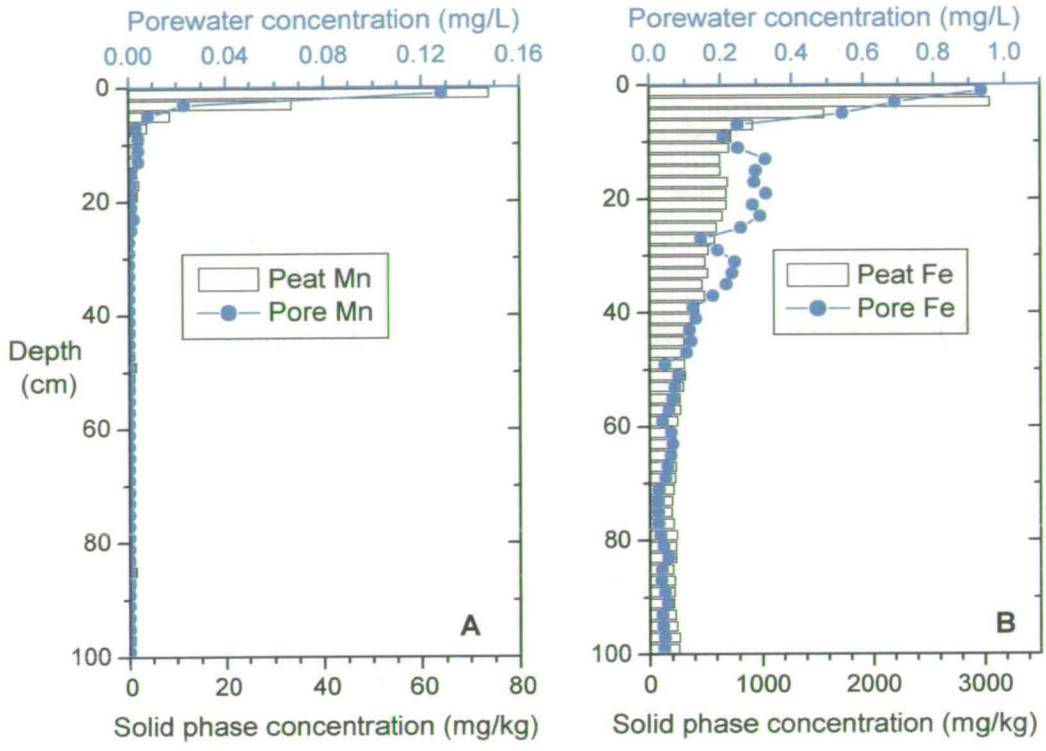

Figure 3.8A-B: Vertical variations in the concentrations of Mn and Fe in porewaters (and solid phase) from a Flanders Moss peat core

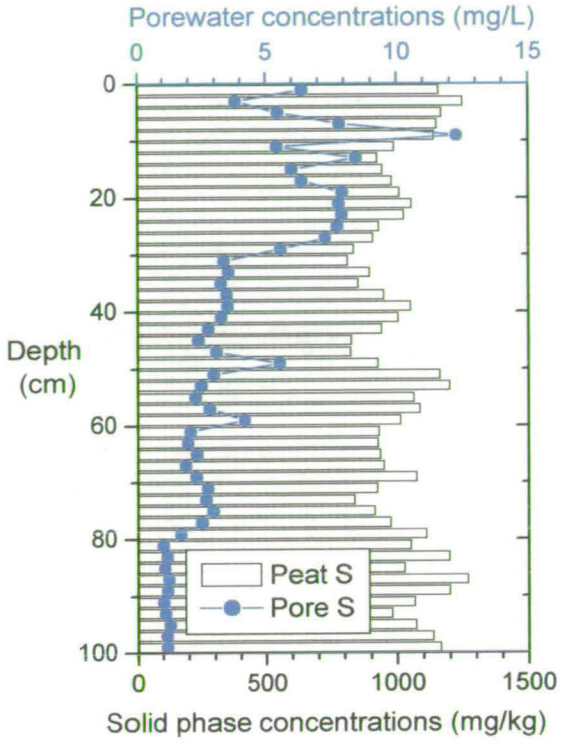

Figures 3.9: Vertical variations in the concentration of S in porewaters (and solid phase) from a Flanders Moss peat core

More specifically, there was a sharp peak at 8-10 cm and then a broad peak at 20-30 cm. The latter occurred at the same depth as a slight but broad peak in the solid phase profile. A broad peak at 70-80 cm coincided with a peak in DOC. No porewater data was obtained for P.

3.5.3 Group III – Al and Ti

The porewater and solid phase concentrations of Al in peat Core 1 are shown in Figure 3.10A. The general shape of the two profiles was similar to a certain extent with highest concentrations occurring in the 0-20 cm section of the core. However, the highest concentrations of Al were found in the porewater from the 0-2 cm section whilst the solid phase maximum occurred in the 4-6 cm section. The shoulder at 10-20 cm in the porewater profile and the sharp decrease in Al concentration at 20-22 cm did match the solid phase profile. The porewater peaks at 30-40 cm and 70-80 cm were absent from the solid phase profile.

Although there was a strong similarity between the solid phase profiles of Al and Ti, the porewater profiles of these elements exhibited differences that were more significant (Figures 3.10A and B). The peak concentration of 0.013 mg/l for Ti in the porewaters occurred at 4-6 cm, the same depth as the solid phase maximum concentration. From 6-38 cm, the concentrations, although centred on 0.007 mg/l varied from 0.003 to 0.010 mg/l. Below this depth, there was a sharp decrease to 0.001 mg/l, and in the deeper sections, the concentration of Ti was often below the concentrations of Ti in the blank.

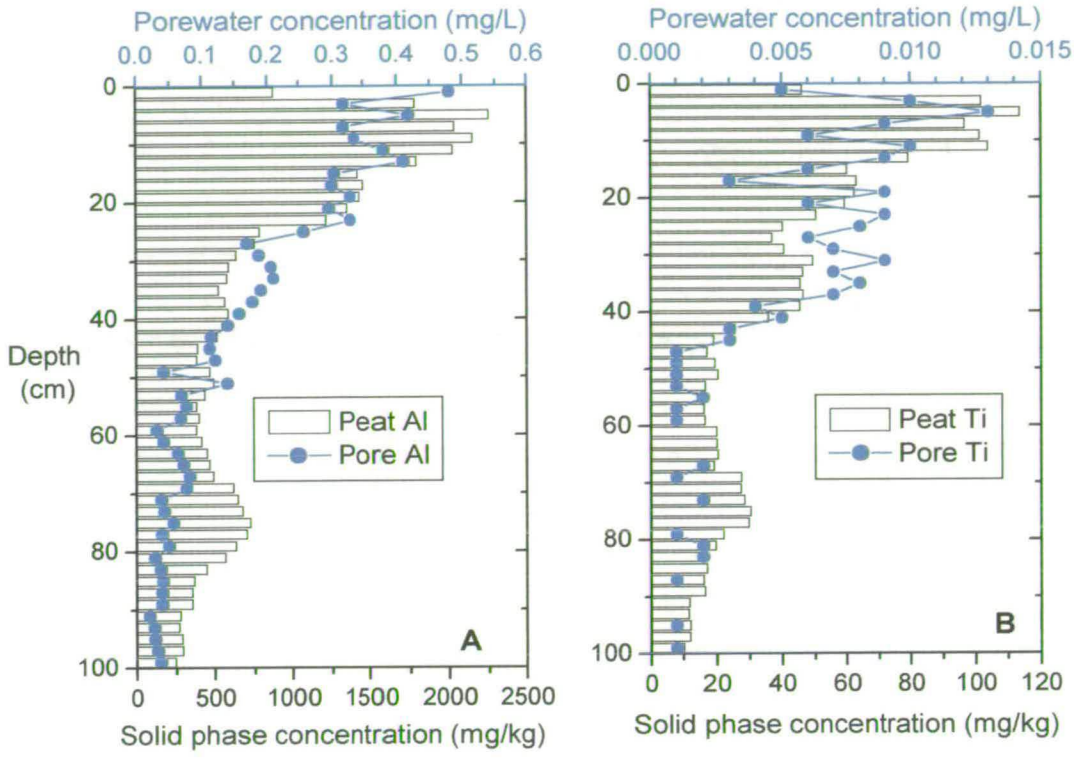

Figures 3.10A-B: Vertical variations in the concentrations of Al and Ti in porewaters (and solid phase) from a Flanders Moss peat core

3.5.4 Group IV – Na, K, Mg, Ca, Sr and Ba

As for the solid phase profiles, there was a sharp peak at 0-2 cm in the porewater profiles for Na (~13 mg/l), K (~18 mg/l) and Ca (~5 mg/l) (Figures 3.11A, B and D). There was also the suggestion of a small but sharp peak at 0-2 cm in the porewater profile of Mg (~3 mg/l) and Sr (~0.03 mg/l) (Figures 3.11C and 3.11E). All of the porewater profiles were different, just as observed for the solid phase profiles.

Below the 0-2 cm section, there was a broad peak at 10-20 cm in the porewater profile for Na that was absent from the respective solid phase profile. This broad peak in Na concentration (10-12 mg/l) did coincide with the peak in the S profile. Below 40 cm, unlike the S profile, however, the Na concentrations were relatively constant at ~5-7 mg/l).

The porewater concentrations for K were only above the detection limit in the 0-6 cm section of the core. It would appear that the concentrations of K in the porewater decreased much more rapidly than in the solid phase peat.

The shape of the porewater profile for Mg exhibited most similarity to the respective solid phase profile. In particular, the maximum concentrations of Mg (2.8-3.3 mg/l) were again obtained for the bottom sections of the core.

The porewater profile for Ca was relatively featureless. Below the sharp surface peak, concentrations decreased down the core from 1.4 mg/l to 0.6 mg/l.

The porewater and solid phase profile of Sr is shown in Figure 3.11E. There was little evidence of a strong relationship between the concentrations of Sr in the porewater and in the solid phase peat material. Instead, there appeared to be some similarity between the porewater profile of Sr and the conductivity/DOC/UV profiles. Sr concentrations were at a maximum of ~0.03 mg/l at 18-24 cm, overlapping the position of the peaks in the conductivity and DOC/UV absorbance profiles. Lower concentrations of 0.008–0.13 mg/l were observed in the porewaters from the 60-100 cm sections.

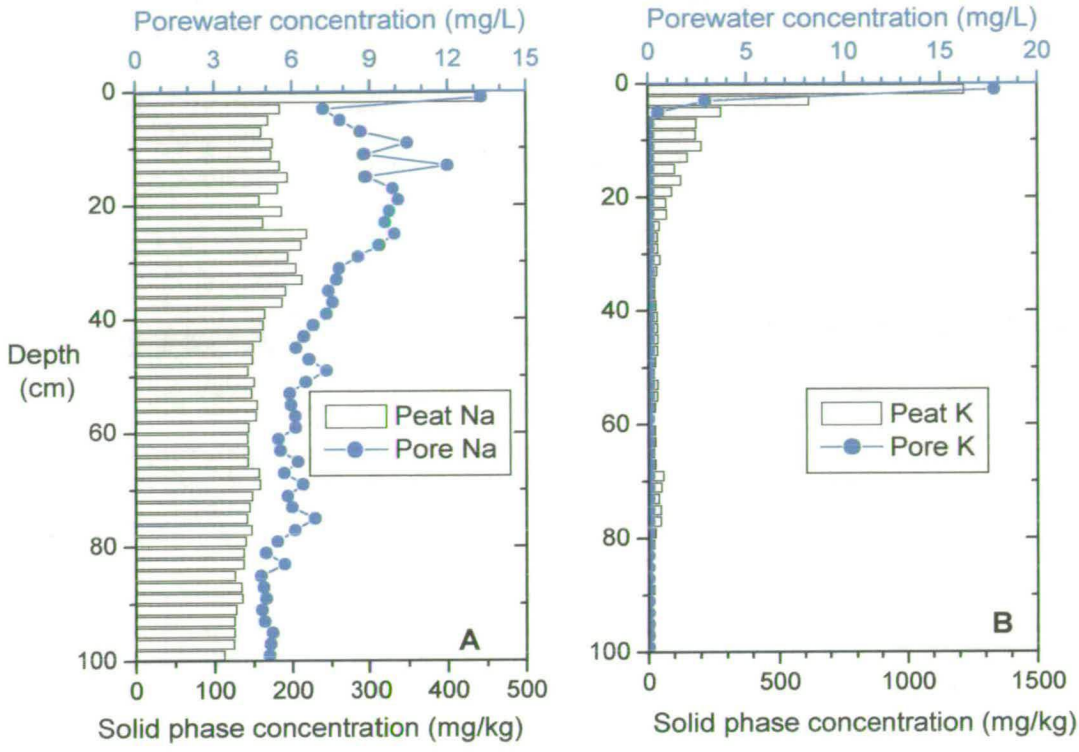

Figures 3.11A-B: Vertical variations in the concentrations of Na and K in porewaters (and solid phase) from a Flanders Moss peat core

Figure 3.11F shows the porewater and solid phase profile for Ba. The concentrations of Ba were frequently below the limit of detection but there would appear to be some correlation between the porewater and solid phase concentration profiles.

3.5.5 Group V – Zn, Cu and Pb

Figure 3.12A-C shows the porewater and solid phase profiles of Zn, Cu and Pb. The porewater profile for Zn shown in Figure 3.12A is particularly noisy. Higher concentrations (0.3-0.4 mg/l) were typically found in the upper sections compared with values of (0.1-0.2 mg/l) in the lower sections of the core. The main decrease in concentration occurred at ~ 40 cm in the porewater but at ~60 cm in the solid phase peat.

Although the porewater and solid phase concentrations of Cu were highest in the 0-20 cm sections, the position of the peaks in the porewater profile did not match those in the solid phase profile (Figure 3.12B). The maximum concentration (0.035 mg/l) in the porewater occurred in the 0-2 cm section, whilst the maximum in the solid phase occurred at 2-4 cm. Similarly, the second peak in the porewater (0.019 mg/l) occurred at 8-12 cm whilst the solid phase maximum was sharper and occurred at 10-12 cm. There was no porewater peak at the position of the solid phase peak at 18-20 cm.

The peak porewater concentrations of 0.043 mg/l and 0.024 mg/l at 4-6 cm and 20-22 cm in the Pb profile coincided exactly with those in the solid phase profile (Figure 3.12C). Moreover, the shape of the two profiles matches very closely over the top 0-40 cm. From 40-80 cm, both solid phase and porewater concentrations of Pb were extremely low. Below, this it would appear that there was a sharp increase from 0.001 to ~0.007 mg/l in the porewater profile which was not mirrored by an increase in concentration in the solid phase peat. There was no indication of a correlation between porewater concentration of Pb and pH, conductivity, or DOC/UV absorbance.

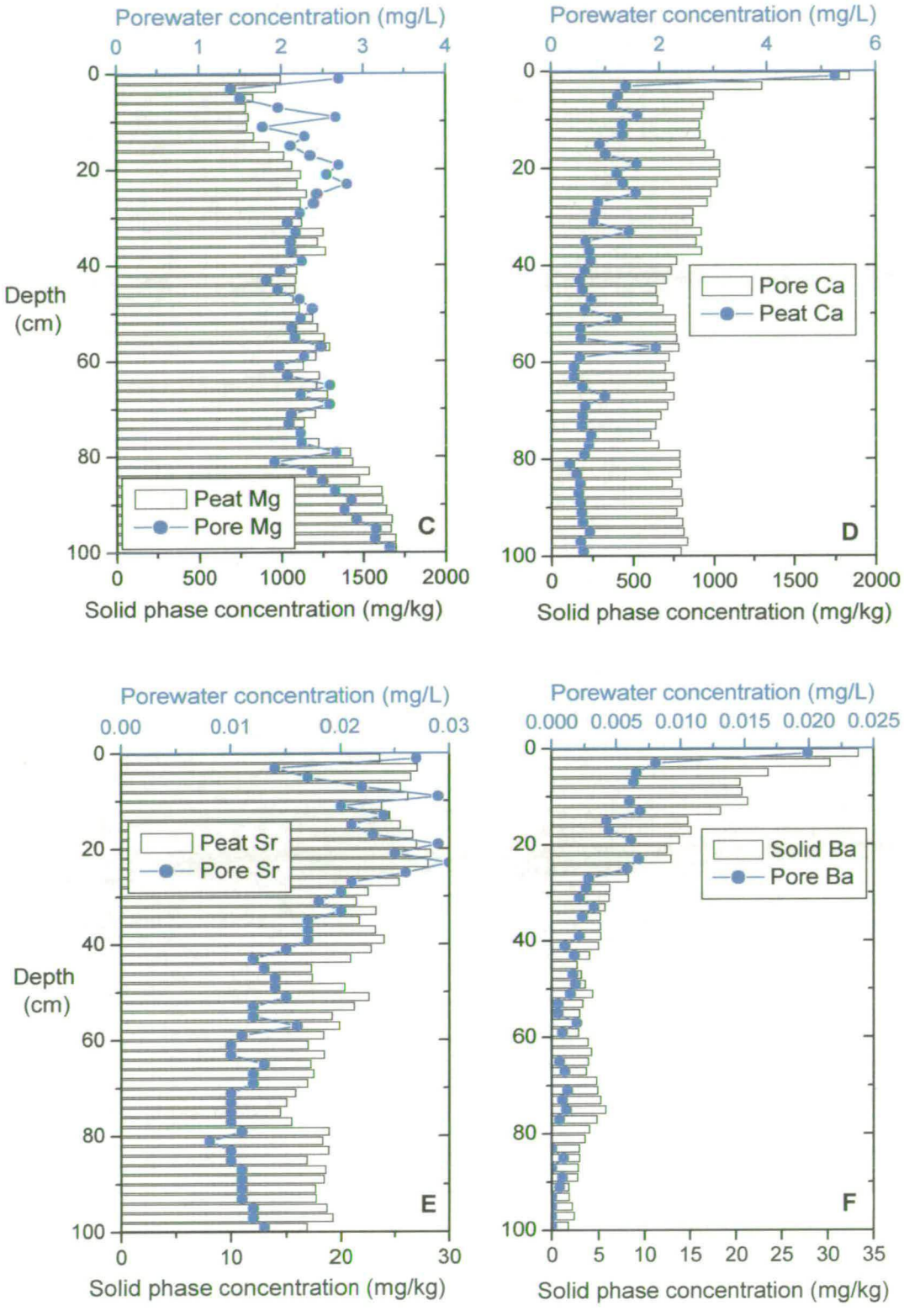

Figures 3.11C-F: Vertical variations in the concentrations of Mg, Ca, Sr and Ba in porewaters (and solid phase) from a Flanders Moss peat core

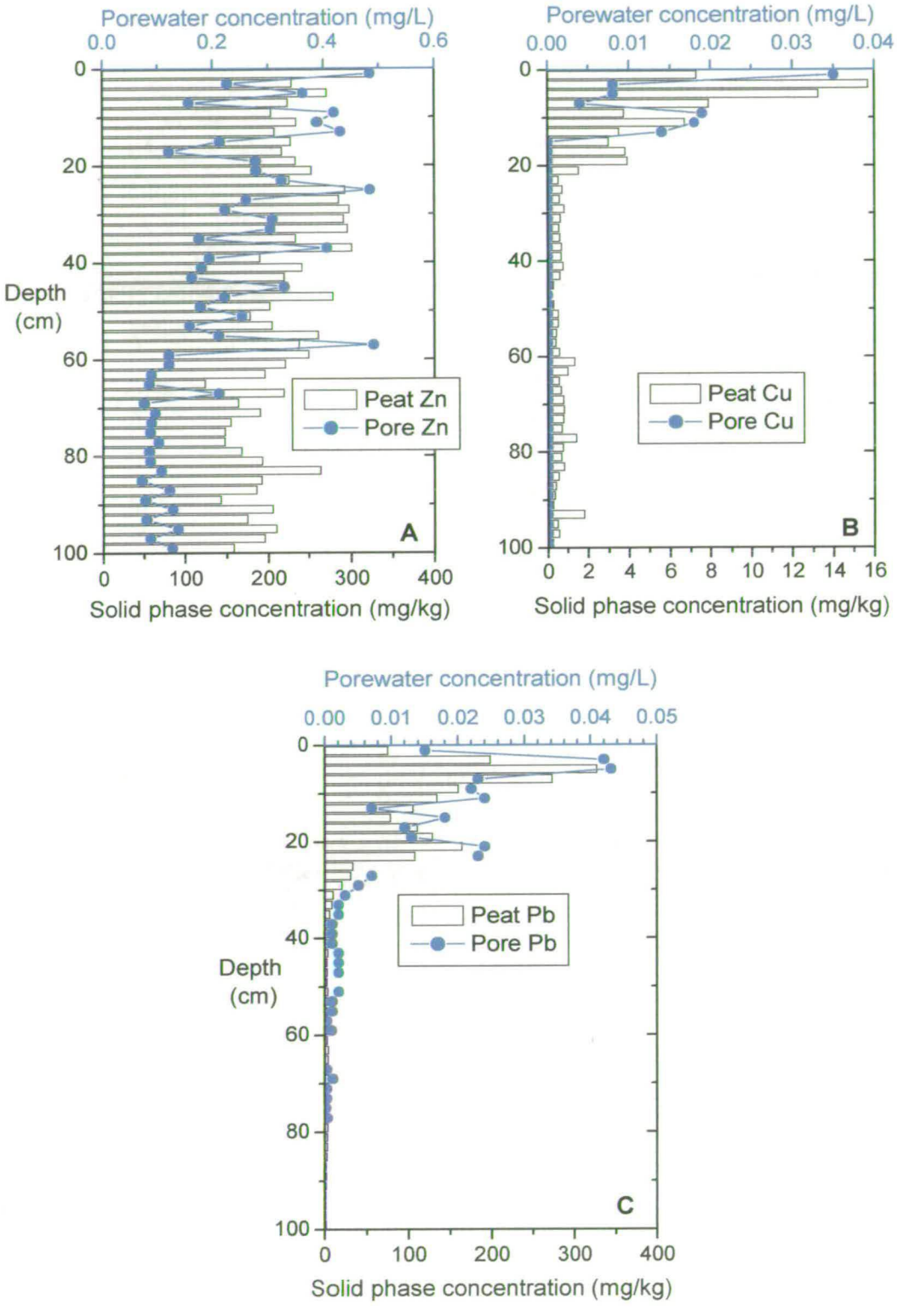

Figures 3.12A-C: Vertical variations in the concentrations of Zn, Cu and Pb in porewaters (and solid phase) from a Flanders Moss peat core

3.6 DISCUSSION: CHARACTERISATION OF THE SOLID PHASE SAMPLES FROM FLANDERS MOSS PEAT CORE 1

3.6.1 The position of the water table at the time of sampling

The volume of water contained within each section (5 cm x 5 cm x 2 cm depth) of the peat increases from the surface down to ~20 cm. Below 20 cm, the water volume is reasonably constant, which suggests that the water table was situated at ~20 cm depth at the time of sampling (summer). The reduced volume of water associated with the upper sections is probably associated with evaporation and transpiration processes. The level of the water table marks the onset of anaerobic conditions within the peat, and is of relevance to the zone of redox recycling, which will be discussed in later sections.

3.6.2 Moisture content and density of the peat

Peat typically has a high moisture content and from the results presented in Table 3.1 the dry weight constituted less than 10% of the fresh weight of peat, indicating that more than 90% of the peat was water. Natural organic matter can retain water equivalent to 20 times its mass (Stevenson, 1982) and so values between 85-95% are not unexpected for an organic-rich peat bog environment.

The near surface density values (0-6 cm sections) are much lower than the underlying sections. This strongly suggested that the material from these sections comprised mainly living plant material rather than peat. At the time of sampling, the sections appeared to contain more vegetation and less peaty material. The amount of the latter increased towards the bottom of the 0-6 cm zone. From 6-20 cm, the material in each section was dominated by darker, more cohesive peaty material and the highest densities were found in these sections. The increase in density was consistent with the formation of peat from slowly decaying bog vegetation. A minimum at ~40 cm suggested that the material from this depth was less humified/ less altered than that from the 6-20 cm sections. In some sections around 40 cm, recognisable plant material was observed at the time of sampling and this would be consistent with a lower extent of humification.

If the local climatic conditions had been different, e.g. wetter, leading to strongly reducing conditions even at the surface of the peat bog, this could account for the preservation of barely altered plant material. Below 40 cm, there were further minor fluctuations in peat density, which may also have resulted from the influence of climatic conditions on the preservation of organic matter.

3.6.3 Organic matter and ash content

Peat is characterised by very high organic contents, resulting from preservation of organic matter under conditions of low temperature, high rainfall, high acidity and lack of oxygen, which inhibit microbial activity. Values of ~98% dry weight over most of the core are consistent with those obtained for other ombrotrophic peat bogs (Shotyk *et al.*, 1996). The minimum organic content in the 4-6 cm section of the peat is due to the high ash content. The higher relative proportion of ash prevalent in the top 20 cm of the peat is attributed to the increased deposition of atmospheric particulate matter in the recent past (more specific time-scales to be discussed in Chapter 5).

3.7 DISCUSSION: CHARACTERISATION OF THE POREWATERS EXTRACTED FROM PEAT CORE 1

3.7.1 Porewater pH and DOC concentration

The pore water pH values were low indicating that the peat was quite acidic. In some previous studies, a constant pH has been measured down the peat profile whilst in others, variations in pH have been observed, (Shotyk and Steinmann, 1995). In Flanders Moss porewaters, the pH minimum coincided with the highest concentration of DOC in the porewaters, suggesting a link between organic acids and pH. Steinmann and Shotyk (1997) in a study of peat pore waters suggested that the pH balance of a peat bog is maintained by organic acids and carbonic acid. They proposed that, based on Thompson *et al.* (1927), at pH's less than 4.2, organic acids control pH, whereas above pH 4.2, carbonic acid is the most important species controlling the pH.

It is important to note at this stage that, not only was the DOC maximum found at the pH minimum, the increase in pH at greater depth corresponded to a concomitant decrease in DOC concentration in the porewaters. This is contrary to the relationship between pH and DOC in outputs from geochemical models, e.g. WHAM. Typically, such models predict decreasing DOC concentrations (Tipping *et al.*, 1995). This will be discussed further in Chapter 6.

3.7.2 Porewater conductivity

The conductivity maximum between 6-20 cm coincided with the density maximum, and was undoubtedly affected by the increased amount of solid phase peat in contact with the porewater. Importantly, the conductivity profile does not inversely mirror the pH profile, illustrating that the conductivity is a measure of other ions as well as protons in solution, and it is bulk solution ionic strength which controls the conductivity.

3.7.3 Porewater organic matter concentration from UV absorbance at 254 nm

There was a good degree of similarity between the DOC profile and the UV profile in that the maxima for DOC and absorbance coincided. Examining the DOC and UV absorbance profiles more closely, however, yielded important information about the changing characteristics of the organic material in the porewaters.

Given the small extent of peat formation, the DOC in the near surface sections most probably consisted of small, low molecular weight organic molecules (e.g. acids, alcohols, and phenols) that did not contain "chromophore" groups and thus did not significantly absorb UV light (254nm). In comparison with the change in DOC concentration, the more rapid increase in the value of UV absorbance from 6-20 cm reflected increased functionality of the molecules. In contrast, towards the base of the core, the more rapid decrease in UV absorbance compared with DOC concentration was attributed to the loss of functionality from the organic molecules during diagenesis.

3.8 DISCUSSION: VERTICAL DISTRIBUTION OF ELEMENTS IN THE SOLID PHASE AND POREWATERS FROM PEAT CORE 1

3.8.1 Distribution co-efficients

Dividing the porewater concentrations by solid phase concentrations, distribution co-efficients for each of the elements were calculated. These distribution co-efficients are indicative of the affinity of the elements for the porewaters relative to the solid phase, with lower values having a much greater affinity to the solid phase. Taking the average of the values for all 50 2-cm sections yielded an average distribution co-efficient, and these are displayed in Figure 3.13.

The larger the distribution co-efficient for an element indicates the greater the preference of that element for the aqueous phase. Unsurprisingly, the values are highest for elements known to have a very low binding affinity for organic matter such as Na and K. In contrast, elements with very high affinities for the solid phase and binding to organic matter exhibit the lowest co-efficient values, as evidenced by the lowest values obtained for Ti, Pb and Al.

Steinmann and Shotyk (1997) conducted one of the few studies in which distribution coefficients were determined, and the results from Flanders Moss show some similarities to the distribution co-efficients calculated by Steinmann and Shotyk.

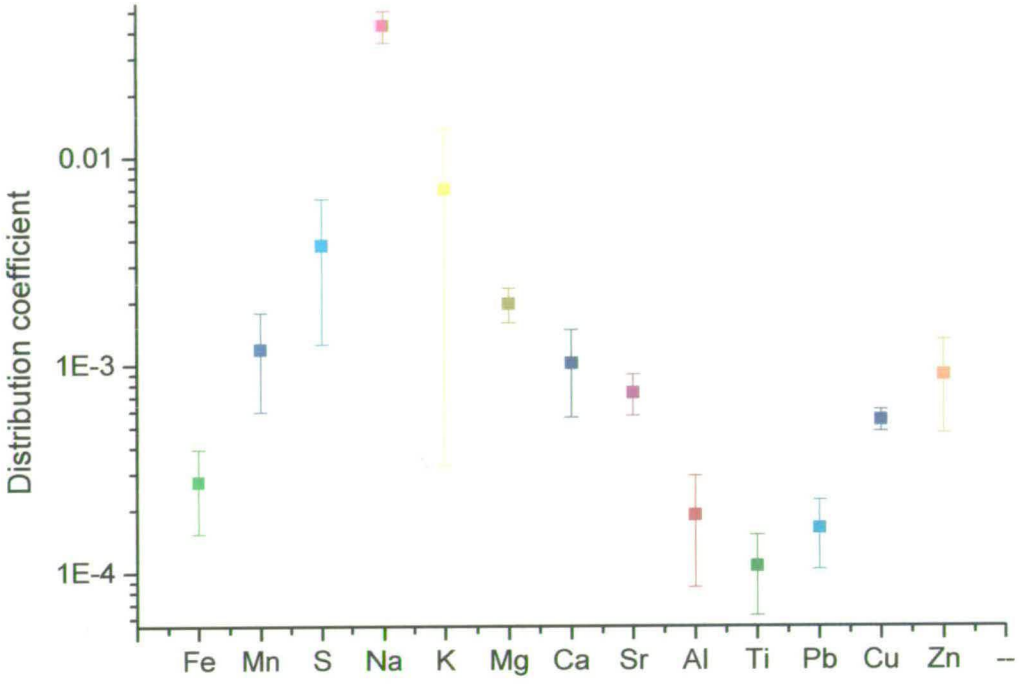

Figure 3.13: Average distribution co-efficients for partitioning between porewaters and solid phase peat from Flanders Moss

3.8.2 Group I – Mn and Fe

The solid phase Mn concentrations (< 0.075%) in the peat were much lower than observed for lake sediments, e.g. Loch Bradan: 1-6% dry weight (Gavin, 1999), Loch Lomond (southern basin): ~0.7% dry weight (Eades, 1999), Lake of Menteith: ~2.6% dry weight (Eades, 1999) and, more generally, soils. Most of the Mn in Core 1 was located close to the surface in line with other studies of Mn in peat (Steinmann and Shotyk, 1997). Initially, the peak of Mn in the solid phase suggested that similar redox processes to those observed in sediments were occurring in the peat; i.e. oxidation of soluble Mn(II) to Mn(IV) and precipitation of the latter as $Mn(IV)O_2$, leading to an enrichment of solid phase Mn at the oxic/anoxic boundary. If redox cycling were responsible for the near-surface peak, a minimum in the porewater concentration of Mn would have been expected (Mn removed from solution into the solid phase). The porewater concentrations in sections below the solid phase peak may also have been expected to increase, as Mn was reduced and subsequently released from the solid phase (Stumm and Morgan, 1996). However, from the pore water data, it is obvious that this is not the case, and the porewater Mn profile mirrors that of the solid phase. Another process that could cause near-surface enrichment of Mn is plant uptake and cycling, and this will be investigated further in Chapter 4.

The Fe solid phase concentrations (at ~ 0.3% dry weight) were low compared with Fe concentrations reported in lake sediments, (e.g. ~6.5% dry weight for Lake of Menteith and ~ 9.8% for Loch Lomond's southern basin, Eades, 1999). These values were in line with previous published iron concentrations in peat, (0.1% to 0.4% in the Tourbiere de Genevez (TGE) peat bog, Steinmann and Shotyk, 1997). The Fe variations in the TGE bog were apparently related to the ash content, with Fe peaks occurring at identical depths to the ash peaks. The ash peak in the Flanders Moss peat was quite sharp and was centred in the 4-6 cm whilst the Fe peak occurred in the 0-4 cm sections.

In peat bogs there is generally insufficient phosphate for the formation of vivianite ($Fe_3(PO_4)_2$). Siderite ($FeCO_3$) can from in CO_2-rich bogs, but only those with a pH >7, so the formation of siderite in Flanders Moss peat can be ruled out. Fe can also form sulphates or sulphides. However, most of the S in peat occurs in association with organic matter (Steinmann and Shotyk, 1997), and is not available for the formation of sulphates/sulphides. The most probable form of inorganic Fe in peat (and soils) is in the form of amorphous/crystalline oxides.

The Fe porewater profile exhibits maximum concentrations in the uppermost sections, and the concentration trend follows a similar pattern to that for the solid phase peat. As was observed with Mn, there was not a minimum in the porewater at the position of the solid phase maximum, which would suggest that the Fe was not subjected to significant cycling due to redox reactions. This would agree with the proposed position of the water table being at 20 cm depth, implying that, at the time of sampling at least, the peat was aerobic at the surface.

Some other mechanism is required to account for the surficial enrichment of Fe observed in both the solid phase peat and pore waters. One such mechanism is the uptake of Fe by plants. Fe is an essential micronutrient, and is required by plants. Although high concentrations exist in most soils, the plants can only take up Fe in a soluble form, either as aqueous ferrous iron or bound to small organic complexes (Wild, 1988). The exact mechanism of uptake is unknown, but it has been speculated (Uren, 1982) that the ferric iron-organic complexes are broken down in the vicinity of plant roots, and the reduced soluble ferrous Fe is taken up. Excess ferrous Fe is rapidly removed from solution by binding to fresh organic litter in the surface horizons of the peat.

The solid phase and porewater profiles for Fe also have an additional feature at ~20 cm. The peak was more pronounced in the porewaters relative to the solid phase, and coincided with the DOC peak. This suggests there is a relationship between DOC released from the solid phase, and the concentration of Fe in the pore waters.

It is proposed that the oxic-anoxic boundary occurs at ~ 20 cm and that reductive dissolution is a possible process by which Fe may be released into the porewater (in association with DOC).

3.8.3 Group II – S and P

Unlike the Fe and Mn, the solid phase S showed no significant near surface enrichment in either the solid phase or porewaters. In fact, there was a slight depletion of S in the pore waters between 0 and 8 cm. The constant concentration of S in the solid phase may reflect the role of S as a constituent in organic matter within the peat, with the S gradually being converted from functional groups on the surface of the small, fulvic type molecules to being incorporated into the backbone of the humic molecule.

In the porewaters, there would appear to have been a strong relationship between the S and organic matter, shown in Figure 3.14A. From a plot of S/DOC (Figure 3.14B), however, it can be seen that there is an overall trend of decreasing ratio of S to DOC down the porewater profile. On a w/w basis, the S would comprise ~2-6% of the dissolved organic matter, significantly higher than would be expected even for solid phase organic material (Steelink, 1985). More probably, not all of the S in the solid phase is in the form of organic S. Release of S from inorganic forms into the porewater must have occurred at ~ 20 cm, i.e. this may not be directly related to the increased concentration of DOC at this depth.

The solid phase P profile exhibited a near surface enrichment, in accordance with the growth-limiting role P plays in plant nutrition. There was also a peak between 70 and 80 cm depth in the peat, which correlated with similar peaks in the Al and Ti profile. This would suggest that this P peak is related to an inorganic component in the peat (see Section 3.8.3).

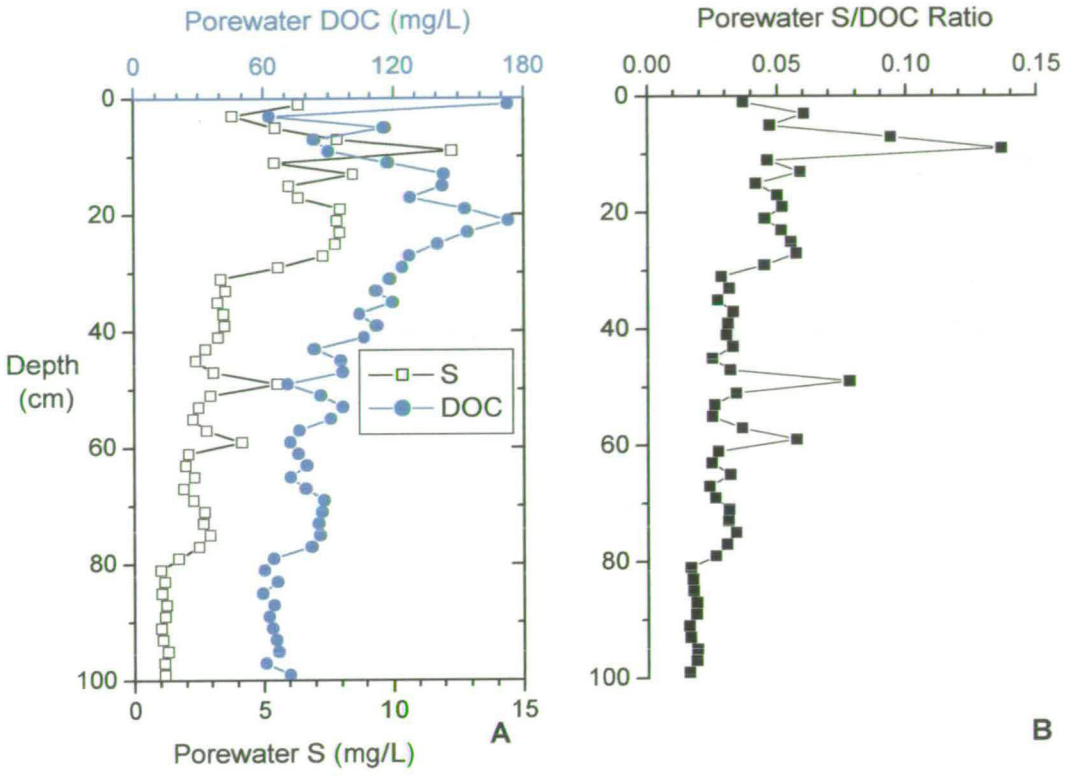

Figures 3.14A-B: Comparison of S/DOC porewater concentrations for a Flanders Moss peat core

3.8.4 Group III: Mineral Constituents: Al and Ti

Although the solid phase Ti and Al profiles show very similar shapes of profile, a Ti peak at 40 cm was absent from the Al profile. This is illustrated by the Ti/Al ratio for the solid phase (Figure 3.15A) which is almost constant over the entire profile except at ~30-40 cm. With the exception of this zone, a common origin for both elements would be predicted and for example, either element might be used as an indicator soil inputs over time. Using both of these elements as indicators of soil inputs to the peat bog on the basis of the 30-40 cm data, however, would yield significantly different results. The Ti/Al profile for the porewaters, although similar in shape, suggested that Ti, particularly at 30-40 cm was less soluble than Al.

A further feature of the data was the broad peak in porewater/solid phase concentration ratio for each of these elements (more so for Al which did not have a marked solid phase peak at this depth). This clearly suggested a change in the solubility of Al and Ti at depth in the peat bog. Although total solid phase elemental concentrations have not been determined in this study (HF is required for a complete dissolution of mineral material), such changes with depth need to be considered when using elemental data for normalisation purposes.

The relationship between the Al and Ti profiles and the ash profile also requires comment. This is best observed in a plot of Ti/Ash and Al/Ash ratios (Figure 3.15B). Generally, both the Ti/Ash and Al/Ash profiles fluctuate little in the upper and lower zones of the peat core, but there are several marked peaks in the middle of the profile, with both Al and Ti enhanced relative to the ash content. This would suggest a change of provenance for the source particles, or a change in rates of deposition of these elements to the peat surface. Numerous other authors (Shotyk, 1998, Kempter and Frenzel, 1999) have attributed peaks in conservative elements within the profile to increased disturbance of the surrounding land, e.g. forest clearances or intensification of agriculture.

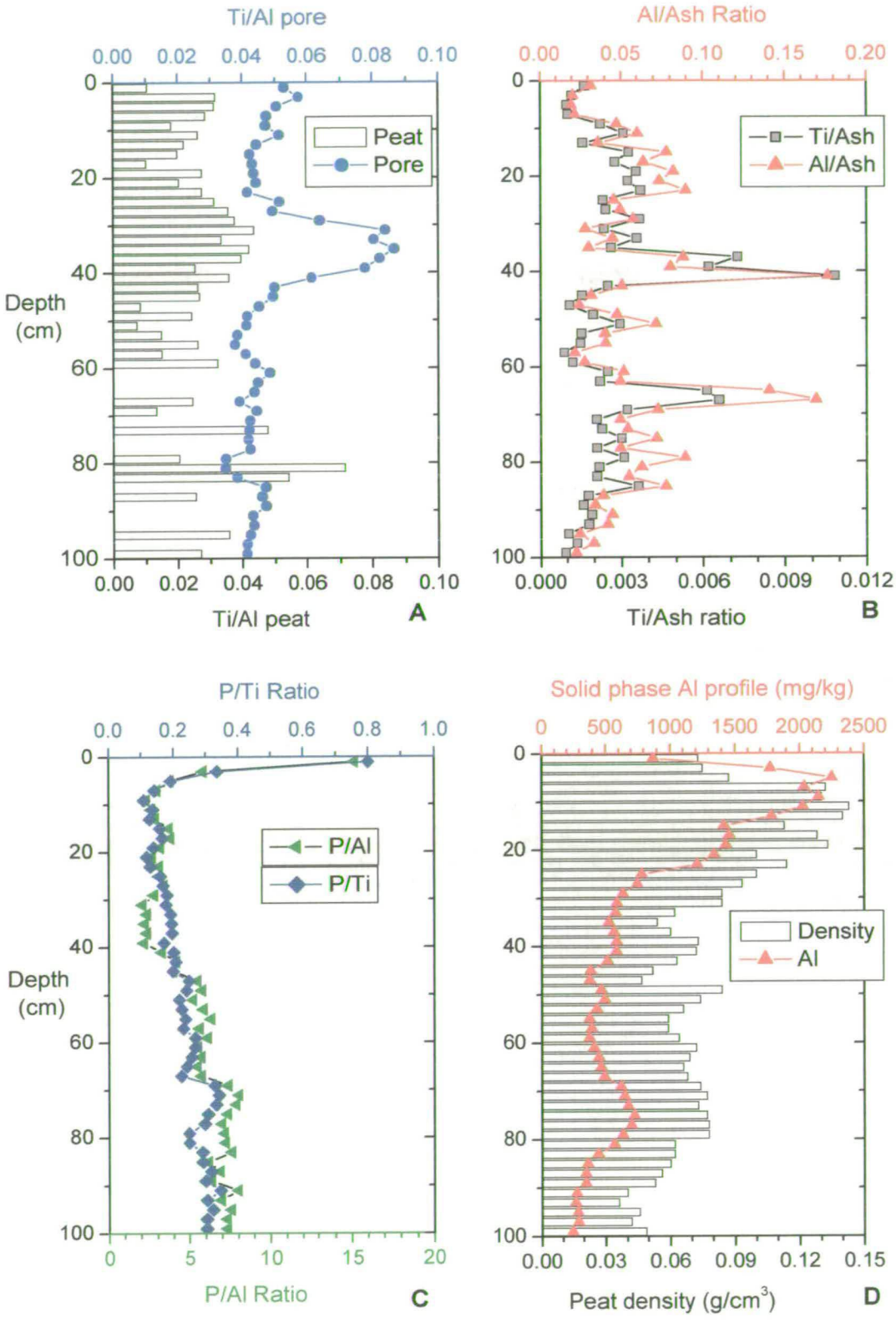

Figures 3.15A-D: Comparison of Al, Ti, porewater and solid phase profiles with P and ash solid phase profiles

The peak between 70 and 80 cm is also perceptible. As commented on with P above, there is marked similarity between the P and Al/Ti profiles at this depth (Figure 3.15C). It could be suggested that a component of the total P input is indicative of P-containing minerals, and while this cannot be ruled out, there is doubt as to whether the pseudo-total extraction would remove P within the mineral component. However, comparing the Al, Ti and P profiles with the peat density (Figure 3.15D) we can see the elevated concentrations of Al, Ti and P correspond to an increased density within the peat in this horizon. Therefore, the apparent increased concentrations at this depth may simply relate to greater compaction of the peat.

3.8.5 Group IV: Na, K, Mg, Ca, Sr and Ba

The order of distribution co-efficients for the alkaline metals and alkaline earth metals (Figure 3.13) is as follows; Na>K>Mg>Ca>Sr. The common factor in most of the solid phase profiles is the near-surface enrichment in the 0-2 cm section due to evapo-transpiration and plant uptake of these elements. The most pronounced enrichment is observed for K, in line with the important role of K in plant nutrition. K is one of the three growth limiting elements, the other two being P (see above) and N. The surface enrichment is least obvious for Mg and Sr.

An additional feature is the relative increase in Mg but decrease in Ca concentrations towards the bottom of the core. A similar situation has been observed in other ombrotrophic peat cores peat cores (Shotyk, 1996). As discussed in section 1.4.6, the Ca/Mg ratio has been used as an indicator of whether the peat is ombrotrophic or minerotrophic, by comparing the Ca/Mg ratio in rainwater with Ca/Mg ratios lower in the peat. Increases in the Ca/Mg ratio with increasing depth were attributed to an influx of Ca-rich groundwaters into the bog, thus marking the division between ombrotrophic and minerotrophic. In the Flanders Moss peat, the opposite situation is observed (Figure 3.16A). Most of the Ca input to the peat is in rainfall, whereas a significant proportion of the Mg input is in mineral material deposited on the surface of the peat bog.

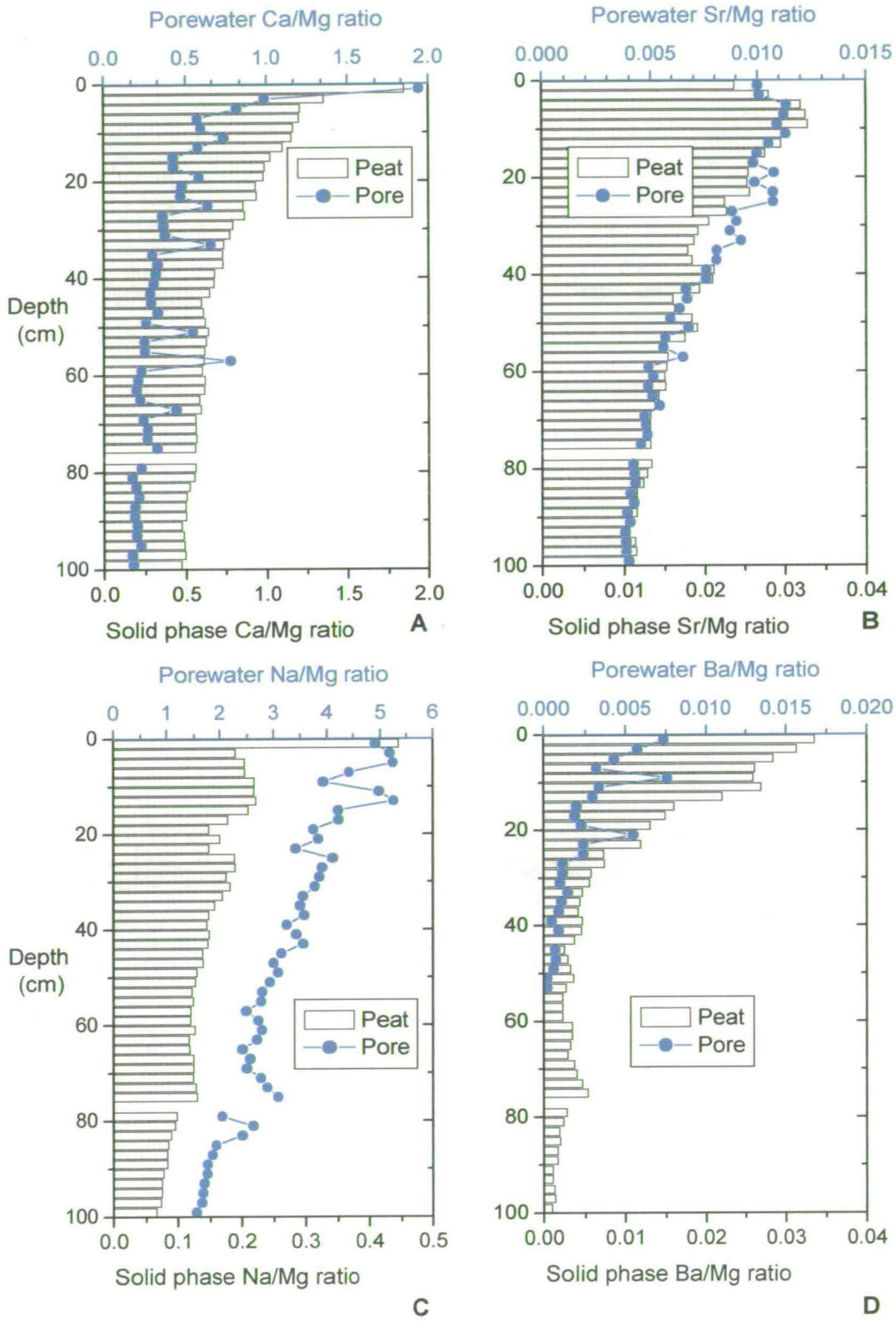

Figures 3.16A-D: Solid phase and porewater ratios Ca, Sr, Na and Ba vs Mg

One of the main Mg-containing minerals is biotite (section 1.2.6), which upon weathering forms clays such as vermiculite. Mg in these clays is held within the silicate lattice and is not readily released upon weathering. The increase in Mg relative to Ca within the peat solid phase and porewaters may reflect the release of Mg from these minerals.

Similar decreases are observed in the Sr/Mg ratio (Figure 3.16B) the Na/Mg ratio (Figure 3.16C), and given that rainfall is again likely to be the dominant source of both Sr and Na (Halstead *et al.*, 2000), then this adds further support to the above hypothesis.

The much higher affinity of Na for the porewaters is observed by the higher values of the distribution coefficient relative to Mg, Ca, Ba and Sr (Figure 3.13). This is consistent with the size of the hydrated sodium ion and the resultant low affinity to organic matter and surface sites on inorganic material.

In contrast to the other alkali and alkaline earth metals, the Ba solid phase and porewater profiles have a completely different shape, which is in fact more akin to the Al, Ti (and at depth P) profiles (Figure 3.16D). This would suggest that the predominant source of Ba to the solid phase peat is in the form of mineral material, and not as a cation within rainfall.

3.8.6 Group V – Zn, Cu and Pb

Although the Zn profiles are extremely noisy, there is a degree of agreement in the shapes of the solid phase and porewater profiles. Both exhibit higher concentrations in the near-surface sections; the decrease in the porewater concentrations occurs more rapidly from 40 cm downwards. The only interpretation that can be substantiated is that Zn is less strongly attached to the solid organic component, and is able to diffuse more significantly (over much greater depth) than either Cu or Pb.

This finding is entirely consistent with previous findings in Scottish peat bogs (Mackenzie *et al.*, 1998). The exact mechanism of vertical migration is unclear, and a number of possibilities have been suggested including formation of Zn sulphides (Damman, 1982). Having already investigated the distribution of sulphur between the solid phase and porewaters (see above), it was concluded that most of the sulphur in the peat was associated with organic matter. Comparison of the Zn profile with the shape of other anthropogenic contaminants Cu and Pb indicate that the Zn profile is unsuitable for use as providing an historical record of anthropogenic inputs.

The solid phase Cu profile is similar but not identical to the solid phase Pb profile, with differences in the position of the subsurface peaks. The presence of most of the Cu in the upper 20 cm of the peat could be consistent with anthropogenic inputs. The Cu porewater profile does not entirely agree with the solid phase profile, with the porewater exhibiting a maximum concentration of Cu in the 0-2 cm section, while the solid phase peak is in the 2-4 cm section. The subsurface peak of Cu ~ 20 cm is not reflected in the porewaters.

The low concentrations of Cu in the porewaters meant that they were close to concentrations of Cu in the blanks. The peak of Cu in the 0-2 cm section in the porewaters may reflect the role of Cu in plant nutrition. Evidence for the requirement of Cu by plants can be seen in deficiencies that have been identified in wheat growing on soils derived from Cu deficient Devonian sandstones in Scotland (Macbratney *et al.*, cited in Wild, 1988), which is the underlying bedrock beneath Flanders Moss.

Sixty to ninety percent of Cu in aqueous extracts of a peat with a pH of 3.5 was organically complexed, which rose to 98% at pH 6 (Hodgson *et al.*, 1965). This association of cations and organic matter with varying pH will be explored in Chapter 6.

It would appear that the Pb porewater profile mirrors the solid phase profile and that there are indeed two peaks in the porewater profile. This indicates that the small amount of Pb in the porewater is not able to diffuse over distances of several cm in this part of the core. The fact that the shape of the solid phase peat profile is reproduced in the porewaters would suggest equilibrium between the solid and aqueous phase. The similarity in solid phase and profiles also clearly indicates that the processes affecting the concentration variations in the Group I-IV elements do not operate with respect to Pb. The low distribution coefficient for Pb (Figure 3.15) shows that the Pb has a very strong preference for the solid phase. These lead to the conclusion that Pb is likely to be immobile in the peat bog.

There is, however, some evidence to suggest a slight downwards diffusion of porewater Pb just below the second peak in the solid phase as evidenced by an apparent increase in the distribution co-efficient profile for Pb with depth (Figure 3.17). It is possible that with increasing burial, the form of Pb in the peat could be altered. Notably, the second peak for Pb in the solid phase and porewaters coincides with maxima in the DOC (and porewater S). It was thus necessary to investigate further the associations of Pb with organic matter, and the results of this investigation are presented in Chapter 4.

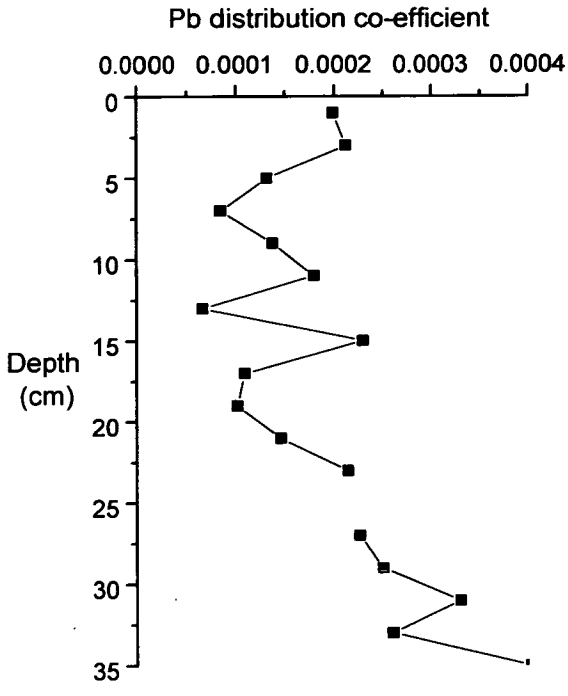

Figures 3.17: Vertical variation in the calculated distribution co-efficient for Pb in Flanders Moss peat

3.9 CONCLUSIONS

Characterisation of the solid phase peat showed that it generally had a low ash content, consistent with designation as an ombrotrophic peat bog. Further evidence for this designation was provided by the Ca/Mg ratio (both for solid phase and porewater), which decreased with increasing depth. High values for moisture content and organic matter were also consistent with those expected for a peat bog. More importantly, the changes in density of the peat with increasing depth helped to characterise different zones of the peat:

(i) 0-6 cm – dominated by vegetation
(ii) 6 cm - marked transition from the vegetation zone to cohesive peaty material
(iii) 6-20 cm –highest density of peat
(iv) 30-50 cm – low density peat – a less humified zone
(v) 50-100 cm – small variations in density indicating differing extents of humification

Characterisation of the porewater samples revealed an inverse relationship between pH and DOC with the maximum DOC concentration at ~20 cm occurring at pH 3.6. This is contrary to the relationship used in certain geochemical models. The relationship between DOC concentration and UV absorbance indicated that there were changes in the nature of the DOC with increasing depth. This is again highly relevant for modelling studies as a change in functionality with depth has implications for the metal binding characteristics of the DOC.

From the elemental data, the major conclusions are detailed below.

Nutrient uptake in the uppermost sections (0-6 cm) was an important process influencing the solid phase and porewater profiles of Na, K, Mg, Ca and perhaps Mn and Fe – the redox behaviour of this second group does not appear to control the vertical distribution of Fe and Mn in this zone.

In the 10-20 cm zone, there were elevated concentrations of some of the more soluble elements (Na, Mg, Sr + perhaps Zn) in the porewaters relative to the solid phase. The peaks in the porewater concentrations of these elements at this depth also correlated with the conductivity maximum.

Although the Al/Ti ratio was constant over much of the profile, the absence of an Al peak resulted in a significant change in the Al/Ti ratio at 40 cm. This has implications for the use of these elements as indicators of soil inputs, i.e. where a constant ratio is assumed on the basis that both elements are always from the same source. The data also indicated changes in the solubilities of Al and Ti with depth Maximum release into the porewaters at 30-40 cm coincided with the zone of low-density peat. It is suggested that both changes in Al/Ti ratios and in elemental solubilities would need to be rationalised before adopting data normalisation procedures.

None of the processes described above which influence the shapes of the elemental profiles appeared to influence the solid phase Pb profile. The results strongly support the post-depositional immobility of Pb in the peat. However, further investigations were warranted because the second Pb peak, present in both the porewater and the solid phase coincided with the porewater DOC, S and Fe peaks. To provide a better understanding of Pb behaviour, a more detailed investigation of Pb associations within the peat was proposed.

Chapter 4 –

Vertical Distribution of Elements in the IHSS and Tris-Borate Humic Substance Extracts from a Flanders Moss Peat Core

4.1 INTRODUCTION

This chapter contains the results of the elemental analysis of (i) humic and fulvic acids obtained using a modified IHSS extraction method (see section 2.5), and (ii) humic substances isolated using a milder extraction method (0.045 M Tris Borate). The humic and fulvic acids, and humic substances were extracted from each of the 50 2-cm depth increment sections from the core designated Core 2 (see Section 2.1.3).

4.2 EXTRACTION AND QUANTIFICATION OF IHSS HUMIC AND FULVIC ACIDS FROM FLANDERS MOSS PEAT

The extraction of fulvic and humic acids (as operationally defined – see Section 1.5.1) was undertaken using the method prescribed by the International Humic Substances Society (outlined in Section 2.4). Three separate materials, designated Fulvic Acid 1 (FA1), Fulvic Acid 2 (FA2), and Humic Acid (HA), were obtained using this method.

Appendix 9.7 contains the concentration of DOC for the FA2 extracts and the freeze-dried weights of HA for each 2-cm depth section of the peat core. The third column in Appendix 9.7 contains the calculated dry weight of FA2 in each section of the core. The conversion of the organic carbon to organic matter values was achieved by multiplying the DOC concentrations by 1.7. No DOC values for FA1 were obtained because these extracts were too lightly coloured to allow DOC determination. The calculation of the percentage of the total peat organic matter extracted by the IHSS method was therefore obtained by comparison of the sum of FA2 and HA with the total OM in the peat. In the following chapter, all values are expressed on a dry weight basis.

4.2.1 Vertical variations in the concentration of FA2

The concentration of FA2 in each 2-cm section of the peat core is displayed in Figure 4.1A. In the three uppermost sections of the core, concentrations ranged between ~10-30 mg/kg. Concentrations then decreased rapidly to 6.8 mg/kg at ~10-14 cm. Below this, there was an increase to a broad maximum (~30 mg/kg) between 30 and 40 cm. Almost constant values of around 20 mg/kg were obtained for the 60-80 cm sections whilst concentrations of up to ~40 mg/kg were obtained for the 80-100 cm sections. The large peaks at 50-52, and 78-80 cm were probably the result of accidental puncturing of the 0.2 μm filter membrane in the filtration process (see Section 2.4.3.

4.2.2 Vertical variations in the concentration of HA

The concentration of HA extracted from each section of the peat core is shown in Figure 4.1B. The shape of the HA profile differs markedly from that observed for FA2. Greatest concentrations of HA were extracted from the 0-20 cm sections and a maximum of ~180 mg/kg was obtained for the 14-16 cm section. No data was available for the 12-14 cm section, which was accidentally spilt. It is notable that the position of the HA sub-surface maximum is very similar to the position of the FA2 minimum. Below 20 cm, HA concentrations decreased to a minimum of 26 mg/kg at 38-40 cm (this is also the position of the FA2 sub-surface maximum). Thereafter, concentrations increased gradually with increasing depth to a smaller maximum of ~140 mg/kg at 88-90 cm.

4.2.3 Vertical variations in the concentration of TB HS

The vertical concentration profile for TB-extracted HS (Figure 4.1C) had a similar shape to that for HA. The sub-surface maximum of ~75 mg/kg (dry weight peat) at 14-16 cm coincided exactly with the position of the maximum in the HA profile. There was also a gradual decrease in concentration below 20 cm to values of ~15 mg/kg (dry weight peat) at 48-50 cm. Thereafter, concentrations again increased to a localised maximum of ~ 65 mg/kg (dry weight peat) at 94-96 cm.

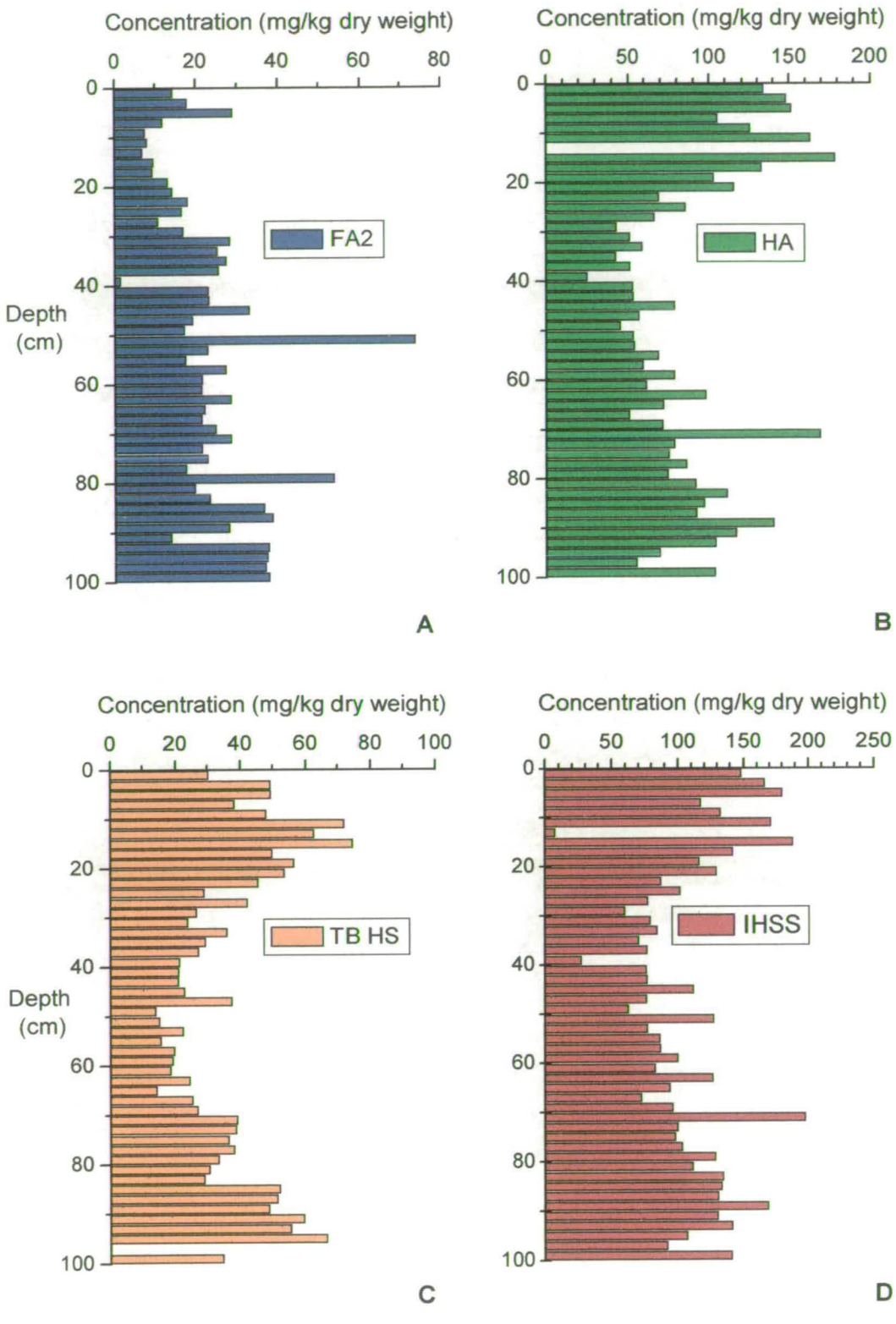

Figures 4.1A-D – Vertical variations in the concentration of organic matter extracted in FA2, HA, TB and IHSS materials from a Flanders Moss peat core

4.2.4 Vertical variations in the concentrations of IHSS (FA2+HA)

The sum of the concentrations of organic matter in the FA2 and HA extracts provides an estimate of the overall amount of organic material extracted by the IHSS methodology. The IHSS vertical concentration profile is displayed in Figure 4.1D. Comparing the HA and IHSS graphs (Figures 4.1B and D respectively) we can see that the profiles exhibit a common shape. From this, it can be seen that the HA component is the most important component of the IHSS procedure for extracting OM. Despite the variations in the FA2 profile in Figure 4.1A, these changes have little effect on the IHSS profile alongside the dominating HA component.

4.2.5 Comparisons between HA- and TB-extracted humic materials

The fraction of the HA material extracted by the TB HS extraction is expressed in Figure 4.2A. The average proportion of the HA component extracted by the TB HS extraction was 43.1 ± 16.7 % (42% at the HA and TB maxima at 14-16 cm). A higher fraction of the HA was extracted as TB HS in the 30-40 cm zone of the peat, with relatively less extracted in the in the 40-60 cm zone. In the lower sections of the profile, the fraction of TB HS increased to values between 50 and 60%. Overall, the profile illustrates that the fraction of the HA extracted by the TB was not constant.

4.2.6 Comparisons between IHSS- and TB- extracted humic materials

The fraction of the "total" IHSS is displayed in Figure 4.2B. The average fraction of IHSS extracted by the TB HS was 33.3 ± 13.3, (although this rose to 39 % at the maxima in 14-16 cm section). As with the TB/HA comparison the fraction of the IHSS extracted by the HA was not constant, but varied with depth. With the addition of the FA2 component to the HA component, there is a slight decrease in the fraction extracted by the TB HS in the upper sections. The largest relative decrease in the two profiles is in the 40-60 cm zone, with the fraction of IHSS extracted about 10% lower than equivalent HA values. The shape of the two profiles is generally the same, indicating that the TB/HA and TB/IHSS values show similar disparities.

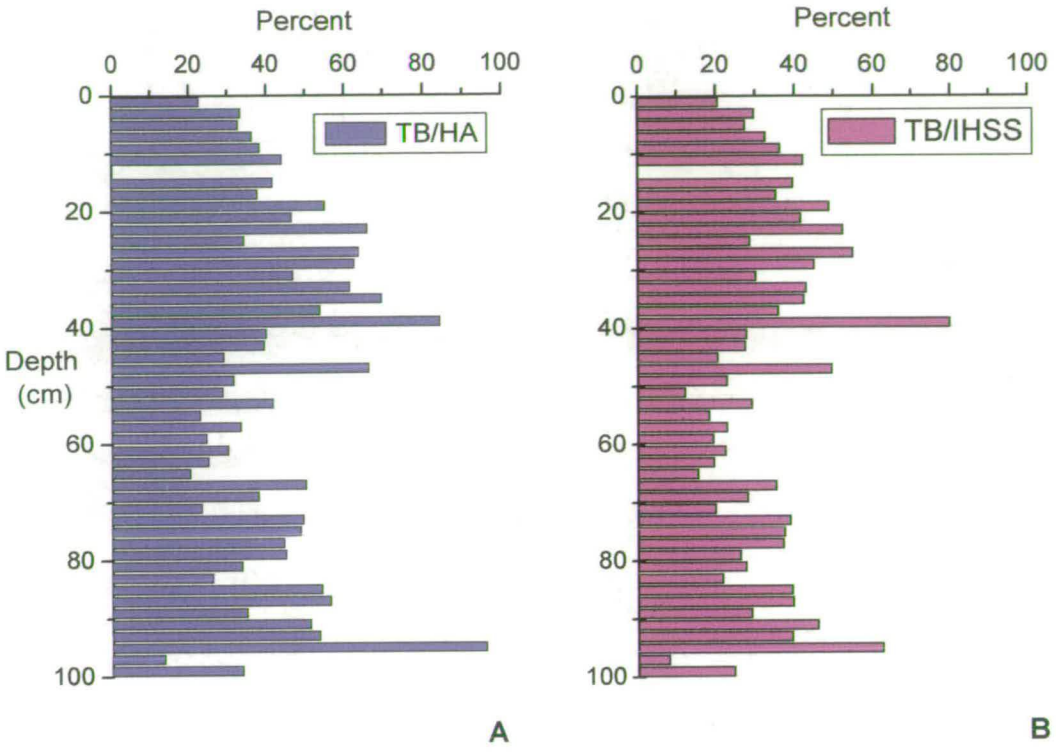

Figures 4.2A-B – TB extracted O.M. expressed as a fraction of HA extracted and IHSS extracted O.M. respectively

4.2.7 Percentage of total organic matter extracted by the IHSS and TB methods

The percentage total OM extracted by the IHSS method averages 12 ± 4% down the core, (but rises to 20% at the IHSS maximum in the 12-14 cm section). The average value for the TB extraction is somewhat lower at 4 ± 2%.

The IHSS profile (Figure 4.3A), exhibits a near surface maximum (>20%) in the 4-6 cm section. Below the second peak (in the 14-16 cm section), the percentage decreases with depth to a minimum (<3%) in the 38-40 cm section of the core. The percentage values increase with depth below 40 cm, reaching a maximum of 17% in the 88-90 cm section.

The TB profile (Figure 4.3B) also exhibits a maximum at 14-16 cm, extracting 8% of the peat OM. The lowest fraction of OM extracted (~2%) occurs between 50 and 66 cm. As with the IHSS profile, values in sections below 66 cm increases to a peak of 6.7% in the 94-96 cm section. The main difference in terms of the shapes of the IHSS and TB profiles is found in the near-surface sections. This difference may arise from the FA2 fraction, which although extracted in the TB profile, had the potential to be lost during the dialysis stage of the TB extraction (see Section 2.5.2). The differences may also be due to the slightly different mechanisms behind the operation of the two extractants (see Section 1.6.1).

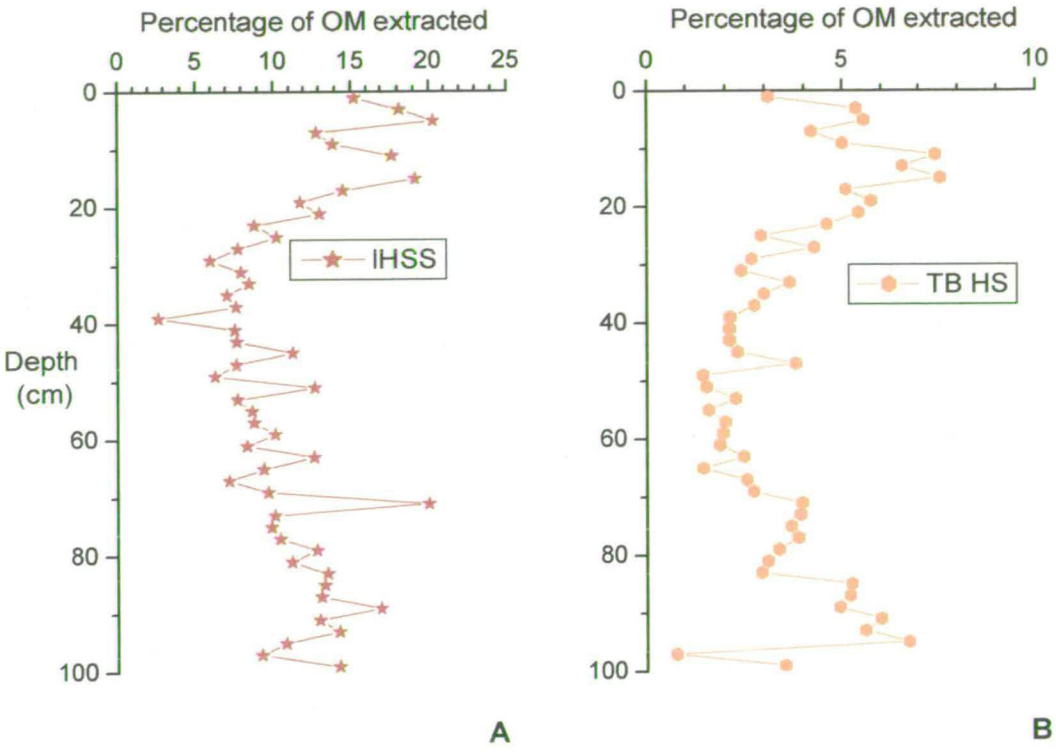

Figures 4.3A-B – The percentage of the peat OM extracted by the IHSS and TB HS extracts

4.3 VERTICAL DISTRIBUTION OF ELEMENTS IN THE FA1, FA2, HA AND TRIS EXTRACTS OF THE FLANDERS MOSS PEAT CORE

The elemental concentrations for each of the extracts are displayed in Appendices 9.8-9.11 respectively. As in Chapter 3, the elements have been divided into the following groups

Group I – Mn and Fe – potential to participate in redox cycling
Group II – S and P – participate in other important biogeochemical cycles
Group III – Al and Ti – indicators of mineral inputs
Group IV – Mg, Ca and Ba* - major and minor nutrient cations
Group V – Zn, Cu and Pb – heavy metals mainly from anthropogenic sources

*The Group IV elements, Na and K, have been omitted here because (i) Na is added to the peat samples in the form of 0.1 M NaOH as part of the IHSS extraction procedure; (ii) K concentrations had lower concentrations than the corresponding blanks for almost all of the extracts.

Where possible, the same scale has been used to aid comparison of the elemental concentrations in each extract. All results in the following sections have been expressed as mg/kg (dry weight peat).

4.3.1 Redox active elements: Mn, Fe and S

The vertical variation in Mn concentration for each of the FA1, FA2, HA and TB HS extracts is shown in Figures 4.4A-D, respectively. The same concentration scale has been used for FA1, FA2 and HA extracts but the scale for the TB HS extracts is one order of magnitude smaller.

With the exception of the TB HS profile, the maximum concentration of Mn was found in the 0-2 cm section (0-4 cm for HA). For FA1, the maximum concentration was ~2 mg/kg, almost double the maximum value for FA2. This in turn was more than three times the maximum value for HA.

Below the near-surface peaks in the FA1, FA2 and HA profiles, some variation with depth was observed. For FA1 (Figure 4.4A), there was a small sub-surface peak (0.6 mg/kg) at 8-14 cm, which was absent from the other profiles.

Below this peak, concentrations decreased gradually down to 0.08 mg/kg (dry weight peat) at 76-78 cm. Below 2 cm, the concentration of Mn in the FA2 (Figure 4.4B) and HA (Figure 4.4C) extracts was generally very low (<0.23 mg/kg and < 0.29 mg/kg, respectively). Mn concentrations in the TB extracts were extremely low (typically < 0.07 mg/kg) over the entire length of the core (Figure 4.4D).

Data was not included for the bottom 6 sections of the HA core, as these exhibited signs of contamination, and due to lack of sample and time, the extraction and analysis could not be repeated.

Figure 4.5A-D illustrates the vertical concentration profiles for Fe for each of the FA1, FA2, HA and TB HS extracts. As for Mn, the same concentration scale has been used for FA1, FA2 and HA extracts but the scale for the TB HS extracts is one order of magnitude smaller. As for Mn, the highest concentrations of Fe were extracted from the 0-2 cm section for FA1, FA2 and HA. In general, highest concentrations were found in the FA1 extracts.

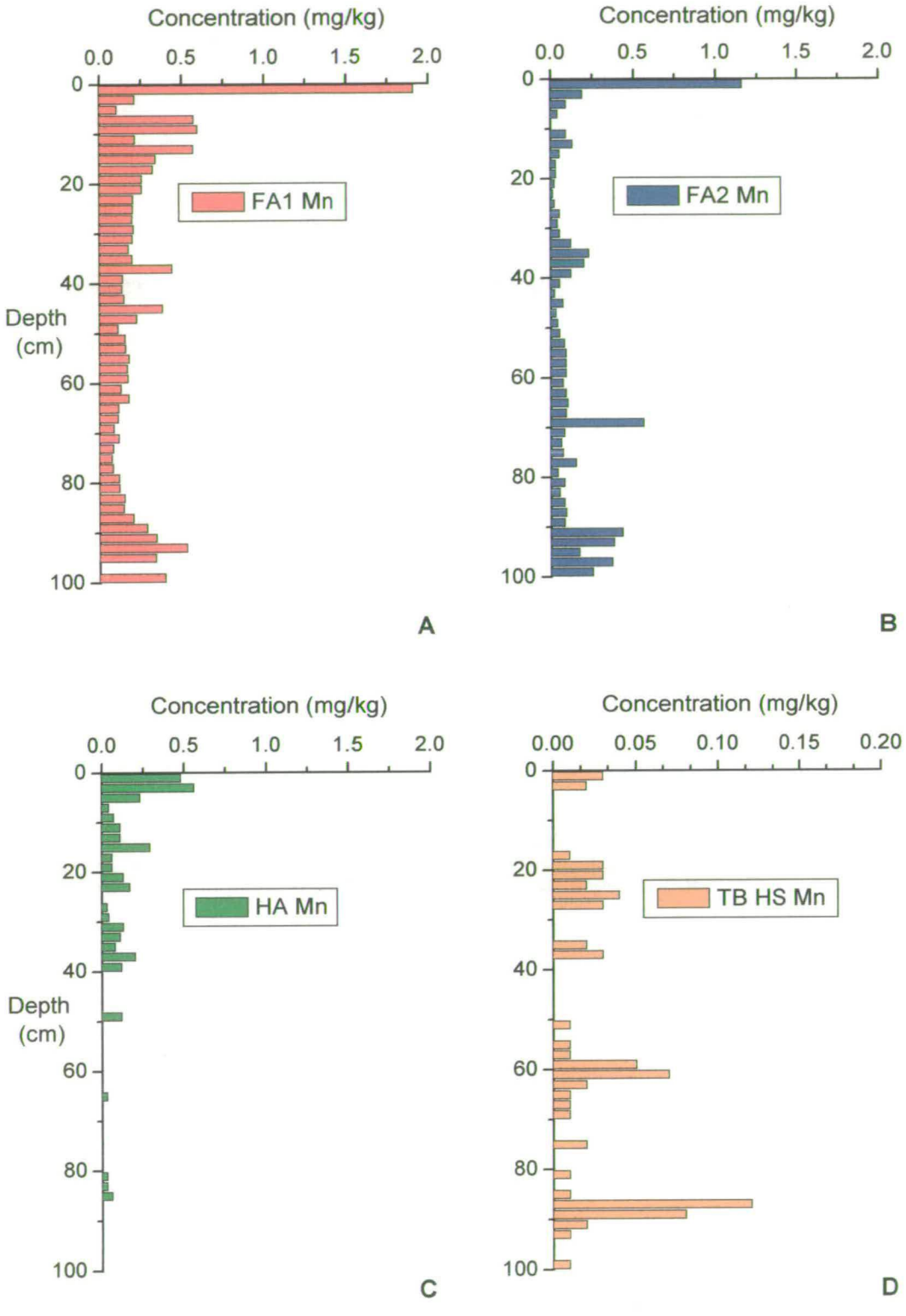

Figures 4.4A-D: Vertical concentration profiles of Mn with FA1, FA2, HA and TB HS extracts of Flanders Moss peat

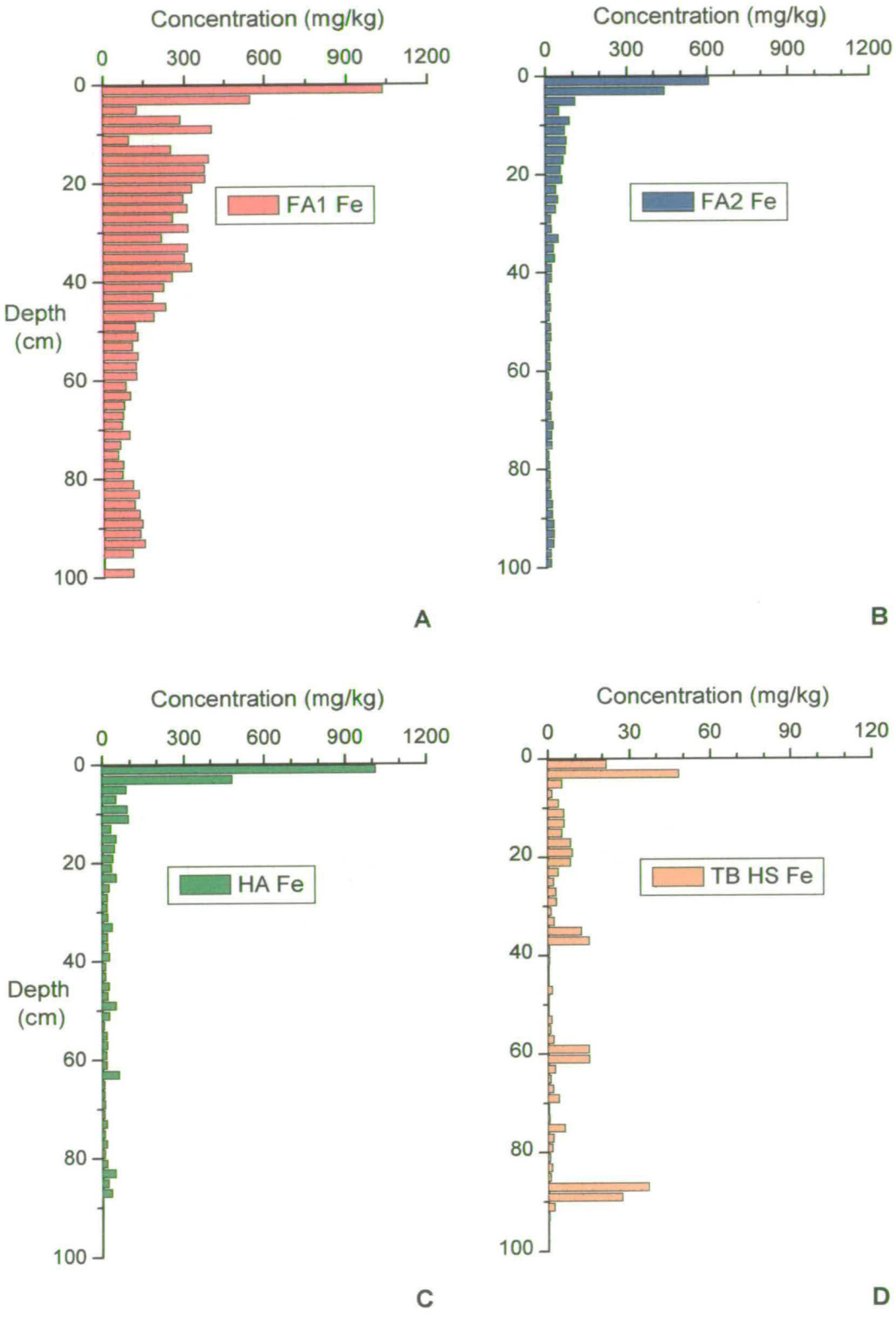

Figures 4.5A-D:Vertical concentration profiles of Fe with FA1, FA2, HA and TB HS extracts of Flanders Moss peat

Values of 1035 mg/kg and 1011 mg/kg were obtained for FA1 and HA respectively whilst the maximum value for FA2 was only 605 mg/kg. Clearly, the distribution of Fe amongst the IHSS extracts differs from that of Mn. The near-surface peaks were also broader than those for Mn and extended over the 0-4 cm sections of the core. There was a near-surface peak in the TB HS profile but with the maximum value of only 48 mg/kg occurring in the 2-4 cm rather than the 0-2 cm section.

Below the near-surface peak in the FA1 profile there were two broad sub-surface maxima, centred at ~16-20 cm (up to 376 mg/kg) and ~34-40 cm (up to 325 mg/kg), respectively. Below these peaks, there was a gradual decrease in Fe concentration. For the FA2 profile, concentrations below 6 cm were generally low (<100 mg/kg) and below 40 cm, concentrations were generally < 20 mg/kg. A similar pattern was observed for HA although concentrations decreased more rapidly to ~ 20 mg/kg by ~ 30 cm depth. For TB HS, excluding the 0-4 cm sections, Fe concentrations were always below 10 mg/kg.

4.3.2 Group II; S and P

The graphs in Figure 4.6A-D show the S concentrations for the FA1, FA2, HA and TB HS extracts. The scales have been selected in the same way as for Mn and Fe.

In contrast to Mn and Fe, the maximum concentration of S was extracted from the 4-6 cm sections in all cases (2-6 cm for TB HS). Values of 399 mg/kg, 403 mg/kg and 1349 mg /kg were obtained at this depth for FA1, FA2 and HA, respectively. The maximum value for TB HS was an order of magnitude lower than the FA1 and FA2 values at 43 mg/kg. In further contrast particularly to Fe, the greatest concentrations were generally found in the HA extracts (excluding the 4-6 cm peak, 160-950 mg/kg). Very low concentrations of S were present in the FA1 extracts (<30 mg/kg) whilst S concentrations in the FA2 extracts ranged from ~ 50-250 mg/kg below the near-surface peak.

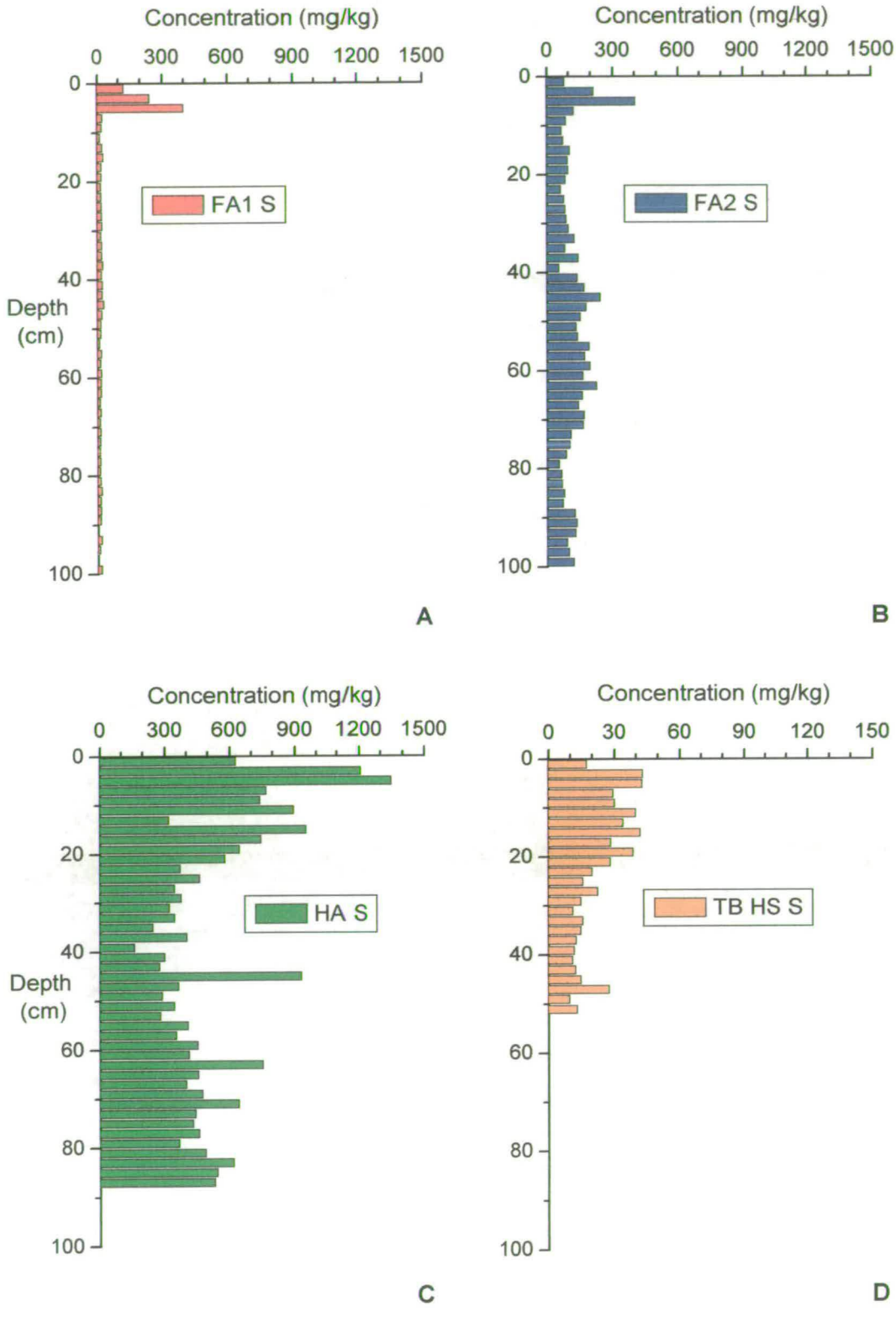

Figures 4.6A-D:Vertical concentration profiles of S with FA1, FA2, HA and TB HS extracts of Flanders Moss peat

Comparing the HA and FA2 profiles, there was a broad subsurface peak centred at 16-18 cm in the HA but not the FA2 profile. Additionally, below a minimum at 38-40 cm in the HA profile, concentrations increased towards the bottom of the core. However, for FA2 a broad maximum was evident at ~ 60 cm and concentrations then decreased towards the base of the core. The TB HS profile was similar to the HA profile in that there was a broad maximum at ~16-18 cm (42 mg/kg) and concentrations decreased to a minimum value at ~ 40 cm (9 mg/kg). No S was detected in the TB extracts below 54 cm. It was also notable that the S concentration at the sharper maximum in the TB HS profile at 4-6 cm was the same as that at the broader sub-surface maximum.

The concentrations of P in the FA1, FA2, HA and TB extracts are presented in Figures 4.7A-D. In the FA1, FA2 and HA profiles, the bulk of P is within extracts from the top 6 cm.

The FA1 and FA2 both have P maxima of 150 and 95 mg/kg respectively at 6-8cm, while the P maximum in the HA profile (230 mg/kg) is at 4-6 cm. Below 12 cm, the concentration of P decreases to >50 mg/kg. In the FA1 and FA2 extracts, the P concentration below 20 cm is negligible, whereas P in the basal HA extracts increases to 50 mg/kg. In the TB profile, the trends are similar to the HA P, with a near surface maximum (at 6 cm), decreasing concentrations down to 70 cm, and an increase in P in the bottom 20 cm.

4.3.3 Group II – Al and Ti

Figures 4.8A-D displays the vertical concentration profiles for Al in the FA1, FA2, HA and TB HS extracts. The scales have been selected in the same way as for the Group I elements.

Maximum Al concentrations in the FA1, FA2 and HA extracts of 662, 496 and 110 mg/kg, respectively, all occurred at 4-6 cm. In the FA1 and HA profiles, there was a small secondary peak at 14-16 cm.

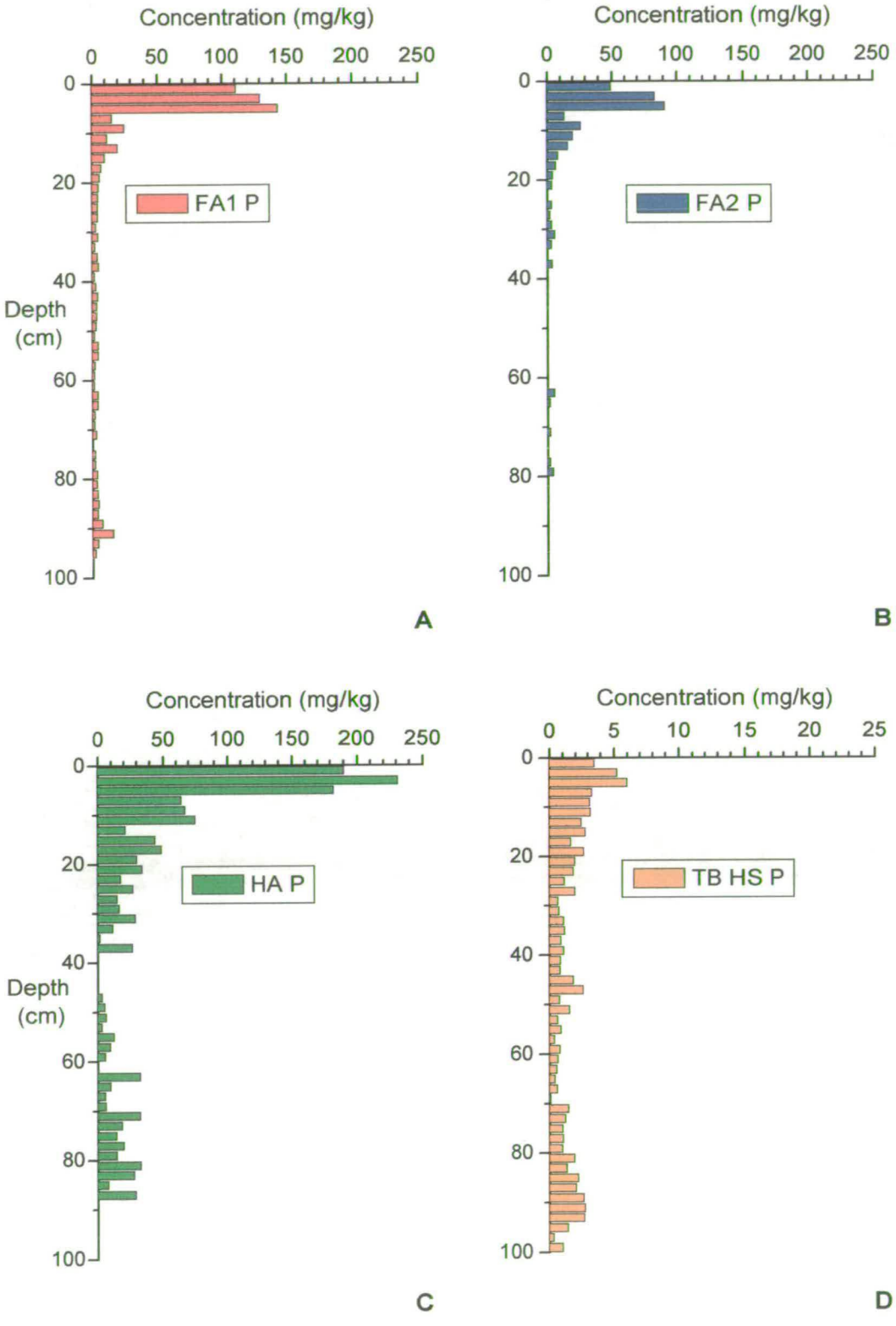

Figures 4.7A-D:Vertical concentration profiles of P with FA1, FA2, HA and TB HS extracts of Flanders Moss peat

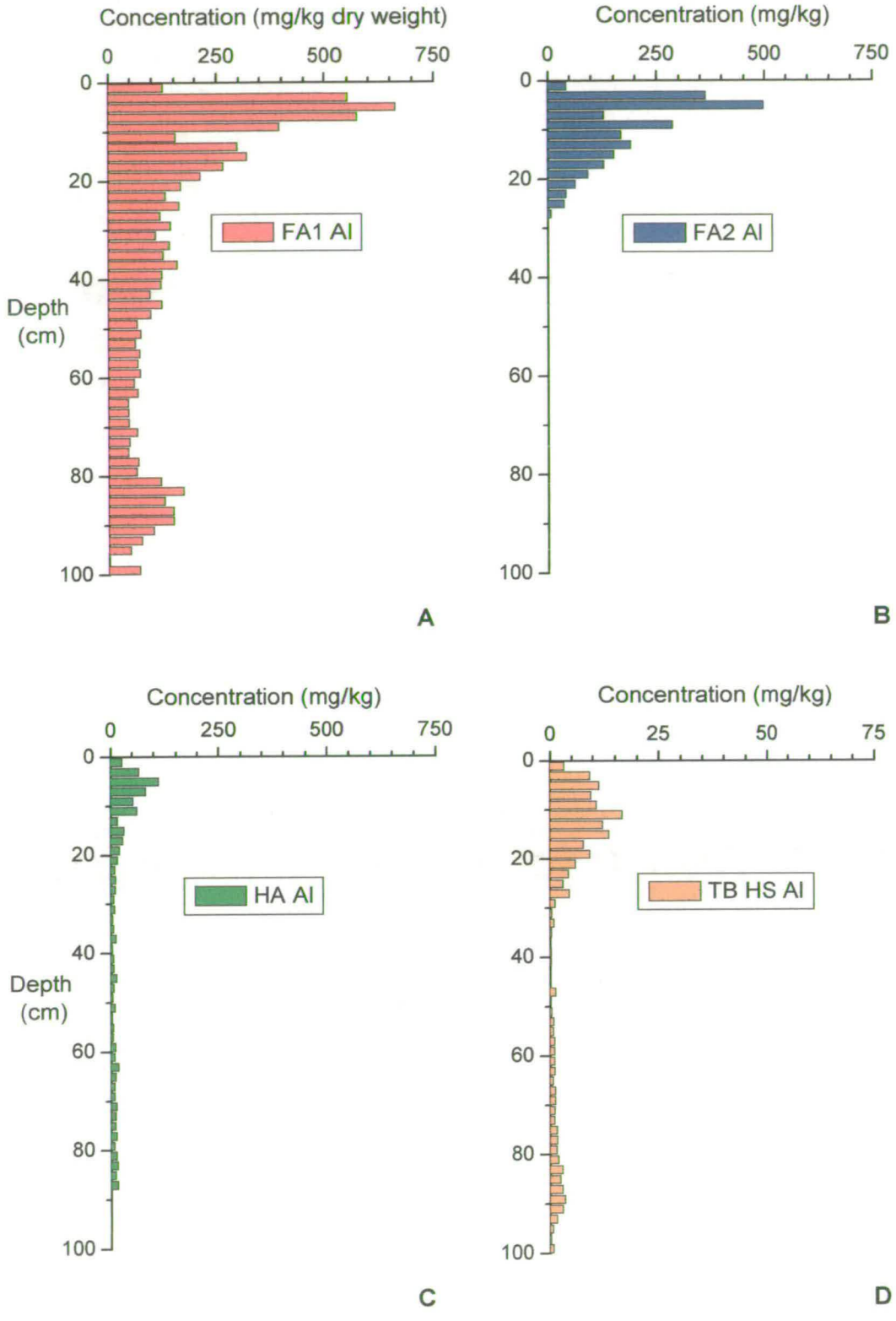

Figures 4.8A-D:Vertical concentration profiles of Al with FA1, FA2, HA and TB HS extracts of Flanders Moss peat

Thereafter, Al concentrations in the FA1 profile decreased with increasing depth whilst those in the HA profile decreased to a minimum of ~ 10 mg/kg at ~ 40 cm and then increased slightly towards the bottom of the core. In comparison with the IHSS materials, the concentration of Al associated with TB HS was typically about one order of magnitude lower. A broader Al maximum (up to 16 mg/kg) centred at around 10-12 cm was found in the upper sections of the TB HS profile. Very low concentrations (<3 mg/kg) were obtained for TB HS from all sections below 30 cm.

The Ti concentration profiles for FA1, FA2, HA and TB HS extracts are shown in Figures 4.9A-D. It should be noted that the scales for FA1, FA2 and TB HS are one order of magnitude smaller than that selected for HA.

Although as for Al there was a Ti peak at 4-6 cm in the FA1 profile, the main maximum of ~ 2 mg/kg occurred at ~ 30-40 cm depth. Below this depth, Ti concentrations were typically < 1 mg/kg. The concentration of Ti in the FA2 extracts was also low (< 2 mg/kg where detected). There was perhaps a small Ti peak at 4-6 cm. The greatest Ti concentrations were found in the HA extracts with the maximum concentration of 30 mg/kg, occurring at 4-6 cm. Clearly, the HA profile for Ti was similar in shape to that obtained for Al. The position of the secondary peak at 16-18 cm was also at a similar depth to that found in the Al profile. Additionally, as for Al, the TB HS profile for Ti had a broader near surface peak and concentrations an order of magnitude lower, compared with the HA profile. The maximum Ti concentration of ~ 1 mg/kg in the TB HS extracts were obtained for the 10-12 cm section. Ti concentrations were below the limit of detection below 30 cm.

4.3.4 Group III – Mg, Ca, Sr and Ba

In this section, no Na and K results are presented because (i) a reagent, namely 0.1 M NaOH, was used in the IHSS extraction scheme and (ii) K concentrations were, with the exception of the 0-2 cm section, below the limit of detection for analysis by ICP-OES.

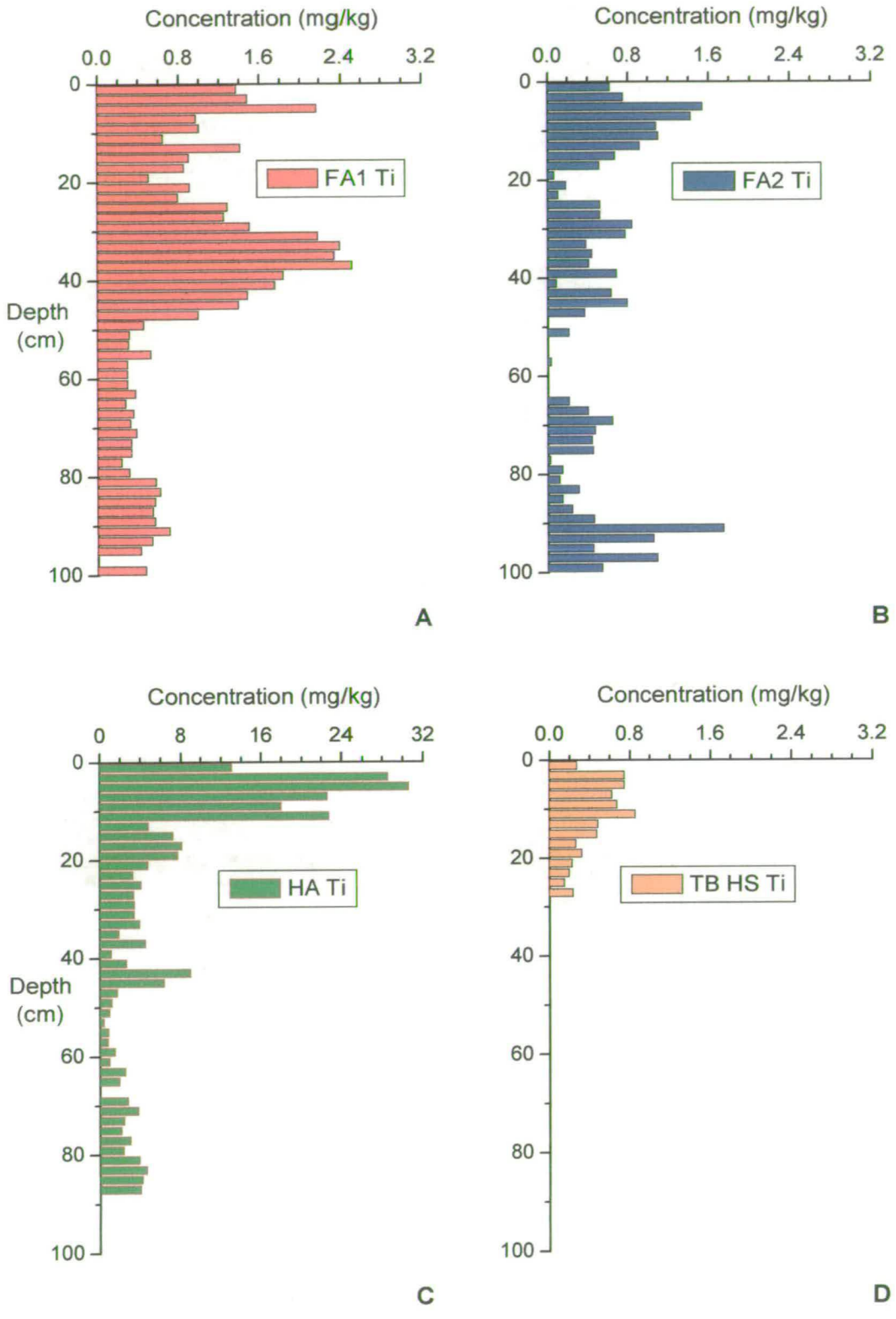

Figures 4.9A-D:Vertical concentration profiles of Ti with FA1, FA2, HA and TB HS extracts of Flanders Moss peat

The vertical variations in the concentration of Mg in the FA1, FA2, HA and TB HS extracts are illustrated in Figures 4.10A-D. The scales differ for each of the four graphs (FA1 > FA2 > HA > TB).

The profile obtained for FA1 had a minimum Mg concentration of ~90 mg/kg in the 0-6 cm sections followed by a relatively rapid increase to >600 mg/kg at ~ 20 cm. Below this depth, there was a slight but broad maximum of ~1000 mg/kg centred at ~40 cm. Mg concentrations then decreased slightly to <800 mg/kg at ~80 cm but increased substantially below this depth (1000-1400 mg/kg). The FA2 profile differed significantly in that there was clearly a broad peak at 10-20 cm (115 mg/kg). A minimum of ~50 mg/kg was observed at ~ 40 cm below which there was a more gradual increase to ~100 mg/kg. The HA profile was distinctive from the FA1 and FA2 profiles as concentrations were highest (up to 30 mg/kg) in the near-surface sections but were typically <10 mg/kg below 20 cm. Finally, the TB HS profile had the lowest concentrations of Mg but major changes with depth were still evident. Low concentrations in the 0-10 cm sections of ~ 3 mg/kg were underlain by a broad peak at ~ 10-20 cm with concentrations of up to 10 mg/kg. Below a minimum at ~ 40 cm, there was a slight increase with increasing depth.

Although each of the four Mg profiles had its own set of distinctive features, it is important at this stage to note the similarities between these profiles and the comparable ones for Sr (see below). In particular, (i) the minimum in 0-6 cm sections in FA1 and TB HS profiles, (ii) the slight but broad maximum at ~ 40 cm in the FA1 profiles, and (iii) the maximum at ~ 10-20 cm in the TB HS profiles.

Vertical profiles showing Ca concentrations in FA1, FA2, HA and TB HS extracts are shown in Figure 4.11A-D. The scales differ for each of the four graphs (FA1 > HA > FA2 > TB).

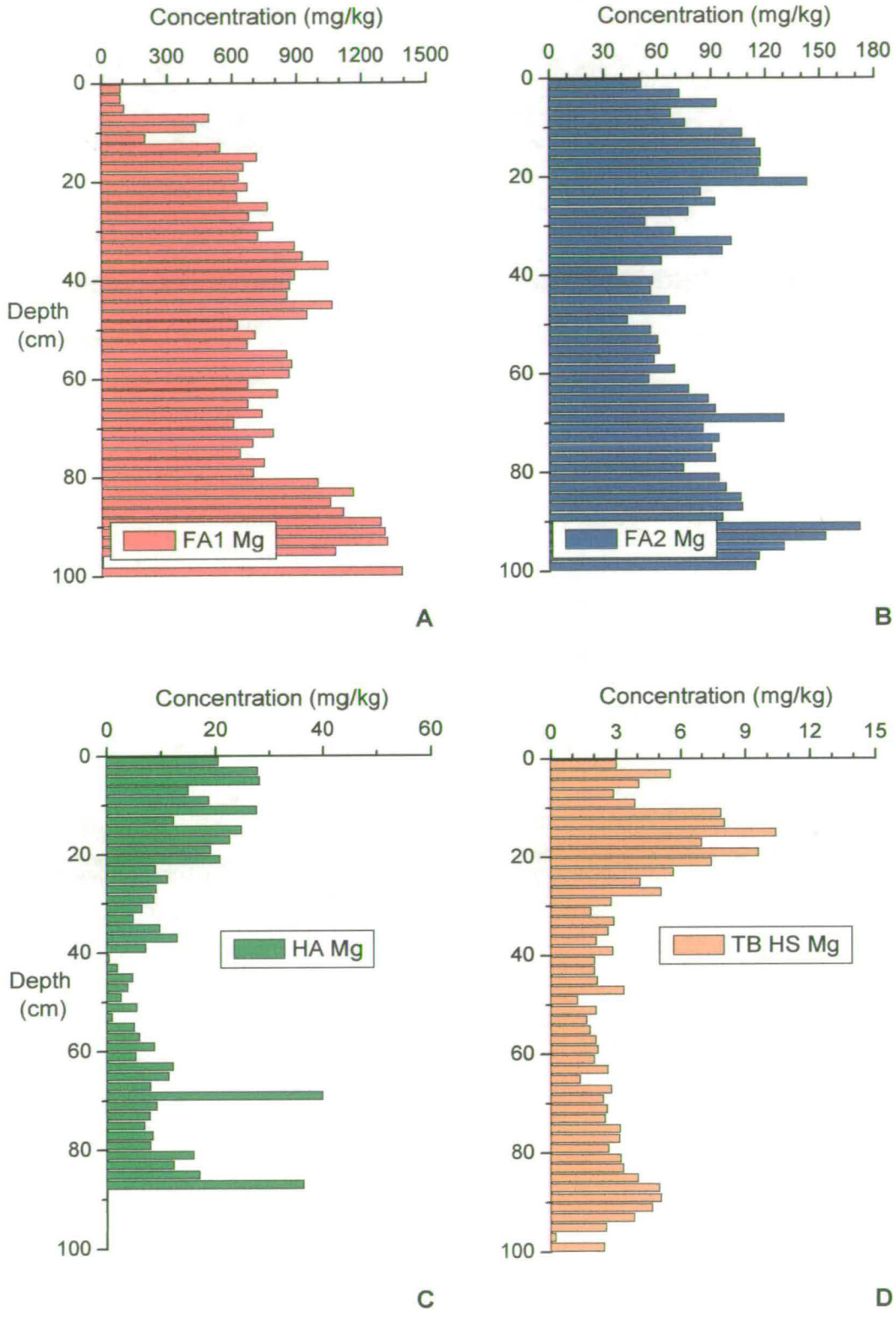

Figures 4.10A-D:Vertical concentration profiles of Mg with FA1, FA2, HA and TB HS extracts of Flanders Moss peat

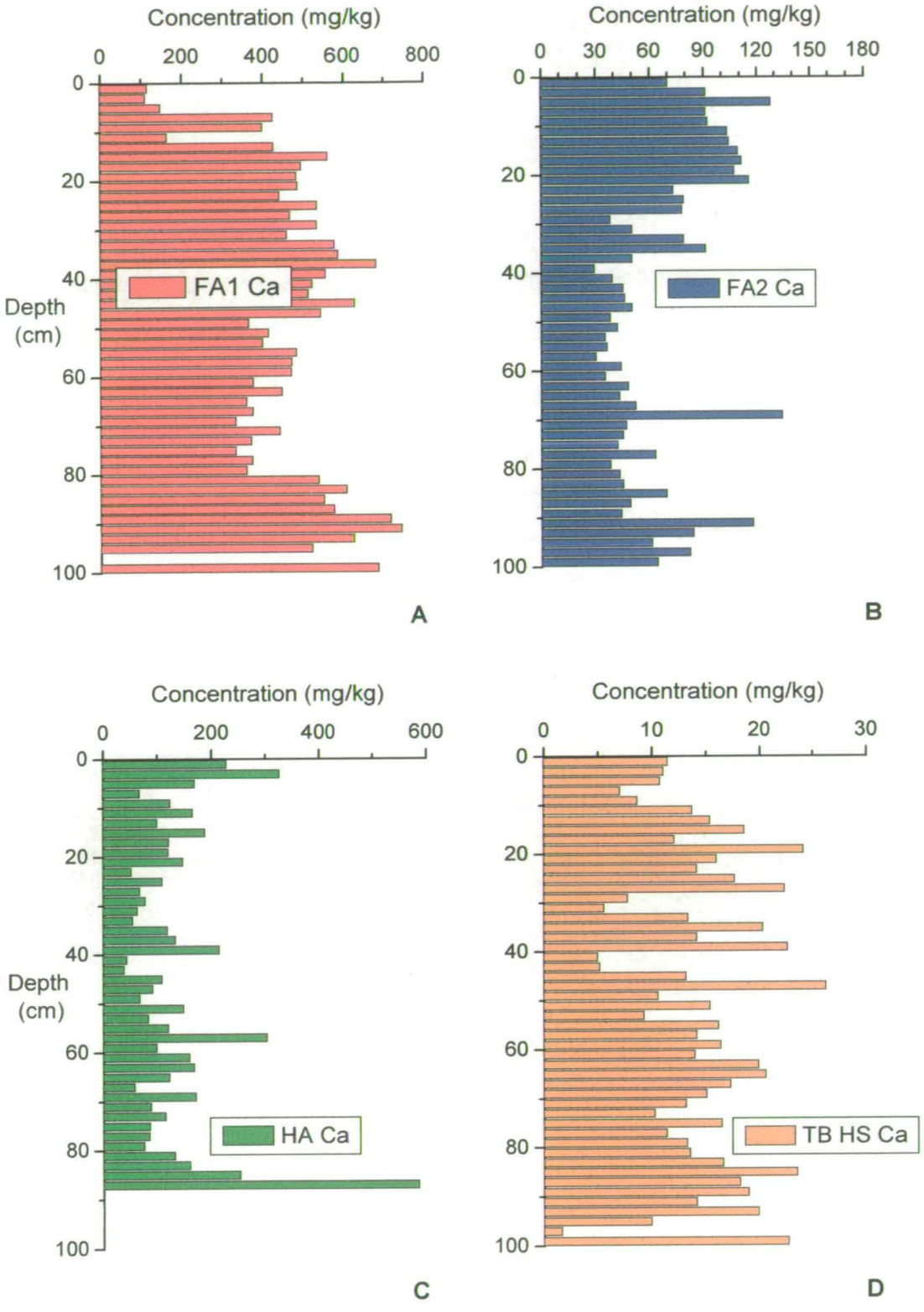

Figures 4.11A-D:Vertical concentration profiles of Ca with FA1, FA2, HA and TB HS extracts of Flanders Moss peat

The FA1 profile for Ca was similar in shape to that for Mg in that there was a near-surface minimum followed by a rapid increase in concentration by 20 cm to ~600 mg/kg. Although the peak at ~ 40 cm was not so pronounced in the Ca profile, further agreement between the Ca and Mg profiles at the bottom of the core was evidenced by the presence of a broad peak at 80-100 cm. It should be noted that the similarity of these profiles did not mean that the Ca/Mg ratio was constant. Values of ~1.5 were obtained for the near-surface minimum compared with ~ 1 at ~ 40 cm and only ~ 0.5 at the bottom of the core. The ratio values will be compared with those obtained for the solid phase peat in the discussion sections appearing later in Chapter 4.

As for FA1, there was some similarity between the Ca and Mg profiles for FA2. In particular, a broad peak in the Ca profile was observed at ~10-20 cm. Concentrations decreased to <500 mg/kg between 50-80 cm and did not increase as markedly towards the bottom of the core. The HA profile for Ca was noisier than the other profile but it appeared that highest values were obtained in the near-surface sections (< 300 mg/kg) and that there was a less significant decrease with depth towards 40 cm. Very little variation with depth was observed in the Ca profile for TB HS and values were typically < 30 mg/kg. In particular, there was an absence of the peak at ~ 20 cm observed in both the Sr and Mg TB HS profiles.

The concentration profiles of Sr in FA1, FA2, HA and TB HS extracts are displayed in Figures 4.12A-D. The scales were selected in a similar manner to those for Group I elements with the exception that the TB HS scale was *two* orders of magnitude smaller.

There was no peak in the 4-6 cm section of the FA1, FA2 and HA profiles. Instead, the FA1 profile has a minimum spanning the 0-6 cm sections and then a broad peak of ~ 15-20 mg/kg over the depth range 6-48 cm. The results showed that concentrations had decreased to ~ 7 mg/kg by 80 cm. FA2 concentrations of Sr were generally lower (< 5 mg/kg). Values were greatest in the 0-40 cm sections.

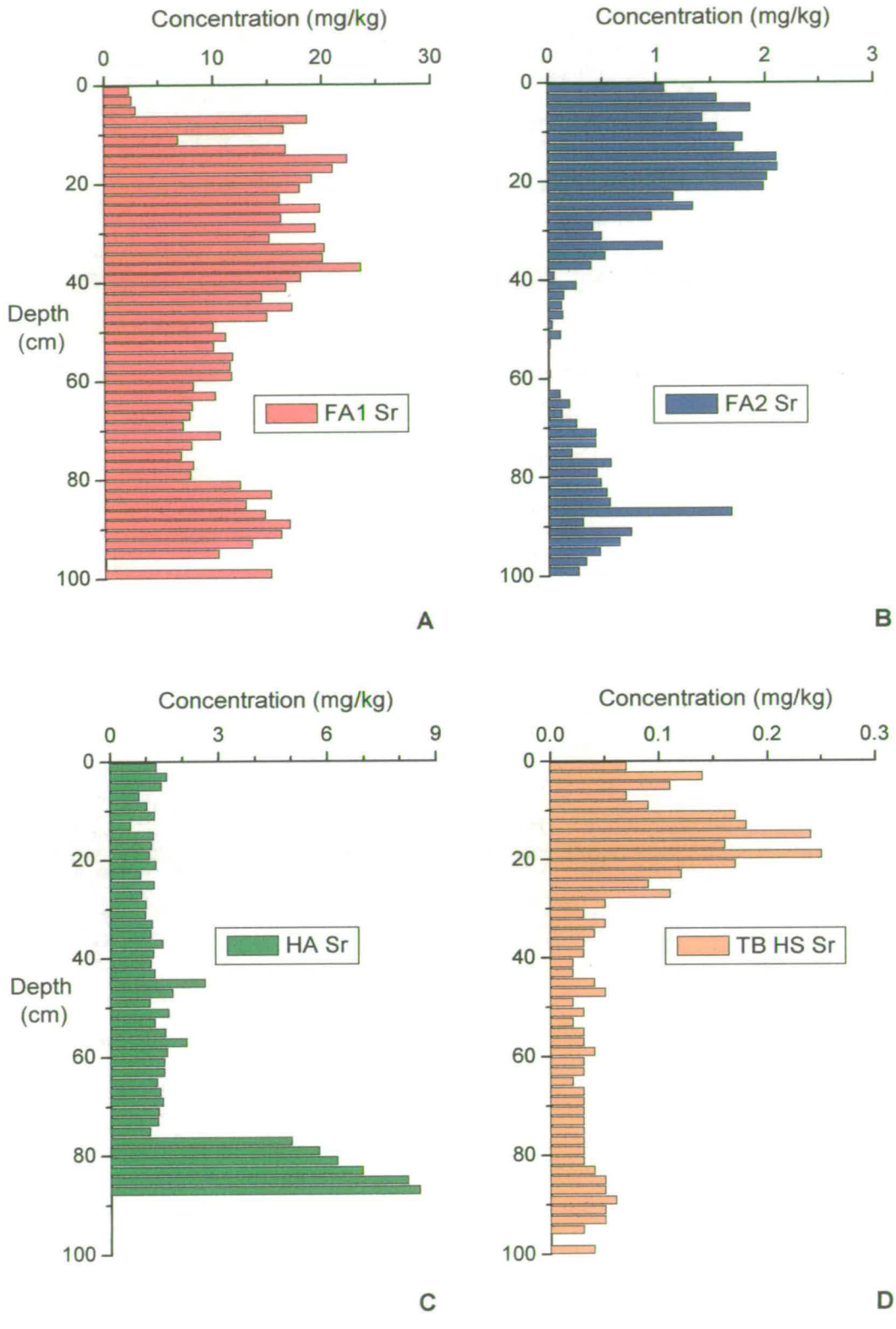

Figures 4.12A-D:Vertical concentration profiles of Sr with FA1, FA2, HA and TB HS extracts of Flanders Moss peat

There was very little variation with depth in the HA profile. Values of < 5 mg/kg were obtained down to ~ 80 cm. Although the concentration scale was significantly different, the shape of the TB HS profile bore some similarity to that of FA1 in that there was a near-surface minimum and a broader peak at 10-28 cm (< 0.3 mg/kg). Below 30 cm, almost constant values of ~ 0.05 mg/kg were obtained for Sr in the TB HS extracts.

The concentration profiles for Ba in the FA1, FA2, HA and TB HS extracts are displayed in Figures 4.13A-D. The scales differ for the graphs, with the order being FA1 = FA2 > HA > TB.

The highest concentration of Ba (12 mg/kg at 8-10 cm) was in the FA1 profile. The localised minimum at 12-14 cm was coincident with similar features in the Mg and Ca profiles. There was a steady decline in concentrations from the peak to concentrations > 2 mg/kg at 98-100 cm. The FA2 profile also has the highest concentrations of Ba in the near surface region, with concentrations decreasing from 2.8 mg/kg at 2-4 cm to > 0.5 mg/kg at depths below 26 cm. The concentrations in both the HA and TB were generally very low, and no significant trends can be identified.

4.3.5 Group IV: Zn, Cu and Pb

Profiles showing the variation in Zn concentration in FA1, FA2, HA and TB HS extracts with increasing depth are shown in Figures 4.13A-D. The scales differ for each of the four graphs (FA1 > FA2 > HA > TB).

The FA1 profile for Zn exhibited little similarity to any of those previously described for other elements. The main features in the Zn profile were a small peak at ~10-16 cm (70 mg/kg), a more prominent peak at 50-60 cm (180 mg/kg) and a broad maximum at 88-98 cm (300 mg/kg). Concentrations were typically < 40 mg/kg in the remainder of the core. The FA2 profile exhibited only one of the three main features in the FA1 profile, namely the broad maximum at the bottom of the core (110 mg/kg).

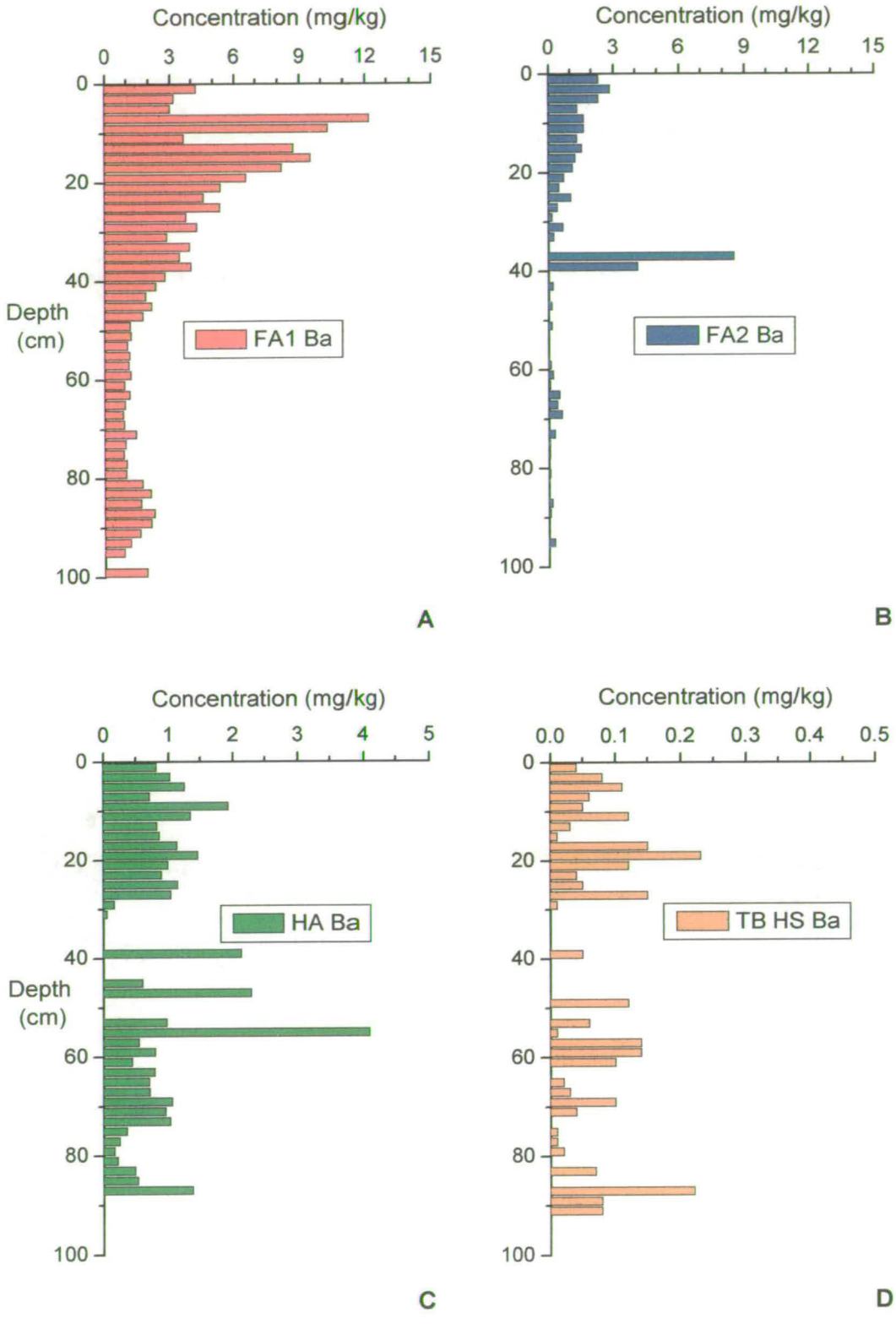

Figures 4.13A-D:Vertical concentration profiles of Ba with FA1, FA2, HA and TB HS extracts of Flanders Moss peat

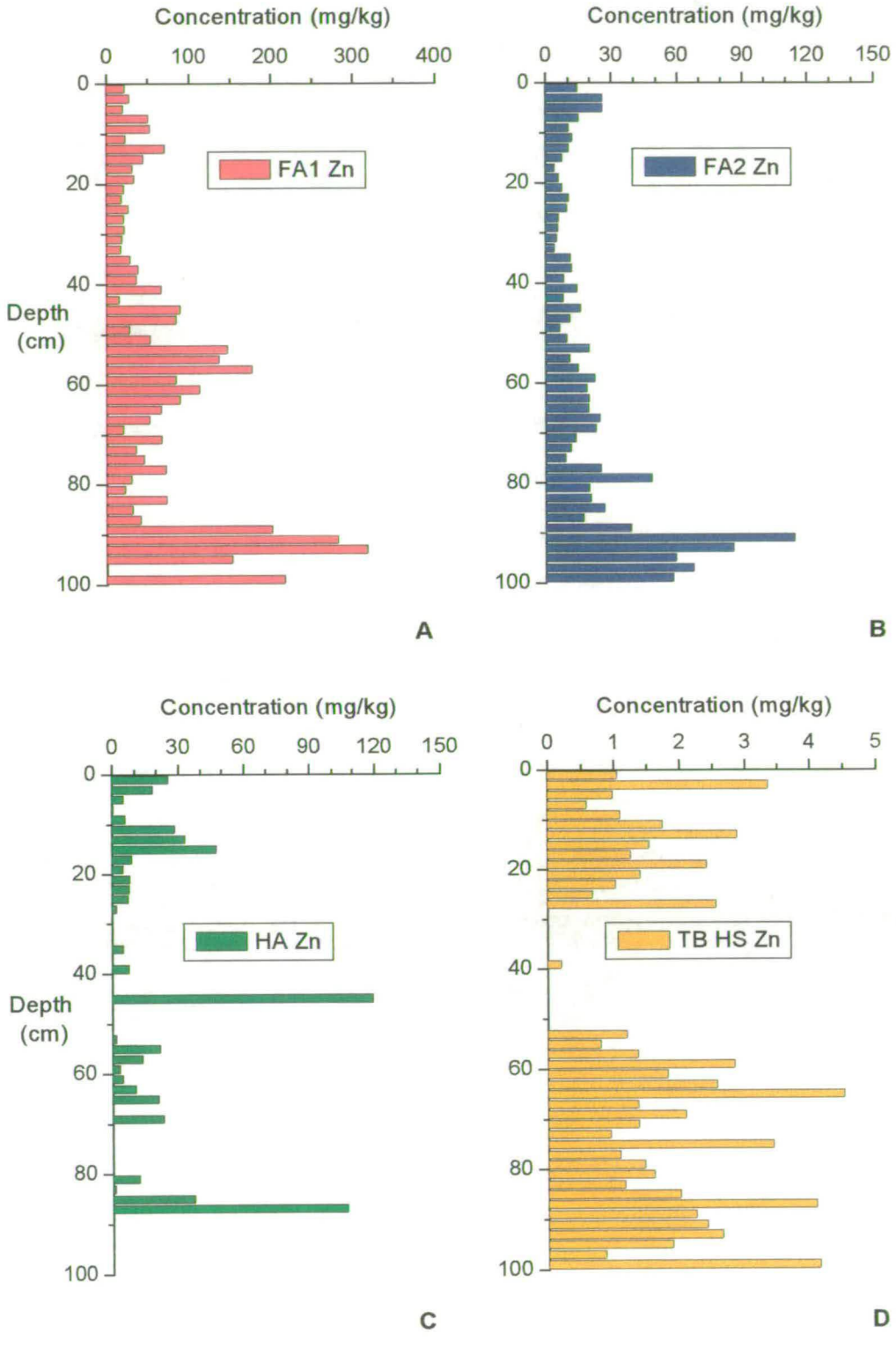

Figures 4.14A-D: Vertical concentration profiles of Zn with FA1, FA2, HA and TB HS extracts of Flanders Moss peat

Again, concentrations in the remainder of the core were low at < 25 mg/kg. Both the HA and TB HS profiles were almost featureless and concentrations were often close to the concentrations of the blanks.

The Cu concentration profiles for FA1, FA2, HA and TB HS extracts are displayed in Figures 4.15A-D. The same scale has been used for FA1, FA2, and TB but a slightly larger scale was required for HA.

The maximum concentration of Cu (< 2 mg/kg) was found for the 0-2 cm FA1 extract. An almost exponential decrease was observed with a minimum of ~0.05 mg/kg at 22-24 cm. Concentrations, although variable (< 1 mg/kg), were small in the deeper parts of the core. Just as for FA1, the maximum Cu concentration (~ 1 mg/kg) was found for the 0-2 cm section of the FA2 profile. No Cu was detected in the FA2 extracts below 6 cm. The highest and most variable concentrations of Cu were found in the HA extracts. Clearly, most Cu was extracted in the upper parts of the core and below 30 cm, the concentration of Cu was frequently below levels in the blank. Very low Cu concentrations if any were determined for the TB HS extracts and there was no discernible trend with increasing depth.

Figures 4.16A-D show the vertical variations in Pb concentration for FA1, FA2, HA and TB HS extracts. The scales are in the order FA1>HA>FA2>TB.

The main feature of the FA1 profile for Pb was the peak at 4-6 cm (73 mg/kg). Below this, Pb concentrations decreased rapidly and by 28-30 cm, concentrations were mainly below the limit of detection. There was perhaps a small secondary peak at 12-14 cm (~10 mg/kg). The FA2 profile also had a peak at 4-6 cm but the concentration of Pb was only 20 mg/kg. Again, concentrations below 20 cm were often below the limits of detection. Most consistently, the main feature of the HA profile is also the (slightly broader) peak at 2-6 cm which was of similar magnitude to that in the FA2 profile (~ 20 mg/kg). The Pb peak in the TB HS profile was at 2-4 cm (~7 mg/kg) but again the overall shape did not differ significantly from the other three profiles.

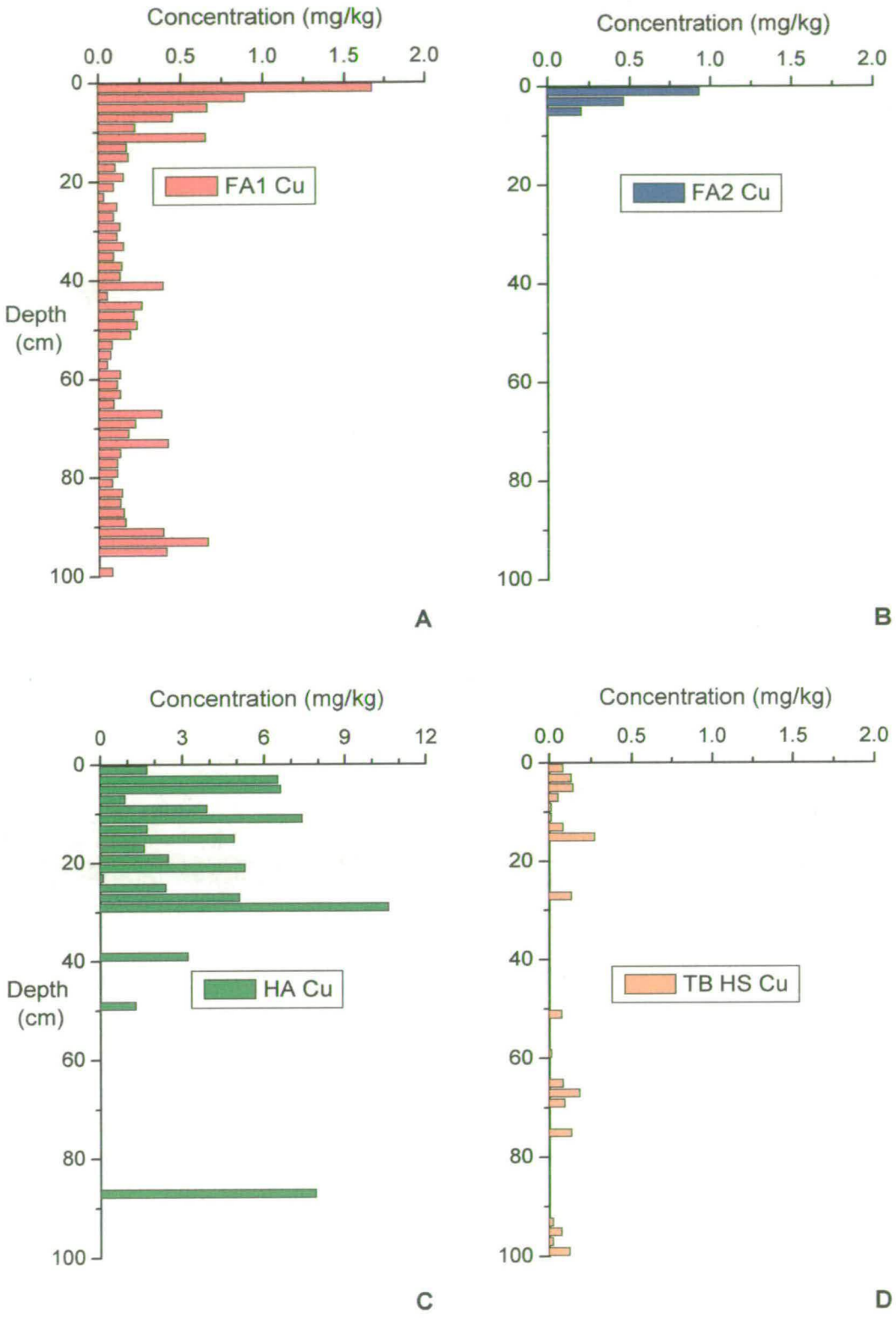

Figures 4.15A-D:Vertical concentration profiles of Cu with FA1, FA2, HA and TB HS extracts of Flanders Moss peat

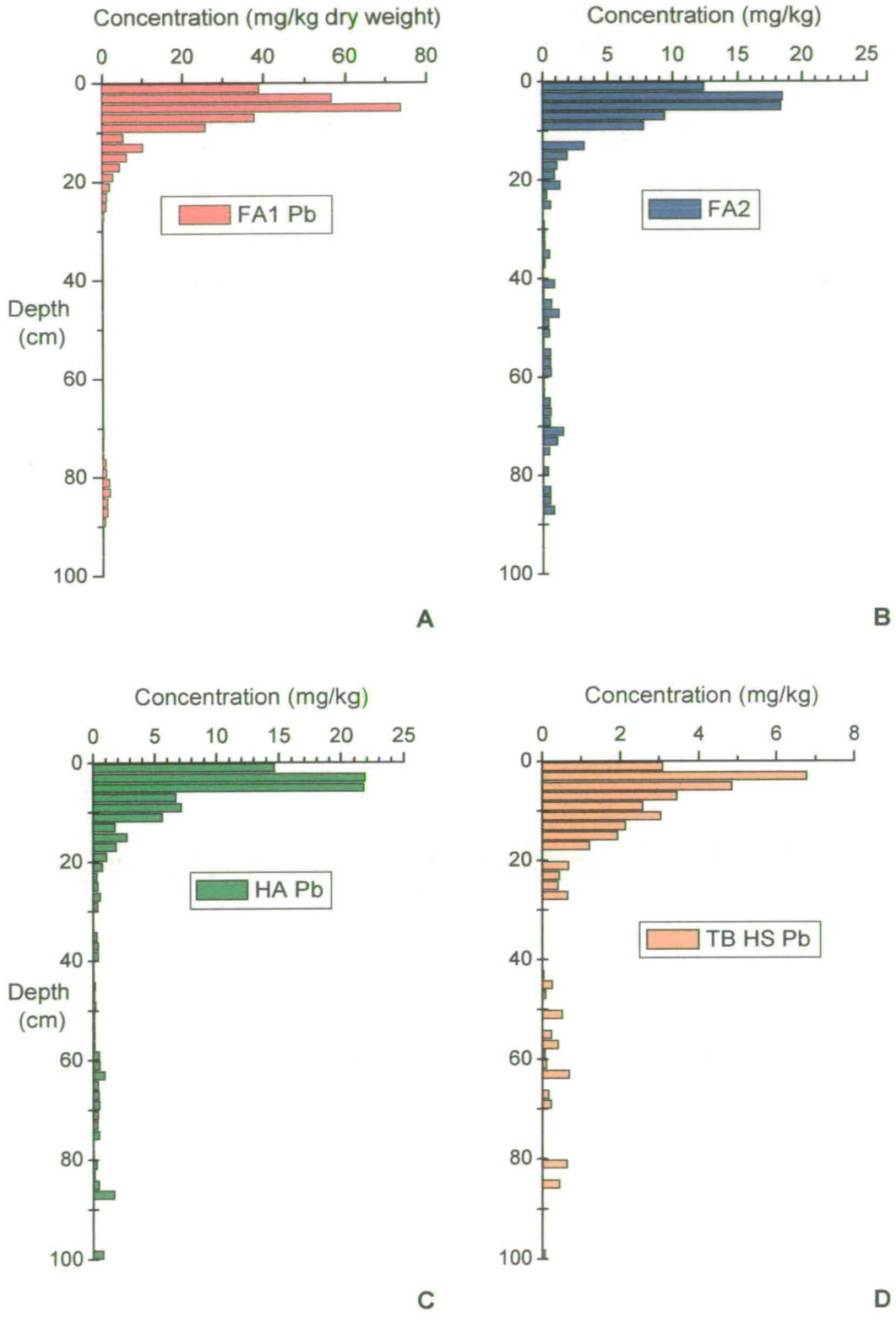

Figures 4.16A-D:Vertical concentration profiles of Pb with FA1, FA2, HA and TB HS extracts of Flanders Moss peat

4.4 DISCUSSION OF RESULTS: HUMIC & FULVIC ACIDS AND HUMIC SUBSTANCES IN FLANDERS MOSS PEAT

4.4.1 Humic and fulvic acids obtained by the IHSS method

It should be recalled that no concentration data was obtained for FA1 because the extract solutions were extremely pale in colour over the entire length of the core. Thus only FA2 and HA concentration data was available. With the exception of a decrease in HA concentration at the position of the total OM minimum, there was little, if any correlation between either FA2 or HA and total OM in the solid phase peat (Figure 3.1C). The total organic matter content was extremely large (> 95% of the total peat on a dry weight basis (except at the position of the ash peak) and did not vary significantly with depth.

The IHSS extraction procedure (FA2 and HA) removed less than 23% of the total OM but generally removed more from the uppermost sections than the lower sections. This suggested that (i) only some of the OM is in the form of humic materials and can be extracted by this procedure and (ii) a greater proportion of extractable material is present in the upper sections of the core. The latter in particular implies that there is a change in the nature of the OM material present at different depths that may be important for elemental associations and indeed element mobility within the peat.

More specifically, FA2 (35.5±12.9 mg/kg) was in general about half the concentration of HA (86.7±24.0%) over the length of the core (46.9±24.0%). A value of 0.5 for the FA/HA ratio agrees with reported values of 0.4 to 0.65 for selected surface soils (Stevenson, 1982). There were, however, some interesting variations in the FA2/HA ratio with increasing depth (Figure 4.17B).

The small peak in the uppermost sections corresponded to the position of the FA2 peak whilst the broad minimum immediately below this coincided with the HA peak at ~ 10-20 cm. The highest values of the ratio ~ 1 were obtained at the position of the broad sub-surface FA peak at ~ 40 cm depth.

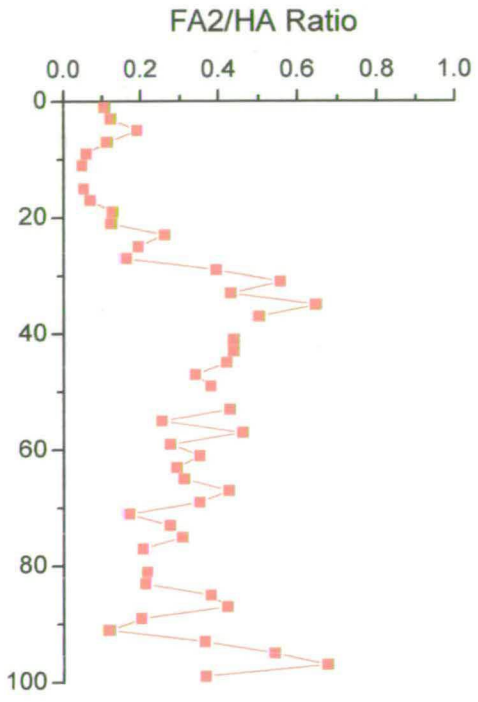

Figure 4.17: Vertical variations in the FA2/HA ratio in Flanders Moss peat

With the exception of the sections below 80 cm, the value of the ratio fluctuated around 0.5. The variations below 80 cm were attributed to the peaks in the FA2 and HA profile, being non-coincident. The FA2/HA ratio profile was highly significant as it highlighted differences in the extent of humification of the peat.

From the results of this study, the prevalence of FA2 in the top sections was interpreted as the initial stages of humification (formation of small humic molecules). The change to predominantly HA in the 10-20 cm sections was indicative of the secondary stages of humification (formation of larger humic molecules). The extent of humification is affected by the prevailing environmental conditions in the locality of the peat bog. Thus, as past conditions may have differed, differing extents of humification may be observed in the deeper sections of the peat. In this study, the higher FA2/HA ratios at ~ 40 cm (and perhaps at 80-100 cm) suggested a past time period where there was a significantly lower extent of humification. The importance of the extent of humification will be discussed further in the sections on ^{210}Pb dating in Chapter 5.

4.4.2 Humic substances obtained by the 0.045 M Tris-borate extraction method (pH 8.5)

The 0.045 M Tris-borate (TB) extraction method is a significantly milder procedure that avoids exposure of the peat material to extremes of pH (0.1 M NaOH – pH 13; 0.1 M HCl – pH 1). This extraction procedure has also been used in other studies Vinogradoff (2000). In agreement with previous work, TB extracts up to ~ 50% of the 0.1 M NaOH extractable material (initial extract – pre-separation of HA and FA2 components). The overall shape of the TB HS profile is quite similar to that of the HA profile suggesting that TB has extracted larger humic molecules. It is not, however, suggested that the IHSS procedure simply isolated more of the same molecules as extracted by TB, as past work strongly suggested that exposure to extremes of pH altered the composition of HA and elemental associations with HA and FA2.

Nor should it be expected that TB HS equal the sum of FA2 and HA, because the TB extracts were dialysed and so smaller molecules would have been lost through the dialysis tubing (MWCO 3500). The elemental associations with each of these materials will be discussed in the following sections.

4.5 DISCUSSION: ASSOCIATIONS OF ELEMENTS WITH IHSS HA & FA AND TB HS IN FLANDERS MOSS PEAT

Traditional extraction procedures, outlined in section 1.6, have been widely used to isolate the operationally defined fractions of humic substances termed HA and FA. These fractions generally undergo extensive purification procedures prior to experimental determination of the metal binding characteristics. Some studies (omitting the purification steps), however, have also determined the concentrations of metals bound directly to HA and FA. The latter approach has been adopted in this study.

Criticism of the traditional extraction procedures has centred on the use of harsh pH conditions (pH 13 and pH 1), which may not only alter the chemical structure of the extracted material but also the associations of bound metals. Thus, prior to the interpretation of the data it is necessary to comment on any likely changes. The FA1 extractant is utilised as a pre-purification step, to remove any $CaCO_3$ prior to the extraction and isolation of the humic materials. Although this was obviously not going to be a serious issue in the case of peat, the extraction was retained to keep consistency with previous studies. This fraction is also expected to contain smaller, non-humic materials such as proteins and carbohydrates.

The low pH can also result in the partial dissolution of solid mineral material, such as clays etc. Finally, the low pH can cause protonation of many of the functional sites on the humic and fulvic acid molecules, and the release of bound metals to solution. The FA2 extraction can also cause dissolution of mineral material at high pH. The dialysis step utilised in both the HA and TB HS isolations can allow the escape of smaller molecules and metal complexes through the membrane. The metal concentrations in the resultant HA extract may not be wholly representative of all the metals bound to organic component in the solid phase peat. Therefore, while these results can be used to provide an insight into the speciation of metals to fulvic and humic acids, it should be noted that many of the observed trends may be an artefact of the method, and not entirely indicative of the "real" situation in the peat.

4.5.1 Group I: Mn and Fe

The shapes of the Mn concentration profiles for FA1, FA2 and HA showed a degree of similarity to the solid phase peat and porewater profiles in that there was a maximum at 0-2 cm. The proportion of pseudo-total Mn extracted in the IHSS and TB HS extracts was very small (<5% of solid phase Mn, Figure 4.18A). This suggested that the bulk of the Mn in the peat was not strongly bound to the humic acid fraction of the organic matter extracted, or liberated from surface sites under the acid conditions employed. Thus either the Mn was bound to the more recalcitrant fraction of organic matter not extracted by the IHSS and TB extractants, or the Mn was in an inorganic form.

In the case of redox cycling, then the Mn could have been associated with Mn(IV)oxides. However, given the depth of the water table in the peat (section 3.6.1), and the relatively aggressive nature of the reagents used to extract FA1 (0.1 M HCl - pH 1), it was unlikely that the major form of Mn in the uppermost sections was Mn(IV)oxides. Therefore, it was concluded that most of the Mn in the 0-6 cm sections was held within the plant material.

In explanation of the absence of a Mn peak in the 0-2 cm section of the TB HS profile (at only pH 8.5), 2 different mechanisms were proposed: (i) the acid conditions employed in the first part of the IHSS procedure released a small portion of total Mn by dissolution of inorganic Mn not liberated by the TB extraction, or (ii) the FA1 and FA2 extractions contained small (<3000Da) organic molecules containing bound Mn.. While these molecules may have initially been present in the TB extracts, they were subsequently lost through the dialysis membrane during the dialysis of the TB extracts.

In the FA1 extracts, it is evident that below the surface peak, the concentrations of Mn were relatively stable down the entire core. There was the presence of slightly greater concentrations in the FA1 extracts at ~10-20 cm, which coincided with the position of the very slight increase in the porewater Mn profile, and the maximum porewater conductivity.

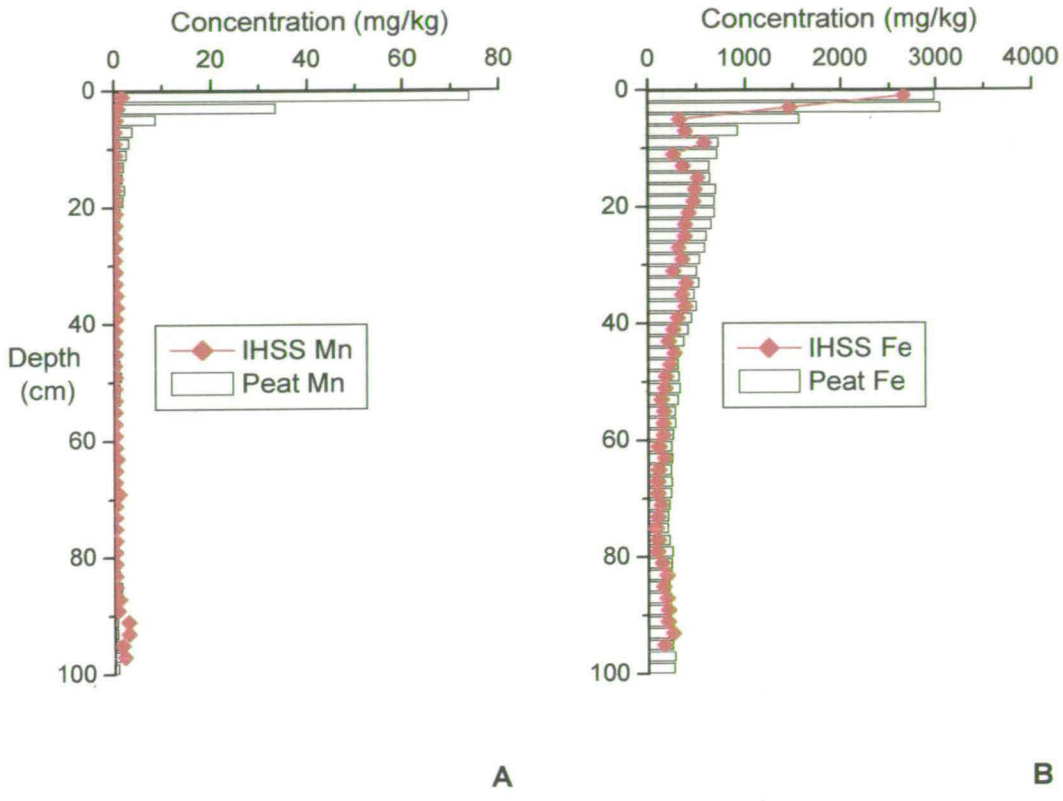

Figure 4.18A-B: Comparison of Mn and Fe concentrations in the solid phase peat and total IHSS extractions for Flanders Moss peat

It was not be determined whether the Mn (and Fe) released in both the FA1 component and the porewaters at these depths was associated with low MW organic complexes, or was released from the dissolution of Mn oxyhydroxides.

Like the near-surface enrichment observed for Fe in the solid phase and porewater extracts, the FA1, FA2, HA and TB profiles also have Fe peaks in the uppermost sections. In contrast to Mn, however, the IHSS extracted Fe represented a much greater proportion of the pseudo-total Fe (Figure 4.18B). With up to 90% of the solid phase, being present in the extracts, it can be seen that Fe is much more readily extractable by the IHSS procedure.

From Chapter 3, the porewater relationship to solid phase in the 0-6 cm sections of the peat strongly suggests that redox cycling was not controlling the shape of the Fe profile. The high extractability of solid phase Fe by the IHSS method suggested that it was not a major constituent within the recalcitrant plant litter, but was in a readily releasable form.

As was the case with Mn, most of Fe at depth is present in the FA1 extracts. Thus even at lower depths in the profile, the Fe remains in an extractable form. This high extractability relative to the fraction of Fe bound to larger humic molecules suggested that the most of the Fe in the peat was in oxyhydroxides, or bound to low MW organic complexes that were released. The only other possibility was that Fe was being released from humic binding sites by increased competition from protons. However, given the strong binding of Fe to the solid phase, as evidenced from the distribution co-efficients in Chapter 3, the last option is less likely.

In the 20-40 cm zone, most of the Fe is readily extractable in the FA1 fraction, suggesting it was present in the peat as amorphous oxyhdroxides and low M.Wt complexes. The release of Fe between 20 and 40 cm in the FA1 extract corresponds to the relative peak in the distribution profile (Figure 3.8.5), although the concentrations of Fe released in the FA1 extraction were much greater than those in the porewaters.

The release of Fe in the FA1 extraction at this depth supports the earlier hypothesis proposed in chapter three that Fe release below the water table may be related to the reduction of Fe in a mixture of "bog ore", releasing both ferrous iron and Fe-organic complexes. As the position of the water fluctuates (according to the time of year), the Fe peak is broadened. Interestingly, a small peak at 20 cm can also be recognised in the TB profile.

4.5.2 Group II: S and P

In the 0-6 cm sections of the peat, the S peak was not at the same position as the Mn and Fe peaks, although as with the Fe and Mn profiles, the peak was present in all of the extracts. The peak did not result from the use of one particular extractant, as the S peak was found independently in all four extracts conducted on two separate sub-samples. This peak in S occurred at the same position as the ash peak and the minimum in peat OM. This could indicate that there was a different form of S at this depth, with inorganic S instead of organically bound S. From Figure 4.19A, it can be seen there was a massive increase in the S:C ratio in the FA2 extract at this depth. S is known to be an important constituent of root exudates, and the prevalence of root exudates in this zone could not be discounted as an explanation for this trend.

To test the earlier theory that S was incorporated into organic matter with increasing depth (Chapter 3), the FA2, HA and TB results were converted into g S/kg (humic material) shown in Figures 4.19B-D. The largest percentage component of S was found in the humic acid extract, and the HA profile exhibited almost constant values (excluding the uppermost sections) of 0.5-0.7% of the organic matter, which is in the range previously reported for humic substances (Steelink, 1988).

The unextracted S may be a constituent of humic materials, but may well be associated with the larger, more aromatic, hydrophobic molecules, which are not readily extractable, even in the HA extract. A similar pattern for the TB HS was observed, except that the value was lower at ~ 0.1%. This would suggest either, that the TB extracted a material with a lower organic-S content, or that the IHSS method co-extracted a form of S which was closely associated with humic acid.

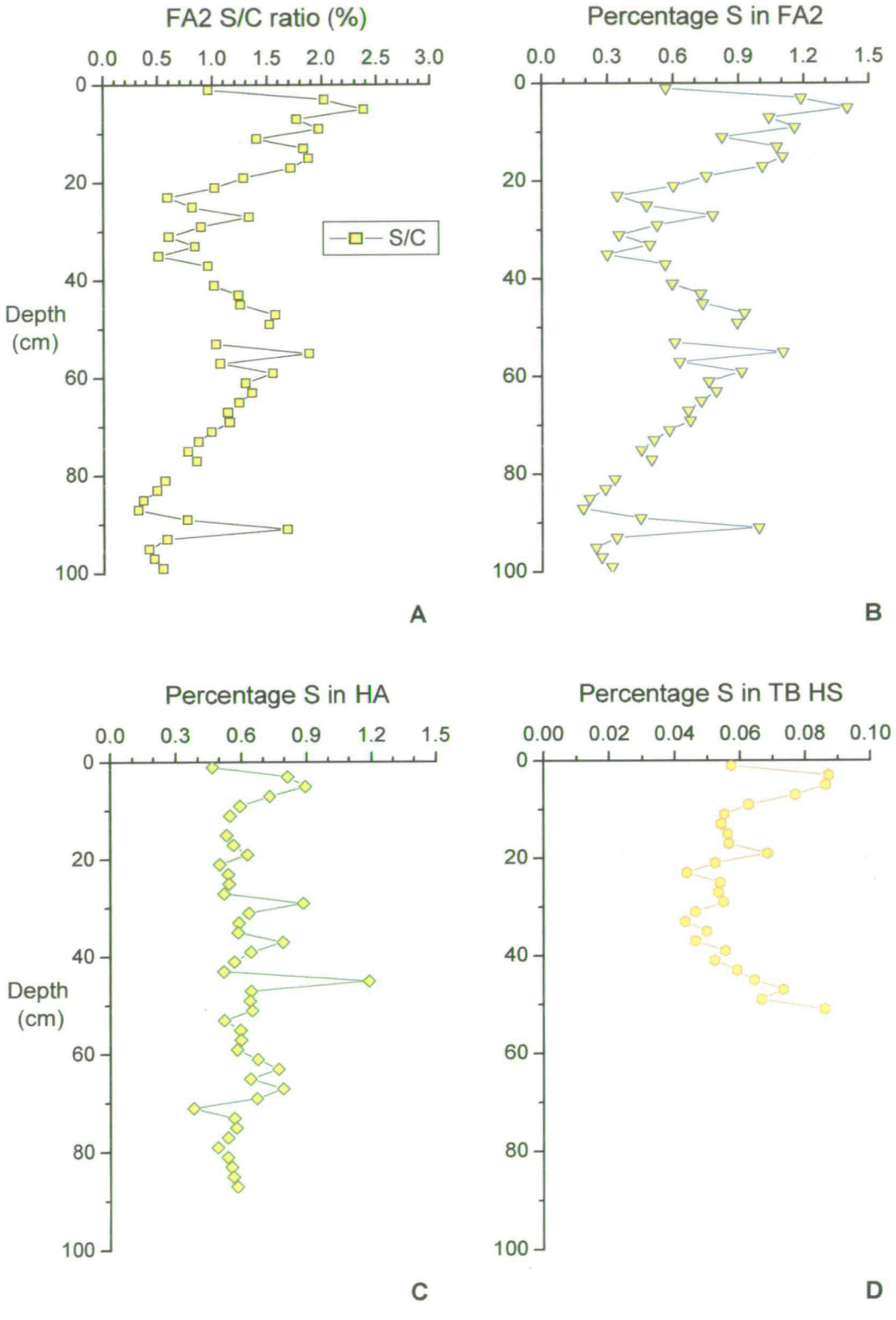

Figures 4.19A-D: Vertical variations in the relationship between S and the FA2, HA and TB HS extracts from Flanders Moss peat

The S component value for FA2 is similar to HA in the 0-20 and 50-70 cm sections of the core but decreases to 0.2-0.3% between 20-40cm and 80-100 cm. These two zones are close to the lower density parts of the core where less humification has occurred (process leading to the incorporation of S) but there is no effect on the HA formed at these depths.

In terms of redox cycling, the absence of a S peak at 20-30 cm (just below the water table) in the FA1 extracts indicates that there is no release of S by acid dissolution. In Chapter 3, a connection between the porewater S profile and the DOC suggested that the S was a component of this DOC. However, comparison with the percentage of S in humic materials reveals that the S in porewater cannot all be part of humic material. The S:C ratio in the porewaters exceeded that in the HA by a factor of ~4-5, and that in the TB HS by a factor of 40-50 times.

For P, the largest amounts were present in the FA1, FA2 and HA extracts from the 0-6 cm section (Figures 4.19B-D). This trend agrees with the trend of the solid phase P +(Figure 3.3B). With the highest fraction of P associated with the HA, this would suggest that most of the extracted P in the extracts is associated with humic material. The relative proportion of the pseudo-total P extracted by the IHSS methodology is shown in Figure 4.20A.

The P distribution in the 0-6 cm section was similar to the distribution of S, and reflected a similar cycling process for P in this upper region.

At depths below 40 cm, the amount of humic acid was important, with P incorporation into humic acid an important process. However, most of the P was still in an unextractable form. From the solid phase profiles, the P profile showed some similarity to shape of Al profile, and this would again seem to suggest that most of the P may be present in an inorganic phase, which is not readily released from the peat by the milder extractants used in the IHSS method relative to the pseudo-total digestion.

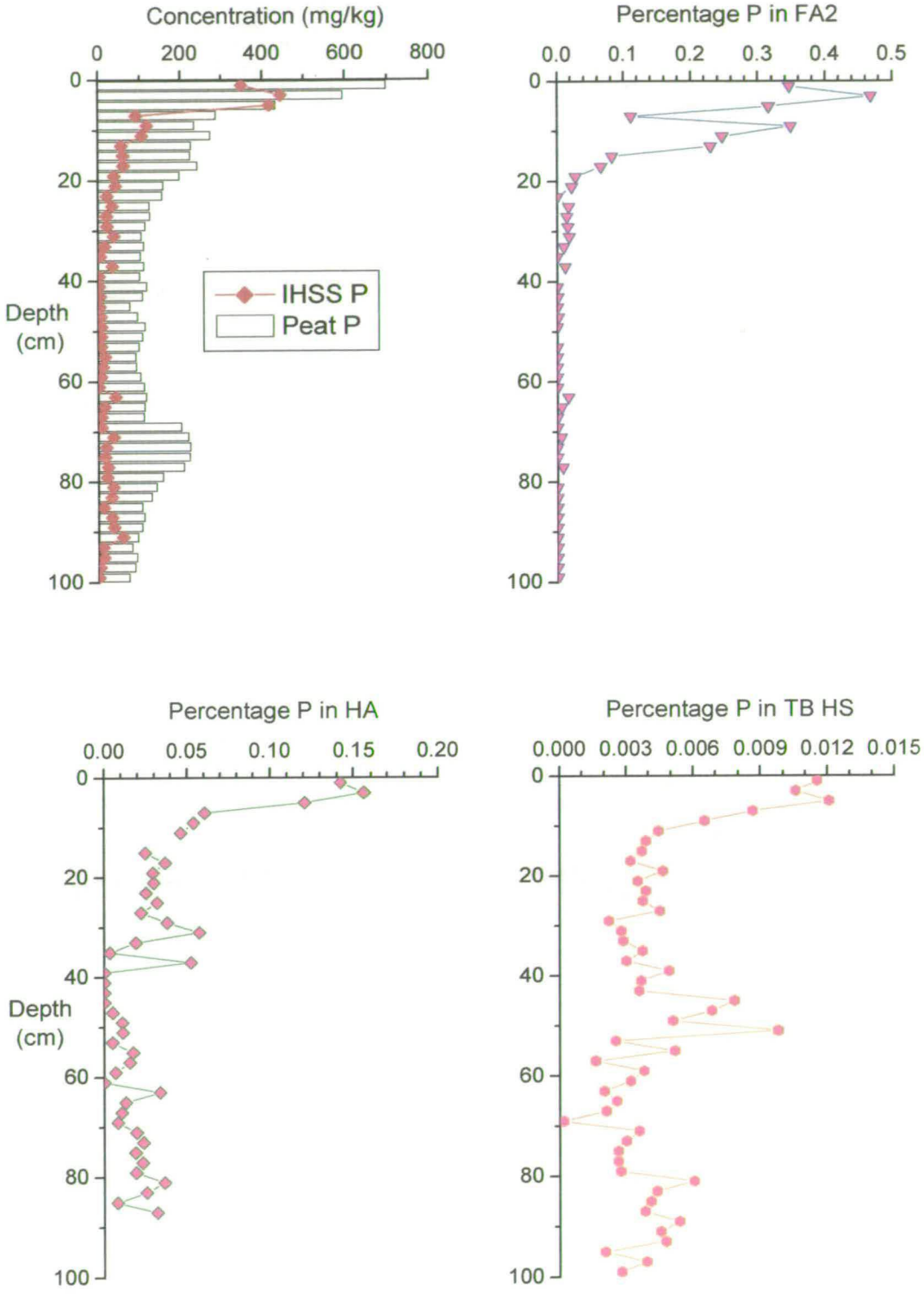

Figures 4.20A-D: Vertical variations in the relationship between P and the IHSS and TB HS extracts from Flanders Moss peat

4.5.3 Group III: Al and Ti

The amount of Al extracted by the IHSS method ranged from up to 60 % in the 4-6 cm section, down to less than 10 % in the 70-75 cm section. Most of the IHSS extractable Al was in the FA1 component. The similarity of the FA1, FA2, HA and TB HS profiles to the Al solid phase profile in the upper sections illustrate that the Al associated with the ash maximum at ~ 4-8 cm was extracted in all of the profiles. The extractability of Al (Figure 4.21A) from this depth was proportionately greater than Al down the rest of the profile. This would also suggest that at least some of the Al in this peak was present in an organic form, otherwise the proportion extracted in the FA1 fraction would have been greater

Comparing the FA1 profile to the porewater Al, a similar peak in the Al profile is observed at 20 cm. Relative to the solid phase, at a depth of around 16 cm, there is a peak present in the FA1 and the solid phase. A slight 'bump' in FA1 profile occurs at the same depth as the position of porewater peak (30-40 cm). This peak is not as pronounced but may be masked because of the major dissolution of Al from solid phase.

The peak at ~ 80 cm in solid phase is absent from all of the organic extract profiles, suggesting that this Al is in a much less available form. This may be related to the increased density of the peat from this section. Conversely, a small peak present in the FA, HA and TB profile lower in the core at ~ 90 cm may be related to the lower density of the peat in this zone.

Overall, on the basis of the HA and FA2 data, the organic complexation of Al does not appear to be very important, with either most of the Al being present in the peat as solid mineral material, or the Al is readily released from binding sites on the humic material, by the acid conditions employed in the FA1 extraction. This would in fact be consistent with the Al being bound as hydroxy complexes, and not as monomeric Al.

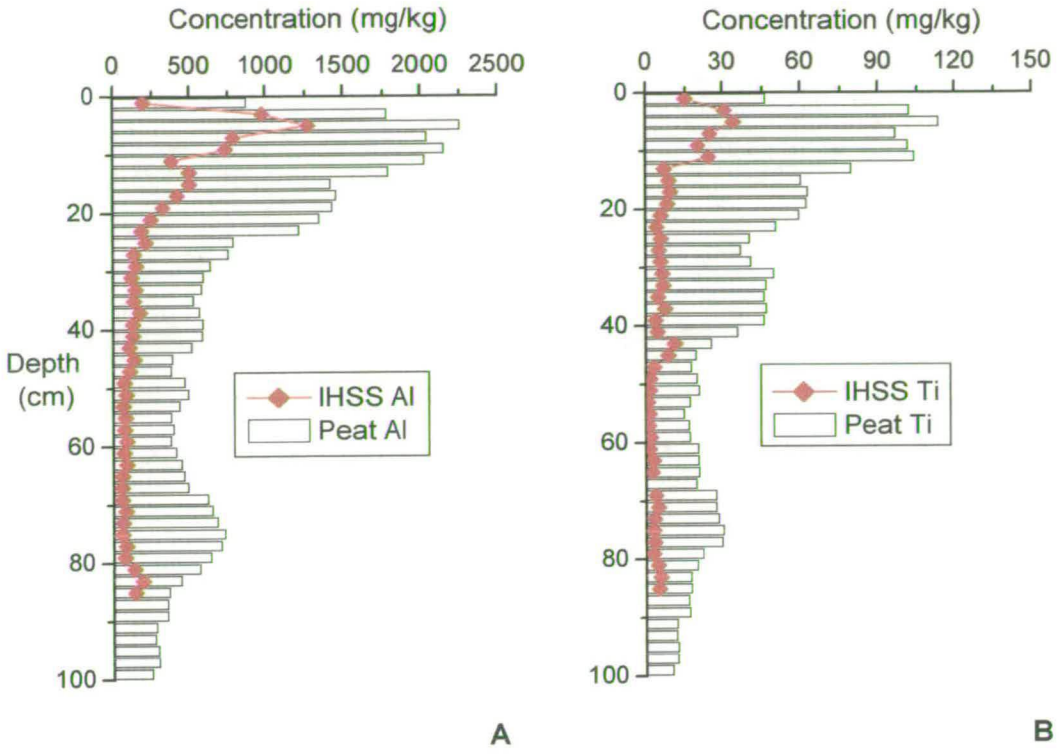

Figures 4.21A-B – Comparison of Al and Ti concentrations in the solid phase peat and total IHSS extractions for Flanders Moss peat

Taking into consideration the relatively low concentrations of Al in the TB HS extraction, it would appear that if the Al is bound to organic matter, it may well be associated with the smaller FA –like molecules and may be lost through the dialysis membrane in the dialysis step. ·The lower extractability of Al at depth corresponds with a reduction in porewater concentrations towards the bottom of the core.

In comparison with the Al concentrations in the organic extracts, the lower Ti concentrations reflect the overall slightly lower extractability of Ti (Figure 4.21B). This can be clearly seen from the Ti distribution co-efficient (Figure 3.13), indicating that Ti has a very strong affinity to binding sites particularly those associated with organic matter. In the upper sections of the core, most of the IHSS extracted Ti is contained in the HA extract (Figure 4.9). In contrast to Fe and Al, it would appear that less of the Ti is extracted during the FA1 extraction, and the Ti is therefore mostly bound to organic matter. The TB HS profile also reflects higher concentrations of Ti, reinforcing this strong organic association of Ti and OM.

The elevated concentrations of Ti observed in the solid phase peat between 20-40 cm are also present in the FA1 extract. These elevated Ti concentrations are coincident with a further zone of low-density peat, and thus the elevated concentrations are likely to originate from mobilisation of some inorganic form rather than humic complexation.

Overall, both the porewater and FA1 extracts demonstrate that Al and Ti can be mobilised under certain conditions. Peaks in the distribution co-efficients occur in the peat bog between 20-40 cm. Given this doubt over the immobility of these elements, it is difficult to see how either element can be used for 'normalising' or to calculate 'enrichment factors'

4.5.4 Group IV: Mg, Ca, Sr and Ba

There is a striking similarity in the shape of FA1 profiles for Mg, Ca, and Sr and, to a lesser extent, Ba, (Figure 4.22).

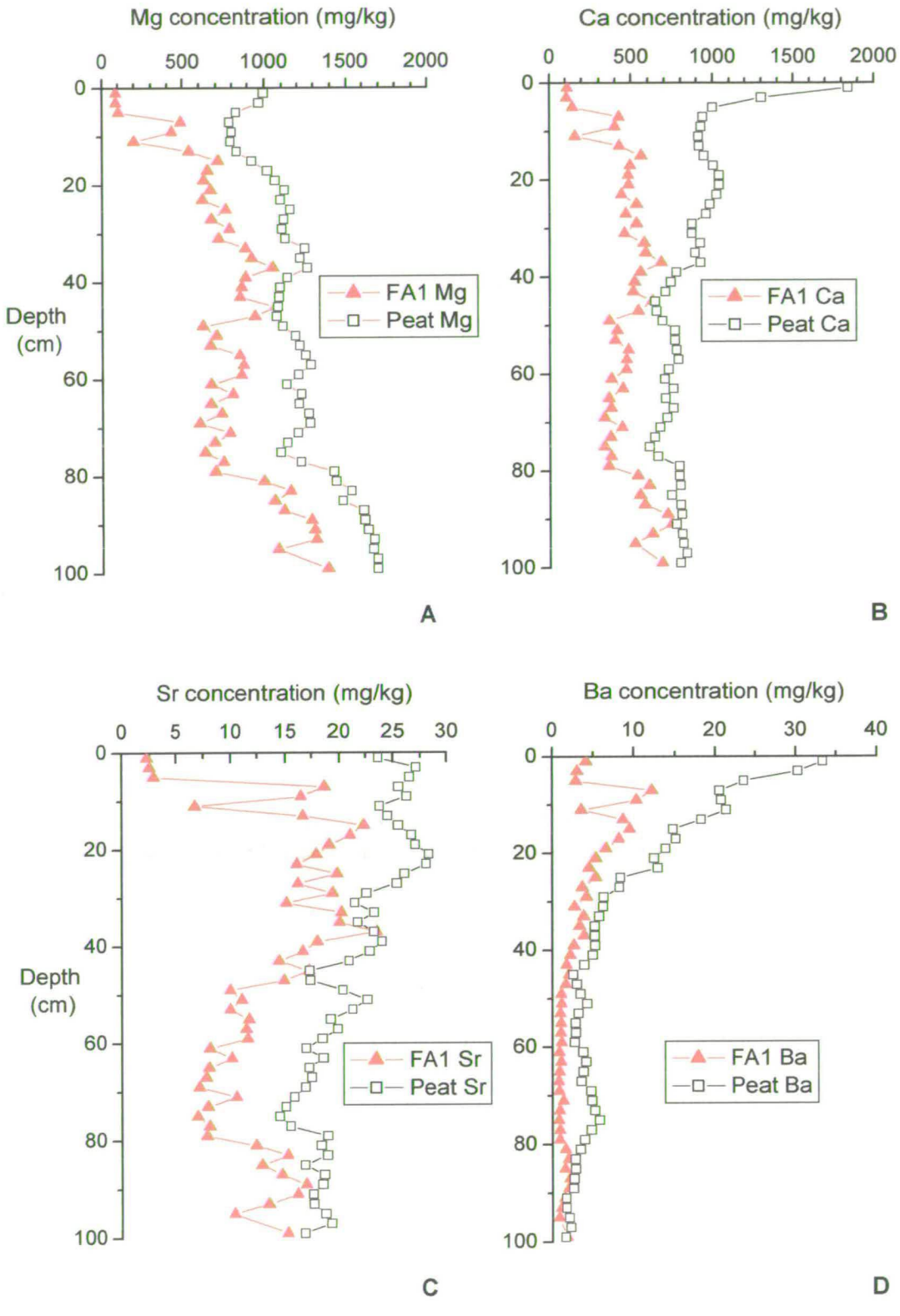

Figures 4.22A-D: Comparison of Mg, Ca, Sr and Ba concentration profiles in FA1 and solid phase fractions for Flanders Moss peat

All of these elements exhibited very marked lower extractability in 0-6 cm (the plant uptake zone), with peaks around 40 cm and 80-100 cm (Mg, Ca and Sr). In all cases, a large proportion of pseudo-total was extracted in FA1. This corresponds to the release of these cations from ion exchange sites, as these metal ions, due to their increased size, are less likely to be bound at specific binding sites on the humic matter, but are more likely to be weakly held in the non-specific sites in the Donnan layer. A dramatic decrease in pH causes a decrease in the volume of the Donnan layer and the displacement of much of the humic bound cations from the exchange sites.

In the FA2 extracts, all of the Group IV have peaks at ~10-20 cm , which was the position of the FA2 minimum. The concentrations of cations in the FA2 extractions do not appear to bear any relation to the concentration of DOC in the FA2 fraction. Thus the FA2 cation concentrations may also reflect the further release of cations from exchange sites during the precipitation of the HA, using 16M HNO_3. Combining the FA2 and HA components yields a profile with a shape similar to that of the HA alone. This suggests that the organically bound fraction of the Group IV cations is determined by the concentration of humic materials. Overall, large proportions of these elements are extracted from all sections of the peat core, apart from the 0-6 cm section where they are mainly held within the plant.

4.5.5 Group V: Zn, Cu and Pb

The Zn associations differ from all other elements described above. Zn is not released to a significant extent in FA1 extracts, except in the bottom sections. A similar trend is followed for the FA2 extracts. Both of these extracts were not dialysed, so any Zn released as part of the extraction procedure would be found in one of these two (even if released from HA by 6 M HCl). There is further confirmation of this low extractability from TB HS, with only a very small amount of Zn extracted from any depth. Notably there is an absence of the 80-100 cm peak in TB HS profile. This suggests that the release under harsher conditions of IHSS procedure is probably due to the dissolution of Zn from solid phase material, with little zinc being held at sites on the humic material.

A further fact is that Zn is not associated with the small molecules that would have been readily extracted. However, the high solubility (distribution coefficient) of Zn suggested the opposite, and there is no clear explanation for this discrepancy.

With the Cu profiles, there is evidence of a link between the FA1 extracts and the porewaters. There is a readily released component in the 0-2 cm section corresponding to a similar peak observed in the pore water. This may reflect the high affinity of Cu to organic binding sites, which in the 0-2 cm section are concentrated on the smaller fulvic-like compounds released through breakdown of plant remains and microbial biomass. In the FA1 and FA2 extracts, the Cu values are very low below ~6 cm. The HA Cu peak at 2-6 cm coincides with the solid phase peak (as does the very small TB HS peak). Below this there are some spurious points in both the HA and TB HS profiles, due primarily to the very low concentrations of Cu in the solutions for analysis.

There is a very good match of Pb in the upper peak position in FA1, FA2, HA and TB HS profiles and solid phase/porewater peat profile. The second peak, however, was absent from all of the humic material profiles, which would indicate that the Pb in the peat was in a different form from the Pb at the surface. The overall IHSS/peat ratio for Pb (Figure 4.22) shows a marked decrease in extractability over the top 20 cm (almost exponential in shape), with the concentrations below 20 cm being extremely low relative to the surface concentrations and close to Pb concentrations in the blanks.

There would appear to be tentative relationships between the FA1 Pb profile and those of Al and Ti (and P/S) in the upper 20 cm. The peak at 80 cm depth for Al, Ti, Ba and P is present to a very small extent in Pb FA1 profile. In the upper section, however the Pb is also bound to humic materials. This is reflected in the Pb concentrations in the FA2, HA and TB HS extracts. Pb in the upper sections of the core is derived from anthropogenic Pb, and as discussed in Chapter 1, the bulk of this Pb is expected to originate mainly from petrol.

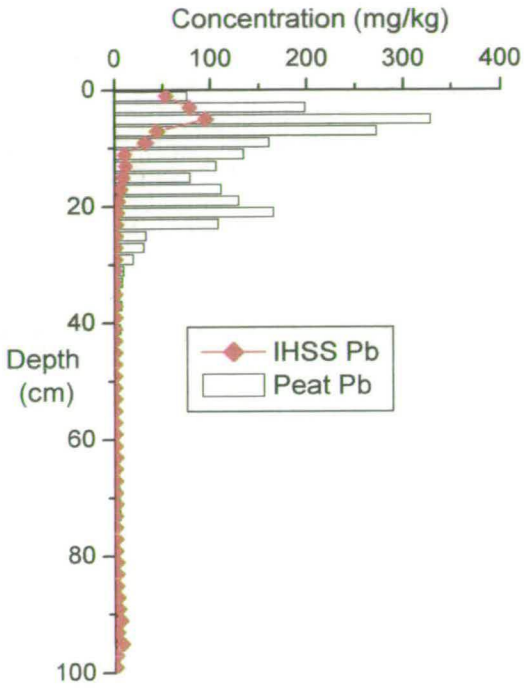

Figures 4.23: Comparison of Pb concentrations in the solid phase peat and total IHSS extractions for Flanders Moss peat

Petrol-derived Pb may be held in inorganic and organic forms within the peat, which become increasingly more extractable towards the surface. In contrast, the older anthropogenic Pb is expected to originate mainly from coal burning. This Pb is not extractable to any obvious extent , and there may be an association with fly ash /PAH type material in soot produced during the combustion

4.6 CONCLUSIONS

The results of the organic matter characterisation illustrate the importance of FA/HA ratio to metal binding, and this ratio is also indicative of the extent of humification. It has also been shown that in many cases the FA1 extract metals concentrations are not necessarily representative of metal bound to fulvic acid and non-humic organic matter.

There is evidence of the mobilisation of relatively large amounts of certain elements by the IHSS procedure, which does have an influence on elemental associations with FA2 and HA, with both generally yielding much higher concentrations than the TB HS extracts. This aside, there is important information to be gained from extraction procedures employed in this study.

There is the possibility of Al and Ti released with decreasing pH, which has implications for the use of both of these elements as 'dust indicators' in peat, ice and sediment cores.

The results also illustrate that the 0-6 cm section of the core is one of active accumulation, with plant uptake and/or evapotranspiration processes causing relative accumulation/depletion of certain elements. However, the role of organic matter in plant uptake would appear to be important for certain elements (notably Fe and Cu) while other elements have sufficient near surface porewater concentrations from rainfall (e.g. Ca, Mg, Na, K etc).

The Group IV elements are generally in a very exchangeable form and this is particularly evident below 6 cm, the zone affected by plant uptake and evapotranspiration.

Overall, for many of the elements, there are points of general similarity (e.g. the surface enrichment of Fe and Mn, or the increasing concentrations of Mg down the core) between the profiles obtained from these two cores (Core 2) and the five cores (Core 1) used to obtain the solid phase and pore water data.

For Pb, there are two peaks in solid phase but only the upper peak is present in the humic profiles. This would suggest that there is a difference in the form of Pb in the upper few sections of the peat from Pb in lower sections of the core. Possible changes in the form of the Pb inputs into the peat will be investigated further with the use of Pb isotopes in the peat. From the evidence above, the Pb appears to be unaffected by the processes 'operating' for other elements within the peat, with even Cu appearing to be mobile to some extent in the top 6 cm.

Chapter 5

An isotopic investigation of Pb mobility and the history of Pb deposition in Flanders Moss peat

5.1 INTRODUCTION

This chapter contains the results of the stable Pb isotope analyses conducted on the solid phase peat, the porewaters and the IHSS- and TB-extracted humic materials from each 2-cm depth section of the core. The isotopic information together with the Pb concentration data (solid phase and porewaters) in Chapter 3 and the Pb associations data presented in Chapter 4 is first used to investigate the vertical mobility of Pb in the peat core. Age dating of the peat, achieved using ^{210}Pb activity measurements from gamma spectrometry, was then undertaken to construct a potential historical record of changing inputs of Pb to the Flanders Moss peat bog.

5.2 DETERMINATION OF THE STABLE PB ISOTOPE SIGNATURE IN THE SOLID PHASE, ASSOCIATED POREWATERS, AND HUMIC EXTRACTS FOR FLANDERS MOSS PEAT

Pb isotopes (^{206}Pb, ^{207}Pb and ^{208}Pb) in the peat, porewaters and humic extracts for each of the 2-cm depth increments were determined as outlined in Section 2.7.3 and isotopic ratios (e.g. $^{206}Pb/^{207}Pb$, $^{208}Pb/^{206}Pb$ and $^{208}Pb/^{207}Pb$) calculated using the method described in Appendix 4. The ratios (±1s.d.) are listed in Tables 5.1, 5.2 and 5.3 for solid phase peat and porewaters, FA1 and HA extracts, and HS extracts, respectively.

5.2.1 $^{206}Pb/^{207}Pb$ isotope ratios for the solid phase peat samples from Core 1

On the basis that most of the Pb in the solid phase is found in the top 0-30 cm, no data below 30 cm will be considered. The 0-30 cm depth profiles of $^{206}Pb/^{207}Pb$ and Pb concentration are shown in Figures 5.1A and 5.1B, respectively.

Table 5.1 – Stable Pb isotopic ratios for Flanders Moss solid phase peat and porewaters from Core 1

Section depth (cm)	Solid phase peat			Pore waters		
	$^{206}Pb/^{207}Pb$	$^{208}Pb/^{206}Pb$	$^{208}Pb/^{207}Pb$	$^{206}Pb/^{207}Pb$	$^{208}Pb/^{206}Pb$	$^{208}Pb/^{207}Pb$
0-2	1.136 ± 0.002	2.115 ± 0.003	2.405 ± 0.003	1.141 ± 0.002	2.111 ± 0.003	2.407 ± 0.003
2-4	1.152 ± 0.000	2.100 ± 0.002	2.418 ± 0.002	1.154 ± 0.002	2.103 ± 0.003	2.425 ± 0.004
4-6	1.161 ± 0.002	2.099 ± 0.002	2.437 ± 0.004	1.167 ± 0.002	2.094 ± 0.002	2.442 ± 0.002
6-8	1.165 ± 0.001	2.081 ± 0.003	2.424 ± 0.003	1.170 ± 0.002	2.092 ± 0.004	2.447 ± 0.003
8-10	1.166 ± 0.002	2.092 ± 0.002	2.439 ± 0.003	1.170 ± 0.001	2.096 ± 0.004	2.450 ± 0.003
10-12	1.164 ± 0.001	2.097 ± 0.002	2.441 ± 0.002	1.170 ± 0.001	2.093 ± 0.003	2.448 ± 0.003
12-14	1.168 ± 0.001	2.084 ± 0.002	2.434 ± 0.002	1.164 ± 0.004	2.100 ± 0.004	2.444 ± 0.008
14-16	1.168 ± 0.002	2.088 ± 0.003	2.439 ± 0.002	1.174 ± 0.001	2.085 ± 0.003	2.448 ± 0.001
16-18	1.171 ± 0.001	2.083 ± 0.002	2.438 ± 0.002	1.168 ± 0.001	2.089 ± 0.001	2.439 ± 0.001
18-20	1.176 ± 0.001	2.074 ± 0.002	2.438 ± 0.000	1.179 ± 0.002	2.080 ± 0.006	2.450 ± 0.004
20-22	1.177 ± 0.001	2.081 ± 0.002	2.447 ± 0.002	1.183 ± 0.000	2.070 ± 0.004	2.447 ± 0.004
22-24	1.177 ± 0.002	2.075 ± 0.003	2.442 ± 0.002	1.182 ± 0.002	2.070 ± 0.003	2.446 ± 0.003
24-26	1.175 ± 0.001	2.083 ± 0.002	2.447 ± 0.002	-	-	-
26-28	1.179 ± 0.000	2.081 ± 0.002	2.452 ± 0.003	-	-	-
28-30	1.177 ± 0.001	2.083 ± 0.002	2.450 ± 0.002	-	-	-

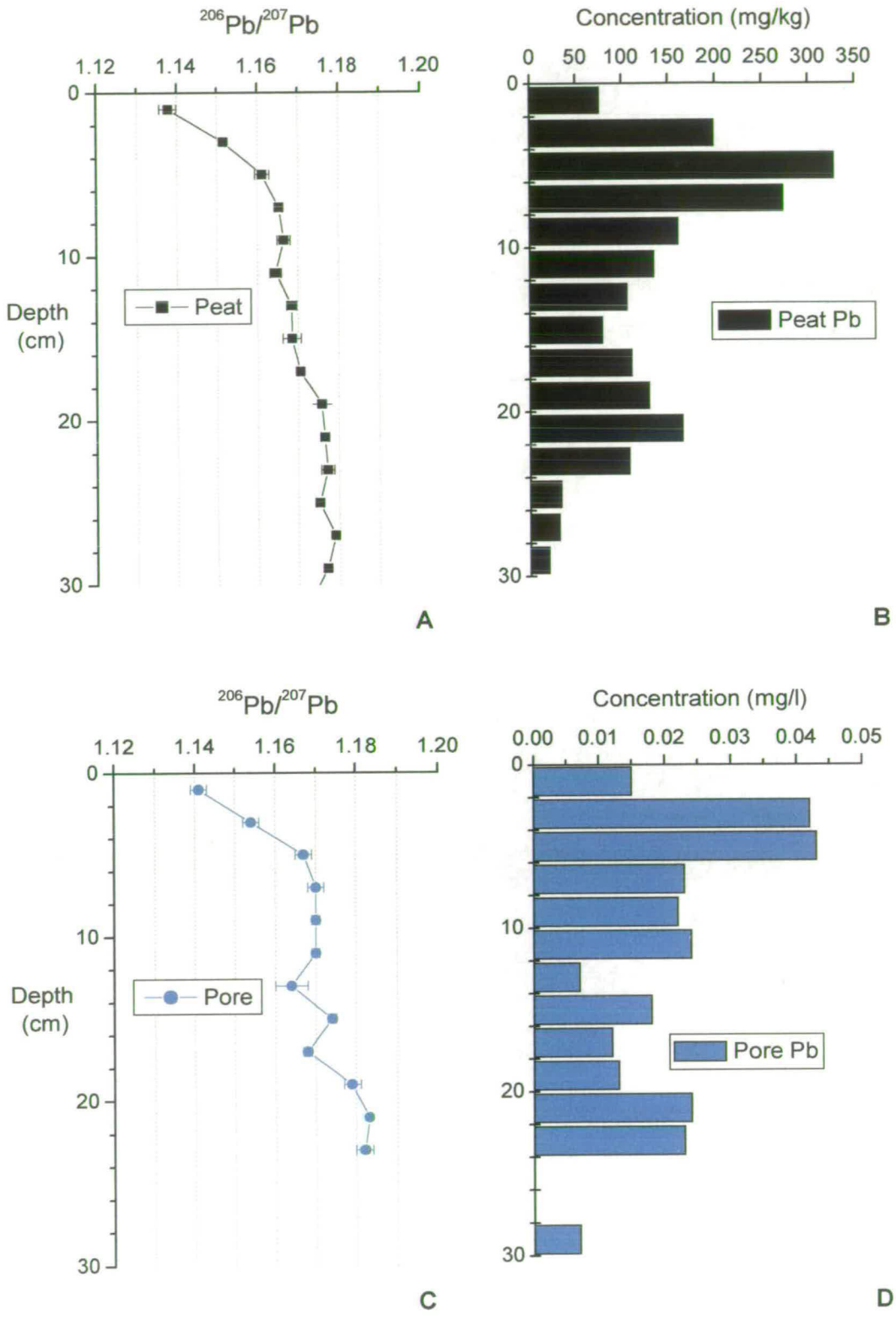

Figures 5.1 – $^{206}Pb/^{207}Pb$ isotopic ratios and Pb concentrations for solid phase peat (A and B) and porewater (C and D) samples from Core 1

The isotopic profile was divided into three distinct portions: (i) a sharp change over the uppermost three sections (1.136 at 0-2 cm to 1.161 at 4-6 cm), (ii) a more gradual change from 1.165 at 6-8 cm to 1.171 at 16-18 cm, and (iii) a portion from 18-30 cm where the $^{206}Pb/^{207}Pb$ isotope ratio is almost constant at ~1.177. The peak in the solid phase Pb concentrations coincided with the boundary dividing (i) and (ii). The second solid phase peak is contained in portion (iii).

5.2.2 $^{206}Pb/^{207}Pb$ isotope ratios for the porewater samples from Core 1

On the basis that Pb concentrations were < 0.01 mg/l below 24 cm, only the data above this will be considered. The 0-24 cm depth profiles of both the $^{206}Pb/^{207}Pb$ ratio and Pb concentration are displayed in Figure 5.1C and D, respectively. Again, the isotopic profile can be divided into three distinct portions: (i) 0-6 cm, (ii) 6-18 cm and (iii) 18-24 cm. There was a sharp change from 1.143 at 0-2 cm to 1.167 at 4-6 cm which was followed by more constant values of ~ 1.17 from 6-18 cm. A small change occurred at 18-20 cm, below which values were near constant at ~ 1.18. As with the solid phase, the peak in porewater Pb concentrations occurred in the 4-6 cm section, which marked the change in gradient from portion (i) to (ii). The second porewater Pb peak was again contained in portion (iii).

5.2.3 $^{206}Pb/^{207}Pb$ isotope ratios for the FA1 extracts from Core 2 peat samples

Only values for 0-20 cm are presented in Table 5.2, as the Pb concentrations in the sections below this depth were too low to permit accurate isotopic analyses. Figures 5.2A and B show the $^{206}Pb/^{207}Pb$ isotopic and Pb concentrations (in mg/kg dry weight peat) profiles for the FA1 extracts, respectively. From the isotopic profile, good agreement between FA1 and the porewater values was obtained for the uppermost sections (1.143 for the 0-2 cm section and a sharp change to 1.164 by 4-6 cm).

Table 5.2 – Stable Pb isotopic ratios for the FA1 and HA extracts of Flanders Moss peat Core 2

Section depth (cm)	FA1 Fraction			HA Fraction		
	$^{206}Pb/^{207}Pb$	$^{208}Pb/^{206}Pb$	$^{208}Pb/^{207}Pb$	$^{206}Pb/^{207}Pb$	$^{208}Pb/^{206}Pb$	$^{208}Pb/^{207}Pb$
0-2	1.143 ± 0.001	2.111 ± 0.004	2.391 ± 0.004	1.140 ± 0.001	2.110 ± 0.004	1.140 ± 0.001
2-4	1.154 ± 0.001	2.102 ± 0.003	2.405 ± 0.003	1.151 ± 0.002	2.102 ± 0.003	1.151 ± 0.002
4-6	1.164 ± 0.002	2.077 ± 0.003	2.418 ± 0.002	1.162 ± 0.001	2.091 ± 0.003	1.162 ± 0.001
6-8	1.176 ± 0.001	2.082 ± 0.002	2.449 ± 0.002	1.178 ± 0.003	2.080 ± 0.004	1.178 ± 0.003
8-10	1.179 ± 0.001	2.083 ± 0.002	2.457 ± 0.002	1.180 ± 0.002	2.079 ± 0.003	1.180 ± 0.002
10-12	1.180 ± 0.001	2.081 ± 0.001	2.456 ± 0.002	1.179 ± 0.004	2.081 ± 0.008	1.179 ± 0.004
12-14	1.182 ± 0.001	2.077 ± 0.002	2.456 ± 0.002	1.181 ± 0.002	2.075 ± 0.005	1.181 ± 0.002
14-16	1.184 ± 0.001	2.080 ± 0.003	2.463 ± 0.002	1.178 ± 0.001	2.078 ± 0.001	1.178 ± 0.001
16-18	1.186 ± 0.002	2.078 ± 0.004	2.465 ± 0.004	1.180 ± 0.005	2.075 ± 0.005	1.180 ± 0.005
18-20	1.190 ± 0.003	2.077 ± 0.004	2.473 ± 0.006	1.178 ± 0.006	2.075 ± 0.012	1.178 ± 0.006

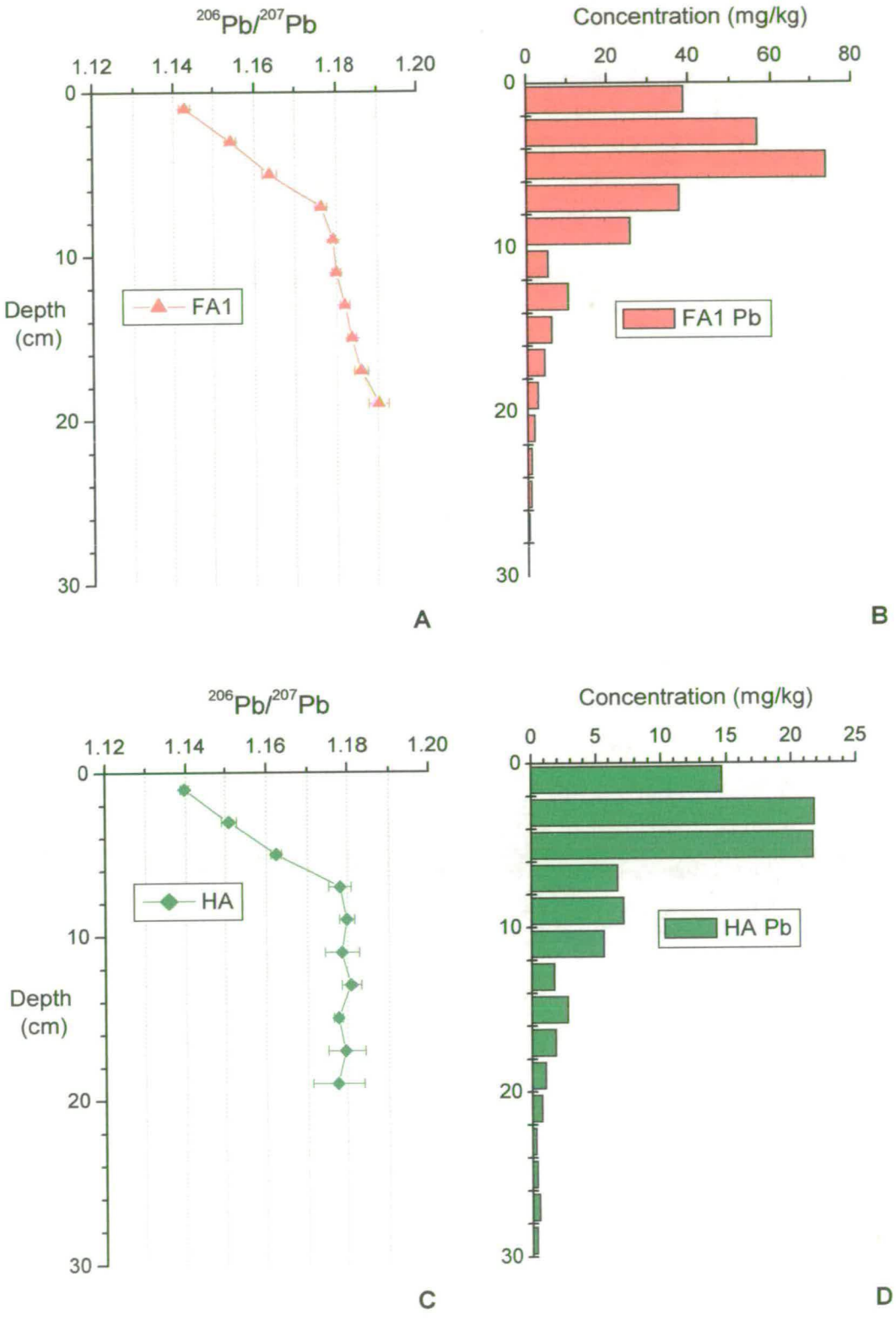

Figures 5.2 – $^{206}Pb/^{207}Pb$ isotopic ratios and Pb concentrations for FA1 (A and B) and HA (C and D) extracts from Core 2 peat samples

The singular peak in the Pb concentration profile for FA1 was in the 4-6 cm section, coincident with the solid phase and porewater Pb concentration profiles. In the 6-8 cm section, however, Pb concentrations started to decrease but the isotope ratio continued to increase to a value of 1.176. A change in gradient then occurred and a more gradual change from 1.179 to 1.190 was obtained over the 8-20 cm sections.

5.2.4 $^{206}Pb/^{207}Pb$ isotope ratios for the HA extracts from Core 2

Again only values for the 0-20 cm sections are presented in Table 5.2. The corresponding 0-20 cm depth profiles for $^{206}Pb/^{207}Pb$ and Pb concentration are shown in Figures 5.2C and D, respectively. As for FA1, the isotopic profile can be divided into two parts: (i) the 0-8 cm section and (ii) the 8-20 cm section. In portion (i) the $^{206}Pb/^{207}Pb$ changed markedly from 1.140 at 0-2 cm to 1.178 at 6-8 cm whilst for portion (ii) the isotopic ratio was constant at ~1.18. Overall, the isotope profile for HA was very similar to that of FA1 except that, for portion (ii) of FA1, the isotopic ratios increased slightly to ~1.19. The peak values in the Pb concentration profile for HA were contained in portion (i) of the isotope profile.

5.2.5 $^{206}Pb/^{207}Pb$ isotope ratios for the HS extracts from Core 2

The HS extracts generally had the lowest concentrations of Pb and only data for the 0-16 cm sections is presented in Table 5.3. The 0-16 cm depth profiles for $^{206}Pb/^{207}Pb$ and the Pb concentrations for the HS extracts are shown in Figures 5.3A and B. Although the changes in the value of the $^{206}Pb/^{207}Pb$ ratio with depth are not as well-defined as for the other humic extracts (sections 5.2.3 and 5.2.4), it was still possible to divide the profile into two parts: (i) the 0-8 cm section and (ii) the 8-20 cm section.

Table 5.3 – Stable Pb isotopic ratios for the HS extracts from Flanders Moss peat Core 2

Section depth (cm)	HS Fraction		
	$^{206}Pb/^{207}Pb$	$^{208}Pb/^{206}Pb$	$^{208}Pb/^{207}Pb$
0-2	1.140 ± 0.001	2.120 ± 0.001	2.416 ± 0.002
2-4	1.165 ± 0.003	2.090 ± 0.005	2.434 ± 0.007
4-6	1.169 ± 0.002	2.095 ± 0.005	2.448 ± 0.006
6-8	1.180 ± 0.003	2.081 ± 0.006	2.454 ± 0.004
8-10	1.180 ± 0.001	2.085 ± 0.004	2.458 ± 0.004
10-12	1.185 ± 0.003	2.077 ± 0.007	2.459 ± 0.006
12-14	1.176 ± 0.005	2.090 ± 0.005	2.457 ± 0.005
14-16	1.192 ± 0.006	2.067 ± 0.006	2.463 ± 0.012

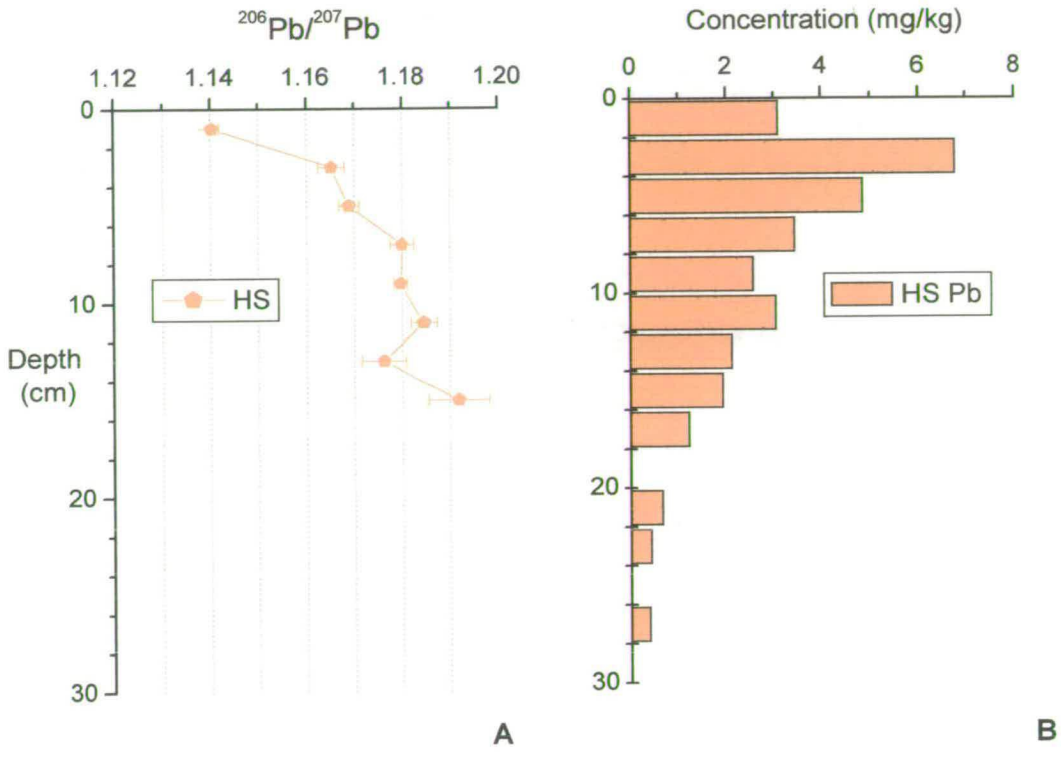

Figures 5.3 A and B – $^{206}Pb/^{207}Pb$ isotopic ratios and Pb concentrations for HS extracts from Core 2 peat samples

The $^{206}Pb/^{207}Pb$ ratio changed in a less linear manner from 1.140 in the 0-2 cm section to 1.180 in the 6-8 cm section. Thereafter, values of the ratio were in the range 1.176-1.192. The peak in the HS profile, in the 2-4 cm section as for all the above profiles, was contained in portion (i) of the isotope profile.

5.2.6 Comparison of $^{206}Pb/^{207}Pb$ profiles for the solid phase, associated porewaters, and humic extracts for Flanders Moss peat

Plotting selected $^{206}Pb/^{207}Pb$ profiles on the same graph enables a comparison of the depth trends. Figures 5.4A-C show the comparison of solid phase and porewater, FA1, HA and HS, and all profiles, respectively.

Figure 5.4A shows the good general agreement between the porewater and solid phase profiles for all depth sections. For both the solid phase and porewater isotopic profiles, there are clearly three main portions as described in sections 5.2.1 and 5.2.2. The slightly greater variability between 10 and 20 cm in the porewater profile is probably attributable to the low concentrations of Pb in the porewaters.

Figure 5.4B shows the broad agreement between the FA1, HA and HS profiles for all depth sections. Each profile was subdivided into two main parts at depths similar to those for the upper two portions described for the solid phase and porewater profiles. There was no data corresponding to the depths of the third portion identified for the solid phase and porewater profiles. Slight variations in isotopic signature of the humic extracts in the second portion of the profiles are again attributable to low concentrations of Pb (particularly in the HS extracts).

Figure 5.4C, showing all the profiles together, highlights the good general agreement over the 0-6 cm sections but also illustrates the difference between the humic extracts and the solid phase/porewater profiles in the 8-20 cm sections. The former group had ratio values which tended towards ~1.18 whilst the latter had values of ~ 1.17.

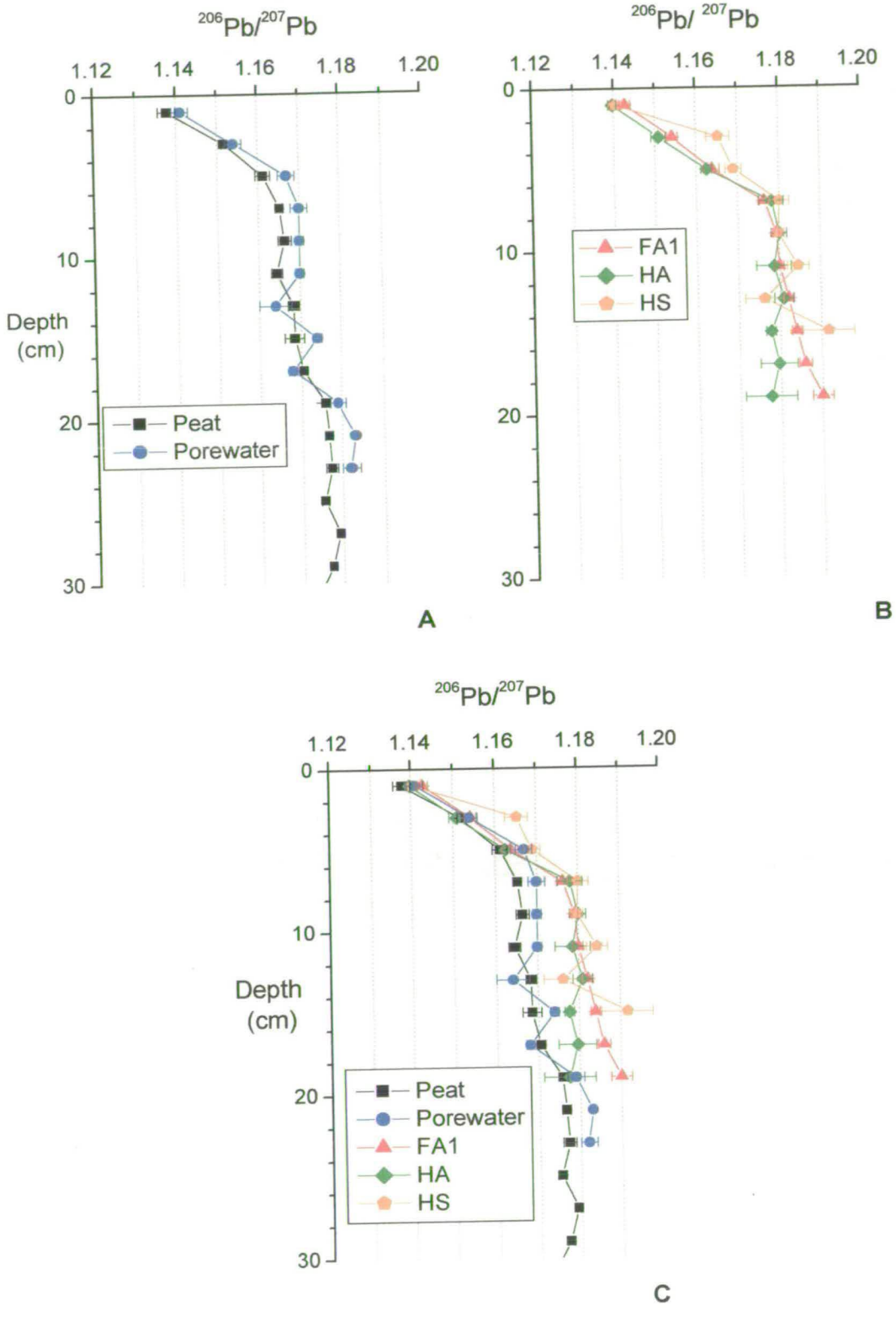

Figures 5.4 A, B, and C– Comparison of $^{206}Pb/^{207}Pb$ isotopic ratios
A = solid phase and porewaters, B = humic extracts, C = all

5.2.7 Comparison of $^{206}Pb/^{207}Pb$ and $^{208}Pb/^{206}Pb$ ratios for the solid phase, associated porewaters, and humic extracts for Flanders Moss peat

A further way of presenting the data involves plotting the $^{208}Pb/^{207}Pb$ vs the $^{206}Pb/^{207}Pb$ ratios and the $^{208}Pb/^{207}Pb$ vs $^{206}Pb/^{207}Pb$ ratios (Figures 5.5A and 5.5B). In previous studies on Pb isotopic signatures (Grousset *et al.*, 1994; Monna *et al.*, 1997; Aberg *et al.*, 1999), these plots have been used to illustrate that the measured isotopic signatures lie between two "end members". In both of these graphs, the data effectively plot on a straight line, with the near-surface ratios representing the less radiogenic end (i.e. lower $^{206}Pb/^{207}Pb$ values), and the ratios from deeper sections in the peat representing more radiogenic values (i.e. higher $^{206}Pb/^{207}Pb$ values). The values associated with the 0-2 cm and 2-4 cm sections for all components (fractions) of the peat are clearly differentiated from the cluster containing most of the data.

The two end members identified are (i) "industrial" Pb (Farmer *et al.*, 1997), with isotopic signatures at the radiogenic end of the spectrum (with an assumed $^{206}Pb/^{207}Pb$ of ~ 1.181), and (ii) petrol-derived Pb, with a less radiogenic signature of 1.06-1.09 (Farmer *et al.*, 1997, 2000). This will be discussed more fully in sections 5.7 and 5.8.

5.3 IMPLICATIONS FOR PB MOBILITY FROM THE $^{206}PB/^{207}PB$ ISOTOPE RATIO AND PB CONCENTRATION PROFILES FOR THE SOLID PHASE, ASSOCIATED POREWATERS, AND HUMIC EXTRACTS FOR FLANDERS MOSS PEAT

From the solid phase and porewater Pb concentration profiles presented in Chapter 3 (Figure 3.12C) and Figures 5.1B and D, it can be seen that most of the Pb is contained in the top 0-30 cm. The two main peaks in the porewater occurred at the same depths as those in the solid phase. Moreover, the value of the distribution coefficient calculated in Chapter 3 was low and almost constant over the top 0-30 cm ($1.5x10^{-4} \pm 5x10^{-5}$ kg/L). This meant that more than 99.8% of the total Pb in the peat bog was associated with the solid phase material. These results *per se* strongly suggested that Pb is not likely to be vertically mobile. However, the associations of Pb within peat had not been determined in other studies.

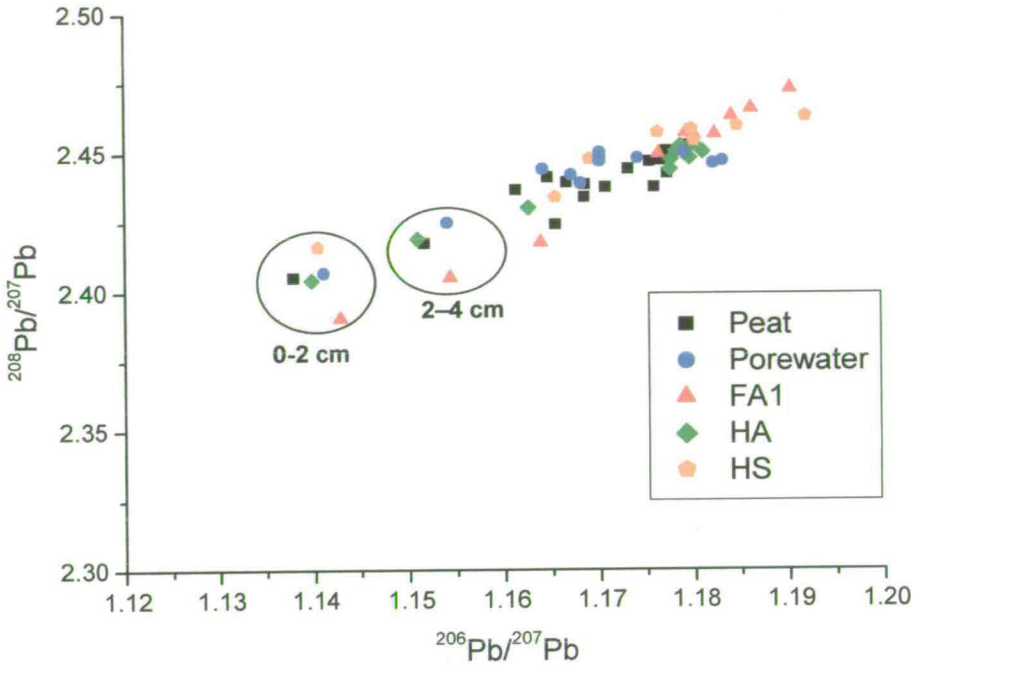

A

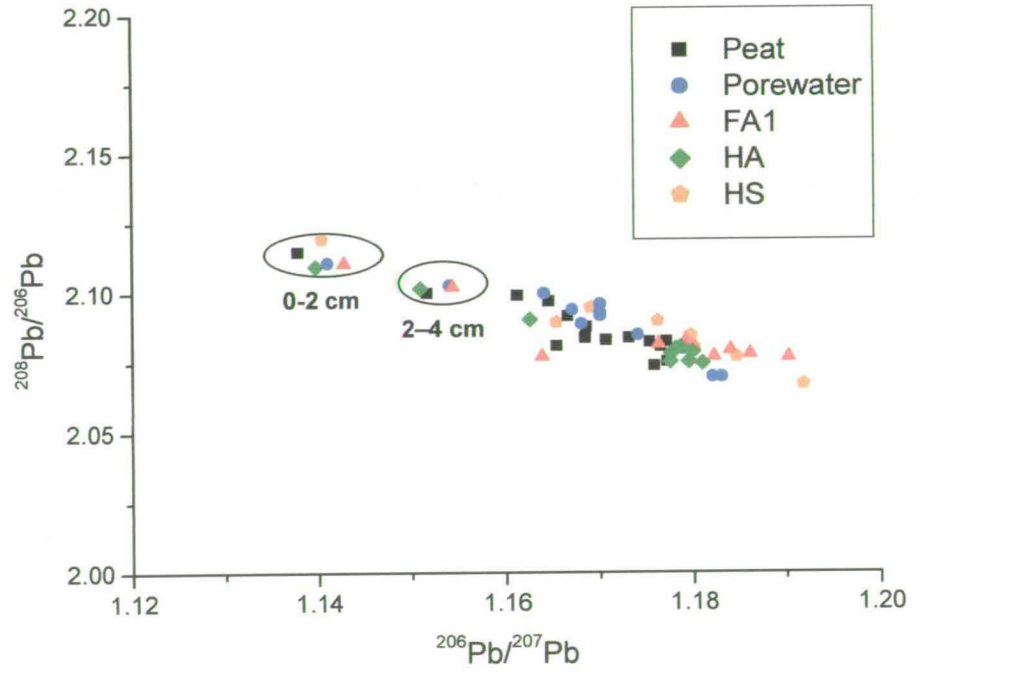

B

Figures 5.5A-B – Plots of $^{208}Pb/^{206}Pb$ (A) and $^{208}Pb/^{207}Pb$ vs$^{206}Pb/^{207}Pb$ (B)

In Chapter 4, the extent of Pb associations with FA1, FA2, HA and HS was determined. By comparing the Pb concentrations in the humic extracts to those in the solid phase, it can be seen that humic materials (perhaps also co-extractable inorganic materials) are solid phase sinks for Pb mainly in the top 0-10 cm of the core (Figure 5.6). The extent of Pb associations with humic materials was not constant even over the top 0-10 cm. In the 0-2 cm section, in excess of 85% of the pseudo-total Pb was extracted along with the IHSS humic materials (Section 4.6.5). In the 4-6 cm section, only 50% of the pseudototal lead in the solid phase was eextracted and this value decreased to 8% at 8-10 cm. Furthermore, the lack of a sub-surface peak in Pb in the organic extracts indicates that with increasing depth, Pb becomes more difficult to extract. At the position of the lower peak in the solid phase concentration profile (20-22 cm), less than 3% of the pseudo-total Pb was extracted. Strong associations with solid phase humic material would favour post-depositional immobility, as would the change to even less extractable inorganic forms.

From the isotopic data presented in this chapter (section 5.2), there was generally good agreement between the $^{206}Pb/^{207}Pb$ isotope ratios obtained for the solid phase, porewaters and humic extracts (Figures 5.4A-C). In particular, the sharp change in ratio in the uppermost sections of the peat, observed in not only the solid phase peat and porewaters, but also in the humic extracts (both extraction methods) illustrated most convincingly that Pb was not vertically mobile within the peat bog.

The only discrepancy in the isotopic data is the difference (~0.01) observed between the $^{206}Pb/^{207}Pb$ ratio determined for the humic extracts and the solid phase peat below 6 cm. This can be explained using information about the sources of Pb inputs into the peat bog, which have changed over the past few hundred years (Farmer *et al*, 1997). Based on previous studies of Scottish freshwater lochs and Flanders Moss peat bog, the sharp decrease in the $^{206}Pb/^{207}Pb$ ratio for the solid phase peat from 6 cm towards the surface is due to increased inputs of petrol Pb during the 20th Century. At depths greater than 6 cm, most of the Pb originated from coal burning and Pb ore smelting.

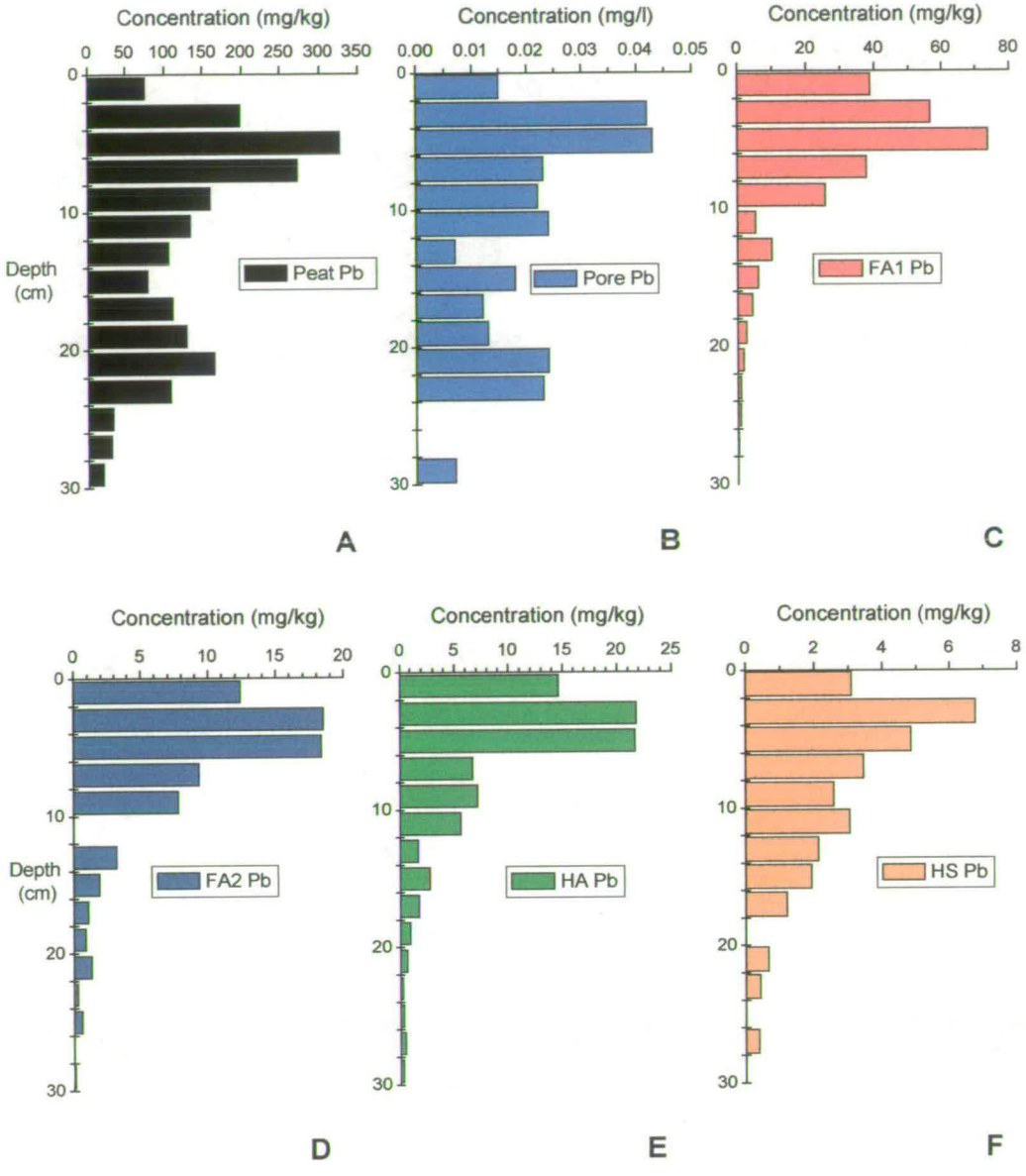

Figures 5.6 – Comparison of Pb concentrations in the solid phase peat (A), pore waters (B), and FA1 (C), FA2 (D), HA (E) and TB (F) extracts

Farmer *et al.* (1999) determined the average $^{206}Pb/^{207}Pb$ ratio for Scottish coals, which was reported as 1.181±0.011, and the $^{206}Pb/^{207}Pb$ ratio for Pb ore from the Leadhills area of Scotland (major source of ore for smelting) which was reported as 1.17 (Sugden *et al*, 1993). The value of ~1.169 for the 6-18 cm sections was close to the latter value whilst the value of ~1.177 for the 18-30 cm portion of the solid phase peat lay closer to the former. It was not surprising that Pb from either of these sources wasn't extracted to any significant extent by the reagents used to extract humic materials. In particular, Pb from smelting activities could be in the form of small particles of galena (PbS), the extremely low solubility mineral comprising the ore. The very small amounts of Pb extracted from 6-18 cm sections had an isotopic signature more similar to the values obtained for Scottish coals than to the Leadhills ores used for smelting. Notably, the $^{206}Pb/^{207}Pb$ ratios for the humic extracts appeared to converge with the solid phase and porewater ratios below 18 cm.

Finally, the data as a whole suggest that Pb entering the peat bog either remains with particulate/mineral material or becomes bound extremely quickly to humic material and so, after deposition, Pb is immobile. Having established this, a historical record of anthropogenic Pb inputs into the peat bog can be constructed.

5.4 ^{210}PB DATING OF THE FLANDERS MOSS PEAT CORE SECTIONS

The activity of ^{210}Pb in known weights of air-dried peat was measured by γ-spectrometry (Section 2.4.2). The total dry weights of peat for each of the 2-cm depth sections were used to calculate the cumulative weight to the mid-point of each of the depth sections analysed. As the cross-sectional area of each of the five bulked cores was 25cm^2, the total surface area receiving deposition was 125 cm^2. The cumulative weight per unit area (g/cm^2) to the mid-point of each section is listed along with the corresponding activities of total and supported ^{210}Pb in the peat in Table 5.4.

Table 5.4 – Total, supported and unsupported activity of ^{210}Pb and weights used to determine the peat accumulation rate for Core 1

Section Depth (cm)	Total ^{210}Pb (Bq/kg)	Supported ^{210}Pb (Bq/kg)	Unsupported ^{210}Pb (Bq/kg)	Section weight (g)	Section half-weight (g)	Cumulative weight (g)	Cumulative half-weight (g)
0-2	427 ± 51	34 ± 2	393	18.33	9.17	18.33	9.17
2-4	271 ± 26	27 ± 5	244	18.88	9.44	37.21	27.77
4-6	159 ± 28	16 ± 3	143	21.73	10.87	58.94	48.08
6-8	80 ± 11	12 ± 2	68	33.07	16.53	92.01	75.48
8-10	44 ± 13	9 ± 2	35	32.54	16.27	124.55	108.28
10-12	68 ± 8	16 ± 2	52	35.82	17.91	160.37	142.46
12-14	48 ± 8	6 ± 1	42	34.94	17.47	195.31	177.84
14-16	37 ± 8		37	28.34	14.17	223.65	209.48
16-18	24 ± 6	4 ± 1	20	32.06	16.03	255.70	239.67
18-20	28 ± 7	4 ± 1	24	33.24	16.62	288.94	272.32
20-22	10 ± 5		10	25.01	12.51	313.95	301.45
22-24	11 ± 3	3 ± 0.3	8	28.41	14.21	342.37	328.16
24-26	13 ± 6	7 ± 1	6	24.92	12.46	367.29	354.83

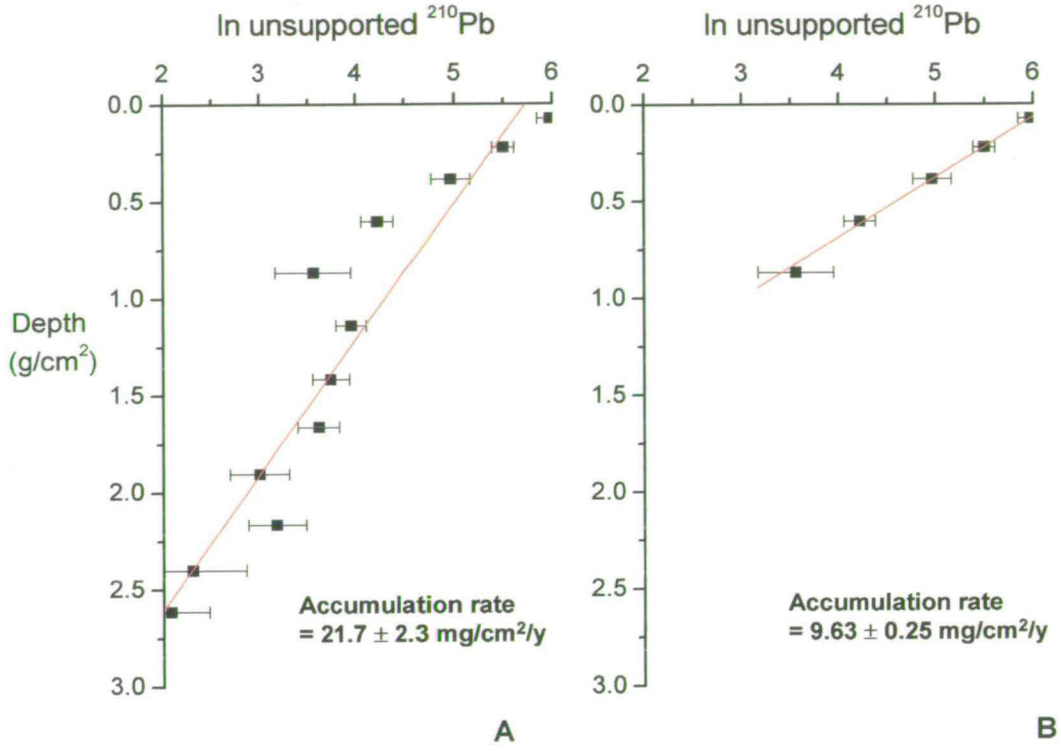

Figures 5.7– Linear regression of unsupported ^{210}Pb vs depth for Core 1 peat samples (A = all data, B = top five sections)

Table 5.5A - ^{210}Pb Dates obtained for 0-10 cm Core 1 (using an accumulation rate of 9.63 mg/cm^2/y)

Depth (cm)		Cumulative weight to midpoint/bottom of section(mg/cm^2)	Years (to midpoint/bottom of section)	Date
0-2	Midpoint	73	7.6	1991
	Bottom	147	15.2	1984
2-4	Midpoint	222	23.1	1976
	Bottom	298	30.9	1968
4-6	Midpoint	385	39.9	1959
	Bottom	472	49	1950
6-8	Midpoint	604	62.7	1936
	Bottom	736	76.4	1922
8-10	Midpoint	866	90	1909
	Bottom	996	103.5	1895

Table 5.5B - ^{210}Pb Dates obtained for 10-24 cm Core 1 (using an accumulation rate of 27.9 mg/cm^2/y)

Depth (cm)	Cumulative weight to bottom of section (mg/cm^2)	Years (to bottom of section)	Date (starting from 1895)
10-12	286	10.3	1885
12-14	554	19.9	1875
14-16	781	28	1867
16-18	1037	37.2	1858
18-20	1303	46.7	1849
20-22	1503	53.9	1842
22-24	1731	61.7	1834

A plot of depth (g/cm^2) vs ln (unsupported ^{210}Pb) enables the peat accumulation rate to be calculated by the CIC method. Using data for the top 12 sections (0-24 cm) in the core, an accumulation rate of 21.7 ± 2.3 $mg/cm^2/y$ was obtained (Figure 5.7A). Clearly, the linear regression did not pass through all of the data points and so the accumulation rate was recalculated using only data for the uppermost 5 sections in the core (10 cm). A significantly different accumulation rate of 9.63 ± 0.25 $mg/cm^2/y$ was obtained (Figure 5.7B). The ^{210}Pb dates for the 0-10 cm sections are shown in Table 5.5A. The non-linear relationship between the ln unsupported ^{210}Pb and the cumulative weight of peat suggests that some process, e.g. humification, that causes compaction and affects the bulk density of the peat, may be occurring. Thus, the dating to 10 cm cannot be extrapolated below this depth. Tentative dates, however, can be obtained if an accumulation rate of 27.9 $mg/cm^2/y$ (based on ^{210}Pb data for 10-24 cm) is taken below 10 cm (Table 5.5B).

5.5 AN INTEGRATED INVENTORY OF PB IN FLANDERS MOSS PEAT CORE 1

The integrated inventory of Pb was calculated by summing the Pb concentration data found in each of the sections. The results obtained are displayed in Table 5.7. The integrated inventory of Pb was calculated at 4.47 g/m^2. This value is comparable to values for the southern basin of Loch Lomond and previous studies on Flanders Moss peat (Table 5.6).

Table 5.6 - Comparison of integrated Pb inventories Loch Lomond (southern basin) and Flanders Moss

Location	Integrated Pb inventory (g/m^2)	^{210}Pb flux (kBq/m^2)	$Pb/^{210}Pb$	Source
Loch Lomond (S basin)	6.36	5.81	1.09	Farmer *et al.* (1996)
Flanders Moss (Core A)	3.39	3.55	0.95	Farmer *et al.* (1997)
Flanders Moss (Core C)	2.44	2.32	1.05	Farmer *et al.* (1997)
Flanders Moss (Core D)	1.78	1.13	1.58	Farmer *et al.* (1997)
Flanders Moss (Core 1) – this study	4.47	1.97	2.27	-

Table 5.7 - Integrated inventory of Pb in Flanders Moss peat Core 1

Depth (cm)	Weight (g)	Pb (mg/kg)	Pb (mg/m^2)	Σ Pb (mg/m^2)	Cumulative %	Date (bottom of section)
0-2	18.33	75.5	110.7	110.7	2.5	1984
2-4	18.88	198.4	299.7	410.4	9.2	1967
4-6	21.74	327.6	569.8	980.2	21.9	1950
6-8	33.07	272.7	721.5	1701.7	38.0	1922
8-10	32.54	160.4	417.6	2119.3	47.4	1895
10-12	35.81	134.1	384.2	2503.5	56.0	
12-14	33.46	105.4	282.1	2785.6	62.3	
14-16	28.34	78.6	178.2	2963.8	66.2	
16-18	32.07	110.5	283.5	3247.3	72.6	
18-20	33.24	128.7	342.2	3589.5	80.2	
20-22	25.01	164.8	329.7	3919.2	87.6	
22-24	28.41	107.5	244.3	4163.5	93.1	
24-26	24.93	33.2	66.2	4229.7	94.5	
26-28	23.21	31.0	57.6	4287.3	95.8	
28-30	21.12	20.0	33.8	4321.1	96.6	
30-32	20.96	9.1	15.3	4336.4		
32-34	15.40	7.7	9.5	4345.9		
34-36	13.45	5.0	5.4	4351.3		
36-38	14.97	7.0	8.4	4359.7		
38-40	18.24	3.1	4.5	4364.2		
40-42	18.07	5.4	7.8	4372.0		
42-44	15.74	3.0	3.8	4375.8		
44-46	13.01	1.9	2.0	4377.8		
46-48	11.70	2.5	2.3	4380.1		
48-50	20.95	2.0	3.4	4383.5		

Table 5.7 (continued) Integrated inventory of Pb in Flanders Moss peat Core 1

Depth (cm)	Weight (g)	Pb (mg/kg)	Pb (mg/m^2)	Σ Pb (mg/m^2)	Cumulative %	Date (bottom of section)
50-52	18.59	3.0	4.5	4388.0		
52-54	16.41	2.3	3.0	4391.0		
54-56	14.85	2.1	2.5	4393.5		
56-58	14.70	1.8	2.1	4395.6		
58-60	16.09	3.4	4.4	4400.0		
60-62	18.05	2.3	3.3	4403.3		
62-64	17.28	3.8	5.3	4408.6		
64-66	16.46	3.4	4.5	4413.1		
66-68	16.95	3.9	5.3	4418.4		
68-70	18.43	4.4	6.5	4424.9		
70-72	19.19	4.8	7.4	4432.3		
72-74	18.29	5.3	7.8	4440.1		
74-76	19.33	3.4	5.3	4445.4		
76-78	19.40	2.9	4.5	4449.9		
78-80	26.49	3.2	6.8	4456.7		
80-82	15.57	2.6	3.2	4459.9		
82-84	15.59	2.7	3.4	4463.3		
84-86	15.13	2.3	2.8	4466.1		
86-88	13.91	1.3	1.4	4467.5		
88-90	13.38	1.9	2.0	4469.5		
90-92	9.92	1.3	1.0	4470.5		
92-94	8.81	1.1	0.8	4471.3		
94-96	11.46	1.0	0.9	4472.2		
96-98	10.43	1.0	0.8	4473.0		
98-100	12.22	1.2	1.2	4474.2		

Using the inventory data along with the dates obtained for the top 10 cm (the base of the 8-10 cm section corresponded to 1895), the percentage of the total Pb inventory in the peat core deposited in the last century can be calculated. The data displayed in Table 5.6 was used to construct Figure 5.8. The results showed that 47.4% of the Pb inventory (to 100 cm) was deposited after 1895. This compared well with the Loch Lomond (southern basin) core, in which 51% of the total Pb inventory in the sediments was deposited after 1900 (Farmer *et al.*, 1997). Between 10 and 30 cm depth, a further 49.2% of the Pb inventory was found for Flanders Moss Core 1 (this study), i.e. a total of 96.6 % in the 0-30 cm sections.

Using the accumulation rate of 27.9 mg/cm^2/yr calculated from ^{210}Pb dating of the 10-24 cm sections, the second Pb peak at 20-22 cm can be dated at ~1845. This means that significant deposition of Pb was occurring by the middle of the 19th Century. Although the dating of sections below 10 cm is tentative, this agreed with the Loch Lomond southern basin, which was also showing significant Pb deposition by that date.

5.6 FLUXES OF PB TO FLANDERS MOSS PEAT

From the Pb concentrations and calculated accumulation rate of the peat, Pb fluxes to the peat can be calculated and these are displayed in Table 5.8. The Pb flux to Flanders Moss peat in the 20th Century peaked at 31.55 mg/m^2/yr (4-6 cm section, corresponding at the midpoint of 3 cm to 1959). Again, this compares well with the anthropogenic Pb flux to Loch Lomond southern basin sediments that peaked at 40-45 mg/m^2/y in the 1950s.

Table 5.8 Fluxes of Pb to Flanders Moss peat

Depth (cm)	Pb (mg/kg)	Accumulation rate (mg/cm^2/y)	Flux (mg/m^2/y)	Date (at midpoint)
0-2	75.5	9.63	7.27	1991
2-4	198.4	9.63	19.11	1976
4-6	327.6	9.63	31.55	1959
6-8	272.7	9.63	26.26	1936
8-10	160.4	9.63	15.45	1909

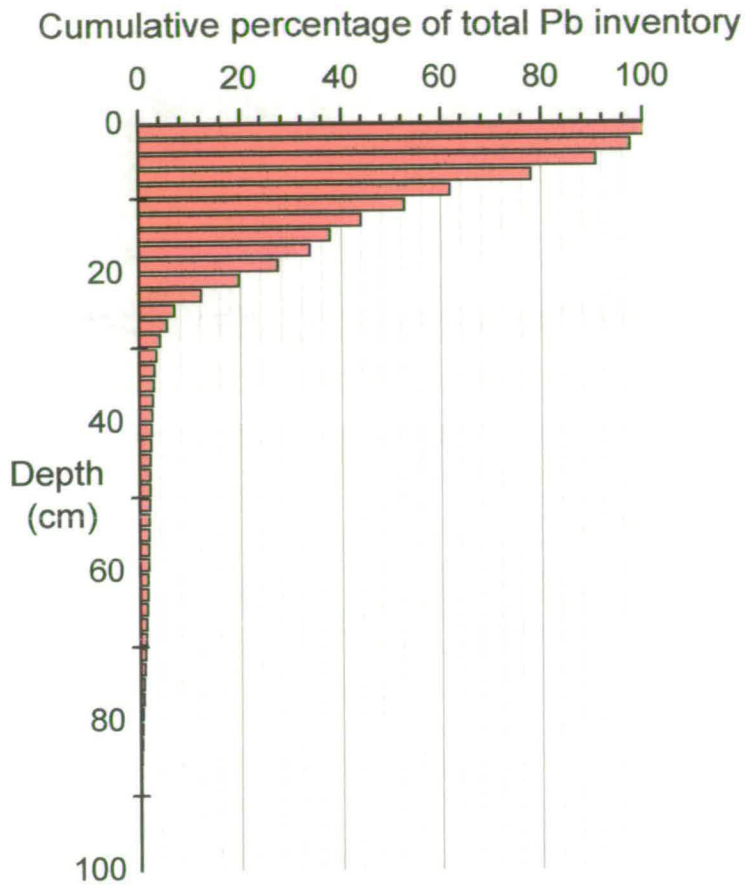

Figure 5.8 - Percentage of total Pb accumulated from the base of Core 1

5.7 HISTORICAL INTERPRETATION OF PB ISOTOPIC RATIOS IN FLANDERS MOSS PEAT CORE 1

As described in Section 5.3, the isotopic ratio in the solid phase peat in the 18-30 cm zone of the peat had an average $^{206}Pb/^{207}Pb$ isotopic ratio of ~1.177 ± 0.001. This value was intermediate between 1.181±0.011 for Scottish coals (Farmer at al, 1999), and 1.170 ± 0.003 for Pb ore derived from the Leadhills/Wanlockhead area.

For the 12-18 cm section of the peat, the $^{206}Pb/^{207}Pb$ averages 1.169 ± 0.002, comparable to the late 19th Century value found for Loch Lomond (southern basin) and Flanders Moss peat cores (Farmer *et al.*, 1997).

The $^{206}Pb/^{207}Pb$ ratio didn't alter much from 10 cm and 6 cm depth, but the onset of the sharp decline in $^{206}Pb/^{207}Pb$ can be taken from 7 cm (midpoint of 6-8 cm section, which corresponds to 1936) to 1.161 at 4-6 cm (dated 1959). The onset of the decline in Loch Lomond (southern basin) occurred at around 1929. It was also notable that the trends identified in this study were similar to those obtained for Flanders Moss peat cores collected some 9 years previously (Farmer *et al.*, 1997). The decrease in $^{206}Pb/^{207}Pb$ isotopic ratio, due to the use of Australian ores in the manufacture of tetra-methyl Pb additives for petrol, has also been observed in many different environmental materials all over Europe (see Chapter 1).

The relative contribution of petrol Pb to the total anthropogenic Pb can be assessed using source apportionment calculations.

5.8 SOURCE APPORTIONMENT OF PB IN FLANDERS MOSS PEAT CORE 1

This type of calculation can be conducted where there are two main anthropogenic sources of Pb with distinct $^{206}Pb/^{207}Pb$ isotopic ratios. Petrol Pb in the U.K has a $^{206}Pb/^{207}Pb$ ratio of 1.06-1.09 (Delves and Campbell, 1993) whilst "industrial" Pb can be taken to have a ratio value of 1.169 (late 19th Century value – 12-18 cm sections). The proportion of total Pb derived from petrol can be determined using the following equation:

$$Pb_{petrol} = \frac{^{206}Pb/^{207}Pb_{industrial} - ^{206}Pb/^{207}Pb_{measured}}{^{206}Pb/^{207}Pb_{industrial} - ^{206}Pb/^{207}Pb_{petrol}}$$ Equation 10

The percentage of total Pb derived from petrol (using both 1.06 and 1.09 as characteristic of the petrol $^{206}Pb/^{207}Pb$ ratio) for each of the top two 2-cm sections of the peat are shown in Table 5.9. Data from previous studies for Loch Lomond (southern basin) sediments and Flanders Moss from the corresponding time period are also shown for comparison.

Table 5.9 - Source apportionment of Pb in Flanders Moss peat and Loch Lomond sediments

Location	Date	Percent of total Pb derived from petrol component, using:	
		$^{206}Pb/^{207}Pb_{petrol}$ A = 1.06	$^{206}Pb/^{207}Pb_{petrol}$ B = 1.09
Loch Lomond (southern basin)	1979-1991	36	50
Flanders Moss (Core A)	1966-1990	20	27
Flanders Moss (Core B)	1965-1990	25	35
Flanders Moss (Core C)	1976-1994	36	49
Flanders Moss (Core D)	1982-1994	35	49
Flanders Moss Core 1 - this study	1984-1999	30.3	41.8
	1968-1984	15.6	21.5

In this study, the 2-4 cm and 0-2 cm sections corresponded to the time periods, 1968-1984 and 1984-1999, respectively. The petrol component, on the basis of a $^{206}Pb/^{207}Pb$ ratio of 1.06, was 15.6% and 30.3% for these two time periods, respectively. In comparison with the former value (for 1968-1984), the petrol component for Flanders Moss Core A (1965-1990) was slightly higher at 20% but this can be attributed the inclusion of petrol contributions from 1984-1990. A similar explanation applies for Flanders Moss Core B (1966-1990).

In comparison with the value for 1984-1999, the petrol components for Loch Lomond (southern basin) (1979-1991) and Flanders Moss Cores C (1976-1994) and D (1982-1994) were greater at 36%, 36% and 35%, respectively. Particularly on the basis of Core D, for which the time period is most similar to that represented by the 0-2 cm section in this study, this suggests that the contribution of petrol Pb to the peat between 1994 and 1999 is decreasing. This would be consistent with the increasing usage of unleaded petrol in the UK over this time period. A similar interpretation can be made on the basis of the calculations using the 1.09 value for the $^{206}Pb/^{207}Pb$ ratio in petrol.

5.9 CONCLUSIONS

Having established that Pb was immobile within the peat bog, a historical record was constructed using ^{210}Pb to date the peat core. Calculation of an integrated inventory for Pb showed that 47.4 % was deposited after 1895. Although the dates obtained for deeper sections of the peat (> 10 cm) were less certain, this study found that, in agreement with results for Loch Lomond (southern basin), significant deposition of Pb was occurring by the middle of the 19th Century. The integrated inventories and fluxes of Pb to the peat bog agreed well with those previously obtained for Flanders Moss. Finally, the source apportionment calculations for the 0-2 cm and 2-4 cm sections enabled changes in recent decades in the contribution of petrol Pb to total Pb deposited to be more clearly established. The calculated data suggested that the effect of increased usage of unleaded petrol had resulted in a decrease in the petrol Pb component for the nearest surface section of the peat bog.

Chapter 6 -

Geochemical modelling of the solid phase-aqueous phase partitioning of Pb and Pb-humic associations in Flanders Moss peat bog using the Windermere Humic Acid Model (WHAM)

6.1 INTRODUCTION

Various geochemical models have been developed to describe the binding behaviour of metals by humic substances. One such model is the Windermere Humic Acid Model (WHAM) (section 1.9). Given the concentrations of selected elements, WHAM calculates the distribution of each of the elements between various specified aqueous inorganic species and humic substances (Tipping, 1994).

The aim was to use the WHAM model to gain an insight into (i) the partitioning of Pb between the solid phase peat and its associated porewaters and (ii) the speciation of Pb in the porewaters. The predicted solubility of Pb within the peat bog was then compared with the porewater results presented in Chapter 3 (Section 3.5.5). A further aim was to assess how sensitive the predicted partitioning of Pb between the solid phase and aqueous phase was to changes in the values of model parameters, e.g. pH, reactive site concentration and metal binding strength. Before discussing the results, it is necessary to understand the procedure utilised by WHAM to achieve a solution.

6.2 THE COMPUTATIONAL MECHANISM OF WHAM

There are two versions of WHAM: (i) WHAM-S for use with soils and sediments, and (ii) WHAM-W for waters. WHAM-W was selected because it enabled the speciation of metals in the porewaters to be determined at the measured values of pH, i.e. the pH could be fixed at the value obtained for each of the 2-cm depth sections. This can't be done using WHAM-S.

The output from WHAM-W is the metal solubility based only on inorganic species (free metal ion + hydroxy species only). The porewaters, however, contained DOC at concentrations in the range ~60-180 mg/l. The measured metal concentrations in the porewaters would have included metal-organic species as well as inorganic species. In order to include metal-organic species in the model output, the partitioning of FA between the solid phase and the porewaters of the peat needs to be described. WHAM-W, because of its intended use only for waters, does not calculate the partitioning of FA between an aqueous and a solid phase. The partitioning can be calculated, however, using FA solid-solution partitioning described by Tipping *et al.*, 1995.

The FA solid-solution partitioning described in Tipping *et al.*, 1995 assumes that FA is the partly soluble form of humic material whilst HA is assumed present only in the solid phase. The required inputs for solid-solution partitioning are: (i) the charge on FAs, (ii) the hydrophobicity factor, γ, and (iii) the amount of solid phase material in a given volume (Tipping *et al.*, 1995). WHAM-W automatically calculates the charge on FAs (Figure 6.1), a value of 1 for the hydrophobicity factor can be assumed, and the dry weight of peat (Core 1) in a given volume (5 x 5 cm x 5 cm x 2 cm = 250 cm^3 per 2-cm depth section) was used to give the concentration of solid material in units of g/L. In this way, the partitioning of FA between the peat porewaters and solid phase was determined for each 2-cm section.

It should be noted that only metal-humic binding (and the formation of hydroxy species) was considered in the model. This was due to the lack of information on the concentration of inorganic anions also present in the peat, which could form, for example, inorganic sulphate, and chloride complexes. In this sense the model input was incomplete, but in terms of considering the metal-humic/fulvic binding, the concentrations of any inorganic anions were considered insignificant compared with the concentration of anionic groups (e.g. carboxyl and phenolic functional groups) on the humic and fulvic acid components of the model.

Figure 6.1 – Flowchart outlining WHAM iteration process

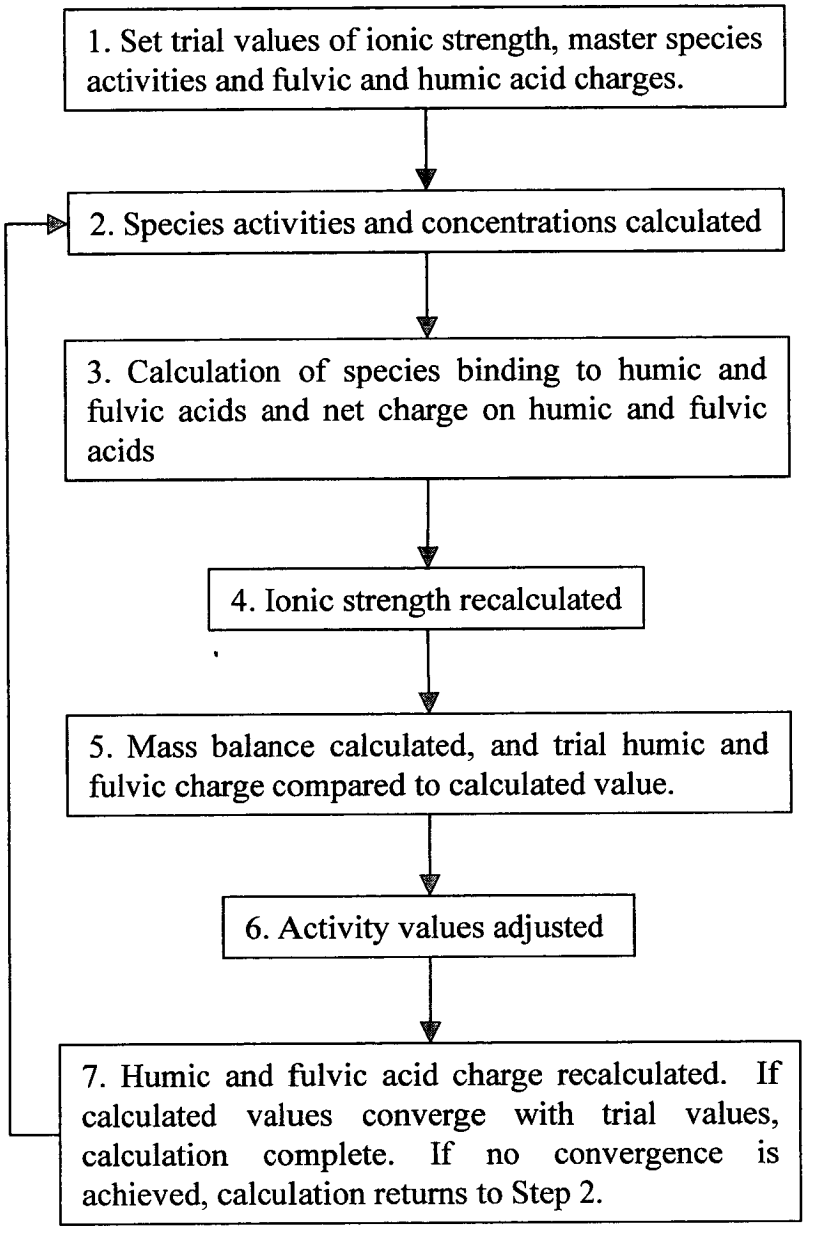

Evidence supporting this assumption comes from Steinmann and Shoytk (1997) who conducted mass balance equations on a Swiss peat using PHREEQE, an earlier speciation model (Parkhurst *et al.*, 1990). Steinmann and Shotyk (1997) reported that in the upper 1m of their peat core, organic ligands represented up to 90% of the anionic mass balance, with the remaining 10% consisting of HCO_3^-.

6.3 INPUT PARAMETERS FOR WHAM

The parameters for input to the model (both experimentally determined and default parameters intrinsic to the model) are discussed in Chapter 1 (Section 1.9.1). The solid phase metal concentrations entered into the model are required to be expressed in units of moles/L but the solid phase peat data presented in Chapter 3 was expressed in units of mg/kg. The transformed input data are listed in Table 6.1. The other input parameters, concentration of solid phase FA (g/L) and solid phase HA (g/L), the concentration of solid peat (g/L) and the pH for each of the 2-cm depth sections, are also contained in Table 6.1.

To reduce the computational complexity, not all of the elements measured in the solid phase peat were used. In addition to Pb, the elements chosen were the major cations (Al, Fe, Na, K, Ca and Mg) and other heavy metals (Cu and Zn). The major cations were selected because of their (i) significant contributions to porewater ionic strength, (ii) role as counterions in the Donnan layer and, in some cases, (iii) potential competition with Pb for binding sites. The heavy metals were also selected for the third reason. For the purposes of modelling, each 2-cm depth section was considered a separate entity, and was modelled in isolation.

6.4 MODEL RESULTS AND INTERPRETATION

WHAM-W was used to generate the aqueous concentration of inorganic metal species for each 2-cm section of the core. Using the FA concentrations from solid-solution partitioning, the aqueous concentrations of FA-metal species were calculated and added to the inorganic component to give total predicted concentrations for each metal.

Table 6.1A - Experimentally determined input data for WHAM

Depth (cm)	pH	Csolid (g/l)	FA content (g/l)	HA content(g/l)
0-2	4.18	152.7	6.08	20.41
2-4	4.02	141.6	4.70	20.91
4-6	3.94	113.1	5.79	17.05
6-8	3.77	172.6	3.50	18.12
8-10	3.79	181.5	2.11	22.67
10-12	3.83	175.5	0.97	28.57
12-14	3.73	173.3	2.30	25.00
14-16	3.74	131.5	2.60	23.45
16-18	3.67	149.2	2.62	19.73
18-20	3.64	143.2	3.27	14.74
20-22	3.7	113.3	2.45	13.02
22-24	3.75	129.2	4.99	8.90
24-26	3.77	108.2	3.80	9.10
26-28	3.67	111.1	2.34	7.34
28-30	3.73	93.6	2.84	3.98
30-32	3.78	93.0	4.13	4.71
32-34	3.88	74.1	3.12	4.34
34-36	3.77	66.9	2.96	2.82
36-38	3.81	68.3	3.23	3.46
38-40	3.77	80.1	3.10	2.00
40-42	3.79	77.5	2.96	4.07
42-44	3.86	71.2	3.10	3.77
44-46	3.87	55.5	3.12	4.35
46-48	3.85	52.1	1.53	2.94
48-50	3.86	95.3	2.35	4.27
50-52	4.02	84.2	2.18	4.45
52-54	3.89	73.2	2.05	3.92
54-56	3.92	69.6	2.05	4.77
56-58	4.19	66.1	2.89	3.90
58-60	3.92	65.4	2.05	5.11
60-62	3.98	82.8	2.72	5.07
62-64	3.96	74.3	3.29	7.24
64-66	3.94	81.5	2.64	5.83
66-68	4.13	64.7	2.08	3.26
68-70	3.96	88.4	2.86	6.27
70-72	4.01	85.0	3.28	14.33
72-74	4.02	82.6	2.35	6.46
74-76	4.05	89.7	3.12	6.71
76-78	4.04	84.6	2.19	7.23
78-80	4	119.1	2.27	8.82
80-82	4.08	72.7	2.45	6.62
82-84	4.07	70.0	2.99	7.74
84-86	4.05	69.5	4.16	6.70
86-88	4.05	61.1	2.59	5.59
88-90	4.06	57.2	2.49	8.01

Table 6.1B - Experimentally determined input data for WHAM

Depth (cm)	Elemental concentrations (moles/l)			
	Na	K	Ca	Mg
0-2	2.94E-03	4.65E-03	6.33E-03	7.03E-03
2-4	1.13E-03	2.17E-03	5.70E-03	4.61E-03
4-6	8.31E-04	7.86E-04	3.90E-03	2.82E-03
6-8	1.20E-03	7.90E-04	5.63E-03	4.05E-03
8-10	1.37E-03	8.12E-04	6.03E-03	4.21E-03
10-12	1.31E-03	8.82E-04	5.78E-03	4.00E-03
12-14	1.39E-03	6.54E-04	6.00E-03	3.96E-03
14-16	1.11E-03	3.32E-04	5.01E-03	3.11E-03
16-18	1.17E-03	4.66E-04	6.31E-03	3.73E-03
18-20	9.78E-04	3.19E-04	6.33E-03	3.72E-03
20-22	9.17E-04	1.87E-04	5.27E-03	2.94E-03
22-24	9.10E-04	2.23E-04	5.88E-03	3.30E-03
24-26	1.03E-03	1.08E-04	5.20E-03	2.66E-03
26-28	1.02E-03	9.44E-05	5.15E-03	2.66E-03
28-30	7.90E-04	7.96E-05	4.29E-03	2.04E-03
30-32	8.29E-04	1.00E-04	4.35E-03	2.02E-03
32-34	6.83E-04	5.74E-05	3.85E-03	1.71E-03
34-36	5.56E-04	3.85E-05	3.39E-03	1.49E-03
36-38	5.55E-04	3.93E-05	3.59E-03	1.58E-03
38-40	5.71E-04	5.21E-05	3.79E-03	1.55E-03
40-42	5.46E-04	6.20E-05	3.52E-03	1.43E-03
42-44	4.92E-04	6.06E-05	3.21E-03	1.25E-03
44-46	3.57E-04	4.86E-05	2.49E-03	8.91E-04
46-48	3.35E-04	4.30E-05	2.32E-03	8.46E-04
48-50	5.88E-04	5.96E-05	4.39E-03	1.63E-03
50-52	5.49E-04	4.21E-05	4.17E-03	1.61E-03
52-54	4.68E-04	6.40E-05	3.71E-03	1.39E-03
54-56	4.66E-04	5.74E-05	3.64E-03	1.34E-03
56-58	4.40E-04	4.13E-05	3.54E-03	1.30E-03
58-60	4.07E-04	2.13E-05	3.29E-03	1.18E-03
60-62	5.11E-04	4.97E-05	3.90E-03	1.45E-03
62-64	4.62E-04	4.83E-05	3.79E-03	1.40E-03
64-66	5.03E-04	4.28E-05	4.11E-03	1.44E-03
66-68	4.42E-04	4.05E-05	3.43E-03	1.22E-03
68-70	6.07E-04	1.24E-04	4.71E-03	1.58E-03
70-72	5.47E-04	1.04E-04	4.26E-03	1.43E-03
72-74	5.17E-04	7.85E-05	3.91E-03	1.32E-03
74-76	5.50E-04	1.03E-04	4.08E-03	1.36E-03
76-78	5.41E-04	9.73E-05	4.31E-03	1.39E-03
78-80	7.20E-04	7.74E-05	7.04E-03	2.35E-03
80-82	4.33E-04	3.64E-05	4.35E-03	1.43E-03
82-84	4.17E-04	2.45E-05	4.47E-03	1.39E-03
84-86	3.81E-04	1.04E-05	4.27E-03	1.29E-03
86-88	3.56E-04	2.14E-05	4.10E-03	1.22E-03
88-90	3.36E-04	3.00E-05	3.85E-03	1.15E-03

Table 6.1C - Experimentally determined input data for WHAM

Depth (cm)	Elemental concentration (moles/L)				
	Al	Pb	Cu	Zn	Fe
0-2	4.94E-03	5.57E-05	1.74E-05	7.66E-04	8.16E-03
2-4	9.31E-03	1.36E-04	3.54E-05	4.97E-04	7.72E-03
4-6	9.43E-03	1.79E-04	2.30E-05	4.70E-04	3.16E-03
6-8	1.30E-02	2.27E-04	2.13E-05	5.92E-04	2.84E-03
8-10	1.44E-02	1.41E-04	1.05E-05	5.70E-04	2.36E-03
10-12	1.32E-02	1.14E-04	1.84E-05	6.32E-04	2.23E-03
12-14	1.15E-02	8.82E-05	9.48E-06	5.55E-04	1.95E-03
14-16	6.92E-03	4.99E-05	6.16E-06	4.59E-04	1.49E-03
16-18	8.06E-03	7.96E-05	8.86E-06	4.96E-04	1.86E-03
18-20	7.60E-03	8.91E-05	8.73E-06	5.13E-04	1.76E-03
20-22	5.64E-03	9.02E-05	2.66E-06	4.41E-04	1.39E-03
22-24	5.79E-03	6.71E-05	1.01E-06	4.47E-04	1.51E-03
24-26	3.01E-03	1.73E-05	1.18E-06	4.88E-04	1.16E-03
26-28	3.09E-03	1.66E-05	1.04E-06	4.87E-04	1.16E-03
28-30	2.20E-03	9.04E-06	1.17E-06	4.29E-04	8.80E-04
30-32	2.02E-03	4.09E-06	8.72E-07	4.16E-04	8.23E-04
32-34	1.58E-03	2.76E-06	6.95E-07	3.38E-04	6.89E-04
34-36	1.30E-03	1.62E-06	6.27E-07	2.40E-04	5.61E-04
36-38	1.42E-03	2.31E-06	7.47E-07	3.16E-04	5.98E-04
38-40	1.74E-03	1.20E-06	8.77E-07	2.34E-04	6.30E-04
40-42	1.67E-03	2.02E-06	9.68E-07	2.88E-04	5.58E-04
42-44	1.36E-03	1.03E-06	6.68E-07	2.40E-04	4.58E-04
44-46	7.94E-04	5.10E-07	2.60E-07	1.89E-04	3.02E-04
46-48	7.32E-04	6.29E-07	8.14E-08	2.23E-04	2.77E-04
48-50	1.65E-03	9.21E-07	4.47E-07	2.96E-04	5.22E-04
50-52	1.54E-03	1.22E-06	6.58E-07	2.32E-04	4.78E-04
52-54	1.17E-03	8.13E-07	5.72E-07	2.31E-04	3.89E-04
54-56	9.78E-04	7.06E-07	4.35E-07	2.80E-04	3.32E-04
56-58	9.68E-04	5.75E-07	4.13E-07	2.41E-04	3.20E-04
58-60	9.14E-04	1.07E-06	6.13E-07	2.52E-04	2.87E-04
60-62	1.26E-03	9.20E-07	1.68E-06	2.80E-04	3.37E-04
62-64	1.23E-03	1.36E-06	1.16E-06	2.24E-04	3.13E-04
64-66	1.40E-03	1.34E-06	7.65E-07	1.56E-04	3.27E-04
66-68	1.18E-03	1.22E-06	7.08E-07	2.17E-04	2.67E-04
68-70	2.02E-03	1.88E-06	1.10E-06	2.23E-04	3.53E-04
70-72	2.02E-03	1.97E-06	1.06E-06	2.50E-04	3.16E-04
72-74	2.06E-03	2.11E-06	1.03E-06	1.97E-04	2.88E-04
74-76	2.41E-03	1.47E-06	9.81E-07	2.04E-04	3.07E-04
76-78	2.19E-03	1.19E-06	1.85E-06	1.91E-04	3.15E-04
78-80	2.79E-03	1.84E-06	1.49E-06	3.06E-04	5.07E-04
80-82	1.52E-03	9.14E-07	7.95E-07	2.16E-04	2.97E-04
82-84	1.15E-03	9.13E-07	8.75E-07	2.83E-04	2.87E-04
84-86	9.33E-04	7.72E-07	5.43E-07	2.05E-04	2.53E-04
86-88	7.93E-04	3.84E-07	3.82E-07	1.75E-04	2.39E-04
88-90	7.42E-04	5.25E-07	2.68E-07	1.26E-04	2.18E-04

The predicted porewater concentrations based on the inorganic components *per se* as well as the total aqueous (inorganic + fulvic) species were compared with the measured concentrations. The results are displayed using plots of p[M] vs depth (Figures 6.2-6.3), where [M] is the metal concentration and p[M] = -log[M]. In general, the use of the default model parameters resulted in the prediction of much higher porewater metal concentrations than were actually measured.

6.4.1 Na and K

For Na, (Figure 6.2A) the predicted inorganic and total concentrations at the surface of the peat are an order of magnitude higher than the actual concentrations observed in the porewaters, although the goodness of fit improves with increasing depth. By comparing the simulated inorganic and total profiles, it is clear that most of the Na in the simulated porewater was in an inorganic form. For K, (Figure 6.2B) due to K concentrations being lower than the reagent blank for most of the core, the goodness of fit could only be judged in the upper 3 sections. In a similar manner to Na, there was an order of magnitude difference between the measured and predicted concentrations, with the simulated profile predicting more K in solution than actually present. The K was also predicted to exist almost entirely in the inorganic form.

6.4.2 Ca and Mg

The Ca and Mg simulated profiles (Figures 6.2C and D) exhibit very similar shapes, which would suggest that the model predicted the binding behaviour of the two metals to be very similar. The differences between the simulated and measured concentrations are greatest in the near-surface sections (excluding the 0-6 cm sections), with fit improving down the core. As with the K and Na, almost all of the metal was predicted to be present as inorganic species.

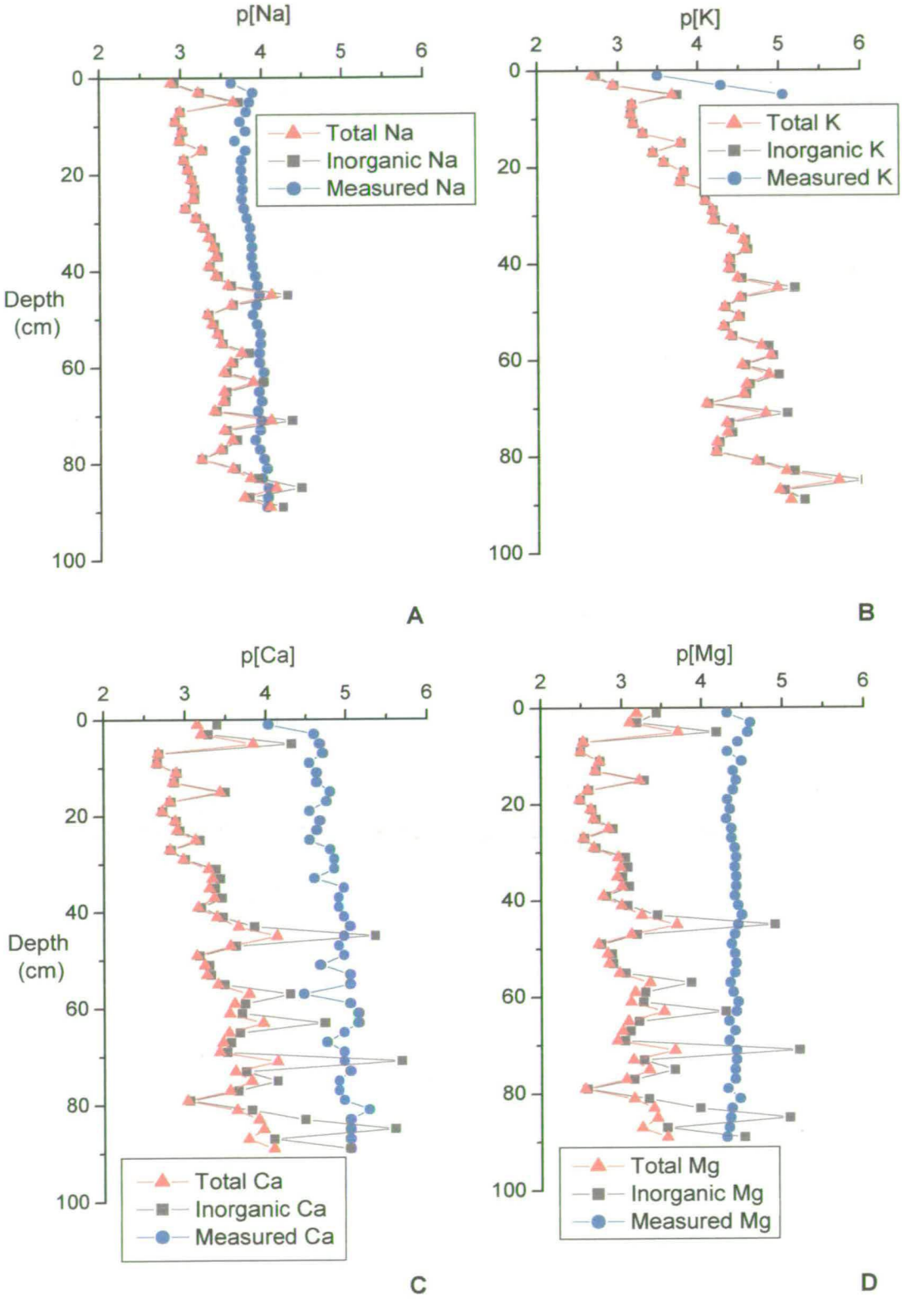

Figures 6.2 A- D – Predicted (inorganic and total aqueous) and measured concentrations for Na, K, Ca and Mg in Flanders Moss porewaters

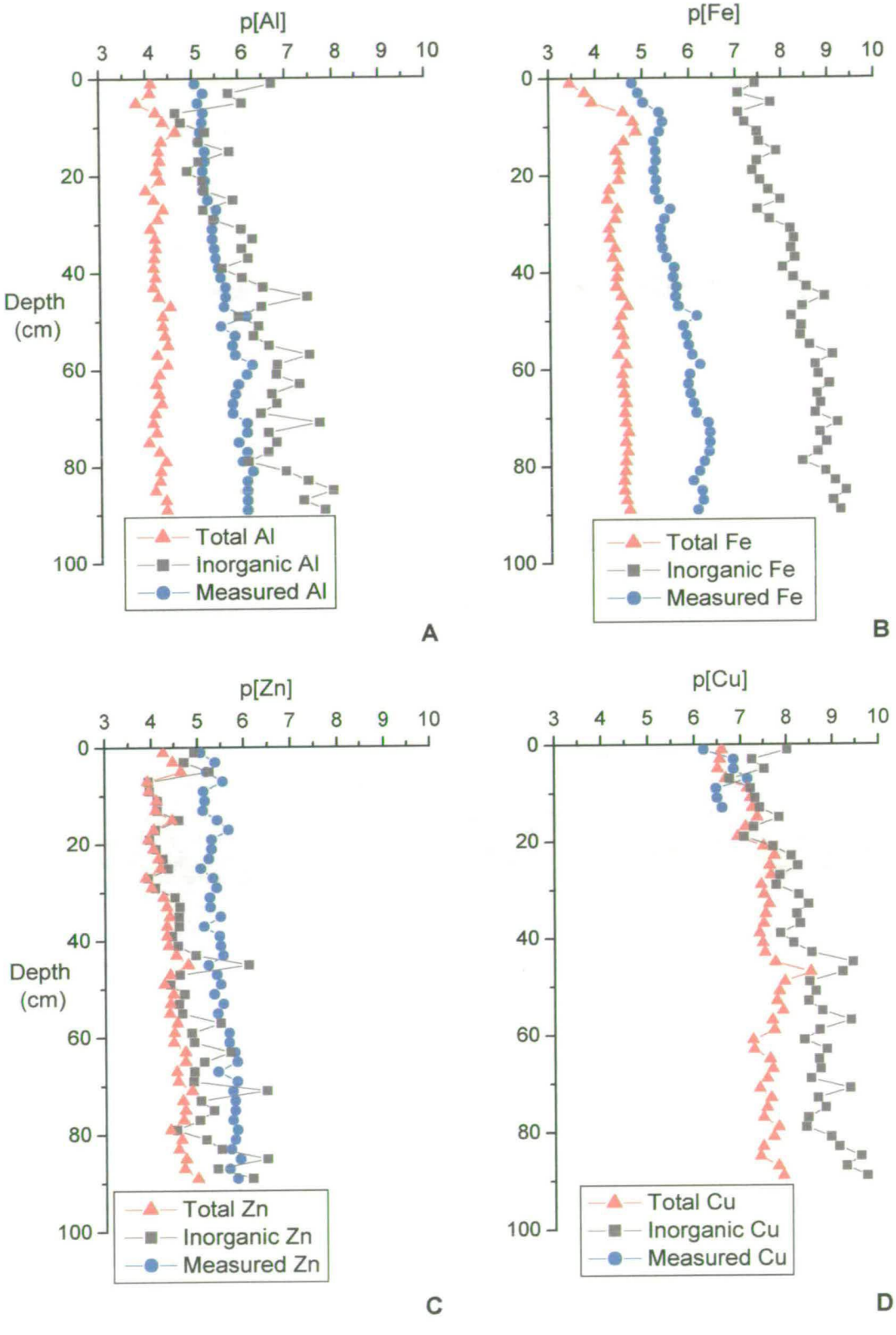

Figures 6.3 A- D – Predicted (inorganic and total aqueous) and measured concentrations for Al, Fe, Zn and Cu in Flanders Moss porewaters

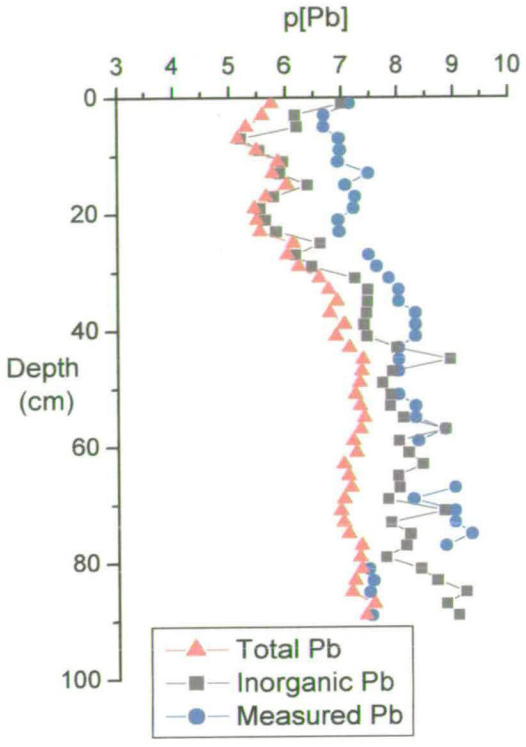

Figures 6.3 E – Predicted (inorganic and total aqueous) and measured concentrations for Pb in Flanders Moss porewaters

6.4.3 Al

The predicted concentrations based only on inorganic components were generally in closer agreement with the measured Al concentrations than were the total predicted concentrations (Figure 6.3A). By including Al bound to soluble FA, the total predicted concentrations were significantly greater than the measured concentrations. The shape of the profile for total predicted Al was, however, quite similar to that of the measured Al. Thus, it is proposed that FA complexation of Al in the porewater is important but that some adjustment of model parameters would be required to obtain a better fit of the measured data.

6.4.4 Fe

The predicted porewater concentrations of Fe based only on inorganic species are several orders of magnitude lower than the measured concentrations (Figure 6.3B). Comparison of total predicted with measured concentrations shows that the inclusion in the model of Fe bound to soluble FA gives an improved fit of the measured data. Nevertheless, the predicted total concentrations of Fe are, as for Al, higher than those measured.

6.4.5 Zn

The predicted concentrations of inorganic forms of Zn in the porewaters showed large fluctuations, particularly below 50 cm (Figure 6.3C). In contrast, the profile for total Zn species was much more similar in shape to that for measured Zn. Although the predicted total and inorganic concentrations were quite similar in the upper sections, below 50 cm, the total values were greater than the inorganic values. This suggested a greater importance of FA-Zn binding at depth in the peat bog. Overall, however, as for Al and Fe, the predicted total concentrations were about one order of magnitude greater than those measured.

6.4.6 Cu

Measurable Cu concentrations were only obtained for the porewaters from the 0-14 cm sections. Solid phase Cu concentrations were obtained for all 2-cm depth sections and so the model was used to predict Cu concentrations in the porewaters from all depths. There was some agreement between the total predicted and measured Cu concentrations for the near-surface sections but limited interpretation can be made on the basis of the small number of data points for measured porewater Cu (Figure 6.3D). From the model results, however, there was a significant difference between predicted inorganic Cu and total Cu concentrations. The model predicts generally greater Cu concentrations in the porewaters when soluble Cu-FA complexes are included.

6.4.7 Pb

The predicted inorganic concentrations of Pb for the upper sections were significantly greater than those measured whilst below ~ 40 cm the predicted and measured values were quite similar (Figure 6.3E). Although, the shape of the total predicted concentration profile was much more similar to that of measured Pb, the model again overestimated the porewater concentrations by about an order of magnitude.

6.4.8 DOC

For Pb and several other metals (Cu, Zn and Al), the inclusion of soluble metal-FA complexes resulted in an overestimation of porewater concentrations mainly in the lower sections (> 50 cm) of the peat core. An immediate concern was that the model was predicting higher concentrations of DOC than had been measured at these depths. Predicted DOC values (in mg/L) were obtained by multiplying the concentrations of soluble FA (in g/L) by 1000 and then by 0.5 (assuming that FA molecules comprised 50% carbon). The predicted and measured DOC profiles are compared in Figure 6.4A and the ratio of predicted to measured DOC is shown in Figure 6.4B. The scattering of the predicted DOC values for the lower sections (>50 cm) is attributable to the variability in measured FA for these sections.

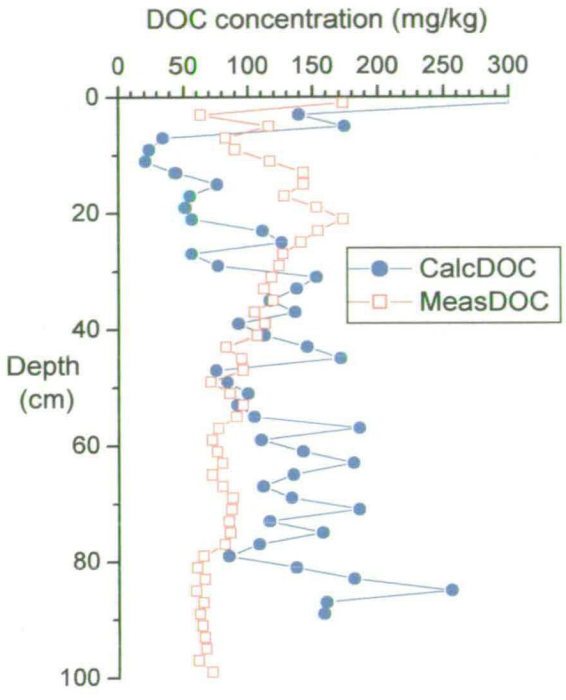

Figure 6.4 – Comparison of model simulated porewater DOC and measured porewater DOC

This variability may have been caused by sample heterogeneity because, in order to avoid problems associated with resuspending dried peat samples, wet peat samples were used. It was therefore not possible to fully homogenise the peat within each section and so some variability in the composition of the sub-sample taken from each section may have been encountered. This apart, Figures 6.4A-B show that good agreement was obtained for the 0-6 cm sections and also for the 60-80 cm sections. For the 6-40 cm sections, the model vastly underestimates the DOC concentration whilst below 80 cm, the model begins to slightly overestimate the DOC concentration. In fact, the predicted profile bears a greater similarity in shape to the measured solid phase FA profile than to the measured DOC profile. Moreover, it should be noted that the measured DOC profile bears a greater resemblance to the measured solid phase total IHSS HA+FA profile than to the measured solid phase FA profile. This is an important point for future work but, for the predicted metal (Pb, Cu, Zn and Al) partitioning between the porewater and solid phase described above, an overestimation of DOC concentrations can't be used to explain the overestimation of total predicted porewater concentrations in the lower sections of the peat core.

6.4.9 Further information about metal speciation obtained using WHAM

More detailed information on predicted metal speciation in the peat bog was obtained using the WHAM model. The model output includes four types of metal association with humic materials:

(i) diffusely bound to humic acids (M-dHA)

(ii) specifically bound to functional groups on humic acids (M-HA)

(iii) diffusely bound to fulvic acids (M-dFA)

(iv) specifically bound to functional groups on fulvic acids (M-FA).

The output values for the association of each metal with these four fractions were divided by the total solid phase concentration and converted to percentage associations with dHA, HA, dFA and FA. The percentage of each metal in dissolved inorganic forms was obtained using the difference between Σ(M-dHA, M-HA, M-dFA, M-FA) and the total solid phase concentration.

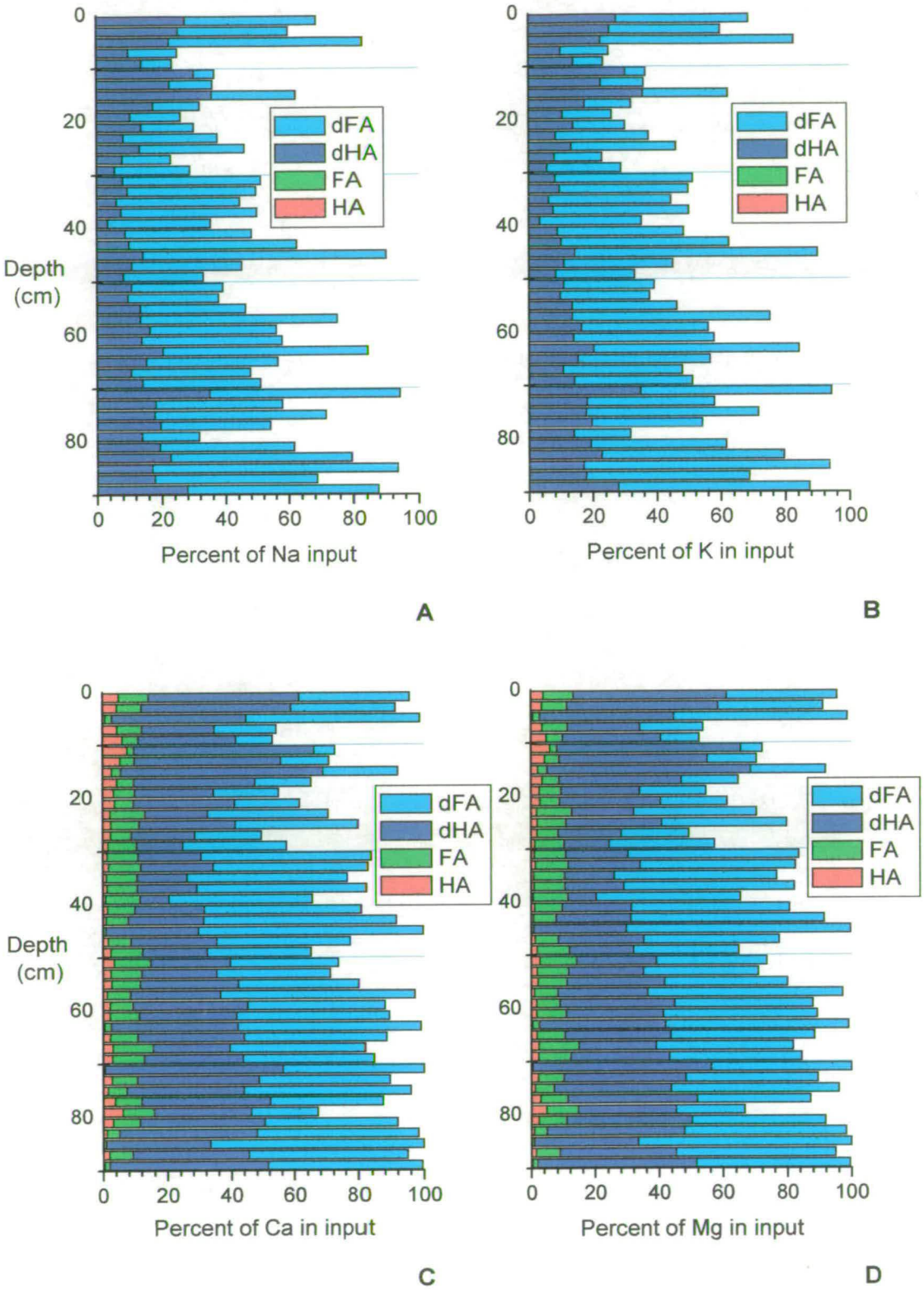

Figures 6.5A-D – Percentage of the input concentrations of Na, K, Ca and Mg bound to the HA and FA components

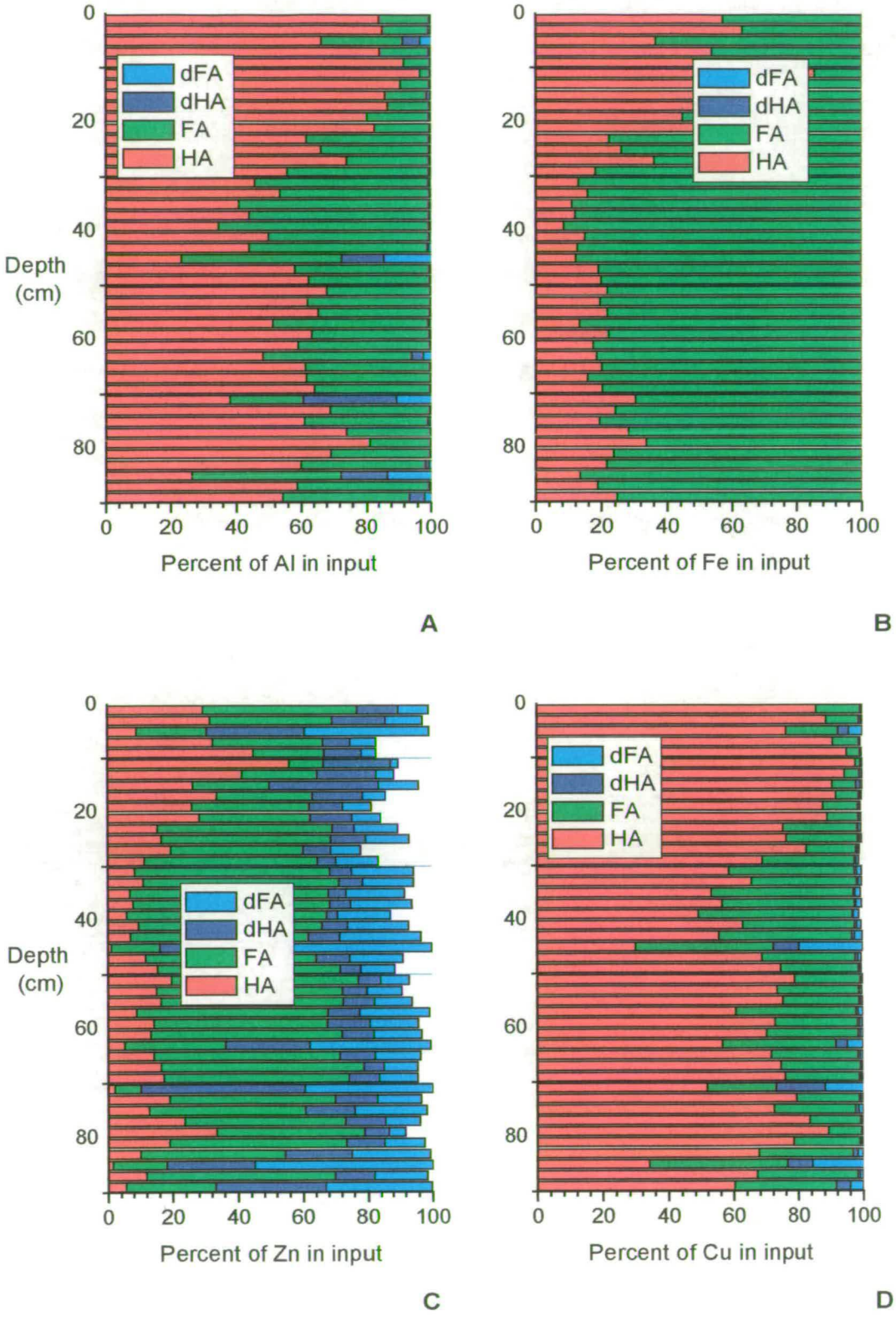

Figures 6.6 A- D – Percentage of the input concentrations of Al, Fe, Zn and Cu bound to the HA and FA components

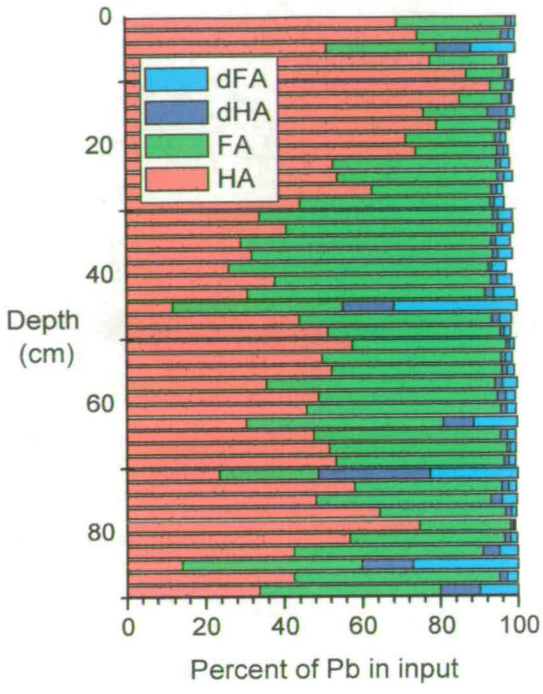

Figure 6.6E – Percentage of the input concentration of Pb bound to the HA and FA components

It should be recalled that, within the model, M-dHA and M-HA represent metal associations with solid phase humic materials but M-dFA and M-FA represent metal associations with humic materials that are partitioned between the solid and aqueous phase. Figures 6.5-6.6 show the vertical variations in the predicted percentage associations of each metal.

As might be expected from well-known properties of Na and K, both had very large dissolved inorganic components (up to ~80%) and the remainder at all depths was mainly diffusely bound to HA and FA (Figures 6.5A and B). Ca and Mg both had large dissolved inorganic components, which were generally greatest in the 6-30 cm sections (up to ~40%: Figures 6.5C and D). In contrast to Na and K, the model predicted some specific associations as well as diffuse layer associations with HA and FA for both Ca and Mg. Higher concentrations in the diffuse layer than in specifically associated forms were predicted. It would be expected that the major cations would be important counterions in the diffuse layer surrounding humic and fulvic acid molecules.

The model predicted that Al would mainly be specifically bound to HA and FA molecules and that the dissolved inorganic component of total Al would be very small (Figure 6.6A). Generally between 60-90% was specifically bound to HA. The shape of the Al-HA profile suggested that the concentration of HA entered into the model was an important factor controlling the output speciation. The model predictions for Fe were quite similar to those for Al in that most was specifically bound to HA and FA (Figure 6.6B). Although ~60% was specifically bound to HA in the upper sections, values were typically ~20% for sections below 40 cm. Overall, the results for Al and Fe suggest that both would potentially compete with Pb for specific binding sites on HA and FA.

The predicted speciation of Zn was quite different from those for Al and Fe (Figure 6.6C). There was a small proportion (up to 20%) of dissolved inorganic forms of Zn, mainly between 6-30 cm. Although there was some Zn specifically associated with HA, more was specifically associated with FA (~40-60%).

In comparison with the specifically associated values for both HA and FA, smaller amounts of Zn were predicted for the respective diffuse layers. The speciation of Cu was most similar to that predicted for Al in that the greatest proportion was specifically associated with HA (Figure 6.6D). The speciation of Pb was again very similar to that for Al thus predicting the importance of solid phase humic materials for Pb binding (Figure 6.6E).

From the results in chapter 4, Ti and Pb would be expected to exhibit the strongest binding to organic matter. In contrast, very little of the Na and K was expected to be associated with the organic matter on the basis of the distribution co-efficients. Metal cations with intermediate binding to FA2 and HA (relative to the proportion released in FA1) include Mg, Sr as well as Al and Fe, with the latter also being involved in formation of hydroxyoxides.

6.4.10 Expression of model output as percentage of metals bound to the solid phase peat

A different way of expressing the output of the model is from the perspective of the percentage of total metal associated with the solid phase. The predicted total porewater metal concentrations were converted to percentages of total metal bound to the solid phase and the vertical variations are displayed in Figures 6.7 and 6.8. Very good agreement is obtained for the upper sections (0-20 cm) where, for Al, Fe and Pb, both the predicted and the measured percentages are greater than 96% of the total metal. This is consistent with the high affinity of these metals for solid phase organic matter.

6.4.11 Reasons for the poor fit of the measured porewater data by the WHAM model

The re-expression of the model results described in section 6.4.10 clearly illustrated that the fraction of total metal predicted to be present in the porewaters is extremely small (in the 0-20 cm sections, often <2% for Al, Fe and Pb).

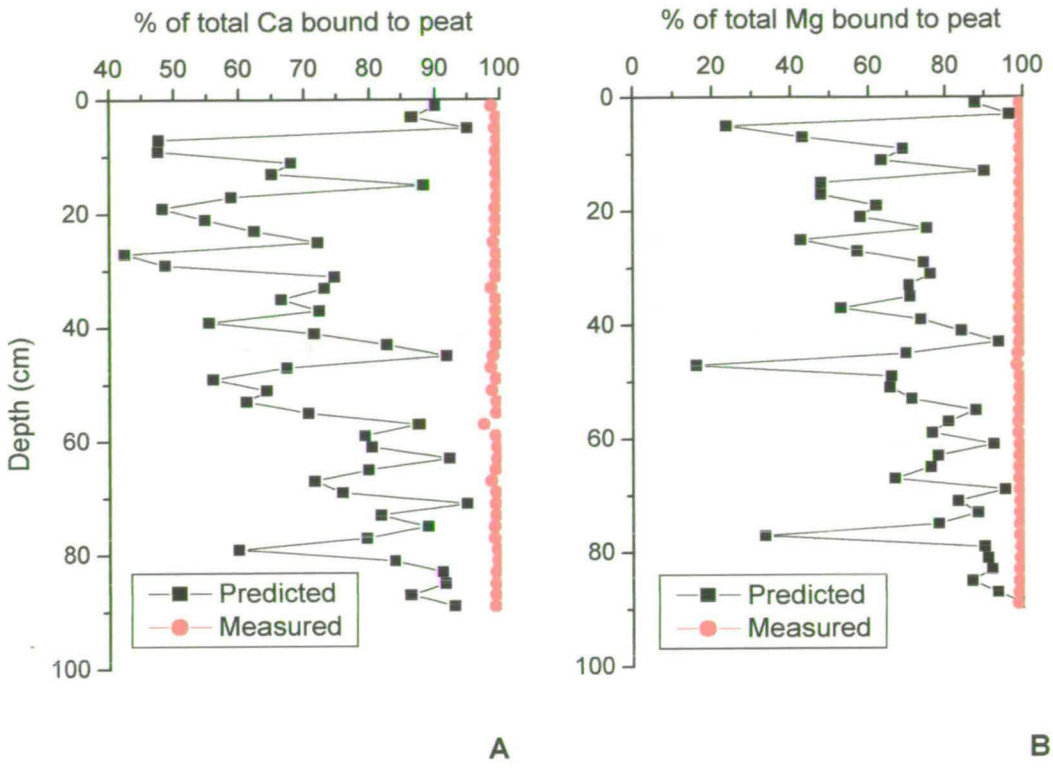

Figures 6.7A-B – Predicted and measured percentages of total Ca and Mg concentrations bound to Flanders Moss peat

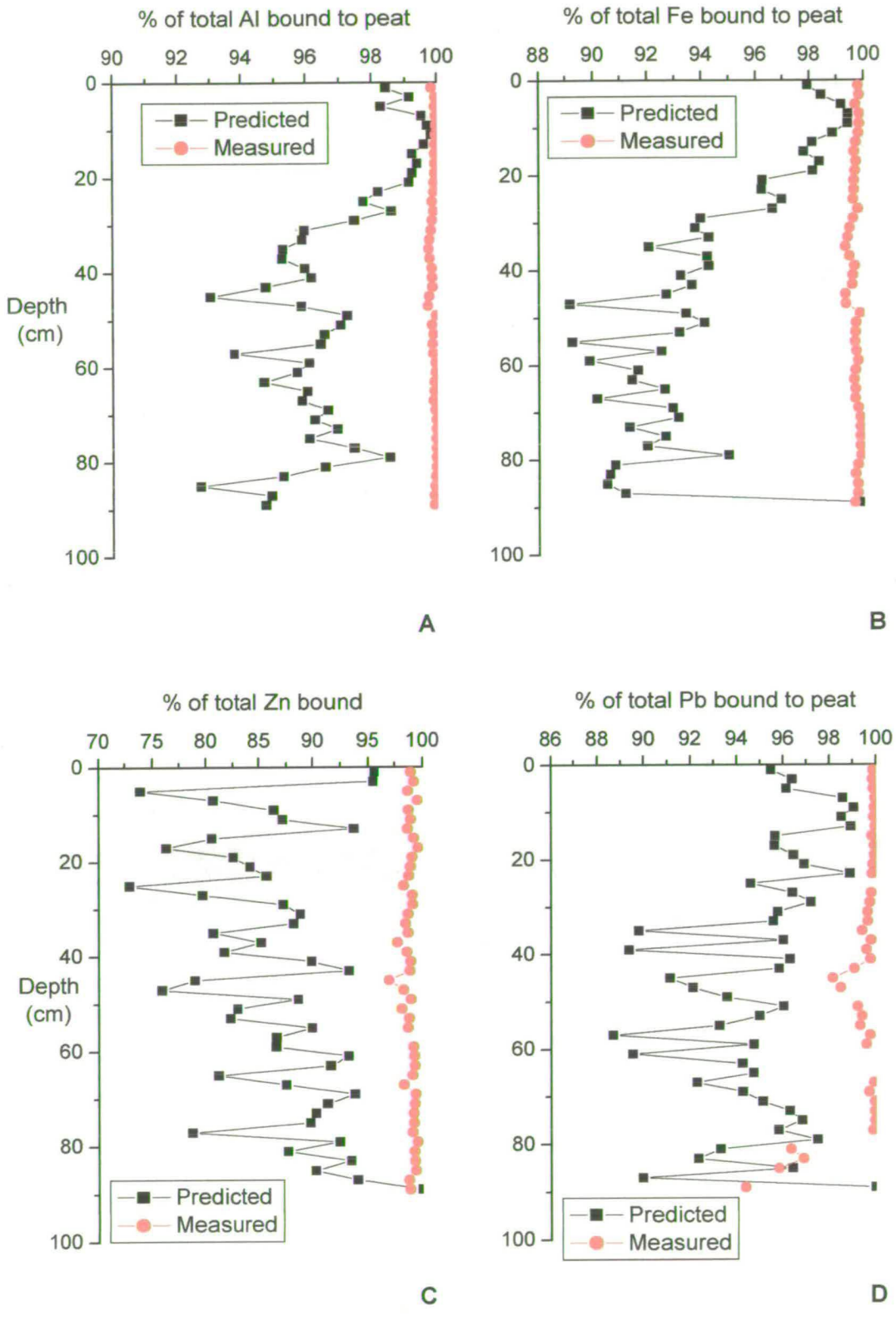

Figures 6.8A-D – Predicted and measured percentages of total Al, Fe, Zn and Pb concentrations bound to Flanders Moss peat

Although predicted total porewater concentrations were often an order of magnitude greater than those measured in the porewaters, it should be taken into account that even a slight error in the predicted binding of the solid phase would result in substantial errors in the simulated porewaters. The predicted associations of metal cations would have a marked effect on the predicted aqueous phase (inorganic and total) concentrations and thus result in substantial differences between predicted and measured values.

Further model calculations were undertaken to investigate the sensitivity of Pb binding to changes in parameter inputs.

6.5 INVESTIGATIONS OF THE SENSITIVITY OF THE WHAM MODEL OUTPUTS FOR PB TO CHANGES IN PH, REACTIVE SITE (HA) CONCENTRATION AND BINDING STRENGTH (K VALUES)

The WHAM model contains a number of adjustable parameters enabling the model to take account of factors that are likely to control metal speciation in the natural environment. These include pH, the number of reactive sites (HA concentration) and metal binding strength (K values). The sensitivity of the model output to changes in the value used for each of these three parameters was investigated. The results are presented in sections 6.5.1-6.5.3 below.

6.5.1 The effect of changing pH

Changing the value of pH entered into WHAM-W will have the effect of increasing the negative charge on HA and FA. This will result in an increased concentration of cations in the Donnan layers (M-dHA and M-dFA) and also an increased concentration of FA (and associated Pb) in the aqueous phase. On the basis that measured pH values ranged from ~3.6 to ~ 4.2, three values, 3.5, 4 and 4.5 were selected.

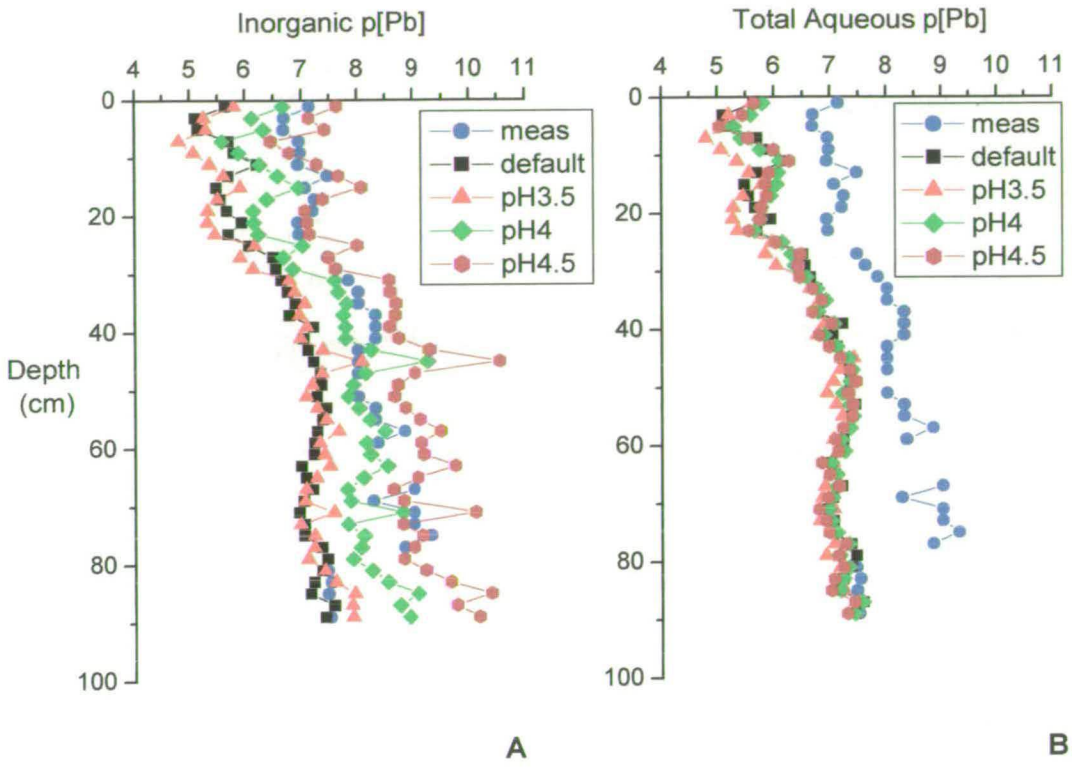

Figures 6.9 A-B – Predicted (A-inorganic; B- total aqueous) vs measured concentrations for Pb : default parameters and varying pH parameter

The three new sets of model results were compared with the original set (measured pH values for each section were used) (Figures 6.9A and B). Increasing the pH had the effect of decreasing the predicted concentration of inorganic forms of Pb in solution (Figure 6.9A).

The best fit of the measured data for the 0-30 cm sections was obtained using a pH value of 4.5. This, however, was generally much higher than the measured values, which for the 10-30 cm sections, were in the range 3.6-3.8.

The best fit of the measured porewater Pb data for the 30-70 cm sections was obtained using a pH value of 4. This was close to the measured pH values which were in the range 3.8-4.0.

Comparison of predicted total porewater concentrations of Pb with the measured values showed that the overall effect of changing pH from 3.5 to 4.5 was very small (Figure 6.9B). This can be explained by considering that the speciation of Pb in the porewaters was dominated by binding to FA and not inorganic species. Thus, the predicted values remained almost an order of magnitude greater than the measured concentrations. It should be noted, however, that increasing the pH did result in a slight decrease in total porewater concentrations of Pb (particularly in the 0-20 cm sections). This was attributable to a small decrease in FA solubility due to increased in metal binding to FA at the higher pH values.

6.5.2 Effects of changing the humic acid concentration

The humic acid content of the peat obtained using the IHSS method was low in comparison to previous reported proportions of humic acid in peat and organic soils (Hayes, 1988; etc). In a recent study to determine the humic and fulvic acid concentrations for input to the model, Lofts *et al.* (2001) used a repeated extraction scheme based on the IHSS methodology. Given that an exhaustive extraction of organic matter was not implemented in quantifying the HA component, it seemed reasonable to investigate the effect of increasing the HA content entered into the model on the Pb binding of the peat.

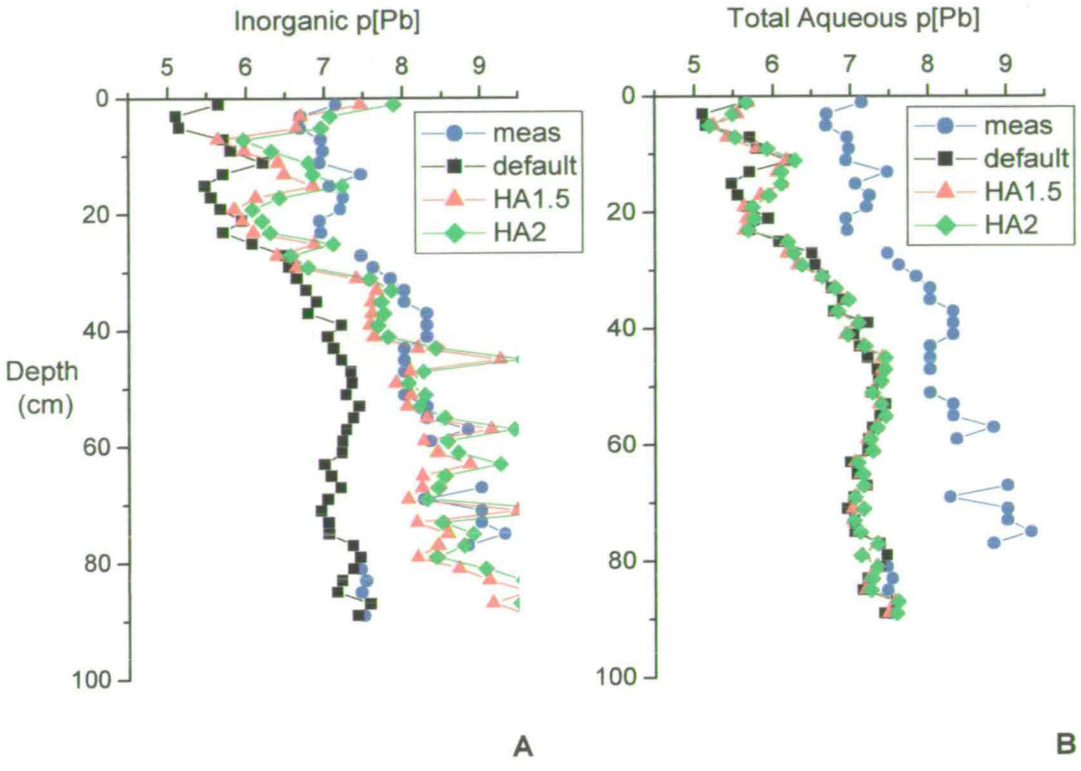

Figures 6.10A-B– Predicted (A-inorganic; B-total aqueous) vs measured concentrations for Pb : default parameters and varying HA parameter

By increasing the HA concentration, the number of solid phase surface sites available for metal binding should increase, lowering the metal concentrations in solution.

The results of increasing the HA concentration by each of a factor of 1.5 and a factor of 2 are presented in Figures 6.10A and B. The predicted concentrations of inorganic forms of Pb were markedly affected by the changes in HA concentration (Figure 6.10A). The predicted values decreased and for, both 1.5 and 2 times the original concentration, the predicted and measured were in good agreement over most of the profile. The poorest agreement was obtained for the 6-30 cm sections.

The generally good agreement described in the preceding paragraph is perhaps misleading because consideration only of inorganic forms of Pb ignores the probable association of Pb with DOC which was present in all porewater samples. The effect of increasing the number of reactive sites on predicted total aqueous concentrations of Pb was neglible (Figure 6.10B). This would suggest that even with the reduced number of sites available for cation binding using the experimentally determined concentrations in the original default run, the number of sites was not limiting the binding of Pb to the solid phase.

6.5.3 Effect of varying the default K (stability constant) value

In previous applications of the WHAM model (Christensen *et al*, 1999), it has been shown that, under certain conditions, use of a default stability constant for metal-humic binding resulted in a model ouput, which was a poor fit of the measured data. After optimisation of the value of the stability constant, a better fit of the data was obtained. By increasing the K values, an increase in the affinity of Pb for functional groups on HA and FA is caused. This should increase the fraction of Pb bound to the solid phase peat thereby decreasing the amount of Pb in the porewaters. For the purposes of this study, the effects of increasing the K value by a factor of 2 and by a factor of 10 were investigated.

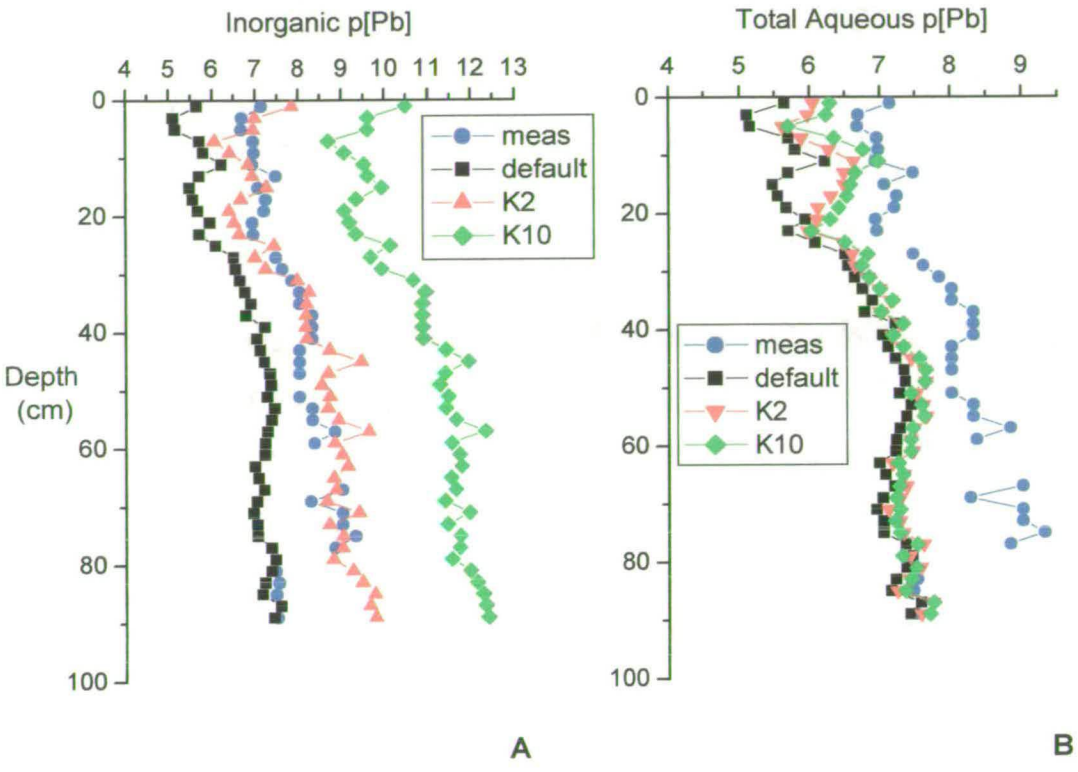

Figures 6.11 A-B – Predicted (A-inorganic; B-and total aqueous) vs measured concentrations for Pb : default parameters and varying Pb K value

Figures 6.11A-B show the results of the calculations based on alteration of the K value for Pb. Remarkably good agreement between the predicted inorganic and measured Pb concentrations were obtained when the K value was increased by a factor of 2 (Figure 6.11A). Clearly, the alteration of K by a factor of 10, an unrealistic increase, resulted in a vast underestimate of the porewater concentrations of Pb.

Comparison of predicted total with measured Pb values, however, again showed that the model continued to overestimate the porewater concentrations (Figure 6.11B) although increasing K (by a factor of 2 or 10) did decrease the predicted concentrations in the uppermost 0-20 cm sections.

Of the three parameters, Pb partitioning between the solid phase peat and the porewaters was clearly most sensitive to the value of the stability constants entered into the model.

6.6 FURTHER ADJUSTMENTS OF PARAMETERS IN THE WHAM MODEL

From the results displayed above, it has been shown that given experimentally determined solid phase concentration data as an input, the model can provide a useful insight into the binding of cations to the solid phase peat although there are difficulties associated in using the model to predict the exact concentrations of these cations in the aqueous phase.

In the peat system, it is suggested that some of these difficulties arise from the poor prediction of DOC. The effect on the output of using the measured DOC values to derive soluble FA concentrations should be considered. The values of the Pb binding constant also warrants further investigation. Doubling the K value for Pb resulted in an improved agreement between predicted porewater concentrations of inorganic Pb species and the measured values.

It is also likely that experimental determination of the specific binding constants of Pb and other cations to the Flanders Moss peat would further improve the agreement between the model output and the measured data. Moreover, the sensitivity of the model output, to a decrease in the binding strength of Pb to FA should also be investigated. It is proposed that this may have a greater effect on predicted total porewater concentrations of Pb.

A further area warranting investigation is the change in characteristics of the humic and fulvic components within the peat with increasing depth. This could be assessed by experimental characterisation of fulvic and humic extracts, both in terms of changes in the concentration of binding sites with depth, and also varying the gamma factor to adjust the relative hydrophobicity/hydrophillicity of the aqueous FA component. It is proposed that these further investigations could be used to improve the model predictions for Flanders Moss peat.

6.7 USE OF THE WHAM MODEL TO PREDICT PB MOBILITY UNDER DIFFERENT ENVIRONMENTAL CONDITIONS

Having shown that WHAM-W works in describing the binding of cations to the solid phase peat, WHAM can then be used to make predictions about the potential mobility of lead in the peat with changing conditions. As discussed in section 6.51, the pH has been shown to have a strong effect on the binding of Pb to organic matter, with lower pH's generally resulting in increased solution concentrations of Pb, which can then be exported from the peat bog in throughflowing surface waters. With increasing levels of acidity being deposited on the peat, there is the possibility that decreasing the pH could result in release of toxic heavy metal cations from the peat into watercourses. One way of predicting the mobility of these elements with changing conditions is through the use of computer models such as WHAM.

For a range of pH values, Pb binding to the peat was investigated using data from one depth increment, which was picked as being representative of the peat core as a whole, but also had sufficiently high lead concentrations to allow meaningful modelling.

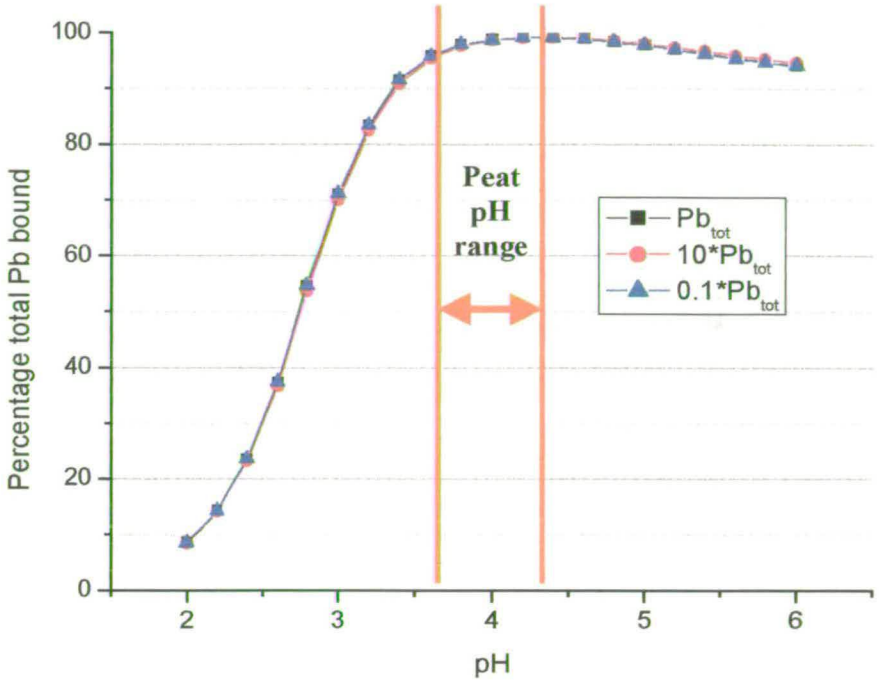

Figures 6.12 – Model prediction of Pb mobility with changing pH

The selected data was rerun through WHAM a number of times, with each run using a different pH input. The remaining parameters were left unchanged, although a small concentration of nitrate anions had to be introduced to allow mass balance on the model at pH's less than 3.4, where the organic material becomes positively charged, and can no longer be used as an anion in the charge balancing. The results were used to create the graph displayed in Figure 6.12. This figure clearly shows that the optimum pH for the binding of Pb to the solid phase peat is achieved between pH's 3.5 and 5. All of the measured porewater pH's in the core are in this zone. This shows that 99.9% of the Pb present in the peat will be bound to the solid phase, and Pb received by the peat from atmospheric deposition can be viewed as immobile within the peat. The graph also shows that the bound Pb is relatively insensitive to minor changes in the pH, and that a major change in the pH is required before Pb will become significantly mobile.

A further investigation involved increasing and decreasing the concentration of Pb in the input parameter to assess the effect of more metal in the system to the binding. With the Pb in the system increased and decreased by a factor of 10 relative to the original input value, the amount of Pb bound was altered very little (Figure 6.12). This agrees with the earlier finding that the predicted Pb profile changes little in response to increased HA concentrations.

6.8 CONCLUSIONS

Using the WHAM model to provide further insight into the speciation and mobility of metals within Flanders Moss peat has proved useful. The model was able to describe the binding of metals to the solid phase peat very well, without optimisation of the default parameters. Given the large number of calculations involved, only the sensitivity of model output to changes in certain parameters could be investigated. Increasing the value of K for Pb did improve the model predictions of total porewater Pb concentrations to a certain extent. From the modelling results, the proposed next step would be to decrease the amount of Pb associated with soluble FA. Finally, an important problem revealed by this work was also the poor prediction of porewater DOC concentrations by the WHAM model.

The selected data was rerun through WHAM a number of times, with each run using a different pH input. The remaining parameters were left unchanged, although a small concentration of nitrate anions had to be introduced to allow mass balance on the model at pH's less than 3.4, where the organic material becomes positively charged, and can no longer be used as an anion in the charge balancing. The results were used to create the graph displayed in Figure 6.12. This figure clearly shows that the optimum pH for the binding of lead to the solid phase peat is achieved between pH's 3.5 and 5. All of the measured porewater pH's in the core are in this zone. This shows that 99.9% of the lead present in the peat will be bound to the solid phase, and Pb received by the peat from atmospheric deposition can be viewed as immobile within the peat. The graph also shows that the bound lead is relatively insensitive to minor changes in the pH, and that a major change in the pH is required before lead will become significantly mobile.

A further investigation involved increasing and decreasing the concentration of Pb in the input parameter to assess the effect of more metal in the system to the binding. With the Pb in the system increased and decreased by a factor of 10 relative to the original input value, the amount of Pb bound was altered very little (Figure 6.12). This agrees with the earlier finding that the predicted Pb profile changing little in response to increased HA concentrations.

6.8 Conclusions

Using the WHAM model to provide further insight into the speciation and mobility of metals within Flanders Moss peat has proved useful. The model was able to describe the binding of metals to the solid phase peat very well, without optimisation of the default parameters. Given the large number of calculations involved, only the sensitivity of model output to changes in certain parameters could be investigated. Increasing the value of K for Pb did improve the model predictions of total porewater Pb concentrations to a certain extent. From the modelling results, the proposed next step would be to decrease the amount of Pb associated with soluble FA. Finally, an important problem revealed by this work was also the poor prediction of porewater DOC concentrations by the WHAM model.

The model slightly overpredicts the concentrations at pH~4 and clearly underpredicts the concentrations at lower pH values (~3.6-3.8). It is important for future modelling of metal partitioning and speciation in peat bogs that a better prediction of porewater DOC is obtained.

Chapter 7 – Conclusions

The objectives for Chapter 3 were to:

(i) determine the distribution of Pb between the porewaters and the solid phase of Flanders Moss ombrotrophic peat bog

(ii) elucidate the processes (e.g. redox cycling, nutrient uptake, mineral dissolution etc.) occurring in the peat bog by including selected other elements which had contrasting chemical behaviour and contrasting mobility within peat bogs

(iii) establish the extent to which the vertical distribution of Pb in the peat bog was affected by the processes in (ii)

In order to provide the context for this study of Pb mobility, various solid phase and porewater parameters were determined. From this it was shown that the peat typically had a low ash content (< 2%) except in the near-surface sections where the peak concentration was ~11%. The peak was, however, attributable to recent atmospheric inputs of anthropogenic particulates and so overall, the results were consistent with those expected for an ombrotrophic peat bog. Confirmatory evidence was provided by the Ca/Mg ratio (both for solid phase and porewater) which decreased with increasing depth. An increase in Ca relative to Mg would have indicated the influx of mineral-rich groundwaters, suggesting that the bog would instead have been minerotrophic.

An important use of the changes in density of the peat with increasing depth was to characterise different zones of the peat. The main distinctions were (i) the 0-6 cm – dominated by vegetation, (ii) at 6 cm - marked transition from the vegetation zone to cohesive peaty material, (iii) 6-20 cm –highest density of peat, (iv) 30-50 cm – low density peat – a less humified zone, and (v) 50-100 cm – small variations in density indicating differing extents of humification.

Characterisation of the porewater samples revealed an inverse relationship between pH and DOC with the maximum DOC concentration at ~20 cm occurring at pH 3.6. This is contrary to the relationship used in certain geochemical models. The relationship between DOC concentration and UV absorbance indicated that there were changes in the nature of the DOC with increasing depth. Small molecules with few chromophores (absorb UV) were found in the vegetation zone whilst maximum functionality was predicted at the position of the DOC maximum. Below this, a more rapid decrease in UV absorbance compared with DOC concentration indicated diagenetic alteration of the organic material. This is again highly relevant for modelling studies as a change in functionality with depth has implications for the metal binding characteristics of the DOC.

Using the results of characterisation in conjunction with the data for the vertical distribution of elements in the peat and porewaters, major processes occurring in the peat were identified.

Sharp concentration peaks in the peat and in the porewater were observed for several alkali and alkaline earth elements as well as for Mn and Fe. Nutrient uptake in the uppermost sections (0-6 cm) was proposed as the process influencing the solid phase and porewater profiles of Na, K, Mg, Ca and perhaps Mn and Fe – the redox behaviour of this second group does not appear to control the vertical distribution of Fe and Mn in this zone.

Comparing the 10-20 cm zone with the remainder of the profile, there were elevated concentrations of some of the more soluble elements (Na, Mg, Sr + perhaps Zn) in the porewaters relative to the solid phase. The peaks in the porewater concentrations of these elements at this depth also correlated with the conductivity maximum. The greatest contribution to conductivity would of course be from the major cations, e.g. Na.

More conservative elements were included in this study for several reasons. It was important to have lower solubility elements to compare with Pb solubility. The inclusion of Al and Ti was also beneficial because of the use made of these elements in other studies, namely to quantify soil dust inputs into the peat bog. Although the Al/Ti ratio was constant over much of the profile, the absence of an Al peak resulted in a significant change in the Al/Ti ratio at 40 cm. This has implications for the use of these elements as indicators of soil inputs, i.e. where a constant ratio is assumed on the basis that both elements are always from the same source. The data also indicated changes in the solubilities of Al and Ti with depth. Maximum release into the porewaters at 30-40 cm coincided with the zone of low density peat. It is suggested that both changes in Al/Ti ratios and in elemental solubilities would need to be rationalised before adopting data normalisation procedures.

The distribution coefficient for Pb (mg/L / mg/kg) was small ($\sim 10^{-4}$) and almost constant over the top 0-30 cm. The former indicates the strong partitioning onto the solid phase whilst the latter indicated that a simple equilibrium between the solid and aqueous phase was controlling the shape of the porewater profile. Most importantly, none of the processes which influence the shapes of the elemental profiles appeared to influence the solid phase Pb profile. The results strongly support the post-depositional immobility of Pb in the peat.

The objectives for Chapter 4 were focused on the associations of Pb within the peat. In particular, characterisation of any changes in association with depth, which might give rise to vertical mobility, was important. The main reason for carrying out this aspect of the work was because the second Pb peak, present in both the porewater and the solid phase coincided with the porewater DOC, S and Fe peaks. Alteration of the solid phase profile was still a possibility.

A further important objective was to determine the concentrations of FA and HA in each of the 2-cm depth sections of the peat core. These were required as input parameters to the geochemical model, WHAM, which was to be used in the later parts of the study to investigate Pb-humic binding.

The results from Chapter 4 highlighted the release of elements upon the addition of 0.1M HCl. The exact mechanism for release was unclear, but dissolution of mineral material by the FA1 extractant was proposed to account for the relatively high proportion of Al in the fraction, whereas for Mg, Ca, and K, release from exchange sites on the organic matter was thought to predominate. Other elements, such as Ti exhibited very strong associations with the humic acid fraction.

The high proportion of solid phase Fe in the FA1 extraction in the 0-6 cm zone provided further evidence for the role of plant uptake in the cycling of this metal in the near surface sections, and reflected the likely association of Fe with root exudate material. This was in contrast to Mn, which displayed low extractability in the upper section, and was attributed to the Mn existing within the plant material itself.

Finally, the lower peak of Pb detected in the solid phase was not present in any of the organic extract fractions, indicating that with increasing depth, the Pb was in a less extractable form. This provided further support for the immobility of Pb in peat. Further work to fully quantify any movement of Pb within the peat using lead isotopes was needed, and this was carried out in Chapter 5.

Following on from the work presented in Chapters 3 and 4, stable lead isotope ratios were determined in order to:

(i) elucidate changes in the solid phase $^{206}Pb/^{207}Pb$ ratio with increasing depth;

(ii) compare the porewater ratio values with those obtained in (i);

(iii) evaluate the importance of Pb associations within the peat bog on the $^{206}Pb/^{207}Pb$ ratios for the upper 0-20 cm of the peat (below this depth, Pb concentrations were too low)

(iv) establish whether a historical record of Pb deposition could be constructed – this would be a valid approach only if Pb was vertically immobile

The good agreement between the peat and porewater lead isotope ratios was a first indication that the conclusions reached at the end of Chapter 3 were indeed justifiable.

Little or no vertical mobility could be substantiated since the change in ratio from 1.136 to 1.161 for the solid phase peat (0-6 cm) was mirrored almost exactly by the change in the porewaters (0-6 cm). Moreover, this trend was also found for HA and FA extracts from the peat, indicating that the timescale for Pb binding to the solid phase is much smaller than downwards diffusion through the peat.

Having established that Pb was immobile within the peat bog, a historical record was constructed using ^{210}Pb to date the peat core. Calculation of an integrated inventory for Pb showed that 47.4 % was deposited after 1895. Although the dates obtained for deeper sections of the peat (> 10 cm) were less certain, this study found that, in agreement with results for Loch Lomond (southern basin), significant deposition of Pb was occurring by the middle of the 19th Century. The integrated inventories and fluxes of Pb to the peat bog agreed well with those previously obtained for Flanders Moss. Finally, the source apportionment calculations for the 0-2 cm and 2-4 cm sections enabled changes in recent decades in the contribution of petrol Pb to total Pb deposited to be more clearly established. The calculated data suggested that the effect of increased usage of unleaded petrol had resulted in a decrease in the petrol Pb component for the nearest surface section of the peat bog.

The final component of this work involved the use of the geochemical model WHAM to compare results obtained in this study for Pb partitioning between the solid phase of the peat and porewaters with the predicted partitioning from the output of the model.

The model was able to describe the binding of metals to the solid phase peat very well, without optimisation of the default parameters. Predicted binding to the solid phase was often > 98% of the total solid phase concentration entered into the model. The model predicted that remainder was present in solution mainly in association with FA (representing soluble humic material). Although the modelled results were consistent with strong partitioning onto the solid phase peat, predicted total porewater concentrations were about an order of magnitude greater than the measured concentrations.

The sensitivity of model output to changes in certain parameters was then investigated. Changes in pH (3.5 to 4.5) and humic acid concentration (measured values x1.5 and x2) had little effect on the model output. Increasing the value of K for Pb did improve the model predictions of total porewater Pb concentrations to a certain extent. The results of the sensitivity studies suggested that perhaps the binding of Pb to FA was too strong. The proposed next step would therefore be to decrease the amount of Pb associated with soluble FA.

Finally, an important problem revealed by this work was the poor prediction of porewater DOC concentrations by the WHAM model. The model slightly overpredicts the concentrations at pH~4 and clearly underpredicts the concentrations at lower pH values (~3.6-3.8). It is important for future modelling of metal partitioning and speciation in peat bogs that a better prediction of porewater DOC is obtained. A better understanding of the processes controlling DOC concentrations in porewaters and of the relationship between solid phase and porewater organic matter concentrations is required.

Overall, this study has provided very strong evidence to support Pb immobility in ombrotrophic peat bogs. More than 99.8% of the total Pb was bound to the solid phase, extractability decreased with increasing depth, but most importantly, the change in $^{206}Pb/^{207}Pb$ isotope, previously observed in the near-surface solid phase of the peat and sediments cores, was observed also in the porewaters and humic extracts from Flanders Moss peat. Calculated dates (^{210}Pb dating), inventories and fluxes agreed well with those obtained previously at Flanders Moss and for nearby Loch Lomond (southern basin). A decrease in the importance of Pb from petrol was also determined for the surface 0-2 cm section. Finally, the study has highlighted that modelling of Pb partitioning between solid phase peat and its associated porewater is extremely challenging because of the small range of pH involved (3.6-4.2), the pH-DOC relationship and also the very low porewater concentrations (in relation to total solid phase concentrations) to be modelled.

Chapter 9 - Appendices to the main thesis

Appendix 9.1 - Specimen calculation of the peat digest solution volumes

The peat digest solution volumes were calculated from the weight of the complete digestion of each sample following decanting of the solution from the Teflon microwave vessels, into Sterilin bottles.

The weight of solution was calculated from

$M_{solution} = M_{total} - M_{empty}$,

where $M_{solution}$ was the weight of the peat digest solution

M_{total} was the combined weight of the solution and the Sterilin bottle, and

M_{empty} was the empty weight of the Sterilin bottle

Having obtained the weight of the digest solution, the volume was calculated by;-

$$\text{Volume} = \frac{\text{Mass}}{\text{Density}}$$

The density of the digest matrix consisting 50% HNO_3 was assumed to be 1.21 g/mL, (from the specific gravity supplied on the bottle of 1.42 g/mL) allowing the calculation of the final digest volumes. This gravimetric technique was also used in a number of other volume determinations (see main text).

Appendix 9.2 - Specimen calculation of peak area for γ spectrometry

The efficiency of the peak counting was calculated using the following equation;

$$\text{Efficiency} = \frac{\text{Count Rate (cps)}}{\text{A(t) (Bq)}} * \frac{100}{1}$$

Where: A(t) is the total activity,

Intensity (count rate) is the number of counts of the spiked sample.

The errors associated with this can be assessed using the equation below

Errors : $S_{eff} = \sqrt{(S_{spike})^2 + (S_{counts})^2}\ \%$

Where S_{spike} is taken as 1%

$$\text{The activity at the time of counting} = \frac{\text{Count rate (cts/s)} * \text{Efficiency}}{\text{Weight (kg)}}$$

$$A(t)\ (Bq/kg) = A(o) * e^{(\gamma t)}$$

Where A(t) is the activity of sample at the time of counting, A(o) is the activity of the sample at the time of counting, and $\gamma = \ln 2 / t_{1/2}$, with $t_{1/2}$ being the half-life of the radionuclide.

Appendix 9.3 – Calculation of elemental concentrations in peat samples (analysis by ICP-OES).

The concentrations of elements in peat samples were calculated as follows:

Corrected concentration in solution (mg/L) = Raw concentration (mg/L) -concentration in reagent blank (mg/L)

Concentration in peat samples (mg/kg) = Corrected concentration (mg/L) x solution volume (L)/weight of peat (kg)

This method was used to calculate the concentrations of elements in solid phase peat, and the FA1, FA2, HA and TB HS extracts from Flanders Moss peat.

Appendix 9.4 – Example calculation of Pb isotope ratios from ICP-MS data

1. Reagent blank correction

Blank corrected counts = Raw counts – blank counts

2. Ratio calculation

$^{206}Pb/^{207}Pb$ ratio = Blank corrected counts for ^{206}Pb/Blank corrected counts for ^{207}Pb

3. Mass bias correction of ratio

corrected $^{206}Pb/^{207}Pb$ ratio = $^{206}Pb/^{207}Pb$ ratio x mass bias correction factor (e.g.~ 1.00)*

*PQVision software use the counts obtained for ^{206}Pb and ^{207}Pb to give a $^{206}Pb/^{207}Pb$ ratio for the SRM 981reference material. The software compares the value of ratio with the certified value and calculates the mass bias correction factor.

4. Average mass bias corrected ratio and standard deviation

average ratio =Σ(ratios calculated for each of the five individual runs of a sample)/5

The standard deviation for the five individual ratios for each sample gives a measure of the internal precision.

Appendix 9.5 – Solid phase elemental concentrations for Flanders Moss peat Core 1

Sample Depth	Concentration (mg/kg)														
	Mn	Fe	S	P	Al	Ti	Na	K	Mg	Ca	Sr	Ba	Zn	Cu	Pb
0-2	73.83	2984	1156	697.8	872.7	46.04	442.8	1217	995	1840	23.62	33.34	325.7	7.305	75.52
2-4	33.33	3044	1249	594.7	1775	101.7	183.8	614.0	967	1302	27.08	30.24	228.0	15.69	198.4
4-6	8.60	1559	1167	431.4	2249	113.6	168.6	277.5	828	998	26.47	23.53	270.4	13.25	327.6
6-8	3.75	918	1149	286.6	2035	96.53	159.7	182.8	783	938	25.49	20.47	223.2	7.910	272.7
8-10	3.02	726	1139	234.5	2146	101.2	174.4	179.4	798	927	26.20	20.68	203.6	3.735	160.4
10-12	2.51	710	988	273.1	2024	103.7	172.2	201.1	790	912	23.76	21.29	234.0	6.695	134.1
12-14	1.84	630	923	225.9	1785	79.23	183.6	151.2	831	914	24.52	18.27	207.7	3.488	105.4
14-16	1.62	634	944	224.0	1420	60.17	193.5	100.8	925	945	25.47	14.76	226.6	2.963	78.61
16-18	2.07	697	979	240.9	1457	62.86	181.3	124.8	1015	1001	26.65	15.08	216.2	3.802	110.5
18-20	1.72	685	1009	197.4	1432	62.33	157.1	88.8	1060	1038	27.01	13.83	232.7	3.916	128.7
20-22	1.17	685	1054	158.2	1343	59.48	185.8	66.3	1117	1037	28.31	12.43	253.0	1.542	164.8
22-24	1.04	651	1025	155.5	1209	50.32	161.6	69.3	1093	1022	28.05	12.87	225.0	0.533	107.5
24-26	0.63	599	929	123.7	782.4	40.17	218.3	40.4	1154	982	26.00	8.37	292.7	0.717	33.22
26-28	0.57	581	906	124.8	749.5	36.86	211.2	33.8	1113	957	25.35	8.24	285.2	0.586	31.01
28-30	0.71	525	835	113.6	633.2	40.58	194.1	34.0	1101	871	22.55	6.25	297.6	0.811	20.01
30-32	0.61	494	812	103.4	587.2	49.32	204.6	43.4	1122	868	21.47	6.19	290.9	0.621	9.09
32-34	0.45	519	893	109.5	575.5	46.27	212.4	30.6	1248	921	23.25	5.69	295.9	0.558	7.7
34-36	0.37	468	851	101.6	525.5	45.53	191.2	22.7	1216	889	21.75	5.18	233.0	0.604	4.96
36-38	0.34	489	949	109.6	563.4	46.39	186.5	22.5	1262	923	23.21	5.19	300.6	0.686	6.96
38-40	0.32	439	1051	99.2	584.5	45.42	163.9	26.2	1134	772	23.99	5.23	190.2	0.672	3.08
40-42	0.34	402	1003	116.5	581.4	35.80	161.7	32.3	1089	738	22.83	4.95	241.5	0.763	5.44
42-44	0.82	359	940	106.4	513.7	25.56	158.6	33.5	1083	704	20.92	3.97	218.9	0.597	3.04
44-46	0.61	304	826	76.1	385.9	19.04	148.4	35.0	1077	642	17.31	2.67	220.5	0.255	1.93
46-48	0.97	297	824	94.2	378.7	17.10	147.9	33.4	1068	650	17.39	3.12	277.7	0.120	2.54
48-50	1.33	306	925	112.6	468.0	19.44	142.3	25.3	1105	686	20.30	3.52	201.9	0.274	2.00

Appendix 9.5 ctd - Solid phase elemental concentrations for Flanders Moss peat Core 1

Sample	Concentration (mg/kg)														
Depth	Mn	Fe	S	P	Al	Ti	Na	K	Mg	Ca	Sr	Ba	Zn	Cu	Pb
50-52	1.01	317	1160	106.7	492.3	20.33	150.0	19.9	1188	763	22.63	4.31	178.8	0.521	3.03
52-54	0.95	297	1197	97.7	432.9	16.62	146.7	34.7	1215	762	21.27	3.27	204.6	0.522	2.26
54-56	0.49	266	1064	90.0	378.6	14.23	154.0	33.2	1253	771	19.17	2.93	260.8	0.419	2.09
56-58	0.49	270	1086	91.3	395.3	16.20	152.7	24.6	1285	784	19.82	2.98	237.2	0.395	1.80
58-60	0.44	245	1011	101.4	376.5	16.55	142.9	12.6	1206	724	18.45	2.82	249.9	0.569	3.36
60-62	0.50	227	929	110.5	411.8	19.93	141.6	24.1	1130	700	16.98	3.81	220.4	1.339	2.34
62-64	0.44	235	926	115.1	447.5	20.06	142.7	25.5	1225	752	18.52	4.18	195.9	1.001	3.84
64-66	0.32	224	935	112.1	464.2	20.30	142.0	20.6	1210	705	17.24	3.86	123.8	0.555	3.40
66-68	0.26	230	949	109.8	490.4	19.11	156.8	25.0	1271	752	17.50	3.63	218.4	0.663	3.89
68-70	0.52	223	1074	201.8	615.6	27.36	158.0	55.9	1280	713	16.92	4.75	163.6	0.781	4.36
70-72	0.58	208	923	219.0	643.3	27.27	147.6	48.9	1203	671	15.85	4.86	190.5	0.813	4.81
72-74	0.54	195	838	223.7	674.4	28.43	144.3	37.7	1135	639	15.02	5.20	154.7	0.779	5.32
74-76	0.43	191	913	222.3	724.1	30.31	141.0	45.5	1092	606	14.44	5.75	147.7	0.694	3.43
76-78	0.45	208	974	207.7	699.8	29.74	146.6	46.4	1222	657	15.49	4.78	147.4	1.419	2.87
78-80	0.42	238	1111	157.0	632.4	21.95	139.2	26.0	1419	789	18.92	3.98	167.8	0.752	3.23
80-82	0.44	228	1050	141.0	564.5	19.57	137.0	20.3	1434	788	18.35	3.50	192.8	0.669	2.60
82-84	0.93	229	1196	128.8	443.2	16.98	137.2	14.0	1532	795	18.90	2.89	262.8	0.809	2.66
84-86	1.38	203	1027	105.3	362.1	17.07	125.7	6.0	1474	740	16.88	2.93	192.0	0.533	2.31
86-88	1.01	218	1267	110.6	349.6	16.09	134.2	13.9	1608	797	18.63	2.78	186.2	0.404	1.32
88-90	0.90	213	1197	104.9	349.7	16.51	135.3	20.7	1614	804	18.49	2.71	142.5	0.343	1.85
90-92	0.48	209	1066	94.6	274.2	11.85	127.2	2.2	1634	770	17.63	1.78	205.3	0.236	1.26
92-94	0.49	223	979	80.8	266.2	11.60	125.1	11.4	1670	806	17.69	1.81	174.9	1.796	1.14
94-96	0.90	237	1071	92.0	286.3	12.16	125.2	17.3	1663	813	18.74	2.15	209.8	0.466	1.03
96-98	1.08	261	1136	88.0	290.6	12.05	124.1	17.4	1692	835	19.26	2.35	195.5	0.546	1.08
98-100	0.68	256	1163	73.7	243.5	10.08	112.0	9.5	1693	795	16.88	1.72	157.7	0.233	1.23

Appendix 9.6 – Characteristics and elemental concentrations of porewaters from Flanders Moss peat Core 1

Section Depth (cm)	UV Absorbance	pH	Conductivity	DOC Conc. (mg/L)	Elemental Concentration (mg/L)												
					Mn	Fe	S	Al	Ti	Na	K	Mg	Ca	Sr	Zn	Cu	Pb
0-2	2.343	4.18	-	172.6	0.128	0.933	6.374	0.480	0.005	13.26	17.79	2.700	5.245	0.027	0.484	0.035	0.015
2-4	2.472	4.02	-	62.86	0.023	0.691	3.798	0.317	0.010	7.189	2.893	1.391	1.372	0.014	0.226	0.008	0.042
4-6	3.654	3.94	113.0	116	0.008	0.541	5.464	0.417	0.013	7.856	0.514	1.501	1.221	0.017	0.364	0.008	0.043
6-8	2.502	3.77	184.1	83.38	0.003	0.247	7.831	0.317	0.009	8.663	< blank	1.962	1.121	0.022	0.158	0.004	0.023
8-10	2.34	3.79	-	89.78	0.004	0.209	12.26	0.335	0.006	10.44	< blank	2.660	1.581	0.029	0.419	0.019	0.022
10-12	3.279	3.83	192.8	117.3	0.004	0.248	5.427	0.38	0.010	8.798	< blank	1.769	1.305	0.020	0.389	0.018	0.024
12-14	2.691	3.73	166.5	143.4	0.004	0.324	8.451	0.410	0.009	11.97	< blank	2.283	1.311	0.024	0.431	0.014	0.007
14-16	3.15	3.74	191.8	142.9	0.001	0.297	5.989	0.303	0.006	8.843	< blank	2.107	0.893	0.021	0.213	< blank	0.018
16-18	3.771	3.67	207.8	127.5	0.001	0.293	6.359	0.299	0.003	9.868	< blank	2.349	0.999	0.023	0.121	< blank	0.012
18-20	3.678	3.64	172.3	153	0.001	0.326	7.931	0.328	0.009	10.09	< blank	2.696	1.568	0.029	0.278	< blank	0.013
20-22	3.429	3.7	158.1	172.9	0.001	0.288	7.801	0.295	0.006	9.728	< blank	2.538	1.205	0.025	0.279	< blank	0.024
22-24	3.651	3.75	-	154	0.002	0.309	7.917	0.328	0.009	9.568	< blank	2.803	1.311	0.030	0.324	< blank	0.023
24-26	3.351	3.77	133.3	140.5	0.001	0.256	7.746	0.257	0.008	9.938	< blank	2.426	1.550	0.026	0.484	< blank	-
26-28	2.673	3.67	-	127	< blank	0.144	7.276	0.169	0.006	9.338	< blank	2.390	0.862	0.021	0.261	< blank	0.007
28-30	2.838	3.73	136.7	123.8	< blank	0.192	5.571	0.187	0.007	8.570	< blank	2.222	0.813	0.020	0.222	< blank	0.005
30-32	3.096	3.78	-	118.1	< blank	0.239	3.350	0.206	0.009	7.800	< blank	2.070	0.772	0.018	0.308	< blank	0.003
32-34	2.907	3.88	119.2	112.2	< blank	0.231	3.529	0.210	0.007	7.697	< blank	2.169	1.425	0.020	0.304	< blank	0.002
34-36	3.078	3.77	128.7	119.4	< blank	0.215	3.231	0.190	0.008	7.374	< blank	2.108	0.626	0.017	0.176	< blank	0.002
36-38	2.772	3.81	129.8	104.5	< blank	0.178	3.455	0.177	0.007	7.541	< blank	2.113	0.696	0.017	0.406	< blank	0.001
38-40	2.55	3.77	130.3	112.5	< blank	0.122	3.490	0.157	0.004	7.298	< blank	2.247	0.715	0.017	0.194	< blank	0.001
40-42	2.572	3.79	127.6	106.8	< blank	0.129	3.240	0.140	0.005	6.794	< blank	1.985	0.605	0.015	0.180	< blank	0.001
42-44	2.258	3.86	112.1	83.42	< blank	0.111	2.748	0.114	0.003	6.438	< blank	1.812	0.513	0.012	0.163	< blank	0.002
44-46	2.386	3.87	119.3	95.43	< blank	0.116	2.372	0.112	0.003	6.131	< blank	1.950	0.563	0.013	0.329	< blank	0.002
46-48	2.016	3.85	112.3	96.28	< blank	0.103	3.064	0.121	0.001	6.625	< blank	2.216	0.728	0.014	0.221	< blank	0.002
48-50	1.676	3.86	-	71.13	< blank	0.041	5.531	0.041	0.001	7.304	< blank	2.373	0.608	0.014	0.178	< blank	

Appendix 9.6 ctd – Characteristics and elemental concentrations of porewaters from Flanders Moss peat Core 1

Section Depth	UV	pH	Conductivity	DOC Conc.	Elemental Concentration (mg/L)												
					Mn	Fe	S	Al	Ti	Na	K	Mg	Ca	Sr	Zn	Cu	Pb
50-52	1.842	4.02	100.3	86.18	< blank	0.080	2.949	0.139	0.001	6.508	< blank	2.229	1.205	0.015	0.253	< blank	0.0020
52-54	1.9	3.89	108.9	96.33	< blank	0.069	2.482	0.068	0.001	5.879	< blank	2.121	0.520	0.012	0.159	< blank	0.0010
54-56	1.896	3.92	111.1	90.83	< blank	0.063	2.256	0.076	0.002	5.932	< blank	2.157	0.533	0.012	0.211	< blank	0.0010
56-58	1.784	4.19	104.9	76.64	< blank	0.052	2.792	0.067	0.001	6.107	< blank	2.470	1.919	0.016	0.490	< blank	0.0002
58-60	1.632	3.92	110.1	72.32	< blank	0.035	4.143	0.031	0.001	6.109	< blank	2.270	0.511	0.011	0.120	< blank	0.0009
60-62	1.5	3.98	98.3	76.17	< blank	0.059	2.067	0.041	< blank	5.444	< blank	1.968	0.403	0.010	0.120	< blank	-
62-64	1.477	3.96	100.0	80.01	< blank	0.064	1.964	0.063	< blank	5.514	< blank	2.066	0.402	0.010	0.088	< blank	-
64-66	1.468	3.94	114.1	72.48	< blank	0.058	2.311	0.071	< blank	6.200	< blank	2.576	0.558	0.013	0.084	< blank	-
66-68	1.389	4.13	-	79.52	< blank	0.049	1.878	0.081	0.002	5.667	< blank	2.227	0.979	0.012	0.211	< blank	0.0002
68-70	1.293	3.96	-	87.67	< blank	0.043	2.282	0.076	0.001	6.391	< blank	2.574	0.610	0.012	0.075	< blank	0.0011
70-72	1.265	4.01	102.3	86.76	< blank	0.024	2.719	0.038		5.796	< blank	2.112	0.557	0.010	0.095	< blank	0.0002
72-74	1.252	4.02	106.9	85.3	< blank	0.022	2.658	0.042	0.002	5.974	< blank	2.082	0.546	0.010	0.088	< blank	0.0002
74-76	1.196	4.05	102.7	85.88	< blank	0.022	2.927	0.056	bdl	6.850	< blank	2.226	0.720	0.010	0.086	< blank	0.0001
76-78	1.189	4.04	102.6	82.13	< blank	0.023	2.500	0.039	bdl	6.093	< blank	2.237	0.677	0.010	0.101	< blank	0.0003
78-80	1.002	4	110.5	64.55	< blank	0.029	1.682	0.049	0.001	5.396	< blank	2.654	0.595	0.011	0.084	< blank	-
80-82	1.082	4.08	89.2	60.26	< blank	0.037	0.995	0.028	0.002	4.956	< blank	1.906	0.320	0.008	0.086	< blank	0.0072
82-84	1.13	4.07	102.1	66.34	< blank	0.051	1.149	0.037	0.002	5.685	< blank	2.363	0.453	0.010	0.106	< blank	0.0061
84-86	1.046	4.05	96.6	59.22	< blank	0.033	1.042	0.040	< blank	4.767	< blank	2.490	0.517	0.010	0.071	< blank	0.0070
86-88	1.092	4.05	-	64.62	< blank	0.031	1.210	0.039	0.001	4.862	< blank	2.639	0.485	0.011	0.121	< blank	-
88-90	1.055	4.06	102.4	62.38	< blank	0.041	1.160	0.039	< blank	4.965	< blank	2.848	0.520	0.011	0.077	< blank	0.0065
90-92	1.093	4.09	101.1	63.82	< blank	0.049	1.011	0.020	< blank	4.801	< blank	2.759	0.545	0.011	0.127	< blank	0.0058
92-94	1.09	4.09	96.8	65.75	< blank	0.034	1.074	0.027	< blank	4.907	< blank	2.911	0.565	0.011	0.079	< blank	0.0085
94-96	1.142	4.1	102.9	66.81	< blank	0.036	1.262	0.028	0.001	5.214	< blank	3.148	0.691	0.012	0.137	< blank	0.0075
96-98	1.147	4.07	106.4	60.82	< blank	0.040	1.135	0.032	< blank	5.134	< blank	3.137	0.523	0.012	0.086	< blank	0.0074
98-100	1.108	4.12	104.0	72.11	< blank	0.038	1.151	0.037	0.001	5.089	< blank	3.312	0.574	0.013	0.126	< blank	0.0075

Appendix 9.7 – Extraction and Quantification data for Humic and Fulvic Acids and Tris Borate Humic Substances from Flanders Moss peat Core 2

Section Depth (cm)	FA2 TOC (mg/L)	HA freeze dried weight (mg)	FA2 extracted (mg/kg dry weight)	Humic Acid (g/kg dry weight)	IHSS extracted (g/kg dry weight)	% of OM extracted by IHSS	TB Humic Substances weight (mg)	TB HS extracted (g/kg dry weight)	% of OM extracted as HS
0-2	801.9	186.5	14.15	133.70	147.85	10.90	43.19	30.23	3.11
2-4	556.8	183.5	17.85	147.97	165.82	14.61	62.15	49.19	5.37
4-6	736	153.6	28.79	151.07	179.86	19.95	51.60	49.32	5.56
6-8	491.5	164.0	11.74	105.19	116.93	8.25	58.32	38.09	4.19
8-10	298.8	194.5	7.51	124.79	132.30	8.90	86.41	47.82	5.01
10-12	328.9	251.8	8.03	162.73	170.75	11.43	107.24	71.84	7.44
12-14	279.8	No data	6.89	0.00	6.89	0.48	94.47	62.35	6.57
14-16	324.3	204.4	9.53	178.29	187.82	16.69	85.72	74.23	7.56
16-18	331.7	174.1	9.34	132.23	141.57	11.01	65.56	49.72	5.09
18-20	434.2	135.2	12.92	102.80	115.72	8.96	71.53	56.38	5.74
20-22	403.9	123.6	14.00	114.90	128.91	12.14	54.72	53.55	5.43
22-24	739.5	83.3	17.99	68.86	86.85	7.27	52.18	45.35	4.60
24-26	551.6	84.3	16.39	84.96	101.35	10.28	28.38	28.97	2.92
26-28	369.7	71.6	10.64	66.09	76.74	7.19	44.49	42.06	4.27
28-30	484.3	37.5	16.77	42.56	59.33	6.76	23.10	26.62	2.67
30-32	652.7	43.6	28.17	50.62	78.80	9.27	20.82	23.76	2.40
32-34	515.5	41.5	25.22	58.54	83.76	11.99	26.52	35.90	3.64
34-36	613.9	28.1	27.30	42.19	69.50	10.61	18.48	29.36	2.99
36-38	521.3	33.1	25.45	50.71	76.16	11.74	17.38	27.22	2.74
38-40	30.6	19.6	1.37	25.09	26.46	3.41	16.37	21.12	2.12
40-42	535.7	39.8	23.05	52.51	75.55	9.99	16.15	20.92	2.10
42-44	508.1	36.9	23.22	52.93	76.15	11.03	13.99	20.84	2.10
44-46	526.2	43.7	32.90	78.29	111.19	20.16	13.11	22.71	2.30
46-48	313.1	29.9	19.16	56.48	75.64	14.49	19.54	37.39	3.80
48-50	398.5	39.1	17.05	44.85	61.90	7.17	12.69	14.12	1.43

Appendix 9.7 ctd – Extraction and Quantification data for Humic and Fulvic Acids and Tris Borate Humic Substances from Flanders Moss Peat

Section Depth (cm)	FA2 TOC (mg/L)	HA freeze dried weight (mg)	FA2 extracted (g/kg dry weight)	Humic Acid (g/kg dry weight)	IHSS extracted (g/kg dry weight)	% of OM extracted by IHSS	TB Humic Substances weight (mg)	TB HS extracted (g/kg dry weight)	% of OM extracted as HS
50-52	1584	41.2	73.64	52.92	126.56	12.74	98.65	15.21	1.53
52-54	433.4	37.9	22.95	53.47	76.42	7.74	54.18	22.25	2.25
54-56	316.2	42.6	17.40	68.53	85.93	8.67	53.36	15.63	1.58
56-58	496.1	35.4	27.25	59.05	86.30	8.79	51.77	19.63	2.00
58-60	371	47.9	21.52	78.18	99.70	10.11	61.04	19.16	1.94
60-62	457.5	50.3	21.43	61.18	82.61	8.33	67.88	18.44	1.86
62-64	519.6	69.0	28.45	97.44	125.89	12.70	89.20	24.38	2.46
64-66	437	55.6	22.19	71.44	93.63	9.39	72.90	14.40	1.44
66-68	378.6	31.9	21.45	50.27	71.72	7.19	45.54	25.20	2.53
68-70	502.9	59.8	24.87	70.93	95.80	9.66	80.73	26.84	2.71
70-72	537.1	132.7	28.47	168.76	197.24	19.98	155.13	38.99	3.95
72-74	400.5	59.5	21.48	78.19	99.67	10.10	75.78	38.63	3.91
74-76	520.1	64.1	22.89	74.78	97.67	9.87	83.73	36.42	3.68
76-78	369.7	70.6	17.48	85.45	102.92	10.44	84.98	38.02	3.86
78-80	1543	60.9	53.75	74.06	127.81	12.87	105.06	33.39	3.36
80-82	402.5	61.0	19.71	91.07	110.78	11.18	74.16	30.57	3.08
82-84	455.7	73.7	23.41	110.70	134.11	13.52	89.30	28.92	2.92
84-86	687	64.1	36.64	96.33	132.97	13.36	88.42	52.14	5.24
86-88	486.1	56.3	38.70	91.46	130.16	13.14	80.12	51.41	5.19
88-90	335.6	80.5	28.01	139.98	167.99	16.97	96.66	48.68	4.92
90-92	162.7	53.9	13.67	116.00	129.67	13.04	60.19	59.41	5.98
92-94	455	48.0	37.77	103.69	141.46	14.25	65.45	55.50	5.59
94-96	453	33.5	37.47	69.19	106.67	10.79	51.65	66.43	6.72
96-98	430.9	25.4	36.99	54.67	91.66	9.25	42.59	7.37	0.74
98-100	406.7	45.9	37.86	103.21	141.07	14.26	62.70	34.80	3.52

Appendix 9.8 – Elemental concentrations for FA1 extractions of Flanders Moss peat Core 2

Section depth	Elemental Concentration (mg/kg)												
	Mn	Fe	S	P	Al	Ti	Mg	Ca	Sr	Ba	Zn	Cu	Pb
0-2	1.91	1035	123.0	110.7	124.7	1.37	87	115	2.29	4.22	21.9	1.67	38.823
2-4	0.21	545	240.6	129.9	550.3	1.48	87	110	2.50	3.18	27.6	0.89	56.777
4-6	0.10	125	399.1	143.2	662.1	2.17	104	146	2.88	2.99	20.1	0.66	73.653
6-8	0.57	284	22.1	15.15	573.2	0.97	490	425	18.65	12.19	50.9	0.45	37.739
8-10	0.59	402	17.8	25.10	394.2	1.00	431	399	16.51	10.33	52.5	0.22	25.618
10-12	0.21	94	9.9	11.34	153.2	0.64	199	162	6.75	3.65	22.9	0.65	5.246
12-14	0.57	248	21.0	19.72	296.7	1.41	541	426	16.69	8.71	70.6	0.17	10.071
14-16	0.34	391	25.5	9.41	319.3	0.90	713	562	22.32	9.51	44.3	0.18	6.113
16-18	0.32	376	16.6	6.70	264.9	0.85	652	495	21.03	8.19	30.9	0.10	4.257
18-20	0.25	376	17.2	5.34	212.7	0.50	628	483	19.06	6.56	32.7	0.15	2.574
20-22	0.25	327	14.5	4.50	165.9	0.91	668	486	17.92	5.34	20.3	0.09	1.715
22-24	0.20	294	15.4	4.00	130.7	0.79	621	441	16.09	4.57	17.5	0.03	0.976
24-26	0.20	308	16.4	3.90	161.7	1.28	762	534	19.79	5.31	25.8	0.11	0.824
26-28	0.20	255	17.6	3.98	118.5	1.24	675	467	16.21	3.75	20.6	0.09	0.254
28-30	0.20	312	19.4	2.38	141.6	1.50	786	534	19.37	4.26	21.1	0.13	0.000
30-32	0.20	213	13.8	4.12	108.1	2.18	716	459	15.11	2.84	18.7	0.11	0.000
32-34	0.17	310	18.1	1.69	139.1	2.39	885	578	20.20	3.93	16.8	0.15	0.000
34-36	0.20	298	18.4	3.74	126.0	2.34	924	586	20.02	3.44	28.2	0.09	0.000
36-38	0.44	326	22.7	4.55	157.7	2.51	1046	681	23.50	3.99	38.2	0.14	0.000
38-40	0.14	253	17.3	1.32	122.4	1.83	886	556	18.01	2.75	35.9	0.13	0.000
40-42	0.14	221	20.1	2.35	120.2	1.75	862	521	16.66	2.33	66.2	0.39	0.000
42-44	0.15	182	19.3	3.92	95.6	1.48	851	511	14.41	1.86	14.7	0.05	0.000
44-46	0.38	228	27.0	3.06	122.5	1.39	1066	627	17.24	2.14	88.4	0.26	0.000
46-48	0.22	185	18.1	3.09	97.0	0.99	944	543	14.88	1.74	83.5	0.21	0.000
48-50	0.11	117	13.3	2.61	65.8	0.45	623	364	9.95	1.16	27.7	0.23	0.000

Appendix 9.8 ctd – Elemental concentrations for FA1 extractions of Flanders Moss peat Core 2

Section depth	Elemental Concentration (mg/kg)												
	Mn	Fe	S	P	Al	Ti	Mg	Ca	Sr	Ba	Zn	Cu	Pb
50-52	0.15	126	12.8	1.24	74.5	0.31	703	413	11.08	1.21	52.4	0.19	0.000
52-54	0.16	106	6.9	4.08	61.3	0.30	667	398	9.97	1.03	146.4	0.08	0.000
54-56	0.18	126	15.9	4.11	72.1	0.52	850	483	11.74	1.14	136.5	0.07	0.000
56-58	0.17	120	11.5	1.66	67.3	0.29	873	471	11.50	1.10	177.0	0.05	0.000
58-60	0.17	122	15.7	1.39	73.3	0.29	860	470	11.63	1.19	83.8	0.13	0.000
60-62	0.13	81	13.9	1.00	58.7	0.29	670	375	8.10	0.89	113.1	0.11	0.000
62-64	0.18	97	13.7	3.85	67.6	0.37	805	447	10.12	1.14	88.9	0.13	0.000
64-66	0.11	76	8.7	3.86	45.2	0.27	669	359	8.01	0.92	66.1	0.09	0.000
66-68	0.11	72	13.4	1.55	46.0	0.35	734	374	7.76	0.83	51.9	0.38	0.000
68-70	0.08	68	9.3	1.29	46.8	0.32	602	332	7.15	0.88	19.7	0.22	0.000
70-72	0.12	94	12.2	2.68	65.9	0.38	786	442	10.58	1.42	67.1	0.18	0.172
72-74	0.08	61	10.1	0.29	48.7	0.33	692	370	7.92	0.95	34.7	0.42	0.082
74-76	0.07	51	9.6	1.71	45.6	0.33	633	333	6.98	0.85	44.8	0.13	0.019
76-78	0.08	71	10.9	1.75	68.5	0.23	744	373	8.07	1.00	72.0	0.11	0.619
78-80	0.12	69	9.5	3.17	64.9	0.31	694	359	7.82	0.97	29.6	0.11	0.774
80-82	0.12	107	11.2	3.12	120.1	0.57	995	537	12.39	1.71	22.1	0.08	1.506
82-84	0.15	128	16.8	3.73	171.7	0.61	1156	606	15.23	2.09	72.5	0.14	1.757
84-86	0.15	113	11.9	4.38	128.1	0.56	1056	551	12.89	1.65	30.9	0.13	1.053
86-88	0.20	131	12.4	3.57	147.7	0.54	1114	578	14.68	2.27	40.6	0.15	1.082
88-90	0.28	142	11.8	7.29	148.5	0.56	1288	716	16.99	2.11	201.4	0.16	0.472
90-92	0.34	133	1.4	15.65	103.9	0.70	1306	742	16.18	1.60	281.5	0.39	0.094
92-94	0.53	151	15.3	3.93	76.5	0.53	1318	624	13.48	1.18	317.5	0.66	0.076
94-96	0.34	105	7.7	1.88	50.2	0.42	1079	521	10.40	0.88	152.5	0.41	0.000
96-98	No data	No data	No data	No data	No data	No data	No data	No data	No data	No data	No data	No data	No data
98-100	0.40	107	15.3	0.00	72.0	0.47	1386	685	15.24	1.92	216.4	0.08	0.000

Appendix 9.9 – Elemental concentrations for FA2 extractions of Flanders Moss peat Core 2

Section depth	Elemental Concentration (mg/kg)											
	Mn	Fe	S	P	Al	Ti	Mg	Ca	Sr	Ba	Zn	Cu
0-2	1.16	605	80	48.9	42.2	0.62	51	70	1.07	2.31	14.3	0.93
2-4	0.19	439	212	83.5	362.1	0.75	72	91	1.55	2.84	25.9	0.46
4-6	0.09	108	403	90.8	496.9	1.54	93	128	1.86	2.31	26.1	0.20
6-8	0.04	48	122	13.0	129.1	1.42	67	91	1.42	1.34	14.9	0.00
8-10	0.00	87	87	26.1	285.8	1.08	75	92	1.55	1.64	10.5	0.00
10-12	0.09	68	66	19.8	167.0	1.10	107	103	1.79	1.64	12.0	0.00
12-14	0.13	75	74	15.8	189.9	0.92	114	104	1.71	1.32	10.3	0.00
14-16	0.05	71	105	7.8	150.8	0.67	117	109	2.10	1.56	7.4	0.00
16-18	0.03	63	94	6.1	128.8	0.51	117	111	2.11	1.24	4.1	0.00
18-20	0.03	53	97	3.6	92.6	0.06	116	107	2.01	1.11	5.9	0.00
20-22	0.02	58	84	3.1	63.3	0.18	143	115	1.98	0.71	7.5	0.00
22-24	0.01	35	62	0.0	41.3	0.10	84	73	1.15	0.48	10.5	0.00
24-26	0.02	43	78	2.9	36.9	0.52	92	79	1.33	1.03	9.4	0.00
26-28	0.05	34	83	1.6	6.0	0.52	77	78	0.95	0.40	6.0	0.00
28-30	0.04	18	88	2.7	0.0	0.84	53	38	0.41	0.16	5.6	0.00
30-32	0.05	20	99	5.2	0.0	0.77	69	50	0.49	0.68	5.0	0.00
32-34	0.12	44	124	2.6	0.0	0.38	101	79	1.05	0.23	4.2	0.00
34-36	0.23	27	81	0.0	0.0	0.44	96	91	0.52	0.00	11.2	0.00
36-38	0.20	31	143	3.2	0.0	0.41	62	50	0.39	8.51	11.7	0.00
38-40	0.12	20	53	0.0	0.0	0.68	37	29	0.05	4.12	8.2	0.00
40-42	0.05	19	137	0.0	0.0	0.08	57	39	0.25	0.00	14.0	0.00
42-44	0.02	8	168	0.2	0.0	0.63	56	45	0.14	0.20	8.0	0.00
44-46	0.07	13	241	0.1	0.0	0.79	66	46	0.12	0.03	15.6	0.00
46-48	0.03	16	177	0.3	0.0	0.37	75	50	0.13	0.14	10.9	0.00
48-50	0.04	10	152	0.0	0.0	0.00	43	38	0.03	0.00	6.4	0.00

Appendix 9.9 ctd– Elemental concentrations for FA2 extractions of Flanders Moss peat Core 2

Section depth	Elemental Concentration (mg/kg)											
	Mn	Fe	S	P	Al	Ti	Mg	Ca	Sr	Ba	Zn	Cu
50-52	0.05	16	132	0.0	0.0	0.21	56	42	0.11	0.14	9.4	0.00
52-54	0.08	17	139	0.0	0.0	0.00	60	35	0.01	0.00	19.5	0.00
54-56	0.09	11	192	0.0	0.0	0.00	61	36	0.00	0.00	10.9	0.00
56-58	0.09	12	171	0.0	0.0	0.03	58	30	0.00	0.00	14.5	0.00
58-60	0.09	14	196	0.0	0.0	0.00	69	44	0.01	0.09	22.3	0.00
60-62	0.07	7	163	0.0	0.0	0.00	55	35	0.00	0.19	18.7	0.00
62-64	0.09	10	226	4.7	0.0	0.00	77	48	0.10	0.05	19.5	0.00
64-66	0.10	19	161	1.3	0.0	0.21	88	43	0.19	0.49	19.4	0.00
66-68	0.09	12	143	0.0	0.0	0.40	92	52	0.12	0.39	24.6	0.00
68-70	0.56	16	168	0.0	0.0	0.64	130	134	0.25	0.61	22.7	0.00
70-72	0.08	23	165	1.6	0.0	0.47	85	47	0.43	0.00	13.6	0.00
72-74	0.06	18	109	0.0	0.0	0.44	94	45	0.43	0.27	11.5	0.00
74-76	0.07	19	103	0.0	0.0	0.45	90	42	0.21	0.04	9.1	0.00
76-78	0.15	7	87	1.4	0.0	0.02	92	63	0.57	0.04	25.2	0.00
78-80	0.04	9	53	3.7	0.0	0.14	74	38	0.44	0.00	48.2	0.00
80-82	0.08	11	65	0.0	0.0	0.11	94	43	0.48	0.05	19.7	0.00
82-84	0.05	11	67	0.0	0.0	0.31	98	45	0.53	0.00	20.4	0.00
84-86	0.08	14	78	0.0	0.0	0.14	106	69	0.56	0.00	26.7	0.00
86-88	0.09	20	71	0.0	0.0	0.24	107	49	1.68	0.16	17.0	0.00
88-90	0.08	20	125	0.0	0.0	0.46	96	44	0.31	0.07	39.0	0.00
90-92	0.43	25	135	0.0	0.0	1.74	172	117	0.76	0.00	114.1	0.00
92-94	0.38	26	128	0.0	0.0	1.05	153	84	0.65	0.00	85.7	0.00
94-96	0.17	25	91	0.0	0.0	0.45	130	61	0.47	0.27	59.3	0.00
96-98	0.37	15	100	0.0	0.0	1.09	116	82	0.34	0.00	67.6	0.00
98-100	0.25	16	120	0.1	0.0	0.54	114	64	0.27	0.00	57.9	0.00

Appendix 9.10 – Elemental concentrations for HA exctractions from Flanders Moss peat Core 2

Section depth	Elemental Concentration (mg/kg)												
	Mn	Fe	S	P	Al	Ti	Mg	Ca	Sr	Ba	Zn	Cu	Pb
0-2	0.48	1011	626	190.0	26.02	13.05	20.4	227	1.28	0.81	25.5	1.7	14.63
2-4	0.56	479	1205	230.9	64.64	28.54	27.7	326	1.57	1.02	18.5	6.5	21.78
4-6	0.23	86	1349	182.6	110.43	30.58	28.1	168	1.42	1.25	5.1	6.6	21.67
6-8	0.04	48	769	63.8	80.70	22.61	14.9	66	0.80	0.71	0.5	0.9	6.67
8-10	0.07	90	739	67.2	51.57	17.96	18.7	123	1.02	1.92	5.7	3.9	7.12
10-12	0.11	94	892	74.9	61.01	22.76	27.5	164	1.23	1.35	28.5	7.4	5.59
12-14	0.11	29	318	21.1	15.02	4.80	12.2	99	0.55	0.82	32.9	1.7	1.72
14-16	0.29	48	950	43.8	30.15	7.20	24.7	187	1.20	0.86	47.4	4.9	2.72
16-18	0.06	41	745	48.5	27.45	8.08	22.5	120	1.14	1.13	8.7	1.6	1.81
18-20	0.06	36	644	30.0	19.61	7.67	19.0	119	1.08	1.46	4.7	2.5	1.03
20-22	0.13	31	576	34.2	14.68	4.76	20.7	146	1.27	0.99	7.8	5.3	0.73
22-24	0.17	48	372	17.2	8.70	3.24	8.9	50	0.84	0.89	7.6	0.1	0.27
24-26	0.00	23	462	27.0	10.22	4.05	11.1	108	1.21	1.14	7.1	2.4	0.36
26-28	0.03	17	344	14.5	9.66	3.31	9.0	66	0.86	1.03	1.7	5.1	0.55
28-30	0.04	16	376	16.1	5.96	3.40	8.6	76	0.99	0.16	0.0	10.6	0.34
30-32	0.13	18	320	29.0	8.03	3.36	6.5	61	0.97	0.05	0.0	0.0	0.00
32-34	0.11	33	344	11.1	3.22	3.93	4.8	53	1.16	0.00	0.0	0.0	0.00
34-36	0.08	17	246	1.4	4.91	1.84	9.7	117	1.12	0.00	4.7	0.0	0.27
36-38	0.20	18	402	26.5	11.03	4.51	12.8	132	1.45	0.00	0.0	0.0	0.39
38-40	0.12	24	161	0.0	2.74	1.11	7.1	213	1.19	2.13	7.2	3.2	0.39
40-42	0.00	10	298	0.0	5.00	2.58	0.3	42	1.12	0.00	0.0	0.0	0.00
42-44	0.00	10	275	0.0	5.56	8.96	1.8	37	1.23	0.00	0.0	0.0	0.02
44-46	0.00	23	929	0.0	12.26	6.32	4.7	107	2.60	0.60	119.2	0.0	0.11
46-48	0.00	18	363	2.8	5.63	1.69	3.8	90	1.71	2.29	0.0	0.0	0.06
48-50	0.12	47	286	4.8	3.32	1.16	2.5	66	1.09	0.00	0.0	1.3	0.16

Appendix 9.10 ctd– Elemental concentrations for HA exctractions from Flanders Moss peat Core 2

Section depth	Elemental Concentration (mg/kg)												
	Mn	Fe	S	P	Al	Ti	Mg	Ca	Sr	Ba	Zn	Cu	Pb
50-52	0.00	24	343	5.9	8.48	0.94	5.5	147	1.61	0.00	0.0	0.0	0.06
52-54	0.00	5	279	2.6	1.86	0.39	0.9	82	1.23	0.97	1.6	0.0	0.06
54-56	0.00	15	407	11.8	4.36	0.82	5.0	119	1.52	4.09	21.5	0.0	0.10
56-58	0.00	17	352	9.1	3.74	0.78	6.0	302	2.09	0.55	13.5	0.0	0.09
58-60	0.00	13	453	5.2	9.89	1.47	8.7	98	1.57	0.79	3.0	0.0	0.46
60-62	0.00	14	412	0.0	7.69	0.95	5.3	158	1.49	0.44	4.4	0.0	0.50
62-64	0.28	57	752	32.6	16.75	2.46	12.0	167	1.49	0.78	10.3	0.0	0.88
64-66	0.03	6	456	9.2	10.28	1.90	11.3	121	1.29	0.70	20.8	0.0	0.37
66-68	0.00	6	399	5.2	8.04	26.93	8.0	56	1.38	0.71	0.0	0.0	0.43
68-70	0.27	8	475	5.7	7.77	2.73	39.8	170	1.45	1.05	23.3	0.0	0.48
70-72	0.00	6	640	32.6	12.09	3.78	9.1	87	1.34	0.95	0.0	0.0	0.37
72-74	0.00	14	443	18.3	10.21	2.35	7.9	114	1.31	1.02	0.0	0.0	0.31
74-76	0.00	7	431	13.9	9.95	2.11	6.9	85	1.09	0.36	0.0	0.0	0.45
76-78	0.00	14	460	19.6	12.28	2.99	8.4	84	5.00	0.24	0.0	0.0	0.00
78-80	0.00	7	365	14.0	7.42	2.28	8.0	74	5.75	0.16	0.0	0.0	0.02
80-82	0.03	16	489	33.0	12.37	3.90	15.9	131	6.27	0.21	11.8	0.0	0.28
82-84	0.03	45	615	27.9	14.92	4.63	12.2	159	6.95	0.49	1.0	0.0	0.08
84-86	0.06	20	543	7.6	10.33	4.21	17.0	253	8.21	0.53	37.1	0.0	0.42
86-88	0.62	31	532	29.1	15.58	4.04	36.2	585	8.53	1.38	107.1	7.9	1.66
88-90	0.40	36	718	29.7	23.58	5.13	29.5	232	8.75	0.77	38.4	5.0	2.86
90-92	2.33	36	674	44.1	18.84	20.81	110.8	979	12.30	2.62	425.2	40.8	5.79
92-94	2.46	67	585	6.6	33.88	3.99	67.4	525	12.23	2.08	96.9	20.3	1.89
94-96	1.37	28	357	10.7	15.25	1.10	67.3	966	8.83	2.59	261.3	44.7	7.74
96-98	1.66	31	269	2.5	17.49	1.43	52.2	349	9.83	1.31	83.7	5.2	1.10
98-100	No data	No data	No data	No data	No data	No data	No data	No data	No data	No data	No data	No data	0.79

Appendix 9.11 – Elemental concentrations for TB HS extractions from Flanders Moss peat Core 2

Section depth	Elemental Concentration (mg/kg)												
	Mn	Fe	S	P	Al	Ti	Mg	Ca	Sr	Ba	Zn	Cu	Pb
0-2	0.03	21.4	17.3	3.49	3.12	0.27	2.99	11.4	0.07	0.04	1.06	0.08	3.085
2-4	0.02	48.2	42.9	5.20	9.17	0.74	5.50	11.0	0.14	0.08	3.36	0.13	6.771
4-6	0.00	4.9	42.6	5.96	11.27	0.74	4.06	10.7	0.11	0.11	0.98	0.14	4.851
6-8	0.00	1.2	29.3	3.30	9.43	0.62	2.86	7.0	0.07	0.06	0.58	0.05	3.438
8-10	0.00	3.6	29.9	3.12	10.73	0.67	3.86	8.6	0.09	0.05	1.10	0.01	2.571
10-12	0.00	5.6	39.6	3.20	16.53	0.85	7.86	13.7	0.17	0.12	1.73	0.01	3.034
12-14	0.00	5.7	33.8	2.43	12.12	0.48	8.03	15.3	0.18	0.03	2.88	0.08	2.121
14-16	0.00	4.9	41.7	2.76	13.51	0.47	10.40	18.5	0.24	0.01	1.53	0.27	1.916
16-18	0.01	8.1	28.1	1.59	7.72	0.26	6.96	12.0	0.16	0.15	1.26	0.00	1.210
18-20	0.03	8.7	38.5	2.63	9.19	0.32	9.59	24.1	0.25	0.23	2.41	0.00	
20-22	0.03	8.0	28.0	1.89	5.75	0.22	7.41	15.9	0.17	0.12	1.40	0.00	0.660
22-24	0.02	3.4	19.8	1.77	4.15	0.19	5.64	14.1	0.12	0.04	1.03	0.00	0.422
24-26	0.04	1.8	15.6	1.09	2.87	0.14	4.10	17.6	0.09	0.05	0.67	0.00	0.387
26-28	0.03	2.6	22.4	1.90	4.32	0.23	5.08	22.3	0.11	0.15	2.55	0.13	0.643
28-30	0.00	2.8	14.6	0.59	1.03	0.00	2.74	7.7	0.05	0.01	0.00	0.00	0.000
30-32	0.00	0.8	11.0	0.66	0.29	0.00	1.83	5.5	0.03	0.00	0.00	0.00	0.000
32-34	0.00	2.0	15.5	1.03	0.77	0.00	2.87	13.3	0.05	0.00	0.00	0.00	0.000
34-36	0.02	11.9	14.6	1.10	0.22	0.00	2.61	20.2	0.04	0.00	0.00	0.00	0.000
36-38	0.03	14.8	12.6	0.82	0.05	0.00	2.07	14.1	0.03	0.00	0.00	0.00	0.002
38-40	0.00	0.3	11.7	1.04	0.15	0.00	2.83	22.6	0.03	0.05	0.20	0.00	0.000
40-42	0.00	0.3	10.9	0.77	0.16	0.00	1.99	4.9	0.02	0.00	0.00	0.00	0.000
42-44	0.00	0.0	12.3	0.75	0.00	0.00	2.00	5.1	0.02	0.00	0.00	0.00	0.029
44-46	0.00	0.0	14.6	1.78	0.01	0.00	2.13	13.1	0.04	0.00	0.00	0.00	0.235
46-48	0.00	1.2	27.4	2.56	1.17	0.00	3.34	26.2	0.05	0.00	0.00	0.00	0.062
48-50	0.00	0.0	9.4	0.72	0.00	0.00	1.20	10.5	0.02	0.12	0.00	0.00	0.000

Appendix 9.11 ctd – Elemental concentrations for TB HS extractions from Flanders Moss peat Core 2

Section depth	Elemental Concentration (mg/kg)												
	Mn	Fe	S	P	Al	Ti	Mg	Ca	Sr	Ba	Zn	Cu	Pb
50-52	0.01	0.1	13.1	1.49	0.26	0.00	2.07	15.3	0.03	0.00	0.00	0.07	0.496
52-54	0.00	1.0	0.0	0.56	0.73	0.00	1.64	9.2	0.02	0.06	1.19	0.00	0.000
54-56	0.01	0.6	0.0	0.81	0.62	0.00	1.79	16.1	0.03	0.01	0.79	0.00	0.219
56-58	0.01	1.8	0.0	0.32	0.91	0.00	2.06	14.1	0.03	0.14	1.36	0.00	0.385
58-60	0.05	14.7	0.0	0.73	0.88	0.00	2.15	16.3	0.04	0.14	2.83	0.01	0.051
60-62	0.07	14.8	0.0	0.59	0.92	0.00	1.99	13.9	0.03	0.10	1.80	0.00	0.083
62-64	0.02	2.3	0.0	0.49	0.96	0.00	2.59	19.8	0.03	0.00	2.56	0.00	0.677
64-66	0.01	0.6	0.0	0.37	0.60	0.00	1.34	20.5	0.02	0.02	4.51	0.08	0.000
66-68	0.01	1.6	0.0	0.53	1.08	0.00	2.76	17.2	0.03	0.03	1.36	0.18	0.146
68-70	0.01	3.6	0.0	0.05	1.08	0.00	2.38	15.0	0.03	0.10	2.08	0.09	0.206
70-72	0.00	0.0	0.0	1.40	0.99	0.00	2.56	13.1	0.03	0.04	1.37	0.00	0.000
72-74	0.00	0.3	0.0	1.16	0.91	0.00	2.47	10.2	0.03	0.00	0.94	0.00	0.000
74-76	0.02	5.8	0.0	0.96	1.48	0.00	3.16	16.4	0.03	0.01	3.43	0.13	0.000
76-78	0.00	1.7	0.0	1.00	1.58	0.00	3.14	11.3	0.03	0.01	1.09	0.00	0.000
78-80	0.00	1.2	0.0	0.92	1.40	0.00	2.63	13.2	0.03	0.02	1.46	0.00	0.000
80-82	0.01	0.4	0.0	1.85	1.81	0.00	3.20	13.5	0.03	0.00	1.60	0.00	0.619
82-84	0.00	1.1	0.0	1.27	2.81	0.00	3.31	16.5	0.04	0.07	1.16	0.00	0.000
84-86	0.01	0.6	0.0	2.15	2.28	0.00	4.00	23.5	0.05	0.00	2.00	0.00	0.427
86-88	0.12	36.8	0.0	1.98	2.76	0.00	5.00	18.1	0.05	0.22	4.09	0.00	0.000
88-90	0.08	27.0	0.0	2.62	3.37	0.00	5.08	18.9	0.06	0.08	2.24	0.00	0.000
90-92	0.02	2.0	0.0	2.71	2.82	0.00	4.67	14.1	0.05	0.08	2.41	0.00	0.000
92-94	0.01	0.3	0.0	2.66	1.48	0.00	3.82	19.8	0.05	0.00	2.64	0.02	0.000
94-96	0.00	0.0	0.0	1.36	0.61	0.00	2.52	9.9	0.03	0.00	1.87	0.07	0.000
96-98	0.00	0.0	0.0	0.29	0.10	0.00	0.19	1.6	0.00	0.00	0.86	0.02	
98-100	0.01	0.0	0.0	0.97	0.69	0.00	2.44	22.7	0.04	0.00	4.14	0.12	0.049

Colloquia Attended

1) "Using Bioassays for Remediation" - Dr Colin Campbell

2) "Modelling Metal Retention in Soils" – Dr David Lumsden

3) "From Obscurity to Stardom – The Story of Inkjet Printers and Colorant" – Prof Peter Gregory

4) "Clean Fuels" – Dr Gordon Finney

5) "The Health Effects of Environmental Particulate Matter; Some Hypothesis" – Dr Vicki Stone

6) "Corrupting the Climate? The Kyoto Protocol and the prospects for Global Action on Climate Change" - Prof Michael Grubb

7) "Diverse Themes on a Common Thread" – Prof Chris Viney

8) "Where There's Brass, there's Muck – A short History of Heavy Metal Pollution" – Dr Geraint Cole

9) "Sourcing Environmental PAH's and Sediment Inputs Using Compound Specific Stable Isotope Measurements" – Prof Colin Snape

10) "Scotch Whisky – More than just Ethanol and Water" – Dr John Conner

11) "Emission, Transport and Chemistry of Organic Carbon in the Troposphere" – Dr Alastair Lewis

12) "Mineral Surface Chemistry of U, Tc and Np in reducing Environments" – Dr Lesley Moyes

13) "Air Quality Issues facing Scotland with Particular Reference to the Forth Valley" – Dr Owen Harrop

14) "Protein Deterioration over Archaeological Timescales; Who cares?" – Dr MJ Collins

15) "Science, a Round peg in a Square Hole" – Sir Harry Kroto

16) "Development of a sequential extraction scheme for use on contaminated land" - Dr Christine Davison

17) "Climate Change – Implications for Scotland" – Dr Andy Kerr

18) "Remediation of Contaminated Land" – Dr Fin Jardine

19) Royal Society of Chemistry – Radiochemical Methods Group "Radionuclides as Tracers of Environmental Processes, 7th January 1998.

20) Annual research presentations at Macaulay Land Use Research Institute

Conferences Attended

The Silver Anniversary International Conference on Heavy Metals in the Environment, 6-10th August 2000, Ann Arbour, Michigan.

The Society for Environmental Geochemistry and Health 16th European Conference, University of Derby, April 1998.

The Society for Environmental Geochemistry and Health 17th European Conference, University of Glasgow, March 1999.

List of Lectures Attended

Atmospheric Chemistry	10 lectures	Dr Matt Heal
Atmospheric Modelling	5 lectures	Dr Matt Heal
Contaminated Land	5 lectures	Dr Richard Bewley

List of Courses Attended

Research Councils' Graduate Schools Programme – High Melton, North Yorkshire, July 2000